

Final report

Optimisation of the application of GRAL in the Australian context

Document control number: AQU-NW-012-21062

Date: 27 October 2017



Project name: Optimisation of the application of GRAL in the Australian context

Document control number: AQU-NW-012-21062

Prepared for: Roads and Maritime Services

Approved for release by: Damon Roddis

Disclaimer & copyright: This report is subject to the copyright statement located at www.pacific-environment.com © Pacific Environment Operations Pty Ltd ABN 86 127 101 642

Document Control

Version	Date	Comment	Prepared by	Reviewed by
01	10/07/2017	First draft	Francine Manansala, Paul Boulter, Jane Barnett, Christian Kurz	Damon Roddis
02	30/07/2017	Second draft, following Steering Group comments	Francine Manansala, Paul Boulter, Jane Barnett, Christian Kurz	Damon Roddis
03	20/09/2017	Revision following client review	Francine Manansala, Paul Boulter, Jane Barnett, Christian Kurz	Damon Roddis
03	27/10/2017	Final for publication	Francine Manansala, Paul Boulter, Jane Barnett, Christian Kurz	Damon Roddis



Adelaide

35 Edward Street,
PO Box 3187,
Norwood SA 5067
Ph: +61 8 8332 0960
Fax: +61 7 3844 5858

Perth

Level 1, Suite 3
34 Queen Street,
Perth WA 6000
Ph: +61 8 9481 4961
Fax: +61 2 9870 0999

Brisbane

Level 19
240 Queen Street
Brisbane Qld 4000
Ph: +61 7 3004 6400
Fax: +61 7 3844 5858

Sydney Head Office

Suite 1, Level 1
146 Arthur Street
North Sydney, NSW 2060
Ph: +61 2 9870 0900
Fax: +61 2 9870 0999

Disclaimer

Pacific Environment acts in all professional matters as a faithful advisor to the Client and exercises all reasonable skill and care in the provision of its professional services.

Reports are commissioned by and prepared for the exclusive use of the Client. They are subject to and issued in accordance with the agreement between the Client and Pacific Environment. Pacific Environment is not responsible for any liability and accepts no responsibility whatsoever arising from the misapplication or misinterpretation by third parties of the contents of its reports.

Except where expressly stated, Pacific Environment does not attempt to verify the accuracy, validity or comprehensiveness of any information supplied to Pacific Environment for its reports.

Reports cannot be copied or reproduced in whole or part for any purpose without the prior written agreement of Pacific Environment.

Where site inspections, testing or fieldwork have taken place, the report is based on the information made available by the client or their nominees during the visit, visual observations and any subsequent discussions with regulatory authorities. The validity and comprehensiveness of supplied information has not been independently verified and, for the purposes of this report, it is assumed that the information provided to Pacific Environment is both complete and accurate. It is further assumed that normal activities were being undertaken at the site on the day of the site visit(s), unless explicitly stated otherwise.

Executive summary

E1 Background and objectives

The GRAMM-GRAL system is a coupled suite that contains a meteorological model (GRAMM¹) and an air pollution dispersion model (GRAL²). The system has recently been used to support the Environmental Impact Statements for the WestConnex M4 East, New M5 and M4-M5 Link projects. Prior to WestConnex, it had not been used extensively in Australia, but it could potentially be used to assess other future road and tunnel projects. To inform such assessments, a study was undertaken to examine the performance of the system in an Australian urban context.

The main objectives of the study were:

- To assess the performance of GRAMM (version: July 2016) against meteorological measurements, and to compare it against another meteorological model (CALMET, version: 6.334) that is commonly used in Australia.
- To assess the performance of GRAL (version: August 2016) against air pollution measurements, and to compare it against another road dispersion model (CAL3QHCR, version: 2.0) that is commonly used in Australia.
- To make recommendations regarding the configuration and application of GRAMM and GRAL to the assessment urban road networks/projects in Australia.

E2 Methodology

E2.1 Evaluation of meteorological models

Measurements

The evaluation of the meteorological models was based on data for the full calendar year of 2015. The study area was located in Western Sydney, where the terrain was relatively flat. The model domain (15 km by 12 km) incorporated five monitoring stations: St Lukes Park station (operated by Roads and Maritime Services - RMS), Sydney Olympic Park and Canterbury Racecourse (operated by the Bureau of Meteorology - BoM), and Rozelle and Chullora (operated by Office of Environment and Heritage - OEH). The measurements at these stations were made at a height of 10 metres.

The evaluation focused on two of the most important meteorological parameters affecting the dispersion of air pollution from roadways: wind speed and wind direction (both as 1-hour averages). There were some differences between the stations in terms of the equipment used. Notably, ultrasonic anemometers were used at the RMS and OEH stations, whereas mechanical (cup-and-vane) anemometers were used at the BoM stations.

Model tests

Various tests were conducted to evaluate CALMET and GRAMM at the five stations. For both models the most important input was a reference (surface) meteorological dataset. Two series of tests were conducted to broadly reflect different approaches to defining the reference meteorology, with specific model set-up parameters being modified in each case. These were as follows:

¹ GRAMM = Graz Mesoscale Model.

² GRAL = Graz Lagrangian Model.

- **Series A:** The reference measurements for both CALMET and GRAMM were taken from a single monitoring station (St Lukes Park), and the model predictions were compared with observations at all monitoring stations. In these tests the following were assessed:
 - CALMET and GRAMM performance.
 - The effects of the horizontal grid spacing in GRAMM (50 metres, 100 metres and 200 metres).
 - The effects of using the 'Re-Order' function in GRAMM.
- **Series B:** The reference meteorological data were taken from multiple measurement stations (for CALMET) or from a synthetic meteorological file with 'Match-to-Observations' (GRAMM), and the model predictions were compared with observations. Three different approaches were examined:
 - GRAMM Match-to-Observations for *all stations except St Lukes Park*. All stations except St Lukes Park were used to provide the reference meteorological data. In the case of CALMET the reference data were entered directly into the model. As GRAMM will only accept data from a single reference station, an analogous approach was used whereby a synthetic meteorological file was used as input to the model, and then the GRAMM Match-to-Observations function was used for the specific monitoring stations.
 - GRAMM Match-to-Observations for *all stations*. All monitoring stations were used with the GRAMM Match-to-Observations function.
 - GRAMM Match-to-Observations for *St Lukes Park only*. This test was used to examine the performance of GRAMM in the dispersion model domain around St Lukes Park, and for the conditions that were used in the GRAL modelling. The results for other stations were therefore considered to be less important in these tests.

E2.2 Evaluation of dispersion models

Measurements

The evaluation of GRAL and CAL3QHCR focussed on the dispersion of oxides of nitrogen (NO_x)³ from surface roads. The reasons for selecting NO_x are provided in the report. Some consideration was also given to the estimation of nitrogen dioxide (NO₂) concentrations, given the focus on the health impacts of this pollutant rather than total NO_x.

The dispersion modelling part of the study involved the analysis of monitoring data and model predictions for an overall period of four months (November 2016 to February 2017 inclusive). Measurements at both roadside and background continuous monitoring stations, as well as multiple passive sampling locations, were used in the assessment.

The study took advantage of the two existing air pollution monitoring stations that were established for the WestConnex M4 East project:

- Concord Oval (roadside), adjacent to Parramatta Road. The average weekday traffic volume on Parramatta Road near this location was around 80,000 vehicles per day.

³ NO_x is, by convention, the sum of nitrogen dioxide (NO₂) and nitric oxide (NO).

- St Lukes Park (background), around 180 metres from the nearest heavily trafficked road (Gipps Street, with around 26,000 vehicles per day). The station was approximately 450 metres to the north-east of the Concord Oval station.

At both these stations air pollution was measured at a height of approximately 3 metres. As noted earlier, meteorology was measured at a height of 10 metres at St Lukes Park. Meteorology was also measured at Concord Oval, but given that this was a roadside site the measurements were at a height of 3 metres.

The continuous monitoring data were analysed as 1-hour averages.

Ogawa passive samplers were used to measure fortnightly-average NO_x and NO_2 concentrations simultaneously at 17 locations in the study area, including co-location with the continuous analysers for calibration. The Ogawa samplers were deployed in triplicate at the 17 locations over two periods (i.e. two rounds of sampling). A third round of sampling was included at Concord Oval and St Lukes Park only, the reason for this being to increase the number of data points available for sampler calibration.

All the main roads in the dispersion model domain were included in the models. Road gradients and widths were estimated from Google Earth. Traffic volumes by lane and by hour at specific junctions and for the whole dispersion model evaluation period were obtained from the Sydney Coordinated Adaptive Traffic System (SCATS). Traffic surveys were also undertaken at seven locations (four video camera sites and three automatic tube count sites) to obtain additional data on traffic composition. Average traffic speeds between specific node points on the network were estimated using the Google Maps Distance Matrix application programming interface (API).

Model set-up

Exhaust emissions were calculated using a simplified version of the NSW EPA emission inventory model. The performance of the emission model was not evaluated separately as part of this study, and most of the work focussed on the effects of changing GRAMM and GRAL parameters on model predictions. However, the sensitivity of the emission model outputs (NO_x only) to changes in specific inputs (e.g. road type, speed, gradient) was examined.

The general set-up of CAL3QHCR and GRAL is described in the report, including road types, meteorological settings, receptor locations (the air pollution monitoring sites) and traffic/emissions data. All dispersion model outputs were defined for a height of 3 metres above ground level. This was equivalent to the height of the air pollution measurements.

NO_2 concentrations were estimated for a limited number of model runs. Five different approaches for converting modelled NO_x to NO_2 were tested, including empirical methods and the ozone-limiting method.

Model tests

The dispersion model evaluation was similar in concept to the meteorological model evaluation. Various tests were conducted to evaluate the performance of CAL3QHCR and GRAL in the dispersion model domain, focussing only on the prediction of NO_x .

Five series of tests were used to broadly reflect different modelling approaches and settings within GRAL, with an initial test using CAL3QHCR:

- **Series C:** Comparison between the predictions of CAL3QHCR and GRAL for a grid spacing of 10 metres and using the Concord Oval meteorological measurements as direct input to the models. Concord Oval was selected in preference to St Lukes Park as there was an emphasis on the prediction of concentrations close to Parramatta Road, and at a height of 3 metres.

- **Series D:** Effects of meteorological input in GRAL. The effects of using GRAMM (Concord Oval Match-to-Observations) in GRAL was compared with the direct observations from Concord Oval. All subsequent GRAL runs (in Series E to G) also used the meteorological input from GRAMM based on Concord Oval Match-to-Observations.
- **Series E:** Effects of grid spacing in GRAL (2 metres, 10 metres and 20 metres).
- **Series F:** Effects of particle number in GRAL (200, 400 and 800 per second).
- **Series G:** Effects of including buildings in GRAL, with the separate testing of prognostic and diagnostic approaches.

The model predictions were compared with observations in two different ways:

- A temporal analysis of NO_x at the Concord Oval and St Lukes Park monitoring stations. The model predictions were compared with observations using 1-hour average data for the period between November 2016 and February 2017. As with the wind speed analysis, this included a consideration of descriptive statistics, use of the `timeVariation` function in Openair, regression plots, and the calculation of specific model-evaluation metrics.
- A spatial analysis of NO_x and NO₂ for the period-average concentrations measured using the Ogawa samplers, as well as contour plots of air quality metrics.

E3 Main findings and recommendations

The main findings of the study are summarised below:

- The observational data illustrate how complex and variable air quality is in an urban location with a complex road network, and how demanding the modelling task is. Any poor agreement between model results and observations (for any model) may be caused by several factors, including
 - Limitations of the model itself.
 - Significant processes or factors influencing observations that have not been modelled (e.g. due to lack of input data, or processes that are highly localised).

This study was not designed to distinguish between these possibilities.

- The results show that the combination of GRAMM and GRAL can produce good average predictions which reflect the spatial distribution of concentrations near roads with reasonable accuracy. The model chain gives results that are at least as good as those produced by other models that are currently in use in Australia. As with all air pollution models, the prediction of short-term (1-hour) concentrations remains a challenge. This is not surprising given the complexity of the processes involved. The GRAMM-GRAL model system is therefore suitable for any type of study involving the modelling of road networks. One caveat here is that it may be an unnecessary complication to use GRAMM where appropriate meteorological data are already available.
- One of the challenges for the study was the treatment of short-term average NO₂ concentrations. This was because of the need to simulate several complex processes, including adequate representation of background concentrations, quantification of primary NO₂ (which is especially uncertain), and the short-term chemical formation of NO₂ through its reaction with ozone. The latter point was particularly

important for this study; the time scales for atmospheric mixing and chemical reactions are very similar, which makes this task difficult. Ideally, what is required is a closely-coupled treatment of mixing and chemistry. As shown in the study, no empirical approach to short-term NO₂ estimation works especially well.

Various recommendations for the application of GRAMM and GRAL have resulted from this study. When considering these, the following should be borne in mind:

- The purpose of the study was not to provide a complete validation of the GRAMM-GRAL system itself, but rather to evaluate its performance for the set-up of the study.
- Any recommendations made for the use of the model system in an Australian regulatory assessment context should be viewed with an understanding that they are based on the set-up for the study.

In particular, it should be noted that the recommendations apply to *road traffic sources in a small study area with relatively simple terrain and few large buildings*. However, it can reasonably be assumed that the findings are transferable from Sydney to similar urban areas of Australia.

The recommendations are as follows:

- For the type of study area investigated, the direct use of measured meteorological data in GRAL can result in model performance that is at least as good as when GRAMM is used. Nevertheless, it would generally be advisable to run GRAMM to confirm this, and to run GRAMM for more complex situations and larger domains.
- Where GRAMM is used, then it will be important to use the Match-to-Observation function for an appropriate (nearby and representative) meteorological station.
- In order to reduce the uncertainty in emission calculations, it is important to use an accurate temporal profile of traffic volume and traffic composition. It will also be important to accurately characterise traffic speed, especially when this is outside the range of around 30-60 km/h. These factors have been known for a long time, and are not exclusive to GRAL.
- The results of GRAL will probably not be sensitive to settings such as grid resolution and number of particles, although these should clearly be within the recommended ranges.
- The likely advantages of including buildings in a model run should be considered prior to modelling, given the implications on grid resolution (fine resolution required) and therefore computation times.
- In general, the prediction of short-term NO₂ concentrations needs to be improved to properly account for local chemical processes. Empirical methods should be further investigated. It would be useful to know, for example, how NO₂ predictions vary according to conditions.

The data obtained in the study could be useful in future studies, and there are further opportunities for data mining. The information presented in the report will be available to anyone interested in understanding or modelling near-road air quality.

For more detailed recommendations on specific model settings the GRAMM and GRAL documentation should be consulted.

Table of contents

1 Introduction	1
1.1 Background	1
1.2 Objectives	1
1.3 Project organisation	2
1.4 Overview of methodology	3
1.4.1 Models	3
1.4.2 Study area	4
1.4.3 Model evaluation parameters	4
1.4.4 Measurements	5
1.4.5 Model evaluation periods	6
1.5 Report structure	7
2 Study area and characteristics	8
2.1 Location and model domains	8
2.2 Emission sources	10
3 Experimental methodology	15
3.1 Continuous air pollution measurements	15
3.1.1 Monitoring station locations	15
3.1.2 Parameters and methods	17
3.2 Passive air pollution sampling	19
3.2.1 Samplers and handling procedure	19
3.2.2 Sampling locations	20
3.2.3 Sampling periods	22
3.2.4 Data checking and processing	22
3.3 Meteorology	24
3.3.1 Monitoring station locations	24
3.3.2 Parameters and methods	25
3.4 Roads and traffic	26
3.4.1 Road links	26
3.4.2 Traffic data	29
4 Modelling methodology	33
4.1 Overview	33
4.2 Emission modelling	33
4.2.1 Model set-up	33
4.2.1.1 Emission factors	34
4.2.2 Weekday emission profiles	36
4.2.3 Model evaluation	36
4.2.4 Traffic data	36
4.2.5 Sensitivity testing	38
4.3 Meteorological modelling	38
4.3.1 CALMET	39
4.3.2 GRAMM	41

4.4 Dispersion modelling	42
4.4.1 CAL3QHCR	42
4.4.2 GRAL	42
4.4.3 Receptors	43
4.4.4 Post-processing	43
4.5 Model evaluation	47
4.5.1 Meteorological model evaluation	47
4.5.2 Dispersion model evaluation	49
4.5.3 Estimation of NO ₂ concentrations	51
5 Results of experimental work	52
5.1 Traffic volume and composition	52
5.2 Traffic speed	54
5.3 Emissions	55
5.4 Meteorological measurements	56
5.5 Continuous air pollution monitoring	61
5.5.1 Statistical overview	61
5.5.2 Temporal analysis	61
5.5.3 Directional analysis	70
5.6 Passive air pollution sampling	78
5.7 Background concentrations	88
5.8 Road traffic contribution	88
5.8.1 Continuous measurements	88
5.8.2 Passive sampling	93
6 Results of modelling	96
6.1 Emission model sensitivity	96
6.2 Meteorological model evaluation	98
6.2.1 Overview	98
6.2.2 Wind speed analysis	98
6.2.3 Wind direction analysis	106
6.2.4 Wind roses	106
6.3 Dispersion model evaluation	106
6.3.1 Temporal analysis of NO _x	106
6.3.2 Directional analysis of NO _x	112
6.3.3 Spatial analysis of NO _x	114
6.4 Treatment of NO ₂ concentrations	119
7 Summary and conclusions	121
7.1 Summary	121
7.1.1 Emission model sensitivity testing	121
7.1.2 Meteorological modelling	121
7.1.3 Dispersion modelling	122
7.2 Conclusions	122
8 Recommendations	125
9 References	126

Appendix A:	The GRAMM-GRAL system
Appendix B:	Model evaluation principles
Appendix C:	Review of GRAL validation studies
Appendix D:	Statistical summary of meteorological measurements
Appendix E:	Results of met model evaluation
Appendix F:	Results of dispersion model evaluation

1 Introduction

1.1 Background

The GRAMM-GRAL model system is a coupled suite that contains a meteorological model (GRAMM⁴) and an air pollution dispersion model (GRAL⁵). The model system – which is often simply referred to as GRAL - was developed with the simulation of pollutant dispersion from complex urban road networks as a core capability.

GRAL has recently been used to support the Environmental Impact Statements (EISs) for the WestConnex M4 East, New M5 and M4-M5 Link projects (Boulter et al., 2015; Manansala et al., 2015; Pacific Environment, 2017). Prior to WestConnex, GRAL had not been used extensively in Australia, but it could potentially be used to assess other future road and tunnel projects. To inform such assessments, and to identify and assess potential improvements to the application of the model in Australia, Pacific Environment was commissioned by NSW Roads and Maritime Services (Roads and Maritime) to undertake a 'GRAL optimisation study'. The study examined the performance of both GRAMM and GRAL, with an emphasis on the following:

- Application in an **urban area** with relatively **flat terrain**.
- The dispersion of **oxides of nitrogen** (NO_x)⁶ from **line sources** (i.e. surface roads); other types of source, such as tunnel ventilation outlets and tunnel portals, were not considered. The reasons for selecting NO_x are provided in the report. Some consideration was also given to the estimation of nitrogen dioxide (NO₂) concentrations.

This report describes the study and presents the findings and recommendations.

1.2 Objectives

The general objectives of the study were as follows:

- Model description
 - To review the GRAMM-GRAL system and previous evaluation studies. The purpose of this review was to identify key issues relating to model set-up, and thus guide the study methodology. The review included:
 - A description of the model system.
 - Model settings and inputs, the physical effects that these simulate, and their qualitative effects on model predictions.
 - Appropriate values (or ranges) for the settings and inputs, with a focus on application in urban areas.
 - General guidance on model evaluation.

⁴ GRAMM = Graz Mesoscale Model.

⁵ GRAL = Graz Lagrangian Model.

⁶ NO_x is, by convention, the sum of nitrogen dioxide (NO₂) and nitric oxide (NO).

- Previous validation studies, with an emphasis on surface roads.
- Assessment of GRAMM performance
 - To undertake GRAMM simulations using local meteorological measurements.
 - To investigate the response of GRAMM to model inputs and settings.
 - To assess the performance of GRAMM against meteorological measurements at several sites, and to compare it against another meteorological model (CALMET) that is commonly used in Australia.
- Assessment of GRAL performance
 - To undertake GRAL simulations using local emission factors and traffic measurements from the study area.
 - To investigate the response of GRAL to model inputs and settings.
 - To assess the performance of GRAL against air pollution measurements in the study area, and to compare it against another road dispersion model (CAL3QHCR) that is commonly used in Australia. Measurements at both roadside and background continuous monitoring stations, as well as multiple passive sampling locations, were used in the assessment.
- Recommendations for model application
 - To identify and assess potential improvements to the application of the GRAMM-GRAL model system in Australia.
 - To make recommendations regarding the configuration and application of GRAMM and GRAL to the assessment complex urban road networks/projects in Australia, taking into account issues such as scaling (e.g. size of study area and number of road links) and practicality (e.g. processing time).

These objectives are reflected in the structure of the report.

1.3 Project organisation

The project was undertaken by Pacific Environment with support from FVT in Austria. It was funded by Roads and Maritime, acting on behalf of other stakeholders including the NSW Advisory Committee on Tunnel Air Quality (ACTAQ). A Steering Group was established to provide guidance on the study. The members of the Steering Group were:

- Emily Kemp, Andrew Mattes, Vince Taranto (Roads and Maritime)
- Carrie Waring (NSW Office of Chief Scientist & Engineer)
- Dr Ian Longley (NIWA)
- Dr Mark Hibberd (CSIRO)

- Dominic Crinnion (NSW Department of Planning and Environment)
- Aleks Todoroski (Todoroski Air Sciences)

Dr David Carslaw of the University of York in the United Kingdom acted as a technical peer reviewer.

1.4 Overview of methodology

The evaluation of meteorological models and air pollution models can be a complex process involving various different steps. Two terms are commonly used when evaluating model performance:

- Model validation. This generally refers to detailed, peer-reviewed studies that have been carried out by the model developer or a regulatory agency.
- Model verification. This generally refers to checks carried out on model performance at a local level. It usually involves the comparison of predicted and measured concentrations.

The study focused on model verification rather than model validation. Models applied for regulatory air quality assessment are commonly verified on the basis of comparison against observations, and this element of the process is known as ‘operational model evaluation’ or ‘statistical performance analysis’ (Denby et al., 2010). However, it is noted that this approach does not provide comprehensive insight into all the properties of models.

1.4.1 Models

The meteorological models and dispersion models included in the study are briefly summarised below. More detailed information on the specific configuration of each model is provided later in the report.

1.4.1.1 Meteorological models

Meteorological models can be classified as either ‘diagnostic’ or ‘prognostic’. Diagnostic models create meteorological fields through interpolation based on measurements. They use a relatively simple mass conservation approach without solving fundamental equations of momentum, energy, or moisture conservation. Their accuracy is often limited by insufficient measurements, and the fields can lack dynamic consistency between meteorological variables. Prognostic models have been developed to overcome some of the shortcomings of diagnostic models by solving the equations that describe atmospheric dynamics. Prognostic models can provide a better representation of certain meteorological phenomena, such as sea breezes and slope/valley circulations. The capability of prognostic models to produce accurate meteorological fields has improved dramatically through, for example, better physical parameterisation and increased spatial resolution (Hu et al., 2010).

CALMET

CALMET⁷ is a diagnostic model that is the meteorological pre-processor for the CALPUFF dispersion model. CALMET requires surface and upper air data. At the surface, the following variables are needed with hourly resolution: wind speed, wind direction, temperature, cloud cover, ceiling height, surface pressure, and relative humidity. The upper air data, needed at least twice daily, must contain the following for each vertical level: wind speed, wind direction, temperature and pressure. CALMET constructs three-dimensional wind

⁷ <https://www.enviroware.com/calmet/>

fields and temperature fields from the meteorological measurements, terrain data and land use data. CALMET also determines two-dimensional fields of the micro-meteorological variables that are needed for dispersion modelling (e.g. mixing height, Monin-Obukhov length, friction velocity, convective velocity). The diagnostic wind field module uses a two-step approach to determine the wind fields. Firstly, an initial estimate of the wind field is made, allowing for the effects of terrain. Secondly, observational data are introduced to produce a final wind field.

GRAMM

GRAMM is a prognostic meteorological model, and is described in Appendix A.

1.4.1.2 Dispersion models

For road traffic sources Gaussian models are most commonly used. Gaussian models assume that pollutant dispersion follows a normal probability distribution. In recent years several roadway models have employed non-steady-state Lagrangian algorithms. A Lagrangian model follows pollution plume 'particles' (also referred to as 'parcels') as they move through the atmosphere, and models their motion using a random-walk process. The model then calculates the bulk dispersion by computing the statistics for the trajectories of a large number of particles.

CAL3QHCR

CAL3QHCR was developed in 1995 by the United States Environmental Protection Agency (USEPA), and is commonly used for road project assessments in Australia. Based on CALINE, it is a steady-state Gaussian model which can determine concentrations at receptor locations downwind of 'at grade', 'fill', 'bridge' and 'cut section' roads located in relatively uncomplicated terrain. The model is applicable to any wind direction, roadway orientation and receptor location. CAL3QHCR is an enhanced version of CALINE that is able to process up to a year of meteorological data and allows for traffic queuing at intersections. CAL3QHCR reads up to seven sets of hourly emissions data in the form of diurnal patterns. These data are synchronised to the day of the week applicable to the meteorological data year being used. The model does not allow for the effects of terrain or buildings on dispersion, uses homogeneous wind fields, and has no atmospheric chemistry.

GRAL

GRAL is a Lagrangian model, and is described in Appendix A.

1.4.2 Study area

To meet the objectives of the study, the meteorological and dispersion models were applied to an urban area containing busy roads, and the model predictions were compared with the measurements from local meteorological and air quality monitoring stations. In order to evaluate dispersion model performance across a range of concentrations, the study required air pollution data from monitoring sites both near roads and at background locations where there was minimal influence from the road network. The study relied upon the data from existing monitoring stations established for the WestConnex M4 East project, supplemented by a passive sampler network established specifically for the work.

1.4.3 Model evaluation parameters

1.4.3.1 Meteorological models

The evaluation of CALMET and GRAMM focused on two of the most important meteorological parameters affecting the dispersion of air pollution from roadways: wind speed and wind direction.

1.4.3.2 Dispersion models

The evaluation of CAL3QHCR and GRAL focussed primarily on the prediction of NO_x for reasons similar to those described elsewhere (e.g. Longley et al. (2013)):

- One of the components of NO_x, NO₂, is a concern from a health perspective.
- Road traffic is the dominant source of NO_x in urban areas. There is therefore generally a stronger road traffic signal for NO_x than for other traffic pollutants. For example, for PM the local impact of traffic on ambient concentrations is relatively small, even at roadside, as there are numerous other sources that contribute to background (non-road) levels in urban areas.
- Although NO₂ is both formed and destroyed by chemical reactions in the atmosphere during dispersion in near-road environments, NO_x is conserved during dispersion. NO_x is therefore more useful for assessing how models perform with respect to dispersion alone, without the complicating effects of atmospheric chemistry.
- The technology for monitoring NO_x is well established, with instruments having a high sensitivity relative to the ambient concentration gradients observed in urban areas.

Several methods for estimating NO₂ concentrations were also included in the study, as NO₂ is important in terms of health and air quality criteria. However, NO₂ is strongly influenced by atmospheric chemistry, and GRAL does not include a chemical reaction scheme. The evaluation of NO₂ did not, therefore, represent an evaluation of GRAL itself.

Other pollutants and metrics are mentioned in the report, such as airborne particles with a diameter of less than 10 µm (PM₁₀), airborne particles with a diameter of less than 2.5 µm (PM_{2.5}), carbon monoxide (CO), volatile organic compounds (VOCs), and ozone (O₃), but these were not modelled or considered in detail. Ozone measurements were, however, used in some of the approaches for calculating NO₂.

1.4.4 Measurements

1.4.4.1 Continuous air pollution measurements

There are relatively few established air quality monitoring stations at roadside sites in Sydney. The study took advantage of the following existing stations from the WestConnex M4 East project:

- Concord Oval roadside. For the M4 East project a roadside station was established in the grounds of Concord Oval, adjacent to the northern edge of Parramatta Road, Concord.
- St Lukes Park background. A background monitoring station for the M4 East project was established in St Lukes Park, approximately 450 metres to the north-north-east of the Concord Oval station.

These monitoring stations are described in more detail later in the report.

Ideally, pollutant concentrations would have been measured continuously on both sides of Parramatta Road. This would have enabled background concentrations to be determined for most wind directions, by simply using the data measured at an upwind station as the background. However, as in many studies of this type, there were various practical limitations, and the establishment of an additional continuous monitoring station on the southern side of Parramatta Road was not possible. This meant that continuous measurements of background concentrations for southerly winds were not available, and hence there was more uncertainty in the background concentrations that were applicable to these situations.

1.4.4.2 Passive air pollution sampling

To supplement the continuous monitoring a temporary, short-term network of low-cost passive samplers (measuring NO_x and NO₂) was installed within the dispersion model domain (see Section 2.1). These measurements of NO_x and NO₂ were made at 17 locations. This sampling increased the spatial coverage of the air pollution measurements, and contributed to the understanding of pollution gradients in the domain. In particular, the passive samplers were deployed so as to characterise concentration gradients perpendicular to Parramatta Road (both to the north and to the south), and broadly between the road, the Concord Oval monitoring station and the St Lukes Park monitoring station. There was a particular emphasis on the environment close to Parramatta Road, where the steepest concentration gradients would be expected. The passive sampling also included co-location and calibration against the reference analysers at the two air quality monitoring stations.

1.4.4.3 Meteorological measurements

Meteorological parameters were measured at the two M4 East stations. Four additional meteorological stations were located within the study area: Bureau of Meteorology (BoM) stations at Sydney Olympic Park and Canterbury Racecourse, and Office of Environment and Heritage (OEH) stations at Rozelle and Chullora. The OEH Earlwood station was also located in the study area, but it was close to the boundary and was therefore excluded from the analysis.

All stations except Concord Oval were used in the evaluation of GRAMM and CALMET. The Concord Oval station was at a roadside location rather than at a more open type of location that is typically used for characterising regional meteorology, and the measurements were made at a height of 2-3 metres, compared with 10 metres at all other stations. In practice, the meteorological data from Concord Oval and St Lukes Park were found to be quite similar (see Section 5.4), and these differences do not appear to have been so important. In addition, on the scale of the GRAMM domain the two M4 East sites were relatively close together. The inclusion of St Lukes Park alone was therefore considered to be sufficient to characterise this area of the GRAMM domain.

On the other hand, for the dispersion model evaluation Concord Oval was selected as the reference meteorological site in preference to St Lukes Park, as there was an emphasis on the prediction of concentrations in the vicinity of Parramatta Road, and at a height of 3 metres.

1.4.5 Model evaluation periods

The evaluation periods were different for GRAMM and GRAL:

- The evaluation of GRAMM covered the calendar year 2015. This permitted model evaluation over the range of meteorological conditions that is typically used in dispersion modelling exercises.

- For GRAL the study involved the analysis of monitoring data and model predictions for an overall period of four months (November 2016 to February 2017 inclusive). This period was limited by the constraints of the study, such as the availability of air quality and traffic data, and the overall timetable for delivery.

1.5 Report structure

The remainder of the report is structured as follows:

- Chapter 2 defines the characteristics of the study area, including the model domains, land use, roads, and emission sources.
- Chapter 3 describes the experimental methodology, including the measurement of air pollution and meteorology.
- Chapter 4 describes the modelling methodology.
- Chapter 5 presents the results of the experimental work.
- Chapter 6 presents the results of the modelling.
- Chapter 7 gives the summary and conclusions.
- Chapter 8 provides the recommendations from the study.

2 Study area and characteristics

2.1 Location and model domains

The study area was located in Western Sydney, as shown in Figure 1. The centre of the study area was approximately 9 km to the west of the Sydney Central Business District (CBD) and 9 km to the north-west of Sydney Airport.

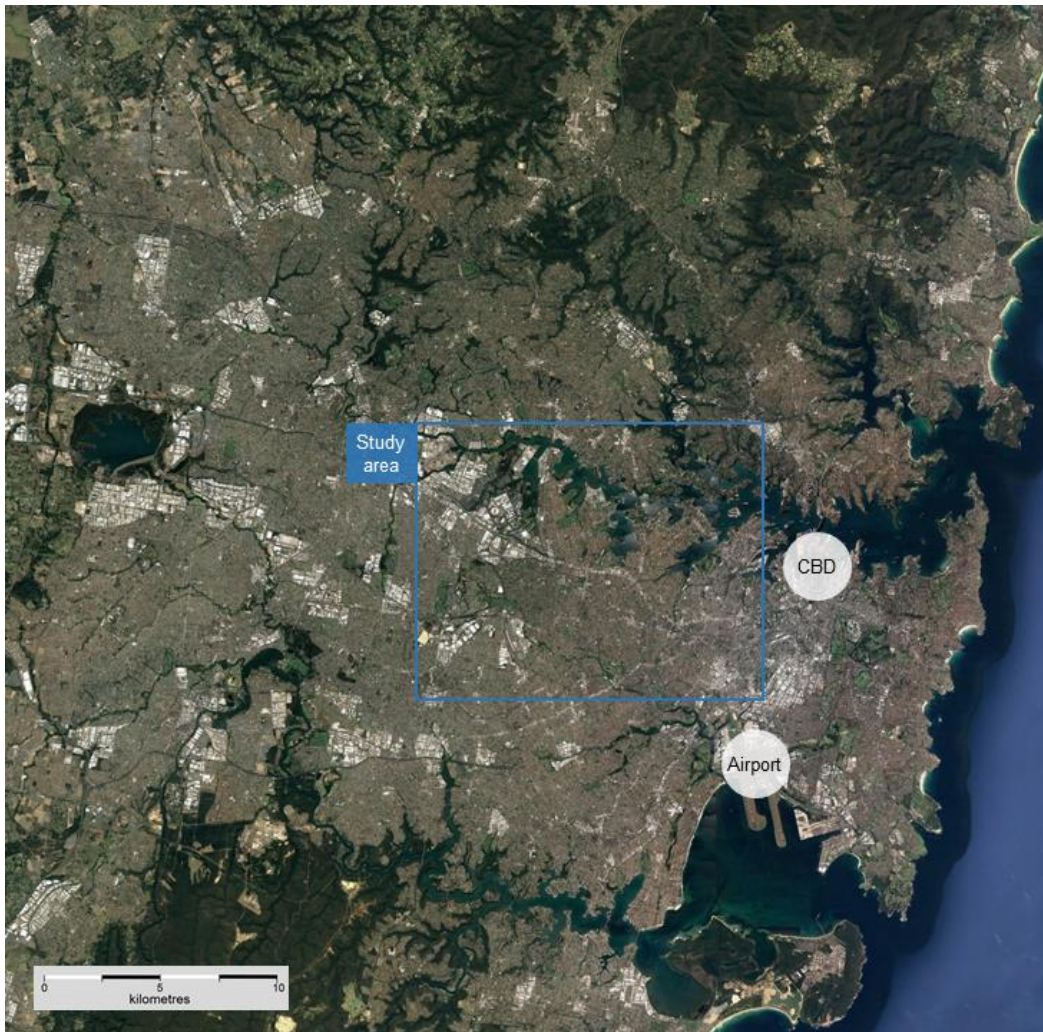


Figure 1: Location of study area – regional context

Two model domains were defined: a larger one to examine the meteorological models, and a smaller one within this to evaluate the dispersion models. Given that one of the aims of the study was to compare the performance of GRAMM with that of CALMET, the domain for meteorology had to be large enough to incorporate several monitoring sites with a sufficient buffer. This domain – which is shown in Figure 2 and is equivalent to the study area defined in Figure 1 – was 15 km by 12 km in size. The much smaller dispersion model domain (2 km by 2 km) is also included in Figure 2. The two M4 East air quality monitoring stations were close to the centre of the dispersion model domain.

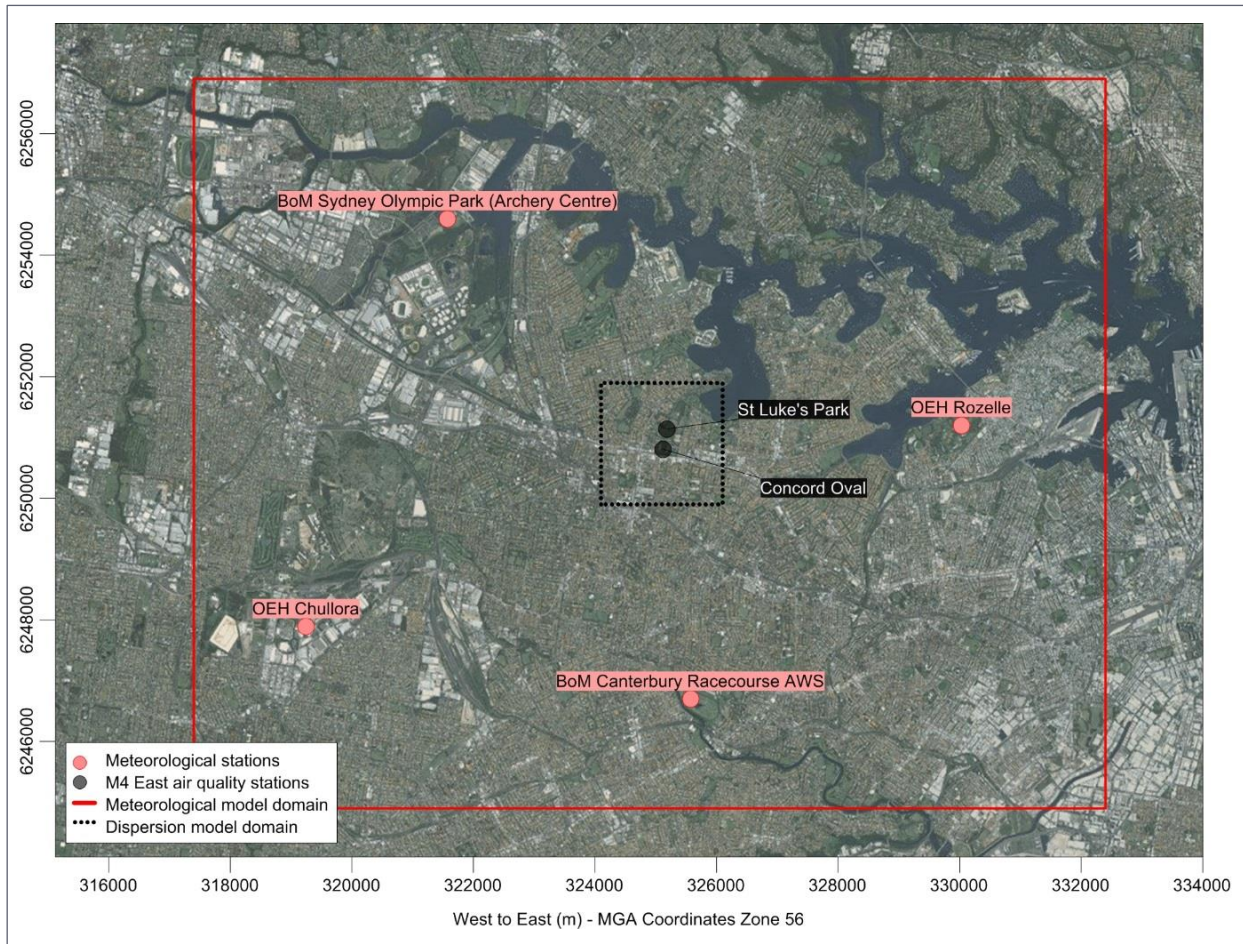


Figure 2: Model domains and locations of monitoring stations

The land use in the meteorological model domain was mainly low-rise and residential in nature, with commercial areas in the north-west, south-west and south-east, and Sydney Olympic Park in the north-west. The northern part of the domain included the Parramatta River, the Lane Cove River, and a large number of bays and inlets. The terrain in the domain was relatively flat and simple, with the ground level elevation ranging from sea level to approximately 62 metres.

The dispersion model domain is reproduced on a larger scale in Figure 3. The land use in the dispersion model domain was again mainly residential in nature, with commercial/retail use along the Parramatta Road, Queens Road and Burwood Road corridors. There was a substantial amount of parkland and recreational space (St Lukes Park, St Lukes Oval, Cintra Park and Concord Oval near the centre of the domain; Barnwell Park Golf Club in the north-east; Cheltenham Road Park and Blair Park in the south-east; Burwood Park in the south-west; Goddard Park and Queen Elizabeth Park in the north-west). The domain also included a short section of railway line to the west of Burwood station, and an area of Canada Bay in the north-eastern corner. The highest point in the domain, in the extreme south, was around 30 metres above sea level.

Figure 3 also identifies the main roads in the dispersion model domain, as well as some minor roads in the general vicinity of the air quality monitoring stations, and the approximate weekday traffic volumes. The domain is bisected by the Parramatta Road corridor, which is aligned on an approximate east-west axis. Parramatta Road is one of Sydney's oldest roads and a strategically important transport route, being the major historical artery connecting the Sydney CBD with Parramatta. It is by far the most heavily trafficked road in the domain with around 80,000 vehicles on weekdays.



Figure 3: Dispersion model domain, with main roads and typical weekday traffic volumes

2.2 Emission sources

The most detailed and comprehensive source of information on current and future emissions in the Sydney area is the emissions inventory⁸ that is compiled periodically by NSW EPA. The base year of the latest published inventory is 2008, and projections are available for 2011, 2016, 2021, 2026, 2031 and 2036 (NSW EPA, 2012a). The data for emissions in Sydney were extracted from the inventory by NSW EPA⁹ and are presented in Figure 4 and Figure 5 for the 2016 projection year.

⁸ An emissions inventory defines the amount (in tonnes per year) of pollution that is emitted from each source in a given area.

⁹ The data were provided for the project Economic Analysis to Inform the National Plan for Clean Air (Particles), undertaken by Pacific Environment on behalf of the NEPC Service Corporation.

The importance of road transport as a source of pollution in Sydney can be illustrated by reference to the sectoral emissions. Figure 4 shows that road transport was the second largest contributor to emissions of CO (34%) after the domestic-commercial sector, and the largest contributor to NO_x (47%). Road transport was also responsible for a significant proportion of emissions of VOCs (13%), PM₁₀ (9%) and PM_{2.5} (11%). The main contributors to VOCs were domestic-commercial activity and biogenic sources. The most important sources of PM₁₀ and PM_{2.5} emissions were the domestic-commercial sector and industry. The contribution to PM from the domestic sector was dominated by wood burning for heating in winter. Emissions from natural sources, such as bushfires, dust storms and marine aerosol, also contributed significantly to PM concentrations. Road transport contributed only one per cent of total SO₂ emissions in Sydney, reflecting the desulfurisation of road transport fuels in recent years. SO₂ emissions in Sydney were dominated by the off-road mobile sector and industry.

The breakdown of emissions in 2016 from the road transport sector by process and vehicle type is presented in Figure 5. Petrol passenger vehicles (mainly cars) accounted for a large proportion of the vehicle kilometres travelled (VKT) in Sydney¹⁰. Exhaust emissions from these vehicles were responsible for 65% of CO from road transport, 37% of NO_x, and 76% of SO₂. They were a minor source of PM₁₀ (3%) and PM_{2.5} (4%). Non-exhaust processes were the largest source of road transport PM₁₀ (70%) and PM_{2.5} (57%). This is a larger proportion than in, say, most European countries, as there are relatively few diesel cars in Australia. Emissions of non-exhaust particles will increase in line with projected traffic growth, as there are currently no controls or legislation. Heavy-duty diesel vehicles are disproportionate contributors of NO_x and PM emissions due to their inherent combustion characteristics, high operating mass (and hence high fuel usage) and level of emission control technology (NSW EPA, 2012b). Evaporation was the main source of VOCs.

The dispersion model domain was located within the suburbs of Concord (post code 2137) and Burwood (post code 2134). Specific information on emissions in these suburbs was obtained using the EPA's 'Air emissions in my community' web tool¹¹. This information was only available for the inventory base year of 2008¹², and is summarised in Figure 6. For NO_x, road traffic is the dominant source in the two suburbs (Parramatta Road is the most important contributor). Whilst commercial water transport is a significant contributor to emissions in Concord, this activity occurs outside the dispersion model domain itself, although it would contribute to background concentrations in the domain. For PM₁₀ and PM_{2.5} residential wood heating is the dominant source. There is a minor contribution from rail transport. The spatial distribution of emissions is also dependent on the source. For example, NO_x emissions are concentrated on Parramatta Road, whereas domestic/commercial combustion is distributed homogeneously.

¹⁰ Diesel passenger vehicles have represented only a very small proportion of the total passenger vehicle fleet. However, the improved performance of light-duty diesel vehicles over the last 10 years, together with superior fuel economy, has boosted sales and the market share is increasing (NSW EPA, 2012b).

¹¹ <http://www.epa.nsw.gov.au/air/airemissionsapp/airemissionswebtool.aspx>

¹² The inventory data for Sydney show that, between 2008 and 2016, emissions from road transport decreased. The reductions were as follows: 47% for CO, 28% for VOCs, 36% for NO_x, 17% for PM₁₀, 26% for PM_{2.5} and 18% for SO₂. The proportional contribution of road transport to total emissions also fell during this period, by between 2 and 16 percentage points, depending on the pollutant. The percentage contribution to SO₂ emissions did not change. However, the inventory data for Sydney in 2016 show that road transport remained the dominant source of NO_x in 2016, and this is also likely to be the case for the study area.

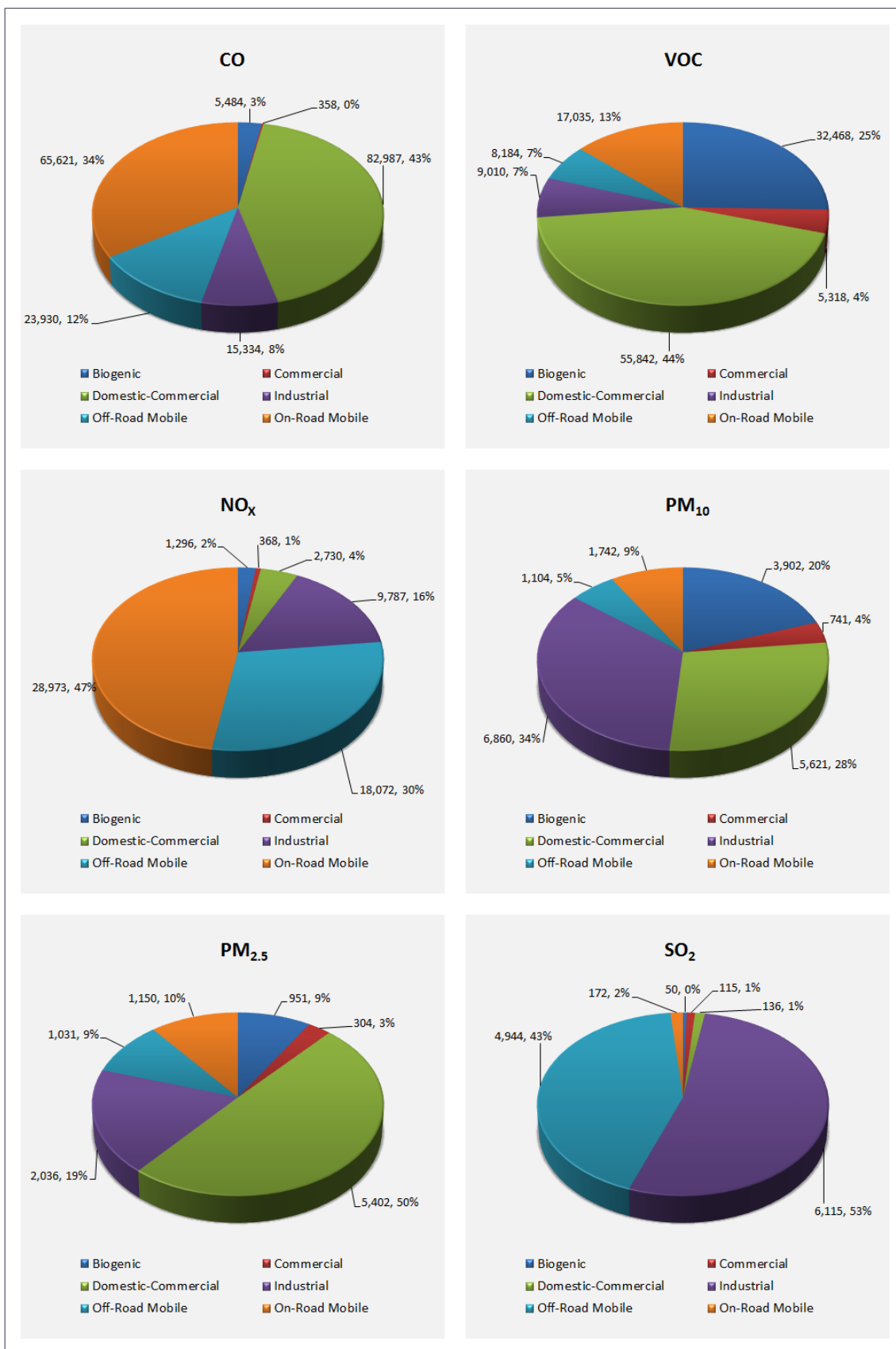


Figure 4: Sectoral emissions in Sydney, 2016 (tonnes per year and percentage of total)

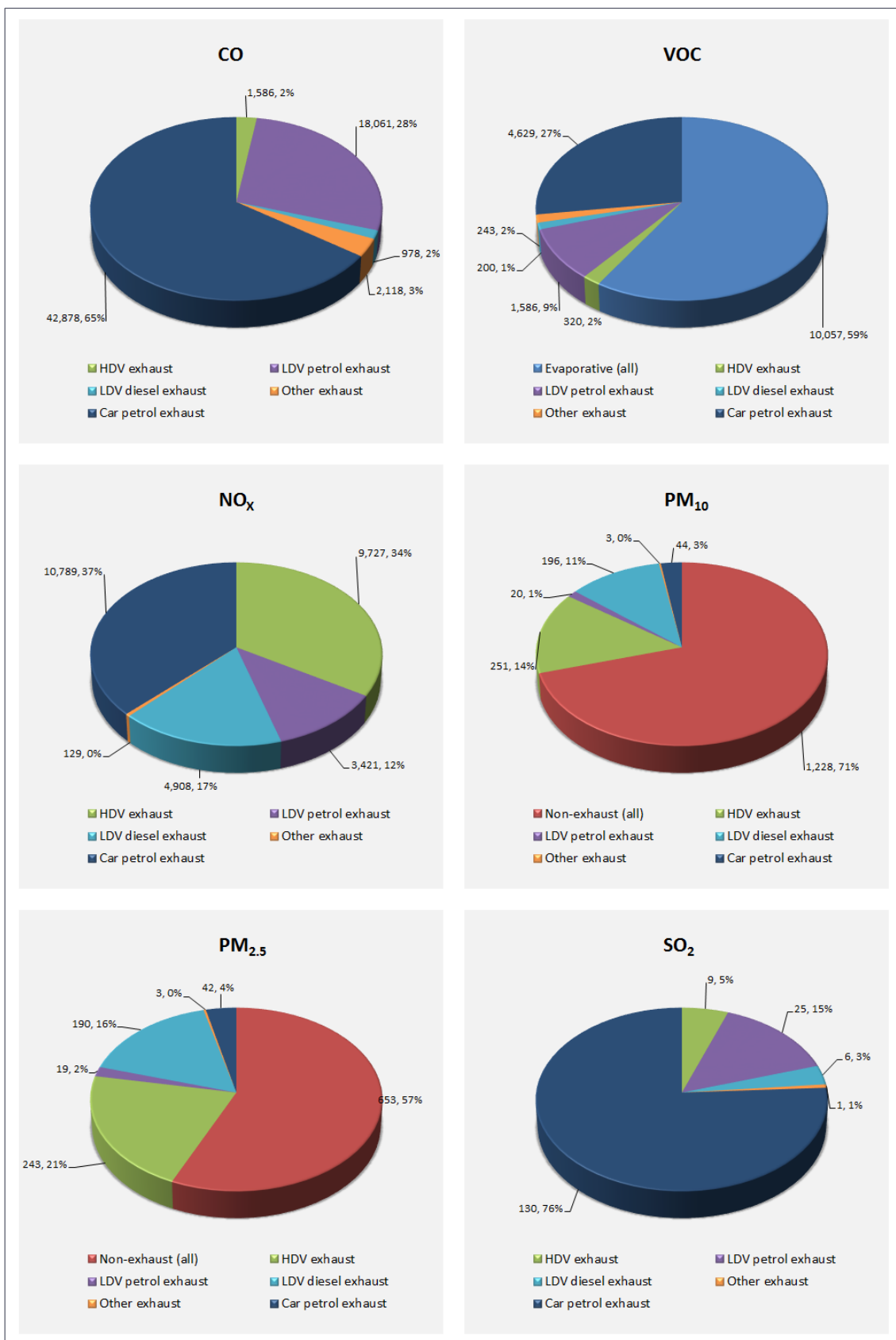


Figure 5: Breakdown of road transport emissions – Sydney, 2016 (tonnes per year and percentage of total)

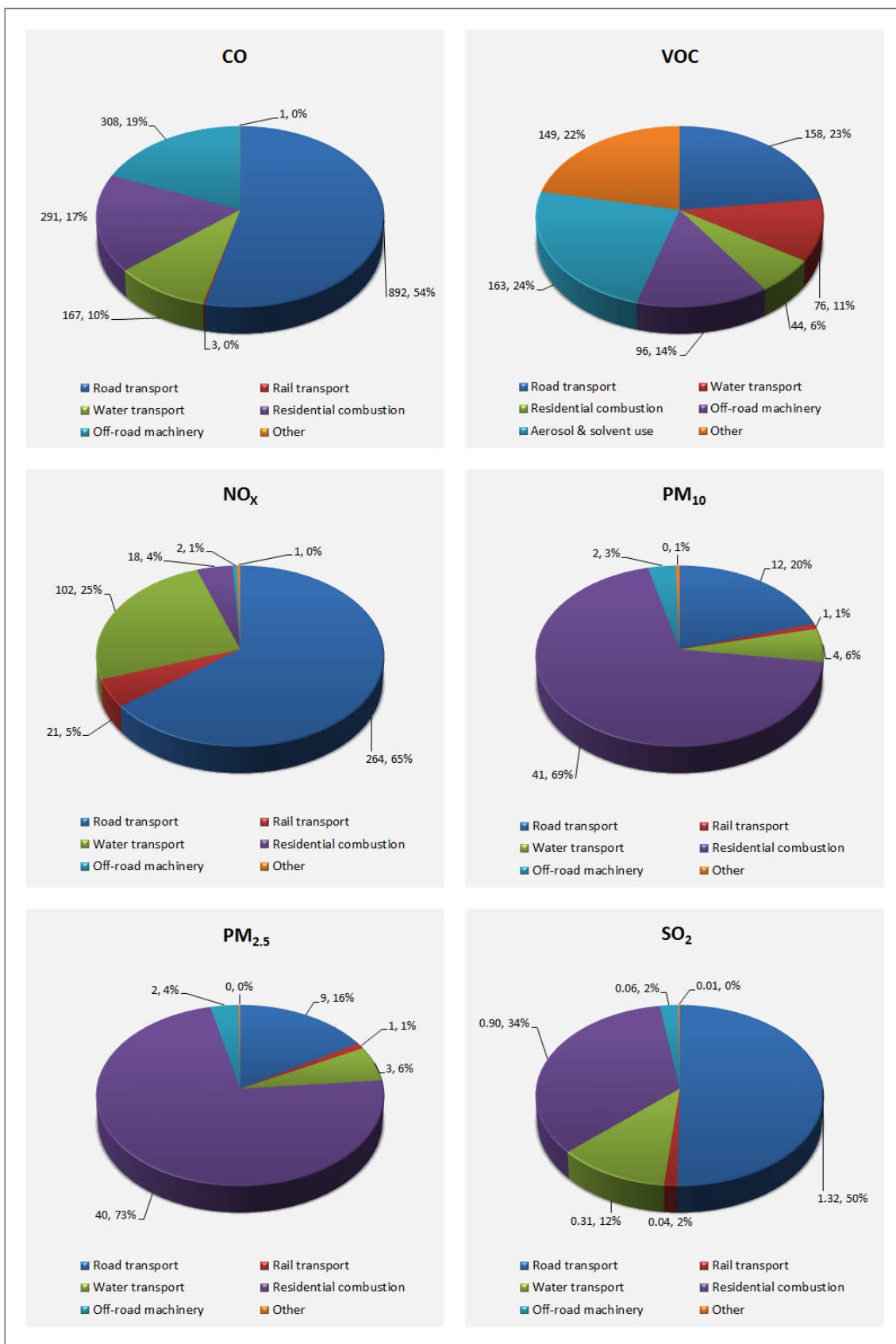


Figure 6: Breakdown of road transport emissions – Concord and Burwood post codes, 2008 (tonnes per year and percentage of total)

3 Experimental methodology

3.1 Continuous air pollution measurements

3.1.1 Monitoring station locations

The study took advantage of the two existing air pollution monitoring stations which were established for the WestConnex M4 East project:

- Concord Oval (roadside). For the M4 East project a roadside station was established in the grounds of Concord Oval, to the south of the car park and adjacent to Parramatta Road (Figure 7, Figure 8). The air inlets were located approximately 11 metres from the kerb of Parramatta Road. The average weekday traffic volume on Parramatta Road near this location was around 80,000 vehicles per day. There were no large buildings close to the monitoring station.
- St Lukes Park (background). A background monitoring station for the M4 East project was established in the grounds of St Lukes Park (Figure 9, Figure 10). The station was approximately 50 metres from the closest roadway¹³, Stanley Street, which is a cul-de-sac with traffic limited to that accessing Concord High School and the sports fields. The station was around 180 metres from the more heavily trafficked Gipps Street (around 26,000 vehicles per day), and approximately 450 metres to the north-east of the Concord Oval station.



Figure 7: Location of Concord Oval monitoring station

¹³ In terms of distance from roads the monitoring station complies with *Australian Standard AS/NZS 3580.1.1:2007 - Methods for sampling and analysis of ambient air - Guide to siting air monitoring equipment*. However, the station is located near a large tree which may act to restrict airflow around the station and influence the meteorological data. The measurements at St Lukes Park may also be affected by the change in the level of the terrain near the station; the ground elevation increases from 3 metres to 6 metres within a horizontal distance of around 20 metres to the south of the site.



Figure 8: Photograph of Concord Oval monitoring station



Figure 9: Location of St Lukes Park monitoring station



Figure 10: Photograph of St Lukes Park monitoring station

3.1.2 Parameters and methods

The pollutants and measurement methods for the two M4 East monitoring stations are summarised in Table 1. The instrument specifications and averaging periods for the data are given in Table 2. The averaging period for each parameter was determined by the Australian Standard methods, as well as NSW air quality assessment criteria (NSW EPA, 2016). In this study, the continuous monitoring data were analysed as 1-hour averages, focussing primarily on NO_x and NO_2 . The data for PM_{10} , $\text{PM}_{2.5}$, CO, hydrocarbons and ozone were not considered in detail.

Instrument calibration was performed in accordance with the relevant Australian Standards and NATA procedures. Daily precision checks (zero and span) were conducted automatically for the gaseous pollutants to identify any instrument drift or malfunction. A dynamic gas calibrator was used at each station to supply the zero air and span gas to each analyser. Operational calibrations were conducted and scheduled in accordance with the relevant Australian Standard. Single-point calibrations were conducted on a monthly basis, and when instruments faults had been rectified or services had been otherwise interrupted. All data were reported in Australian Eastern Standard Time (AEST).

The data validation process was based on procedures by NSW OEH in Australia (NSW OEH, 2014), Defra in the UK (Stevenson et al., 2009) and the National Environment Protection Measure (PRC, 2001). Furthermore, data validation follows guidelines set by the Australian/New Zealand Standards Authority. The data validation process involved steps such as the removal of calibration points, removal of data during servicing and maintenance periods, corrections for instrument drift, and corrections for offsets.

Table 1: Pollutants and measurement methods

Parameter	Units	Instrument	Measurement technique	Australian Standard
Carbon monoxide (CO)	Parts per million (ppm)	Teledyne Carbon Monoxide Analyser (T300)	Gas filter correlation infrared (GFC-IR)	AS/NZS 3580.7.1.2011
Nitrogen oxide (NO) Nitrogen dioxide (NO ₂) Oxides of nitrogen (NO _x)	Parts per billion (ppb)	Teledyne Nitrogen Oxide Analyser(T200)	Chemiluminescence	AS/NZS 3580.5.1.2011
Ozone (O ₃)	Parts per billion (ppb)	Teledyne Photometric Ozone Analyser (T400)	Ultraviolet photometry	AS/NZS 3580.6.1.2011
Methane (CH ₄) Total hydrocarbons (THC) Non-methane hydrocarbons (NMHC)	Parts per million (ppm)	PCF Elettronica hydrocarbon monitor (529)	Flame ionisation detector (FID)	AS/NZS 3580.11.1.2013
Particulate matter with an aerodynamic diameter of less than 10 µm (PM ₁₀)	Micrograms per cubic metre (µg/m ³)	Thermo Electron Corporation Continuous Ambient Particulate Monitor (FH62C14)	Beta attenuation monitor (BAM)	AS/NZS 3580.9.11.2016
Particulate matter with an aerodynamic diameter of less than 2.5 µm (PM _{2.5})	Micrograms per cubic metre (µg/m ³)	Thermo Electron Corporation Continuous Ambient Particulate Monitor (FH62C14)	Beta attenuation monitor (BAM)	AS/NZS 3580.9.12.2013

Table 2: Instrument specifications and data averaging periods

Parameter	Measurement factor	Specification	Averaging periods
CO	Lower detectable limit	< 0.04 ppm	5-minute, 1-hour, 8-hour rolling
	Lag time	10 seconds	
	Full scale value	50 ppm	
	Precision	0.5% of reading or 0.2 ppm	
NO _x , NO, NO ₂	Lower detectable limit	0.4 ppb	5-minute, 1-hour
	Lag time	20 seconds	
	Full scale value	500 ppb	
	Precision	0.5 % of readings above 50 ppb	
O ₃	Lower detectable limit	< 0.6 ppb	5-minute, 1-hour, 4-hour rolling
	Resolution	0.5 ppb	
	Response time	< 5 min to 95 %	
	Full scale value	500 ppb	
	Precision	< 0.5 % of readings above 100 ppb	
THC, NMHC, CH ₄	Lower detectable limit	< 0.02 ppm	5-minute, 1-hour
	Background noise	0.01 ppm	
	Response time	180 seconds	
	Full scale value	20,10,10ppm respectively	
	Precision	+/- 0.5 %	
PM ₁₀ and PM _{2.5}	Lower detectable limit	4 µg/m ³ (1-hour average)	1-hour, 24-hour
	Resolution	1 µg/m ³	
	Full scale value	1,000 µg/m ³	
	Scanning time	1 second	

3.2 Passive air pollution sampling

3.2.1 Samplers and handling procedure

Ogawa passive samplers (model 3300) from a supplier in the United States¹⁴ were used to measure period-average NO_x and NO_2 concentrations simultaneously at multiple locations. The Ogawas were selected following an initial review which considered the performance, cost and feasibility of different sampling options. The review also included diffusion tubes and low-cost active samplers, and concluded that the Ogawas would be the most appropriate for the study based on suitability, cost and lead time for delivery. Whilst Ogawas are more expensive than standard diffusion tubes sourced from overseas, they are comparable in price to diffusion tubes from Australian suppliers, and considerably cheaper than active samplers.

The Ogawa samplers measure NO_x and NO_2 with a limit of detection of 0.4 ppb. Samples are typically taken over a 1-2 week period, resulting in an average concentration for the period. Continuous measurements are not available. According to the supplier, tests have demonstrated a good level of comparability between the results from the Ogawa sampler and average measurements from continuous gas analysers. This has also been shown through this study (see Section 5.6).

A schematic of the Ogawa sampler is provided in Figure 11. The sampler is composed of a Teflon cylindrical body with an air inlet at each end. It is possible to sample more than one gas simultaneously because the two inlets are separated by a central solid section in the body of the sampler. In this study, each sampler housed two 14.5 mm-diameter pre-coated cellulose filter pads, one to absorb NO_2 and a second to absorb NO_2 and NO_x , thus allowing the measurement of both NO_2 and NO_x .

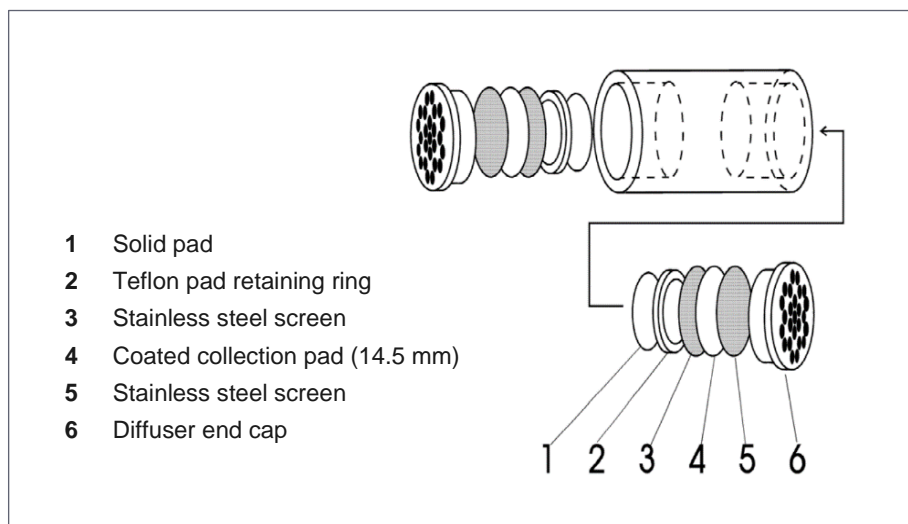


Figure 11: Schematic of the Ogawa sampler

When deployed in the field the body of the sampler is usually mounted on a clip that is housed in a protective PVC outdoor shelter. The shelter protects the sampler from rain and dust contamination. The Ogawa sampler and shelter are pictured *in situ* in Figure 12.

¹⁴ <http://ogawausa.com/>

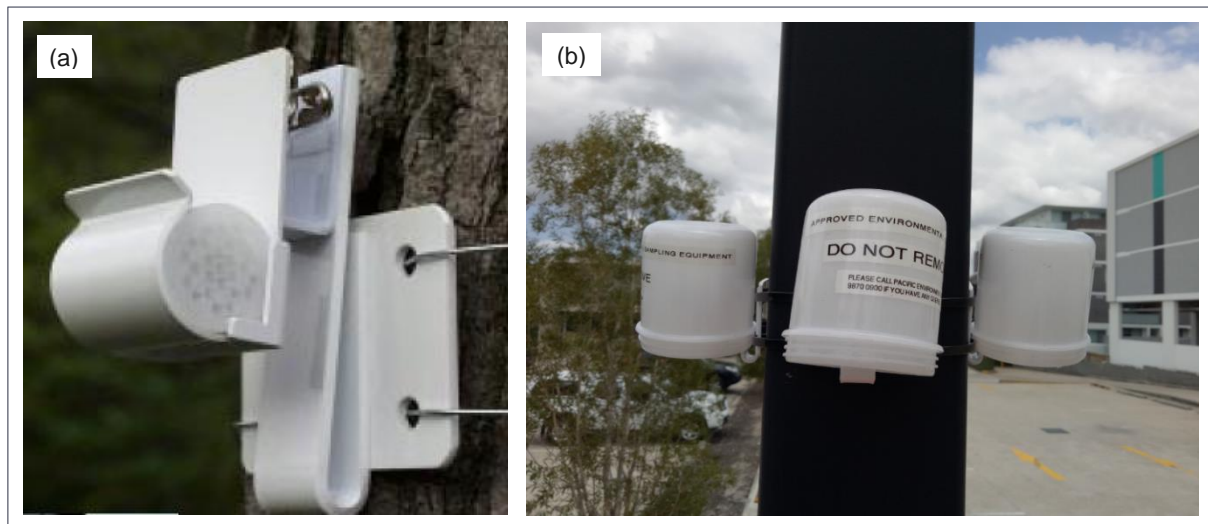


Figure 12: Ogawa passive sampler *in situ*: (a) sampling unit and (b) with shelter attached

As a precaution, the sampling pads were refrigerated before and after deployment in the field. In order to minimise contamination of the filter pads the samplers were assembled and loaded with the filter pads in a clean environment, with the operator wearing latex gloves and using tweezers. All subsequent contact with the samplers was undertaken using latex gloves. The body of each sampler was labelled to clearly distinguish the NO_x and NO_2 sampling ends. All samplers were transported in sealed, labelled containers.

Following exposure, the pads were returned to the supplier for analysis. The analysis of the pads took place in a laboratory using routine analytical procedures to determine the average gas concentration during pad exposure, including a correction for the average temperature and relative humidity over the sample exposure duration.

3.2.2 Sampling locations

The Ogawa samplers were deployed in triplicate at 17 locations over two periods (i.e. two rounds of sampling), as shown in Figure 13 and summarised in Table 3. A third round of sampling was completed at only two locations (Concord Oval and St Lukes Park).

The sampler deployment and collection was undertaken by Pacific Environment.

The sampling locations reflected the objectives of the passive sampling work, and included:

- Co-location with Australian Standard reference analysers. When using passive samplers in the field it is good practice to verify their accuracy by comparing their response with that of reference instruments. The sampler results can then be adjusted accordingly. In this study, Ogawas were co-located with the reference analysers at the Concord Oval and St Lukes Park monitoring stations to cover the high and low ends of the concentration range. The samplers were installed as close as possible to the station gas inlets so that they were measuring the same air as the reference analysers.
- Locations alongside both carriageways of Parramatta Road, around Concord Oval, and between the St Lukes Park and Concord Oval monitoring stations. The samplers were attached to street furniture (traffic lights, sign posts), lamp posts, telegraph poles, fence posts and other structures. Approval for the installation of the samplers was obtained from Roads and Maritime, Ausgrid, Canada Bay Council, and the management of Concord Oval.

The samplers were deployed at a height of around 3 metres above ground level for consistency with the monitoring station gas inlets and to reduce the possibility of theft or vandalism. This is also within the ‘breathing zone’ that is defined for air pollution monitoring¹⁵.

In addition, field blanks were deployed in triplicate during each round of measurements. The field blank samplers and pads were subjected to the same procedures and conditions as the other samplers, but were not exposed to the atmosphere. The results for the field blanks would normally be averaged and subtracted from the concentrations obtained for each exposed pad to give a blank-corrected concentration. However, in this study the blank samples were considered to be erroneous and they were therefore not used. This is explained in Section 5.6.

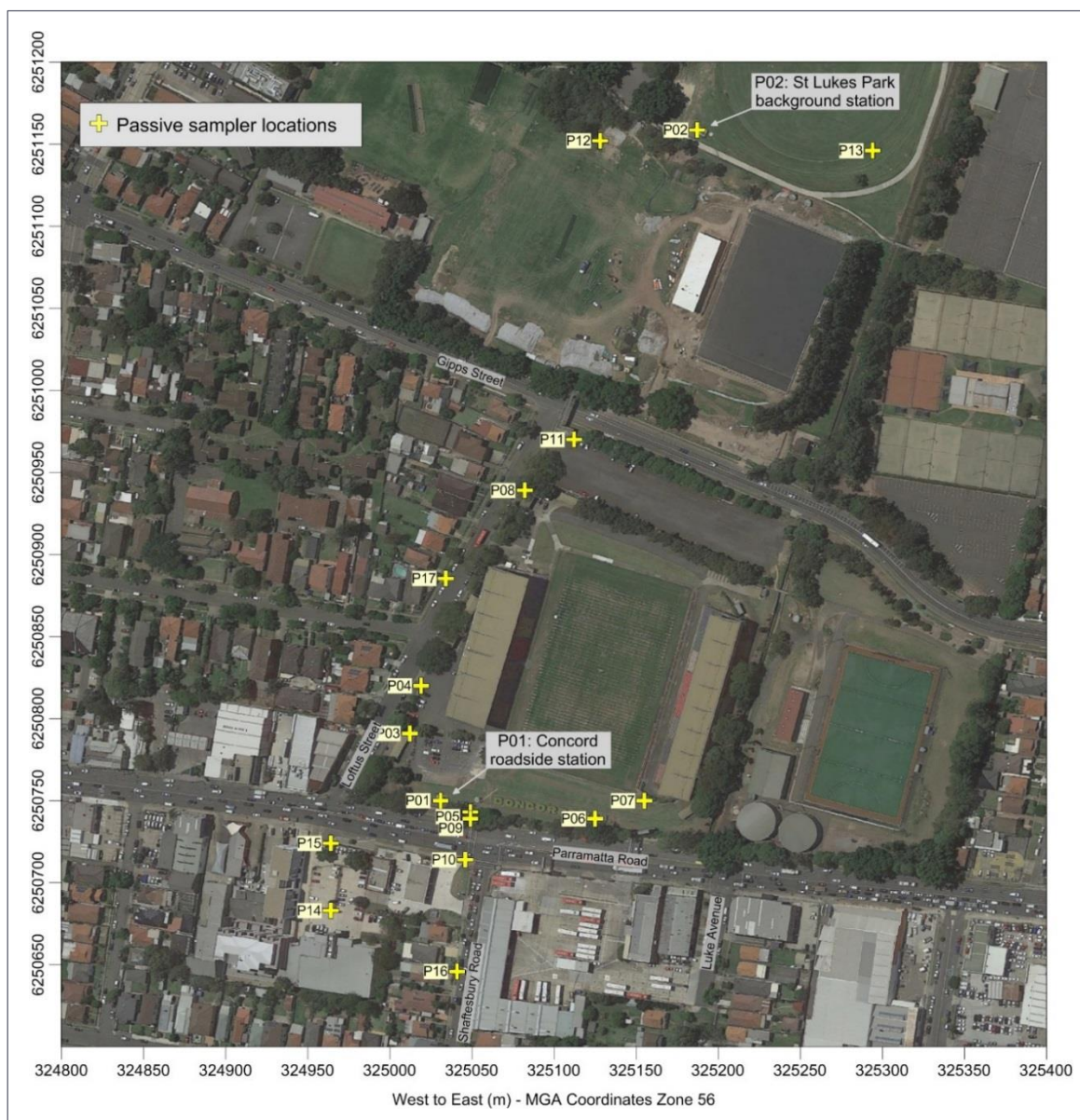


Figure 13: Locations of passive samplers

¹⁵ For example, Annex III.C of EU Directive 2008/50/EC defines the breathing zone as a height between 1.5 and 4 metres.

Table 3: Locations of passive samplers

Code	x (MGA)	y (MGA)	Description
P01	325031	6250750	Concord Oval monitoring station
P02	325187	6251159	St Lukes Park monitoring station
P03	325012	6250791	Lamp post
P04	325019	6250820	Lamp post near entrance gate
P05	325049	6250743	Post attached to disused box in grounds of Concord Oval
P06	325125	6250739	Sign post in grounds of Concord Oval
P07	325155	6250750	Disused metal frame in grounds of Concord Oval
P08	325082	6250939	Lamp post near garage in grounds of Concord Oval
P09	325049	6250739	Traffic signal post near northern kerb of Parramatta Road
P10	325046	6250714	Traffic signal post near southern kerb of Parramatta Road
P11	325112	6250970	Floodlight post near Gipps Street
P12	325128	6251152	Floodlight post, St Lukes Park
P13	325294	6251146	Floodlight post, St Lukes Park
P14	324964	6250683	Lamp post in commercial parking area
P15	324964	6250724	Sign post in commercial parking area
P16	325041	6250646	Telegraph pole near Shaftesbury Road
P17	325034	6250885	Telegraph pole near Loftus Street
Field blanks	325031	6250750	Concord Oval monitoring station

3.2.3 Sampling periods

The time and date of deployment at each sampling location was recorded. The samplers were exposed for three consecutive rounds, of duration 12 days, 15 days and 13 days respectively:

- Round 1: 13 January to 25 January 2017 (at all 17 locations plus a field blank)
- Round 2: 31 January to 15 February 2017 (at all 17 locations plus a field blank)
- Round 3: 15 February to 28 February 2017 (at 2 monitoring stations plus a field blank)

The third round of sampling was included to increase the number of data points available for sampler calibration.

3.2.4 Data checking and processing

The data from the samplers were checked, analysed and interpreted by Pacific Environment. The consistency of the triplicate measurements at each location was examined, and any non-concordant results were rejected. The NO_x concentration for a given location was accepted as being concordant with the other two measurements where the difference between the individual measurement and the median of the three measurements was less than 5 ppb. For NO₂ a value of 2 ppb was applied.

Table 4: Sampling periods

Location code	Round 1				Round 2				Round 3			
	Start date	Start time	End date	End time	Start date	Start time	End date	End time	Start date	Start time	End date	End time
P01	13/01/17	10:00	25/01/17	10:34	31/01/17	08:55	15/02/17	10:06	15/02/17	11:00	28/02/17	10:33
P02	13/01/17	13:38	25/01/17	11:10	31/01/17	09:50	15/02/17	11:50	15/02/17	12:00	28/02/17	11:45
P03	13/01/17	10:53	25/01/17	10:50	31/01/17	09:14	15/02/17	11:15	-	-	-	-
P04	13/01/17	11:01	25/01/17	10:53	31/01/17	09:15	15/02/17	11:15	-	-	-	-
P05	13/01/17	10:16	25/01/17	10:38	31/01/17	09:01	15/02/17	11:05	-	-	-	-
P06	13/01/17	10:26	25/01/17	10:40	31/01/17	09:03	15/02/17	11:07	-	-	-	-
P07	13/01/17	10:33	25/01/17	10:43	31/01/17	09:07	15/02/17	11:10	-	-	-	-
P08	13/01/17	11:23	25/01/17	11:02	31/01/17	09:25	15/02/17	11:30	-	-	-	-
P09	13/01/17	12:13	25/01/17	11:54	31/01/17	10:20	15/02/17	12:10	-	-	-	-
P10	13/01/17	12:08	25/01/17	11:57	31/01/17	10:20	15/02/17	12:25	-	-	-	-
P11	13/01/17	11:32	25/01/17	11:07	31/01/17	10:20	15/02/17	11:35	-	-	-	-
P12	13/01/17	13:15	25/01/17	11:17	31/01/17	09:50	15/02/17	11:30	-	-	-	-
P13	13/01/17	13:30	25/01/17	11:28	31/01/17	10:25	15/02/17	11:30	-	-	-	-
P14	13/01/17	12:41	25/01/17	12:06	31/01/17	10:25	15/02/17	12:40	-	-	-	-
P15	13/01/17	12:44	25/01/17	11:57	31/01/17	10:25	15/02/17	12:40	-	-	-	-
P16	13/01/17	11:52	25/01/17	11:49	31/01/17	10:30	15/02/17	12:30	-	-	-	-
P17	13/01/17	11:15	25/01/17	10:58	31/01/17	09:25	15/02/17	11:20	-	-	-	-
Field blank	13/01/17	08:00	25/01/17	15:00	31/01/17	08:55	15/02/17	10:06	15/02/17	11:00	28/02/17	10:30

3.3 Meteorology

3.3.1 Monitoring station locations

As well as air pollutants, meteorological parameters were also monitored continuously at the Concord Oval and St Lukes Park stations. Four additional meteorological stations were located within the study area: BoM stations at Sydney Olympic Park Archery Centre (Station No. 066212) and Canterbury Racecourse (Station No. 066194), and OEH stations at Rozelle and Chullora. A brief description and photograph (where available) for each meteorological station is given in Table 5. Some potential influences on the measurements are noted in the site descriptions.

Table 5: Meteorological station siting (BoM and OEH stations)

Station	Site description	Photograph and source
BoM Sydney Olympic Park (Archery Centre)	<p>The BoM Sydney Olympic Park (Archery centre) weather station is located at the Archery Centre grounds of Olympic Park.</p> <p>There are no large buildings in the vicinity of the monitoring station, and the closest trees are located approximately 20 metres to the west of the station.</p> <p>The station is located on flat terrain, with a slight dip immediately to the west. The ground elevation at the monitoring station and in the immediate vicinity is approximately 4-5 metres.</p>	 <p>Source: http://www.abc.net.au/radionational/program/offtrack/olympic-park-weather-station/5572982</p>
BoM Canterbury Racecourse	<p>The BoM Canterbury Racecourse weather station is located in a large, open space within Canterbury Racecourse.</p> <p>There are no large buildings or trees in the vicinity of the monitoring station.</p> <p>The area immediately surrounding the station is predominantly flat, with a ground elevation of approximately 5 metres.</p>	 <p>Source: Google Earth Pro accessed 21.08.17</p>
OEH Rozelle	<p>The Rozelle weather station is located in the grounds of Rozelle Hospital, off Balmain Road, Rozelle.</p> <p>The OEH website states that the site does not comply with Australian Standard for siting, as the clear sky angle is <math><120^\circ</math> due to trees within 20 metres to the west of the station.</p> <p>The station is located on a hill, with a steep incline going from approximately 22 metres ground elevation at the station site to 5 metres below.</p>	 <p>Source: Damon Roddis, 2015</p>

Station	Site description	Photograph and source
OEH Chullora	<p>The Chullora weather station is located in the grounds of the Southern Sydney TAFE, Worth Street, Chullora</p> <p>The OEH website states that the site does not comply with Australian Standard for siting, as the clear sky angle is <math><120^\circ</math> due to trees within 20 metres to the northeast and east of the station.</p> <p>The station is located at a ground elevation of approximately 37 metres, with a slight incline immediately to the north reaching approximately 33 metres at the base.</p>	 <p>Source: Google Earth Pro accessed 21.08.17</p>

3.3.2 Parameters and methods

For the two M4 East meteorological stations used in the study (Concord Oval and St Lukes Park), a summary of all parameters, units of measurement, instrumentation and measurement techniques is provided in Table 6. The measurements were compliant with Australian Standard AS/NZS 3580.14-2011.

Table 6: Meteorological parameters and measurement methods (M4 East stations)

Parameter ^(a)	Units	Instrument	Measurement technique
Temperature	Degrees Celsius (°C)	Lufft Compact Weather Station (WS500-UMB)	Negative temperature coefficient (NTC) thermistor
Pressure	Millimetre of mercury (mm Hg)	Lufft Compact Weather Station (WS500-UMB)	Micro-electromechanical systems (MEMS) capacitive
Relative humidity	Percent (%)	Lufft Compact Weather Station (WS500-UMB)	Capacitive
Wind speed	Metres per second (m/s)	Lufft Compact Weather Station (WS500-UMB)	Ultrasonic anemometer
Wind direction	Degrees (°)	Lufft Compact Weather Station (WS500-UMB)	Ultrasonic anemometer
Rainfall	Millimetres (mm)	Lufft Rain Sensor (WTB100)	Tipping bucket rain gauge
Solar radiation	Watts per square meter (W/m ²)	Kipp & Zonen Pyranometer	Actinometer

(a) Meteorological measurements were made at a height of 10 m at the St Lukes Park background site. At the Concord Oval roadside site the meteorological measurements were made at a height of 2-3 m.

For the BoM and OEH stations the meteorological parameters, units of measurement, instrumentation and measurement techniques are provided in Table 7. The OEH stations also measured background air pollution. However, the air pollution measurements were not considered in the study as the stations were well outside the dispersion model domain and the focus was on near-road air quality.

There were some differences between the various meteorological sites in terms of the equipment used, and the most important of these probably related to the measurement of wind speed and direction. Notably, ultrasonic anemometers were used at the M4 East and OEH stations, whereas mechanical (cup-and-vane)

anemometers were used at the BoM stations. Because mechanical anemometers use moving parts, the measurements are affected by the start-up inertia of the cup and vane. For example, the Synchrotac SYN732 wind speed transducer used at the BoM sites has a starting threshold wind speed of 0.7 m/s. Mechanical instruments will therefore not always represent rapid changes in wind speed and direction. In contrast, an ultrasonic anemometer is not affected its inertia; it will measure a change in wind direction or a gust immediately and in real time.

Table 7: Meteorological parameters and measurement methods (BoM and OEH stations)

Station	Parameter	Instrument	Measurement technique
BoM stations	Temperature	Rotronics MP101A-T4-W4W	N/A
	Pressure	-	-
	Relative humidity	Rotronics MP101A-T4-W4W	N/A
	Wind speed	Synchrotac SYN732/706	Cup and vane anemometer
	Wind direction	Synchrotac SYN732/706	Cup and vane anemometer
	Rainfall	Rimco 7499	Tipping bucket rain gauge
	Solar radiation	-	-
OEH stations	Temperature	Vaisala HMP 155	HUMICAP polymer sensor
	Pressure	-	-
	Relative humidity	Vaisala HMP 155	HUMICAP polymer sensor
	Wind speed	Met One Model 50.5	Ultrasonic anemometer
	Wind direction	Met One Model 50.5	Ultrasonic anemometer
	Rainfall	-	-
	Solar radiation	Middleton Solar EQ08-E	Blackened thermal sensor

3.4 Roads and traffic

3.4.1 Road links

The main roads in the dispersion model domain - which were taken to be those with more than 1,500 vehicles per day - were included in the dispersion model. These road links are shown in Figure 14, and their characteristics are summarised in Table 8. The same road links were used in both the CAL3QHCR and GRAL models.

Each road link was defined at a level of detail that reflected its likely importance in terms of pollutant concentrations in the domain. For example, Parramatta Road was split into multiple links to allow each lane of traffic and direction of travel to be represented separately. Separate links were used to represent the direction of travel on Gipps Street and Shaftesbury Road. All other roads were represented as single links (i.e. with combined two-way traffic).

Where direction of travel was taken into account, the gradient of the road link was estimated using height and length data from Google Earth. Road widths were also estimated using Google Earth. On several roads, parked cars occupied the part of the road near to the kerb. These areas were excluded from the road width estimates (i.e. on the 'active' road sections were measured), again taken from Google Earth.

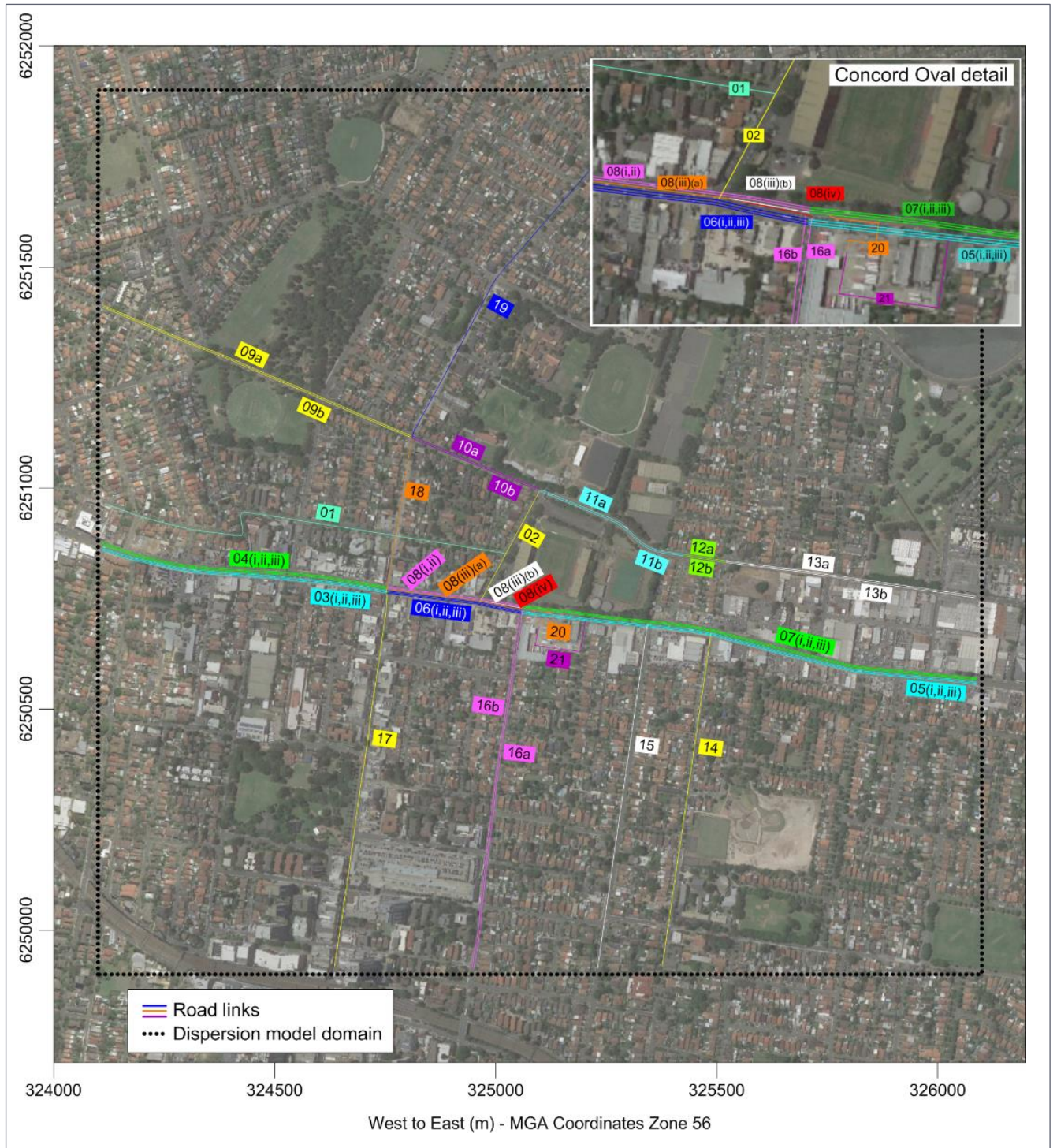


Figure 14: Locations of modelled road links (inset shows more detail close to Concord Oval monitoring station)

Table 8: Characteristics of road links modelling in GRAL

Link number	Road	Section	Direction	Lane	EPA road type	Gradient (%)	Width (m)
01	Burton Street	Between Loftus St and Coles St	WB+EB	Total	Residential	-	6.5
02	Loftus Street	Between Parramatta Rd and Gipps St	NB+SB	Total	Residential	-	8.0
03(i)	Parramatta Road	West of Burwood Rd	WB	Lane 1	Arterial	0.1%	2.6
03(ii)				Lane 2		0.1%	2.8
03(iii)				Lane 3		0.1%	2.8
04(i)	Parramatta Road	West of Burwood Rd	EB	Lane 1	Arterial	-0.1%	2.7
04(ii)				Lane 2		-0.1%	2.8
04(iii)				Lane 3		-0.1%	2.8
05(i)	Parramatta Road	East of Shaftesbury Rd	WB	Lane 1	Arterial	0.0%	2.6
05(ii)				Lane 2		0.0%	2.8
05(iii)				Lane 3		0.0%	2.8
06(i)	Parramatta Road	Shaftesbury Rd to Burwood Rd	WB	Lane 1	Arterial	3.3%	2.6
06(ii)				Lane 2		3.3%	2.8
06(iii)				Lane 3		3.3%	2.8
07(i)	Parramatta Road	East of Shaftesbury Rd	EB	Lane 1	Arterial	0.0%	2.4
07(ii)				Lane 2		0.0%	2.8
07(iii)				Lane 3		0.0%	2.8
08(i)	Parramatta Road	Burwood Rd to Shaftesbury Rd	EB	Lane 1	Arterial	-3.3%	2.2
08(ii)				Lane 2		-3.3%	2.8
08(iii)(a)	Parramatta Road	Loftus St to Shaftesbury Rd	EB	Lane 3 ^(a)	Arterial	-1.1%	2.8
08(iii)(b)	Parramatta Road	Burwood Rd to Loftus St	EB	Lane 3 ^(a)	Arterial	-4.2%	2.8
08(iv)	Parramatta Road	Filter lane to Shaftesbury Rd	EB	Lane 4	Arterial	-1.3%	3.1
09a	Gipps Street	West of Burwood Rd	EB	Total	Residential	-0.3%	5.8
09b	Gipps Street	West of Burwood Rd	WB	Total	Residential	0.3%	5.8
10a	Gipps Street	Between Loftus St and Burwood Rd	EB	Total	Residential	-2.8%	3.2
10b	Gipps Street	Between Burwood Rd and Loftus St	WB	Total	Residential	2.8%	3.2
11a	Gipps Street	Between Loftus St and Taylor St	EB	Total	Residential	-0.3%	3.3
11b	Gipps Street	Between Taylor St and Loftus St	WB	Total	Residential	0.3%	3.3
12a	Queens Road	Between Taylor St and Walker St	EB	Total	Residential	4.2%	3.2
12b	Queens Road	Between Walker St and Taylor St	WB	Total	Residential	-4.2%	3.2
13a	Queens Road	East of Walker St	EB	Total	Residential	-0.9%	3.0
13b	Queens Road	East of Walker St	WB	Total	Residential	0.9%	3.0
14	Cheltenham Road	South of Parramatta Rd	NB+SB	Total	Residential	-	5.5
15	Lucas Road	South of Parramatta Rd	NB+SB	Total	Residential	-	5.8
16a	Shaftesbury Road	South of Parramatta Rd	SB	Total	Residential	2.9%	4.5
16b	Shaftesbury Road	South of Parramatta Rd	NB	Total	Residential	-2.9%	4.5
17	Burwood Road	South of Parramatta Rd	NB+SB	Total	Residential	-	8.5
18	Burwood Road	Between Parramatta Rd and Gipps St	NB+SB	Total	Residential	-	7.0
19	Burwood Road	Between Gipps St and Crane St	NB+SB	Total	Residential	-	7.0
20	Parramatta Road	Filter lane to bus depot	EB	Total	Arterial	0.0%	3.1
21	Luke Avenue	Entrance and exit to bus depot	NB+SB	Total	Residential	-	7.5

(a) This link was split into two section to ensure conservation of traffic at the filter for Shaftesbury Road

3.4.2 Traffic data

The traffic volume, composition and speed for the road links in the dispersion model domain were provided by Roads and Maritime, and were taken from the sources described below. The data were processed by Pacific Environment to provide suitable inputs for the emission model. Any assumptions that were made are also stated below.

3.4.2.1 SCATS

Traffic volumes by lane and by hour at specific junctions and for the whole dispersion model evaluation period were obtained from the Sydney Coordinated Adaptive Traffic System (SCATS)¹⁶. SCATS operates in real-time, adjusting signal timings in response to variation in traffic demand and system capacity. It measures traffic volumes and flows at intersections mainly using inductive loop detectors buried in the road surface. This information is then used to automatically adapt operation of traffic signals on an area-wide basis. The junctions for which SCATS data were obtained are identified in Figure 15.

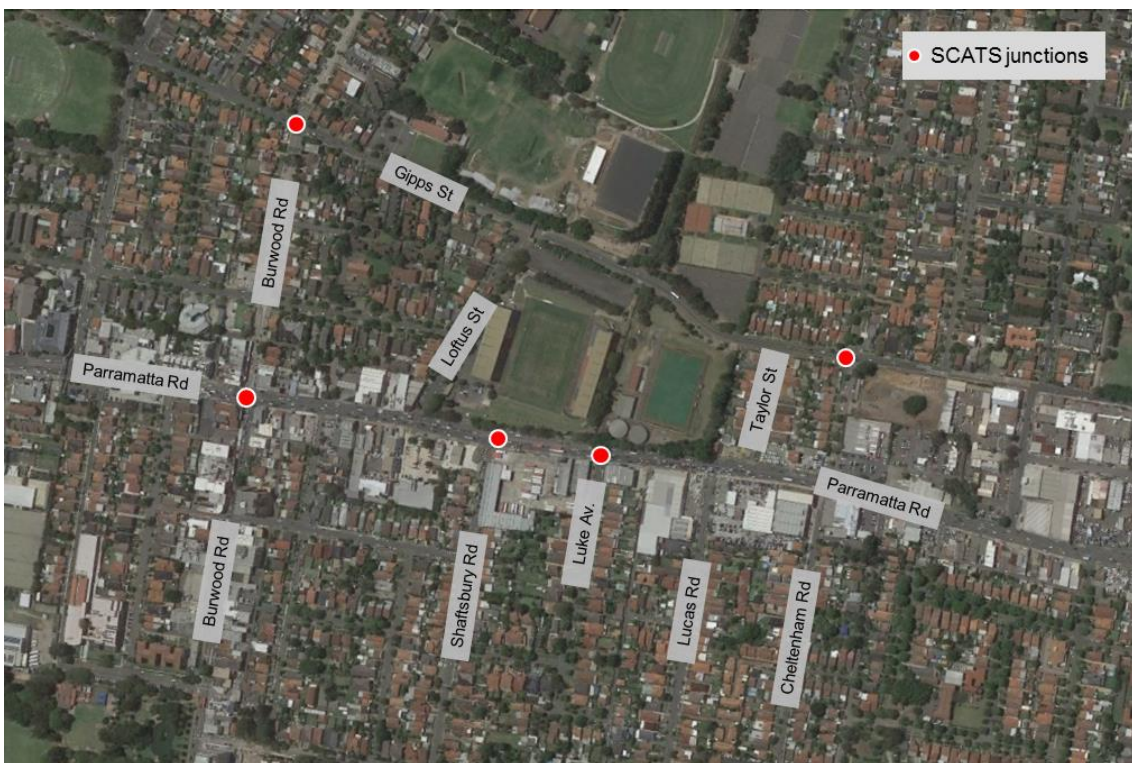


Figure 15: SCATS locations

3.4.2.2 Traffic surveys

Traffic surveys were undertaken specifically for the study at seven locations to obtain composition data: four video camera sites and three automatic tube count sites (Figure 16, Table 9). The video cameras and pneumatic tubes (Metrocounter) were installed on 21 November, with timers used on the video equipment to ensure recording on the correct days. After equipment retrieval, all data files were backed up and checked for quality assurance. The video survey at Shaftesbury Road was initially undertaken between 23 and 26

¹⁶ http://www.qtcts.com.au/media/512152-RTA532_SCATS_A4_Product_Brochure_07.pdf

November. However, some data were lost to equipment failure and therefore the survey was repeated at this site between 14 and 17 December.

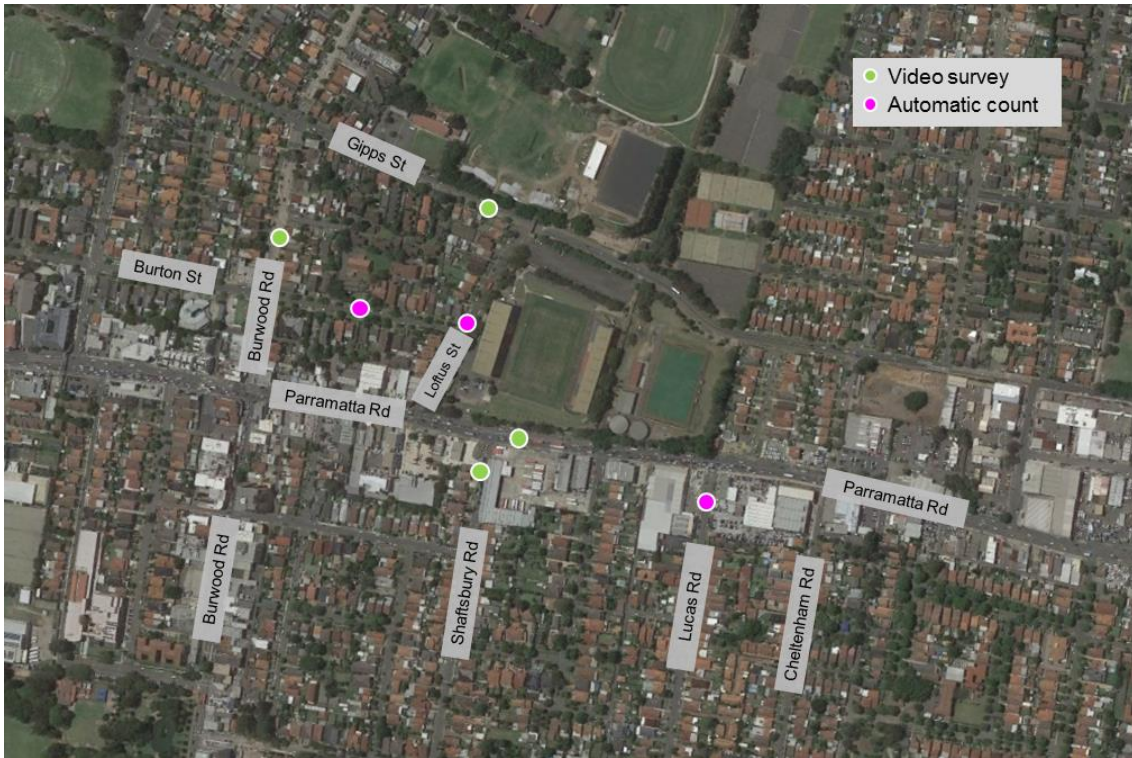


Figure 16: Traffic survey locations

Table 9: Traffic survey summary

Site number	Survey type	Road	Direction	Start date	End date	Time resolution	Vehicle classes	Speed
V01	Video	Parramatta Road	EB/WB	23/11/2016	26/11/2016 ^(a)	15 minutes	6 ^(c)	No
V02	Video	Shaftesbury Road	NB/SB	14/12/2016	17/12/2016 ^(b)	15 minutes	6 ^(c)	No
V03	Video	Burwood Road	NB/SB	23/11/2016	26/11/2016 ^(a)	15 minutes	6 ^(c)	No
V04	Video	Gipps Street	EB/WB	23/11/2016	26/11/2016 ^(a)	15 minutes	6 ^(c)	No
T01	Tubes	Loftus Street	NB/SB	22/11/2016	29/11/2016	15 minutes	12 ^(d)	Yes
T02	Tubes	Burton Street	EB/WB	22/11/2016	29/11/2016	15 minutes	12 ^(d)	Yes
T03	Tubes	Lucas Road	NB/SB	22/11/2016	29/11/2016	15 minutes	12 ^(d)	Yes

(a) No survey on 25/11/2016

(b) No survey on 16/12/2016

(c) Cars, light commercial vehicles, rigid HGVs, articulated HGVs, buses, motorcycles

(d) Austroads 94 classification

For the roads where tubes and video cameras were deployed, average hourly weekday and weekend profiles for traffic volume and composition were determined. For the same roads, these profiles were then applied to all days during the survey period. Where SCATS data were available, these were used to determine traffic volume by lane in preference to the survey data.

3.4.2.3 Google Maps Distance Matrix API

Average traffic speeds between specific node points on the network were estimated using the Google Maps Distance Matrix application programming interface (API). This is a web-based service that provides travel distance and time for a matrix of origins and destinations, based on the recommended route between the start and end points. The calculations are based on crowd-sourced GPS data transmitted to Google by road users. This information is then processed using proprietary algorithms to ensure that speed and location information is anonymous, and that it excludes anomalies such as frequently stopping vehicles.

The start and end points used in the study are given in Figure 17. The distance and time data were used to determine average traffic speed for each road link used in the dispersion models, including by direction of travel. Data were obtained for the periods between 18/11/2016 to 22/12/2016, and between 2/2/2017 and 28/2/2017. These two sets of data were used to represent the November/December and January/February periods of the study respectively. The data were obtained as 15-minute averages, and were aggregated to give 1-hour averages.

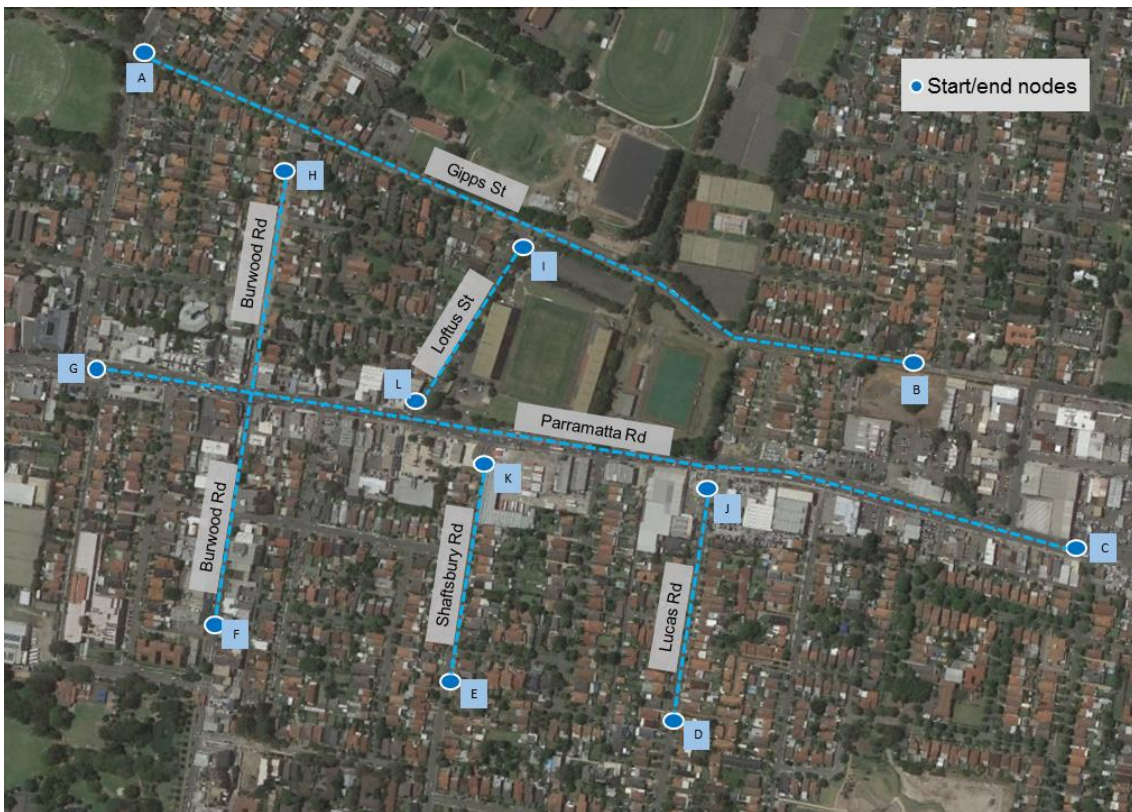


Figure 17: Google Maps Distance Matrix nodes

On analysis, the speed data for Parramatta Road for the period between 15 and 28 February were found to be unusually low. Enquiries with Google revealed that there was an edit on the road segment geometry on 15 February to permit a better match of the road alignment with satellite imagery. The data for this period were therefore rendered invalid.

Any missing hours were filled using an average speed profile for the corresponding month and day type (weekday or weekend).

3.4.2.4 Other information

City of Canada Bay Council was contacted to establish whether there had been any events at Concord Oval that could have led to high levels of vehicular activity in the vicinity, and in particular in the car parks adjacent to Parramatta Road and Gipps Street. No major events were reported, and the Council confirmed that there were no games at Concord Oval during the summer months. However, it was noted that the Gipps Street car park was being leased by WestConnex for staff and contractors.

4 Modelling methodology

4.1 Overview

The modelling work consisted of the following main elements:

- Emission modelling and sensitivity testing to determine the extent to which the emission model outputs were influenced by changes in specific inputs.
- Meteorological model evaluation. This involved a comparison between the GRAMM (version: July 2016) predictions and the meteorological measurements at locations in the meteorological model domain, with systematic changes to model inputs and settings, and a comparison between GRAMM and CALMET (version: 6.334).
- Dispersion model evaluation. This involved a comparison between the GRAL (version: August 2016) predictions (primarily for NO_x) with measurements at locations in the dispersion model domain, again with systematic changes to model inputs and settings, and comparisons between GRAL and CAL3QHCR (version: 2.0).

4.2 Emission modelling

4.2.1 Model set-up

A link-based emissions inventory was developed for the main roads in the dispersion model domain, and this was used in all dispersion model testing. Pacific Environment developed an in-house tool which could be used to calculate emissions for multiple road links and could be readily adapted for processing traffic data. The main aspects of model set-up related to the following:

- Emission factors. These included¹⁷:
 - Hot exhaust emissions. These are the emissions generated once vehicle engine and emission-control equipment are at their full operational temperatures.
 - Cold-start emissions. These are the emissions generated before vehicle engine and emission-control equipment reach their full operational temperatures.
 - Non-exhaust emissions of particulate matter, generated by abrasion processes such as tyre wear and brake wear.
- Fleet data. Vehicle age and technology level (i.e. the sophistication of the engine and emission-control equipment that is fitted to a vehicle) has a large influence on emission rates. This information is difficult to obtain for vehicles in local studies, and therefore the distributions of vehicle age and technology level from a NSW dataset were built into the emission model.

These aspects are described in the following Sections.

¹⁷ VOCs are also released through the evaporation of fuel. The calculation of evaporative emissions is relatively complex, as it requires an understanding of temperature profiles, fuel vapour pressure, fuel composition, and operational patterns. Moreover, it is difficult to link evaporative emissions to traffic activity on specific road links, as running losses are only one component (for example, evaporative emissions also occur when vehicles are stationary). For these reasons, evaporative emissions were excluded from the model. Ambient concentrations of VOCs are also very low, and were not considered in the modelling.

4.2.1.1 Emission factors

For hot running emissions, the NSW EPA emission inventory model was used, as it is specifically designed for use in NSW and takes into account the characteristics of the state's vehicle fleet. The inventory was updated in 2012¹⁸, with significant refinements to the road transport methodology. The emission factors allow for the deterioration in emissions performance with mileage, the effects of tampering or failures in emission-control systems, and the use of ethanol in petrol. They were derived using an extensive database of measurements on Australian vehicles. Emission factors have been provided by EPA for heavy-duty vehicles with and without the implementation of the Euro VI regulation. In line with the WestConnex EIS methodology, only the latter were used in this study.

The method involved the use of matrices of 'base composite' emission factors for the following cases:

- Six pollutants (CO, NO_x, NO₂, PM₁₀, PM_{2.5}, THC). However, only the results of the emission calculations for NO_x were used in this study^{19,20}.
- Nine vehicle types, as summarised in Table 10. The composite emission factor for each vehicle type took into account VKT by age and the emission factors for specific emission standards.

Table 10: Vehicle types in the NSW EPA emissions model

Code	Vehicle type	Vehicles included
CP	Petrol car ^(a)	Petrol car, 4WD ^(e) , SUV ^(f) and people-mover, LPG ^(g) car/4WD
CD	Diesel car ^(a)	Diesel car, 4WD, SUV and people-mover
LCV-P	Petrol LCV ^(b)	Petrol light commercial vehicle < 3.5 tonnes GVM ^(h)
LCV-D	Diesel LCV	Diesel light commercial vehicle < 3.5 tonnes GVM
HDV-P	Petrol HDV ^(c)	Petrol heavy commercial vehicle < 3.5 tonnes GVM
RT	Diesel rigid HGV ^(d)	Diesel commercial vehicle 3.5 t < GVM < 25 t
AT	Diesel articulated HGV	Diesel commercial vehicle > 25 tonnes GVM
BusD	Diesel bus	Diesel bus > 3.5 tonnes GVM
MC	Motorcycle	Powered two-wheel vehicle

(a) Referred to as 'passenger vehicle' in the inventory

(b) LCV = light commercial vehicle

(c) HDV = heavy-duty vehicle

(d) HGV = heavy goods vehicle

(e) 4WD = four-wheel drive

(f) SUV = sports-utility vehicle

(g) LPG = liquefied petroleum gas

(h) GVM = gross vehicle mass

¹⁸ <http://www.environment.nsw.gov.au/resources/air/120256AEITR7OnRoadMobile.pdf>

¹⁹ Ambient concentrations of NO₂ were determined using an empirical method. However, primary NO₂ emissions can still be calculated using the model when required. These are based on NO₂:NO_x ratios ($f=NO_2$) for various vehicle types and emission standards in the COPERT model (Pastramas et al., 2014). A recent update of the evidence for vehicles in Sydney was provided by Boulter and Bennett (2015), and it was noted that there has been a gradual increase in $f=NO_2$ in recent years for highways, from less than 10% before 2008 to around 15% in 2014. It was also concluded that the approach of incorporating the European values for $f=NO_2$ in models for Sydney produced a satisfactory agreement with measurements.

²⁰ Although not used in the study, non-exhaust PM₁₀ and PM_{2.5} emissions were calculated using the method in the EMEP/EEA Air Pollutant Emission Inventory Guidebook (EEA, 2016), and included tyre wear, brake wear and road surface wear. Emission factors (in g/km) were provided for each vehicle type, road type and year. Information was required for parameters such as vehicle load and number of axles, and the assumptions used for vehicles in the NSW GMR are described in NSW EPA (2012b).

- Five road types (residential, arterial, commercial arterial, commercial highway, highway/ freeway), to allow for differences in traffic composition and driving patterns. However, the only road types included in the study were residential and arterial (see Table 8)
- Nine model years (2003, 2008, 2011, 2016, 2021, 2026, 2031, 2036 and 2041). The year defines the composition of the fleet for each type of vehicle, allowing for technological changes. The base year for the inventory is 2008, and therefore the data for years after 2008 are projections. The version of the model developed by Pacific Environment interpolated between years.

The emission factor for a given traffic speed was calculated as follows:

$$EF_{HotSpd} = EF_{HotBasSpd} \times \frac{SCF_{Spd}}{SCF_{BasSpd}}$$

Where:

- EF_{HotSpd} is the composite emission factor (in g/km) for the defined speed
- $EF_{HotBasSpd}$ is the base composite emission factor (in g/km) for the base speed
- SCF_{Spd} is the speed-correction factor for the defined speed
- SCF_{BasSpd} is the speed-correction factor for the base speed

Each base composite emission factor was defined for a VKT-weighted average speed (the base speed) associated with the corresponding road type. Dimensionless correction factors were then applied to the base emission factors to take into account the actual speed on a road. Each speed-correction factor was a 6th order polynomial: $SCF = aV^6 + bV^5 + \dots + fV + g$, where **a** to **g** are constants and **V** is the speed in km/h. The speed correction factors were valid up to 110 km/h for LDVs, and up to 100 km/h for HDVs.

Correction factors were also applied to allow for the effects of road gradient on hot running emissions. NSW EPA did not develop gradient correction factors for the inventory, and therefore these were determined using the emission rates for speed-gradient combinations in PIARC (2012). For each gradient and speed, the gradient correction factor was determined by dividing the corresponding PIARC emission rate by the emission rate for zero gradient.

Cold-start emissions were calculated by applying adjustments to the base hot emission factors to represent the extra emissions which occur during 'cold running'. The adjustments took into account the distance driven from the start of a trip, the parking duration, and the ambient temperature. Cold-start emissions were only calculated for light-duty vehicles, with the amount of 'cold running' being dependent on the road type.

4.2.1.2 Fleet data

In order to combine the emission factors in the models with traffic data, information was also required on the following:

- The fuel split (petrol/diesel) for cars. This was assumed to be the same for all road types.
- The fuel split (petrol/diesel) for LCVs. This was also assumed to be the same for all road types.
- The sub-division of HDVs into rigid HGVs, articulated HGVs and buses. This was dependent on road type. For example, the proportion of HGVs on major roads is typically higher than that on minor roads.

The fuel splits for cars and LVCs were taken from a Roads and Maritime fleet model that was developed to support the calculation of in-tunnel emissions in the WestConnex M4-M5 Link project (O’Kelly, 2016).

The Roads and Maritime fleet model did not differentiate between different types of road. For the sub-division of traffic the default traffic mix information provided by EPA was therefore used. The default traffic mix profiles were derived from state-level statistics. Because the study straddled 2016 and 2017, an average traffic mix for the two years was used in the emission calculations (Table 11).

Table 11: Default traffic mix by road type (average of 2016 and 2017)

Road type	Proportion of traffic (%)								
	CP	CD	LCV-P	LCV-D	HDV-P	RT	AT	BusD	MC
Residential	69.8	10.1	6.1	9.1	0.0	2.8	0.8	0.6	0.5
Arterial	67.0	9.7	6.9	10.4	0.0	3.8	1.2	0.5	0.5

The emission model was also run separately for the years 2016 and 2017 to reflect the changes in emission factors, and the results from the two runs were averaged for input into the dispersion models.

4.2.2 Weekday emission profiles

The emission data were simplified for use in the dispersion models. For each road link, this involved the development of a diurnal (24-hour) emission profile for an average weekday. The average weekday profile was then applied every day of the modelling period, including Saturdays and Sundays. The average weekday emission profiles were examined separately for November, December, January and February, and only some minor differences were identified. These were taken into account using monthly scaling/modulation factors in the dispersion models.

4.2.3 Model evaluation

The performance of the emission model was not evaluated separately as part of this study. Indeed, this would not have been possible within the scope of the study and for the range of conditions being modelled. However, the accuracy of the EPA model (including EMEP for non-exhaust PM) in representing vehicle emissions (CO, NO_x, NO₂, PM₁₀ and PM_{2.5}) has previously been investigated using measurements from the ventilation outlets of the Lane Cove Tunnel during October and November 2013, as described by Boulter and Manansala (2014). It was found that, for the conditions in the tunnel (generally free-flow traffic, typical speed of 80 km/h), the model overestimated emissions by a factor of between 1.7 and 3.3, depending on the pollutant. This overestimation is likely to be due, at least in part, to the over-prediction built into the PIARC gradient factors, as well as other conservative assumptions, and the tunnel environment itself affecting emissions. The piston effect and any forced ventilation in the direction of the traffic flow may combine to produce an effective tail wind that reduces aerodynamic drag on the vehicles in the tunnel (John et al., 1999; Corsmeier et al., 2005). The performance of the model for open roads and lower speeds – such as those in the study – has not been tested. It is therefore difficult to infer the emission model performance in the study.

4.2.4 Traffic data

The collection of traffic data for the main roads in the dispersion model domain was described in Section 3.4. Some further steps were required to convert the traffic data into a suitable format for each road link the

emission modelling, which was undertaken for each hour of the dispersion model evaluation period (November 2016 to February 2017). An overview of the traffic data used for each road is given in Table 12.

Table 12: Processing of traffic data for road links for modelling in GRAL

Link number	Road	Traffic volume	Traffic composition	Traffic speed
01	Burton Street	Tubes. Average 24-hour WD/WE profiles repeated	Tubes (average 24-hour profile)	No data available. Assumed 30 km/h for all periods.
02	Loftus Street	Tubes (average 24-hour profile)	Tubes (average 24-hour profile)	No data available. Assumed 30 km/h for all periods.
03(i)	Parramatta Road	As link 6(i)	As link 6(i)	Google Maps API. Assumed to be same for all lanes.
03(ii)		As link 6(ii)	As link 6(ii)	
03(iii)		As link 6(iii)	As link 6(iii)	
04(i)	Parramatta Road	SCATS	Video (average 24-hour profile)	Google Maps API. Assumed to be same for all lanes.
04(ii)		SCATS		
04(iii)		SCATS		
05(i)	Parramatta Road	SCATS	Video (average 24-hour profile)	Google Maps API. Assumed to be same for all lanes.
05(ii)		SCATS		
05(iii)		SCATS		
06(i)	Parramatta Road	SCATS	Video (average 24-hour profile)	Google Maps API. Assumed to be same for all lanes.
06(ii)		SCATS		
06(iii)		SCATS		
07(i)	Parramatta Road	SCATS	Video (average 24-hour profile)	Google Maps API. Assumed to be same for all lanes.
07(ii)		SCATS		
07(iii)		SCATS		
08(i)	Parramatta Road	SCATS	Video (average 24-hour profile)	Google Maps API. Assumed to be same for all lanes.
08(ii)		SCATS		
08(iii)(a)		SCATS		
08(iii)(b)		SCATS, calculated as 08(iii)(a) + 08(iv)	Video (average 24-hour profile)	Google Maps API. Assumed to be same for all lanes.
08(iv)	Parramatta Road	SCATS	Assumed same as link 16a	Assumed to be 20 km/h for all periods.
09a	Gipps Street	SCATS	As 10a	Google Maps API.
09b	Gipps Street	Assumed same as 9a	As 10b	
10a	Gipps Street	SCATS	Video (average 24-hour profile)	Google Maps API.
10b	Gipps Street	SCATS		
11a	Gipps Street	SCATS	As 10a	Google Maps API.
11b	Gipps Street	SCATS	As 10b	
12a	Queens Road	SCATS	As 10a	Google Maps API.
12b	Queens Road	SCATS	As 10b	
13a	Queens Road	SCATS	As 10a	Google Maps API.
13b	Queens Road	SCATS	As 10b	
14	Cheltenham Road	As Link 15	As Link 15	Assumed same profile as link 15
15	Lucas Road	Tubes (average 24-hour profile)	Tubes (average 24-hour profile)	Google Maps API.

Link number	Road	Traffic volume	Traffic composition	Traffic speed
16a	Shaftesbury Road			Google Maps API.
16b	Shaftesbury Road			Google Maps API.
17	Burwood Road			Google Maps API.
18	Burwood Road	SCATS	Video (average 24-hour profile)	Google Maps API.
19	Burwood Road	SCATS	As link 18	Assumed average of links 17 and 18.
20	Parramatta Road	SCATS	Assumed to be buses only	Assumed to be 20 km/h for all periods.
21	Luke Avenue	SCATS	Assumed to be buses only	Assumed to be 20 km/h for all periods.

4.2.5 Sensitivity testing

Whilst most of the work in the study focussed on the effects of changing GRAMM and GRAL parameters on model predictions, it was also considered important to understand the extent to which the emission model outputs (NO_x only) would typically be influenced by changes in specific inputs.

The traffic volume, composition and speed are the main inputs into the calculation of vehicle emission rates, but it is often the case that the traffic data are coarser than would be desirable (e.g. in terms of composition or time period), incomplete, or based on assumptions. Errors in the traffic inputs therefore result in errors in the emission modelling. For some parameters the relationships between the traffic and emission errors are non-linear (e.g. for speed), whereas in other cases they are linear. For example, an error in traffic volume will result in a directly proportional error in emissions from the network. Traffic volume was therefore not considered in this part of the work. The parameters investigated were:

- Road type, using a default traffic mix for each road type
- Road type, using the same traffic mix for all road types
- Road gradient
- Traffic speed
- The proportion of HDVs in the traffic
- The inclusion of cold start emissions

4.3 Meteorological modelling

This Section describes the general set-up of CALMET and GRAMM. Specific aspects of the GRAMM set-up were investigated in the study, and these are explained in Section 4.5. However, it was not possible to test the effects of all model settings and inputs. For example, it was assumed that the highest available terrain resolution would tend to be used in any assessment, and therefore the effects of terrain resolution were not tested. Similarly, it was assumed that a land use file would be used in any assessment, and therefore the effects of other land use assumptions were not examined.

4.3.1 CALMET

For CALMET the cloud amount and height were sourced from the closest available BoM hourly observation site: Sydney Airport AWS, located approximately 10.5 km to the south-east of the centre of the domain. Upper air information was incorporated through the use of prognostic 3D data extracted from The Air Pollution Model (TAPM) (Hurley, 2008). TAPM was also used to fill in any gaps in the observational data. The TAPM and CALMET domains are shown in Figure 18.

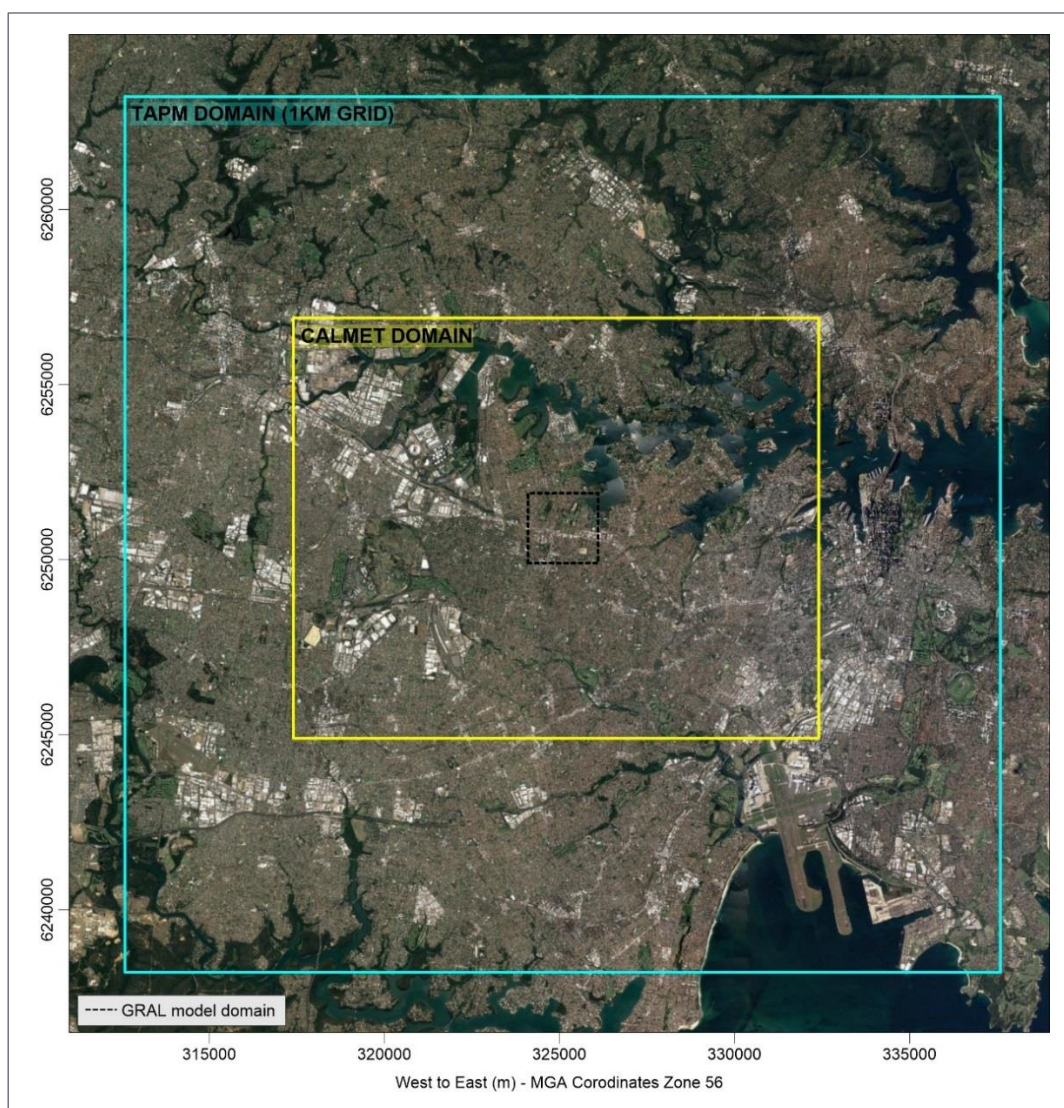


Figure 18: CALMET and TAPM domains

Land use for the model domain was determined from aerial photography (Google Earth) using the land use creator tool in the CALPUFF View software. This software uses the USGS (United States Geological Survey) classification system which are generalised into first and second levels where, Level 1 categories are general area types (e.g. urban, forest land etc.) and Level 2 categories are specific area types (e.g. residential, deciduous forest etc.). Terrain for the modelling was sourced from NASA Shuttle Radar Topographic Mission (SRTM) data. SRTM data for Australia are sampled at one arc second resulting in an approximate resolution

of 30 metres. Further details of the set-up used for TAPM and CALMET - including inputs and the options selected for key model settings - are provided in Table 13, Table 14 and Table 15.

Table 13: TAPM set-up parameters

Parameter	Setting
Model version	4.0.4
Number of grids (spacing)	4 (30 km, 10 km, 3 km, 1 km)
Number of horizontal grid points	25 x 25
Vertical grids/vertical extent	35 / 8,000 m
Terrain and land-use	Default TAPM values based on land-use and soils data sets from Geoscience Australia and the US Geological Survey, Earth Resources Observation Systems (EROS) Data Center Distributed Active Archive Center (EDC DAAC)
Centre of analysis (local coordinates)	Centre of grid domain (325.087, 6250.720 km)

Table 14: CALMET set-up

Parameter	Setting
Model version	6.334
Meteorological grid domain	15 km x 12 km
Meteorological grid spacing	50 metres
Number of grid points	300 x 240
Vertical grids / vertical extent	8 cell heights / 3,200m
Upper air meteorology	Prognostic 3D.dat extracted from TAPM at 1 km grid

Table 15: CALMET model options used

Flag	Descriptor	Default	Value used
IEXTRP	Extrapolate surface wind observations to upper layers	Similarity theory	Similarity theory
BIAS (NZ)	Relative weight given to vertically extrapolated surface observations versus upper air data	No default	-1, -0.5, -0.25, 0 for all other layers*
TERRAD	Radius of influence of terrain	No default (typically 5-15 km)	5 km
RMAX1 and RMAX2	Maximum radius of influence over land for observations in layer 1 and aloft	No Default	5 km, 5 km
R1 and R2	Distance from observations in layer 1 and aloft at which observations and Step 1 wind fields are weighted equally	No Default	2.5 km, 2.5 km

* The BIAS value ranges from -1 to +1, and a value is input by the user for each vertical layer. A value of -1 means the surface station has 100% weight, while a value of +1 means the upper air station has 100% weight (Barclay and Scire, 2011).

4.3.2 GRAMM

Table 16 summarises the general GRAMM set-up parameters. As per the methodology adopted for the WestConnex assessments, GRAMM was run using classified meteorological conditions (7 stability classes, 36 wind direction classes, and multiple wind speed classes), as determined by the spread of the input data.

Table 16: GRAMM set-up parameters

Parameter	Input/value
Model version	July 2016
Reference meteorology	
Meteorological parameters	Wind speed (m/s), wind direction (°), stability class (1-7)
Wind speed classes, single station (m/s)	9 classes (0-0.5, 0.5-1, 1-2, 2-3, 3-4, 4-5, 5-6, 6-9, >9)
Wind speed classes, multiple stations (m/s)	8 classes (0-0.5, 0.5-1, 1-2, 2-3, 3-5, 5-7, 7-9, >9)
Number of wind speed sectors	36
Sector size (degrees)	10
Concentration grids and general GRAMM input	
Horizontal grid resolution (m)	50
Vertical thickness of first layer (m) ^(a)	10
Number of vertical layers	15
Vertical stretching factor ^(b)	1.2
Relative top level height (m) ^(c)	730
Maximum time step (s) ^(d)	10
Modelling time (s)	3,600
Relaxation velocity ^(e)	0.05
Relaxation scalars ^(f)	0.05

(a) Defines the cell height of the lowest layer of the flow field. Typical values are 1-2 metres.

(b) Defines how quickly cell heights increase with height above ground. For example, a factor of 1.1 means a cell is 10% higher than the one below it.

(c) This is the highest vertical level in the model domain, defined as the relative height from the lowest level. The value used here is quite low compared with typical values in other models such as TAPM and CALMET. However, the highest ground elevation within the domain is around 135 metres, and therefore the 730m top level height should be reasonable.

(d) Defines the amount of time taken to ensure that calculations are done efficiently but stably.

(e) These are chosen to ensure the numerical stability of GRAMM simulations.

Terrain data were processed within the GEOM (Geographical/Geometrical grid processor) component of GRAMM. The terrain data for the meteorological model domain were obtained from the ASTER website, and converted into a text file for use in GRAMM. The terrain data used in GRAMM had a resolution of 30 metres. Although the terrain in the dispersion model domain was not especially complex, a spatially-varying terrain file was used to provide an accurate reflection of the situation.

A spatially-varying land use file was developed for use in GRAMM. Various land use types can be specified in GRAMM, and CORINE (Coordination of Information on the Environment) land cover parameters can be imported. The land use file was based on a visual classification using aerial imagery base maps in ArcGIS. Firstly, a polygon shapefile was digitised using eight CORINE land cover classes (continuous urban fabric, discontinuous urban fabric, industrial/commercial units, road/rail networks, airports, green urban areas/sports and leisure facilities, forests, and water bodies), which are also used in GRAMM. Within the meteorological

model domain the visually distinguishable areas were then classified according to these eight classes. The result was converted to a 50-metre resolution ASCII raster file for use within GRAMM.

GRAMM and CALMET use different methods for the inclusion of land use data. As explained above, GRAMM accepts land use data from the CORINE dataset whereas the method used to create the CALMET land use data relies on the USGS classification system. Although the two land use datasets are based on different classification schemes, in both cases, the land use was selected manually using an aerial photograph before the classification codes were applied. Therefore, the general type of land use in both models is the same.

4.4 Dispersion modelling

This Section describes the general set-up of CAL3QHCR and GRAL. As with the meteorological modelling, specific aspects of the GRAL set-up were investigated in the study, and these are explained in Section 4.5. Again, it was not possible to test the effects of all model settings and inputs.

4.4.1 CAL3QHCR

CAL3QHCR is an enhanced version of the CALINE Gaussian dispersion model, and is designed specifically for the assessment of road traffic emissions. Gaussian dispersion algorithms do not perform well under low wind speed conditions (below around 1 m/s) (NZMfE, 2004), and such conditions were observed for almost 30% of the time during the 17-week period of this study at the Concord Oval monitoring station.

The following information was used as input to the model:

- Link type. Different link types can be defined in CAL3QHCR (e.g. 'at grade', 'fill', 'bridge' and 'cut section'). All road links were defined as 'at grade' for this study.
- Meteorological conditions. This is required in the simple hourly format formerly used in the USEPA's Industrial Source Complex (ISC) model. The parameters used are wind speed, wind direction, temperature, stability class and mixing height. As ISC had a tendency to overestimate concentrations under wind speed conditions of less than 1 m/s; hours with these conditions were treated by the model as calm. Following convention, in this study the minimum wind speed was set to 1 m/s to avoid zero concentration predictions for periods with wind speeds below 1 m/s.
- Receptor locations. Both discrete and gridded receptors were used.
- Traffic volume by road link. As noted in section 4.2.2, this involved the use of average weekday profiles for each day of the dispersion model evaluation period.
- Vehicle emission rates (grams per vehicle-kilometre per hour)²¹ of each pollutant for each road link. As for traffic volumes, these included average weekday profiles for each day over the duration of the study period.

4.4.2 GRAL

A general description of GRAL is provided in Appendix A. In GRAL each hour of the average weekday emission profile was represented as a separate source group, resulting in a total of 24 source groups. A

²¹ CAL3QHCR actually requires unit emission rates in grams per vehicle-mile, but for the purposes of this discussion metric units have been used for consistency. Metric units were converted for input into the model.

period-average emission factor was used in conjunction with emission modulation factors, with the latter being used to switch specific hours on or off as required.

4.4.3 Receptors

All dispersion model outputs were defined for a height of 3 metres above ground level. This was equivalent to the height of the air pollution measurements. Two types of receptor were defined:

- Discrete receptors, for which hourly time series were calculated. These coincided with the locations of all 17 air pollution measurement sites, including the air inlets of the roadside and background monitoring stations and the passive sampling locations.
- A Cartesian grid of evenly-spaced receptors, for which basic statistics were calculated for contour plots. GRAL runs were conducted for a number of different grid spacing options (2 metres, 10 metres and 20 metres), but the CAL3QHCR model was only run for the 10 metre spacing option.

4.4.4 Post-processing

4.4.4.1 Calculation of total concentration

The dispersion model predictions for NO_x were combined with a background contribution to give total concentrations. The methods for determining background concentrations are described in Chapter 5. Essentially, two alternative approaches were considered for NO_x:

- 'Unadjusted background' approach. For each hour, the model contribution at each location was added to the corresponding concentration from the St Lukes Park background site.
- 'Adjusted background' approach. For each hour, the model contribution at the background site was subtracted from the observation to give an 'adjusted' background. The adjusted background was then added to the model prediction at each location.

For reasons that are explained later in the report, only the results for the first method have been presented.

4.4.4.2 Calculation of road increment

For NO_x at the Concord Oval site the model predictions were compared directly with the 'road increment', which was calculated by subtracting the St Lukes Park observation from the Concord Oval observation in each hour. The road increment was examined as a function of wind direction.

4.4.4.3 Calculation of NO₂ concentrations

NO₂ is rapidly formed through the atmospheric reaction of NO with O₃, and is destroyed by sunlight during the day. This is one reason why air pollution models are generally configured to predict NO_x concentrations, with the spread of NO_x being simulated as though it were a non-reactive gas. However, as NO₂ is important in terms health it was considered important to include it in the model evaluation exercise²².

The estimation of NO₂ concentrations near roads is not straightforward - it requires an understanding of NO₂ formation and destruction, and here there are a number of challenges. These include:

²² It is essential to consider NO₂ in the context of air quality assessments, but this was not the focus of this study.

- How to account for the amount of primary NO₂ emitted in vehicle exhaust. This is dependent on the composition of the traffic.
- How to account for the amount of conversion of NO to NO₂ in the atmosphere following release from the source, as this is dependent on the local atmospheric conditions, including the amount of ozone available.
- How to determine cumulative NO₂ concentrations, or in other words how to combine the road traffic contribution and the background (non-road) contribution.

Various different approaches have been developed for calculating NO₂ concentrations. When using models such as GRAL for air quality assessments, a common approach is to estimate NO₂ from NO_x using empirical methods. However, this can be problematic for model evaluation purposes, as it simplifies the complex behaviour of NO₂ on short timescales.

In this study NO₂ concentrations were recorded as 1-hour averages (continuous monitoring) and as nominal two-week averages (passive samples). The estimation of average NO₂ concentrations on these short time scales is difficult. For example, Figure 19 compares 1-hour average NO_x and NO₂ concentrations for a range of site types in Sydney and for multiple years. The Sydney dataset includes around 1.7 million data points. The data from the two monitoring sites in the GRAL study are also shown. It can be seen that for any given 1-hour NO_x concentration a wide range of 1-hour NO₂ concentrations is possible. It is not straightforward to derive empirical methods for converting NO_x to NO₂ from these data, as the chemical and photochemical reactions in the roadside environment need to be taken into account, and these will vary from site to site.

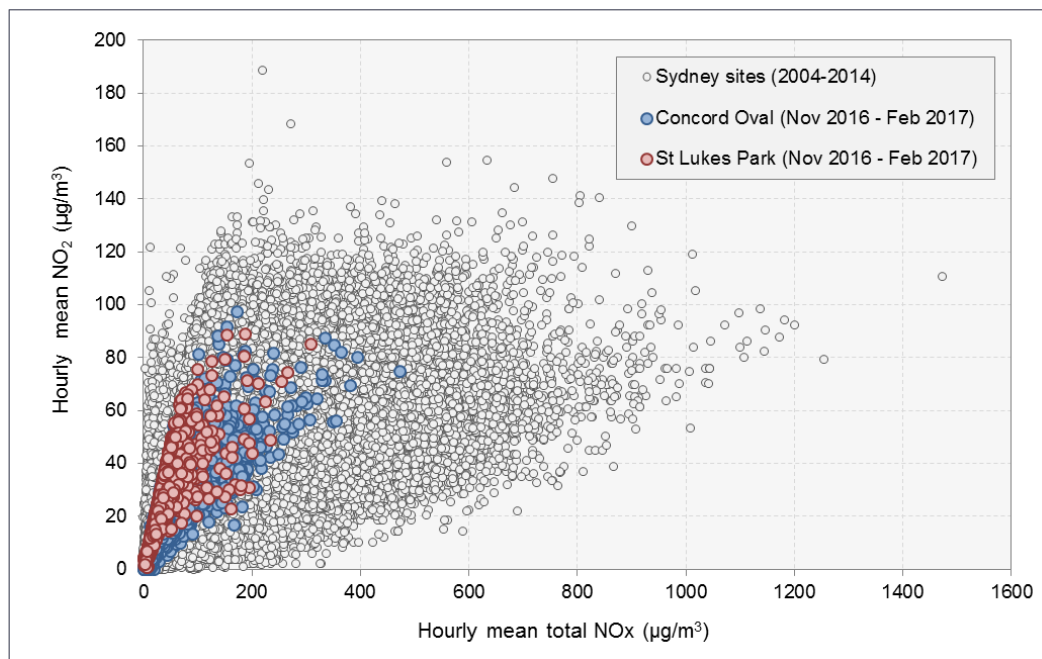


Figure 19: Scatter plot of 1-hour average NO_x and NO₂ concentrations

For the assessment of the WestConnex projects two empirical methods were defined for the conversion of NO_x to NO₂ (Pacific Environment, 2017). The first method is used to determine the annual average NO₂ concentration from the annual average NO_x concentration, and this is shown in Figure 20. In this Figure the solid blue line is a regression fit to the data, and the dashed blue line is an extrapolation. The second method

is used to determine the *maximum* one-hour average NO_2/NO_x ratio (and hence NO_2 concentration) for any given 1-hour average NO_x concentration. This is shown in Figure 21, which is essentially a different way of showing the data in Figure 19, with the NO_2/NO_x ratio as the y axis instead of NO_2 , and an upper bound function fitted to the data. A very small fraction of the measurements is above the upper bound. An alternative upper bound (black line) has also been included based solely on the data collected in the study area and for the dispersion model evaluation period. The functions are summarised in Table 17.

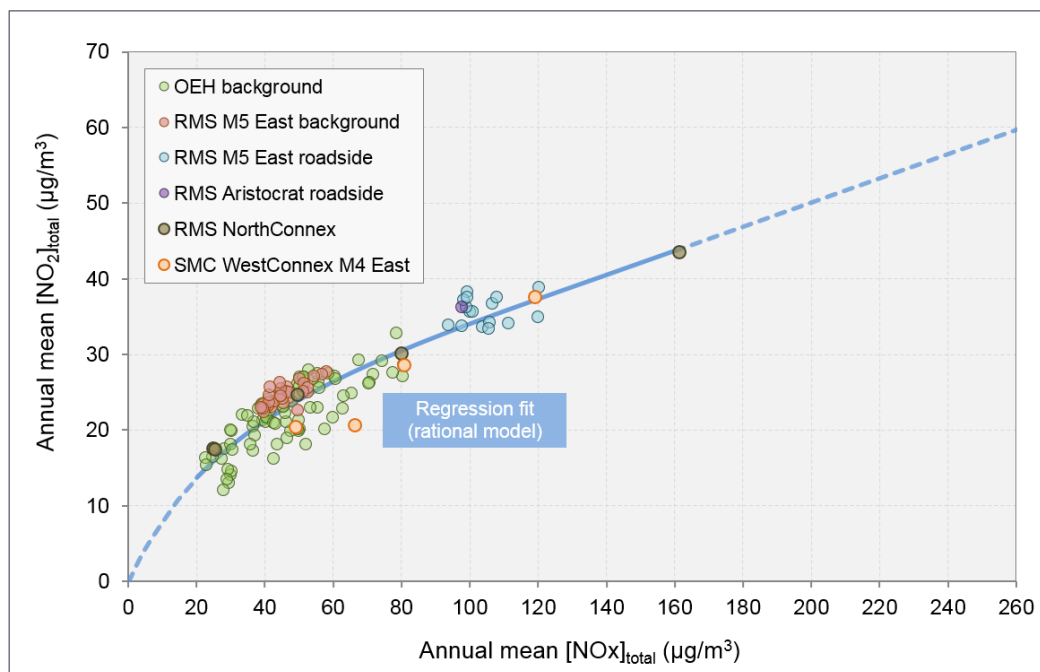


Figure 20: Empirical conversion - annual mean NO_x to annual mean NO_2

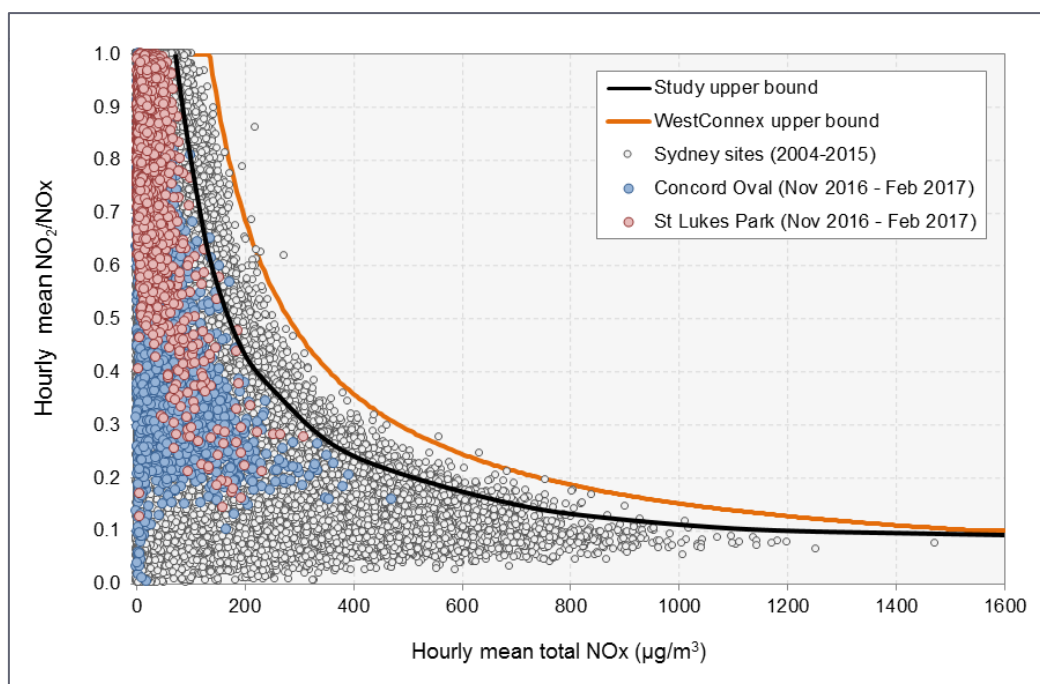


Figure 21: Hourly mean NO_x and NO_2/NO_x ratio for monitoring sites at various locations in Sydney

Table 17: NO_x-to-NO₂ conversion functions

Conversion method	Functional form
WestConnex annual mean	<p>For [NO_x]_{total} values less than or equal to 140 µg/m³:</p> $[\text{NO}_2]_{\text{total}} = \frac{a + b[\text{NOx}]_{\text{total}}}{1 + c[\text{NOx}]_{\text{total}} + d([\text{NOx}]_{\text{total}})^2}$ <p>where:</p> <p>a = -7.6313 x 10⁻⁴ b = 9.9470 x 10⁻¹ c = 2.3750 x 10⁻² d = -4.5287 x 10⁻⁵</p> <p>For [NO_x]_{total} greater than 140 µg/m³:</p> $[\text{NO}_2]_{\text{total}} = 40.513 + (0.16 \times ([\text{NOx}]_{\text{total}} - 140))$
WestConnex 1-hour maximum	<p>For [NO_x]_{total} values less than or equal to 130 µg/m³:</p> $\frac{[\text{NO}_2]_{\text{total}}}{[\text{NOx}]_{\text{total}}} = 1.0$ <p>For [NO_x]_{total} values greater than 130 µg/m³ and less than or equal to 1,555 µg/m³:</p> $\frac{[\text{NO}_2]_{\text{total}}}{[\text{NOx}]_{\text{total}}} = a \times [\text{NOx}]_{\text{total}}^b$ <p>where:</p> <p>a = 100 b = -0.94</p> <p>For [NO_x]_{total} values greater than 1,555 µg/m³ a cut-off for the NO₂/NO_x ratio of 0.10 is assumed</p>
Study-specific 1-hour maximum	<p>For [NO_x]_{total} values less than or equal to 80 µg/m³:</p> $\frac{[\text{NO}_2]_{\text{total}}}{[\text{NOx}]_{\text{total}}} = 1.0$ <p>For [NO_x]_{total} values greater than 80 µg/m³ and less than or equal to 1,180 µg/m³:</p> $\frac{[\text{NO}_2]_{\text{total}}}{[\text{NOx}]_{\text{total}}} = a \times [\text{NOx}]_{\text{total}}^b$ <p>where:</p> <p>a = 38 b = -0.84</p> <p>For [NO_x]_{total} values greater than 1,180 µg/m³ a cut-off for the NO₂/NO_x ratio of 0.10 is assumed</p>

Because these empirical methods were designed for estimating annual mean and maximum one-hour NO₂ concentrations in air quality assessments, none of them were especially well-suited to determining *short-term average* concentrations in the GRAL study.

A commonly used alternative is the USEPA's ozone limiting method (OLM). This employs a simple approach to the reaction chemistry of NO and O₃ in order to estimate NO₂ concentrations on an hourly basis. It is

assumed that all the available O₃ in the atmosphere will react with the NO from the source until either all the O₃ is consumed or all the NO is used up (Cole and Summerhays, 1979; Tikvart, 1996).

The method involves an initial comparison of the estimated maximum NO_x concentration and the ambient O₃ concentration to determine the limiting factor to NO₂ formation:

- If the O₃ concentration is greater than the maximum NO_x concentration, then total NO_x to NO₂ conversion is assumed.
- If the maximum NO_x concentration is greater than the ozone concentration, the formation of NO₂ is limited by the ambient ozone concentration.

The OLM – in the USEPA form – is based on the assumption that 10% of the initial NO_x emissions are NO₂. The emitted NO reacts with ambient ozone to form additional NO₂. If the ozone concentration is greater than 90% of the predicted NO_x concentration, all the NO_x is assumed to be converted to NO₂. Otherwise, NO₂ concentrations are calculated on the assumption of total conversion of the ozone. The predicted NO₂ concentration is then added to the background NO₂ concentration.

In the NSW EPA's submission to the EIS for the NorthConnex project in Sydney, it is stated that that an average value for the NO₂/NO_x ratio of 16% would be more appropriate than 10%. The OLM equation should therefore be adjusted as follows (AECOM, 2014):

$$[\text{NO}_2]_{\text{total}} = \{0.16 \times [\text{NO}_x]_{\text{road}}\} + \text{MIN} \{ (0.84) \times [\text{NO}_x]_{\text{road}} \text{ or } (46/48) \times [\text{O}_3]_{\text{background}} \} + [\text{NO}_2]_{\text{background}}$$

The effect of the adjustment is to increase the amount of NO₂ emitted directly, potentially increasing the NO₂ concentrations that are predicted under low ambient O₃ concentrations.

Several limitations of the OLM have been noted in the literature (e.g. NZMfE, 2004), and the approach is known to overestimate NO₂ concentrations, particularly close to the source. For example, the method assumes that the atmospheric conversion of NO to NO₂ occurs instantaneously, whereas in reality the reaction requires time. The method assumes that all ozone is available to the emission source being evaluated. The OLM will be too conservative when, for example, a new source is to be located in close proximity to existing sources. The USEPA states that the OLM should only be used on a 'plume-by-plume' basis, and this is problematic in relation to road projects.

The conversion methods tested in the study are summarised in Section 4.5.3. Because of the limitations of the calculation methods, the results for NO₂ should only be considered as indicative.

4.5 Model evaluation

4.5.1 Meteorological model evaluation

Various model tests were conducted to evaluate the performance of CALMET and GRAMM in the meteorological model domain, with the model predictions being compared with observations. Each test was conducted using all available 1-hour average data for 2015, but only the hours with valid data in all three datasets for a given station (observations, CALMET and GRAMM) were used in the analysis. For example, in test GM-05 the Rozelle observation/CALMET/GRAMM analysis had 8,467 hours of data, but the St Lukes Park analysis had 8,717 hours of data. The availability of these data was limited by the measured data for each station.

Although the set-up of both models was designed to be similar, there were no exact like-with-like comparisons because of the different principles involved and inputs required. The tests conducted are summarised in Table 18, and are described in more detail below.

Table 18: Summary of meteorological model tests

Test series (reference met approach)	Test	Grid spacing	GRAMM processing method: with Re-Order	GRAMM processing method: Match-to-Observations	Model evaluation site (observations)
Series A Single measurement station (St Lukes Park)	CALMET (CT-01)	50 m	Not applicable	Not applicable	All stations
	GRAMM (GM-01)	50 m	No	Not applicable	
	GRAMM (GM-02)	100 m	No	Not applicable	
	GRAMM (GM-03)	200 m	No	Not applicable	
	GRAMM (GM-04)	50 m	Yes	Not applicable	
Series B Multiple measurement stations (CALMET) ^(a) or synthetic meteorology (GRAMM)	CALMET (CT-02)	50 m	Not applicable	Not applicable	All stations
	GRAMM (GM-05)	50 m	Not applicable	Match to all stations in domain except St Lukes Park	
	GRAMM (GM-06)	50 m	Not applicable	Match to all stations in domain	
	GRAMM (GM-07)	50 m	Not applicable	Match to St Lukes Park only	

(a) For CALMET the reference stations were all stations except St Lukes Park (i.e. Sydney Olympic Park, Canterbury Racecourse, Rozelle and Chullora).

For both models the most important input was a reference (surface) meteorological dataset including hourly records of wind speed, wind direction and stability class from one or more measurement stations deemed to be representative of the study area. Two series of tests were conducted to broadly reflect different approaches to defining the reference meteorology, with specific model set-up parameters being modified in each case. These were as follows:

- **Series A:** In the first series of tests the reference measurements for both CALMET and GRAMM were taken from a single monitoring station (St Lukes Park), and the model predictions were compared with observations at all monitoring stations. This is similar to the approach that was used in the WestConnex assessments. In these tests the following were assessed:
 - CALMET and GRAMM performance. Tests CT-01 and GM-01 involved running CALMET and GRAMM with a grid spacing of 50 metres. The St Lukes Park data were used to generate prognostic wind fields in GRAMM.
 - The effects of the horizontal grid spacing in GRAMM. Tests GM-01, GM-02 and GM-03 involved running GRAMM with grid a spacing of 50 metres, 100 metres and 200 metres respectively, all other model settings unchanged. CALMET was not included in these tests.
 - The effects of the Re-Order function in GRAMM (see Appendix A for a description of this function). Tests GM-01 and GM-04 involved running GRAMM with a grid spacing of 50 metres. These two tests examined the effects of running GRAMM without the Re-Order function (Test GM-01) and with the Re-Order function (Test GM-04) to improve the fit of the simulated flow fields to the

measured data. All other model settings unchanged. The results were again compared with CALMET test CT-01.

- **Series B:** In the second series of tests the reference meteorological data for the models were taken from multiple measurement stations (for CALMET) or from a synthetic meteorological file with Match-to-Observations (GRAMM), and the model predictions were compared with observations. The Match-to-Observations function is described in Appendix A. All tests were conducted with a grid spacing of 50 metres, and three different approaches were examined:
 - GRAMM Match-to-Observations for *all stations except St Lukes Park*. In tests CT-02 and GM-05 all stations except St Lukes Park were used to provide the reference meteorological data. In the case of CALMET the reference data were entered directly into the model. As GRAMM will only accept data from a single reference station, an analogous approach was used whereby a synthetic meteorological file was used as input to the model, and then the GRAMM Match-to-Observations function was used for the specific monitoring stations.
 - GRAMM Match-to-Observations for *all stations*. In test GM-06 all monitoring stations were used with the GRAMM Match-to-Observations function, and the GRAMM predictions were compared with the measurements at all stations. For all stations except St Lukes Park the GRAMM results were compared with CALMET test CT-02. For St Lukes Park the results were compared with CALMET test CT-01 from Series A.
 - GRAMM Match-to-Observations for *St Lukes Park only*. In test GM-07 the GRAMM Match-to-Observation function was applied to St Lukes Park only, and the results were extracted for all stations. This test was used to show the performance of GRAMM in the much smaller dispersion model domain around St Lukes Park, and for the conditions that were used in the GRAL modelling. The results for other stations were therefore less important. The results from this test were compared with this from tests GM-01 and CT-01 from Series A.

The following types of output were considered for each test to determine how the model predictions agreed with, or diverged from, the observations:

- (a) Combined wind speed and wind direction (as wind roses).
- (b) Wind speed only. This included a consideration of descriptive statistics (such as averages, percentiles and percentage of calm winds), a detailed temporal evaluation (using the `timeVariation` function in Openair), regression plots, and the calculation of specific model-evaluation metrics.
- (c) Wind direction only. Radar plots were used to simplify the presentation of the wind direction results, and to allow observations and model performance to be compared more directly than in the wind roses.

This work provided information on model performance, sensitivity to inputs/settings, and uncertainty.

4.5.2 Dispersion model evaluation

The dispersion model evaluation was broadly similar to the meteorological model evaluation. Various tests were conducted to evaluate the performance of CAL3QHCR and GRAL in the dispersion model domain,

focussing only on NO_x. As with the meteorological model evaluation, although the set-up of both models was designed to be similar an exact like-with-like comparison was not possible. The tests are summarised in Table 19 and described in more detail below.

Table 19: Summary of dispersion model tests

Test series	Test	Meteorological input	Grid spacing	Number of particles per second	Buildings	
					GRAL prognostic	GRAL diagnostic
Series C Model comparison	CAL3QHCR (C3-01)	Concord Oval observations	10 m	Not applicable	Not applicable	Not applicable
	GRAL (GL-01)	Concord Oval observations	10 m	400	No	No
Series D Met input	GRAL (GL-02) ^(a)	GRAMM with MtO at Concord Oval	10 m	400	No	No
Series E Grid spacing	GRAL (GL-03) ^(b)	GRAMM with MtO at Concord Oval	2 m	400	No	No
	GRAL (GL-04) ^(b)	GRAMM with MtO at Concord Oval	20 m	400	No	No
Series F Particle number	GRAL (GL-05) ^(c)	GRAMM with MtO at Concord Oval	2 m	200	No	No
	GRAL (GL-06) ^(c)	GRAMM with MtO at Concord Oval	2 m	800	No	No
Series G Buildings	GRAL (GL-07) ^(d)	GRAMM with MtO at Concord Oval	2 m	400	Yes	No
	GRAL (GL-08) ^(d)	GRAMM with MtO at Concord Oval	2 m	400	No	Yes

(a) For comparison with test GL-01.

(b) For comparison with test GL-02.

(c) For comparison with test GL-03.

(d) For comparison with test GL-03.

Five series of tests were conducted to broadly reflect different modelling approaches and settings within GRAL, with an initial test using CAL3QHCR. The tests were as follows:

- **Series C:** Model comparison. Tests C3-01 and GL-01 involved a comparison between the predictions of CAL3QHCR and GRAL for a grid spacing of 10 metres and using the Concord Oval meteorological measurements as direct input to the models. Concord Oval was selected in preference to St Lukes Park as there was an emphasis on the prediction of concentrations close to Parramatta Road, and at a height of 3 metres. This use of a homogeneous meteorological field is an acceptable approach for relatively flat domains and low-level sources, and is the standard approach used in CAL3QHCR.
- **Series D:** The effects of the meteorological input in GRAL. One test (GL-02) was conducted to compare the effects of using GRAMM (Concord Oval Match-to-Observations) in GRAL rather than the direct observations from Concord Oval (GL-01). All subsequent GRAL runs (in Series E to G) also used the meteorological input from GRAMM based on Concord Oval Match-to-Observations.

- **Series E:** The effects of the horizontal grid spacing in GRAL. These tests examined the influence of the grid spacing (2 metres, 10 metres and 20 metres) in GRAL, with the 10 metre case taken from test GL-02. The number of particles in GRAL was fixed at 400 per second.
- **Series F:** The effects of the particle number in GRAL. This series of tests examined the effects of varying the number of particles in GRAL (200, 400 and 800 per second) at a small grid spacing. The 400 particles per second case was taken from test GL-03.
- **Series G:** The effects of including buildings in GRAL. In these tests the larger buildings in the dispersion model domain were included in GRAL to capture any associated effects on dispersion (e.g. building wake effects). This involved the separate testing of prognostic (GL-07) and diagnostic (GL-08) approaches. The results were compared with those from test GL-03.

The model predictions were compared with observations in two different ways:

- (a) A temporal analysis of NO_x at the Concord Oval and St Lukes Park monitoring stations. The model predictions were compared with observations using 1-hour average data for the period between November 2016 and February 2017, and within each test only the hours with valid data in all three datasets (observations, CAL3QHCR and GRAL) were used. As with the wind speed analysis, this included a consideration of descriptive statistics, use of the `timeVariation` function in Openair, regression plots, and the calculation of specific model-evaluation metrics.
- (b) A spatial analysis of NO_x and NO₂ for the period-average concentrations measured using the Ogawa samplers, as well as contour plots of air quality metrics.

For the correlation coefficient (*r*), and the associated coefficient of determination (*R*²), the strength of any relationship was described according to the scheme by Evans (1996) (for *R*²: 0.00-0.04 = “very weak”, 0.04-0.16 = “weak”, 0.16-0.36 = “moderate”, 0.36-0.64 = “strong”, 0.64-1.00 = “very strong”).

4.5.3 Estimation of NO₂ concentrations

NO₂ concentrations were estimated for only the Series C predictions from GRAL (i.e. test GL-01) and CAL3QHCR (i.e. test C3-01). Given the inherent uncertainty in the prediction of NO₂, it was not considered worthwhile to extend this to the other test series. As noted above, NO₂ was also only investigated for the passive sampling locations and the corresponding period-average concentrations.

Five different methods for converting modelled NO_x to NO₂ were tested in the study, and these are summarised in Table 20.

Table 20: NO₂ calculation methods

Method code	Method description
NO2_1	OLM based on roadside O ₃ and NO ₂ measurements
NO2_2	OLM based on background O ₃ and NO ₂ measurements
NO2_3	WestConnex empirical – annual conversion method
NO2_4	WestConnex empirical – one-hour conversion method
NO2_5	Study-specific – one-hour conversion method

5 Results of experimental work

5.1 Traffic volume and composition

The average daily traffic volumes of LDVs and HDVs on the road links in the dispersion model domain are given in Table 21. The most important roads in the vicinity of the monitoring stations and passive samplers were Parramatta Road and Gipps Street. Traffic volumes on Burwood Road were comparable to those on Gipps Street, but the road was slightly further away from the monitoring locations.

Table 21: Average daily traffic volumes for main roads in dispersion model domain

Road link	Road	Direction	Traffic volume (vehicles per day)			Traffic volume (vehicles per day)		
			LDV			HDV		
			Weekday	Saturday	Sunday	Weekday	Saturday	Sunday
01	Burton Street	WB+EB	1,597	1,303	1,052	81	42	33
02	Loftus Street	NB+SB	1,712	1,593	1,193	189	100	72
03	Parramatta Road	WB (all lanes)	35,158	39,351	37,752	3,139	1,550	1,422
04	Parramatta Road	EB (all lanes)	39,829	44,213	37,183	3,637	1,748	1,353
05	Parramatta Road	WB (all lanes)	35,463	39,221	37,579	3,197	1,557	1,422
06	Parramatta Road	WB (all lanes)	35,158	39,351	37,752	3,139	1,550	1,422
07	Parramatta Road	EB (all lanes)	39,878	44,240	37,054	3,639	1,750	1,353
08	Parramatta Road	EB (all lanes)	36,640	40,404	33,592	3,376	1,622	1,240
09a	Gipps Street	EB	12,228	12,179	9,694	366	179	139
09b	Gipps Street	WB	12,986	12,646	10,287	404	164	128
10a	Gipps Street	EB	12,411	12,124	9,532	374	178	136
10b	Gipps Street	WB	12,986	12,646	10,287	404	164	128
11a	Gipps Street	EB	12,411	12,124	9,532	374	178	136
11b	Gipps Street	WB	12,932	12,438	10,099	402	161	126
12a	Queens Road	EB	12,411	12,124	9,532	374	178	136
12b	Queens Road	WB	12,932	12,438	10,099	402	161	126
13a	Queens Road	EB	12,411	12,124	9,532	374	178	136
13b	Queens Road	WB	12,932	12,438	10,099	402	161	126
14	Cheltenham Road	NB+SB	1,356	1,231	1,071	76	22	27
15	Lucas Road	NB+SB	1,356	1,231	1,071	76	22	27
16a	Shaftesbury Road	SB	7,609	8,045	8,045	300	186	186
16b	Shaftesbury Road	NB	7,627	7,958	6,666	300	172	140
17	Burwood Road	NB+SB	12,685	12,559	10,842	761	339	287
18	Burwood Road	NB+SB	11,203	10,718	9,170	678	293	247
19	Burwood Road	NB+SB	9,769	9,626	8,536	590	264	230
20	Parramatta Road	EB	-	-	-	573	371	289
21	Luke Avenue	NB+SB	-	-	-	578	437	313

Figure 22 shows average weekly profiles for traffic volume on Parramatta Road and Gipps Street, and by direction of travel. Numbers of HDVs and LDVs are given separately, along with the percentage of HDVs.

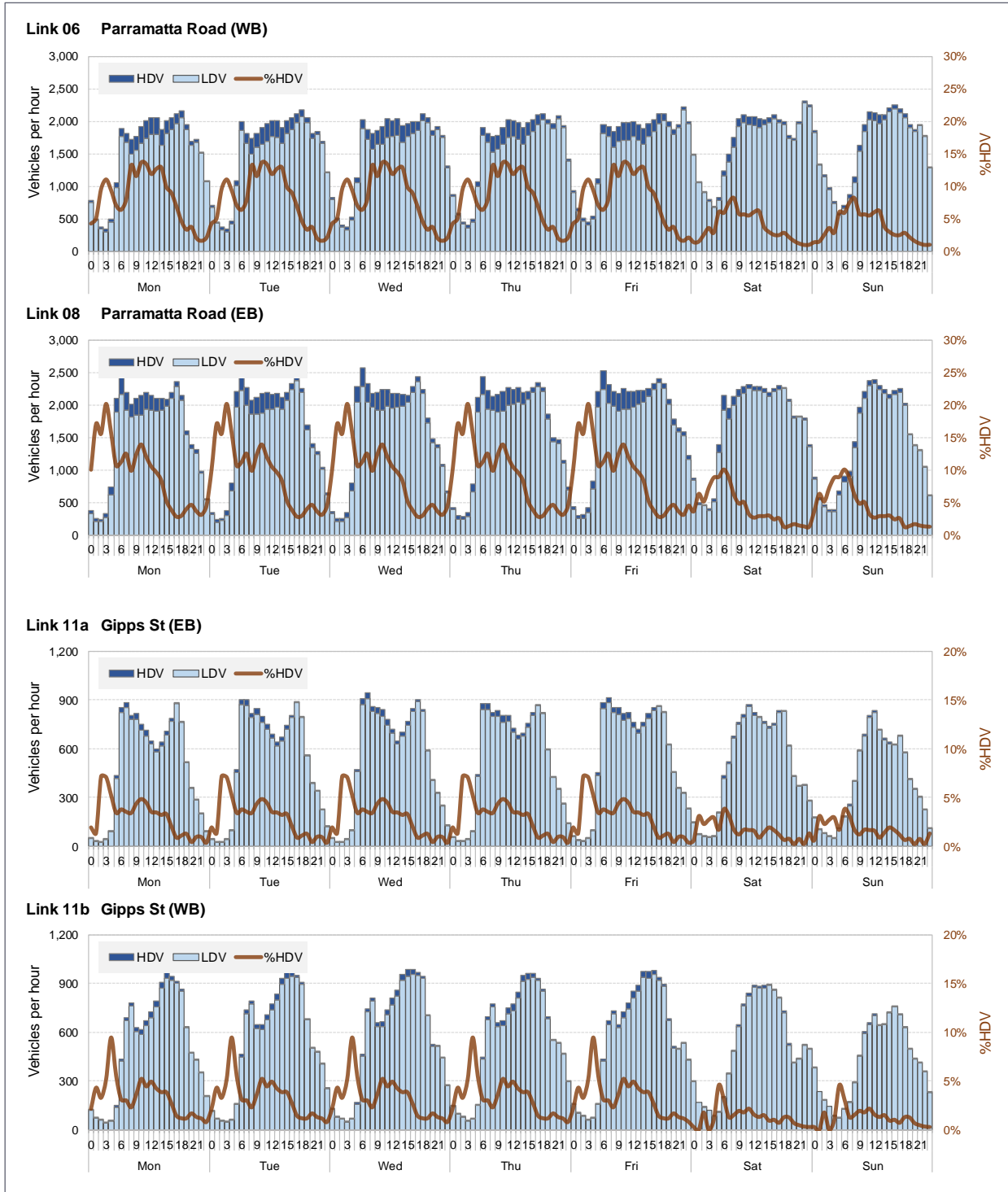


Figure 22: Average weekly LDV, HDV and %HDV profiles for Parramatta Road and Gipps Street

On Parramatta Road the weekday traffic had a broadly similar pattern in both the westbound and eastbound directions. The traffic increased quite sharply from an overnight low of 250-350 vehicles per hour to around 2,000 vehicles per hour at the start of the morning peak period. This peak began between 06:00 and 07:00 in the westbound direction, and an hour earlier in the eastbound direction. High levels of traffic were maintained throughout the day, with typically still more than 1,500 vehicles westbound and 1,000 vehicles eastbound between 22:00 and 23:00. There were pronounced peaks in the westbound traffic on Friday and Saturday

nights between 21:00 and 00:00. The number of HDVs peaked at around 300 vehicles per hour between 10:00 and 12:00. For westbound traffic the percentage of HDVs peaked at around 14% in the late morning, whereas for eastbound traffic it peaked at around 20% between 03:00-04:00. The profiles of traffic volume on Saturdays and Sundays were similar to those on weekdays, the main difference being a lower proportion of HDVs and a later start of the peak traffic period.

On Gipps Street the traffic profiles were different to those on Parramatta Road. Overall volumes were substantially lower, peaking at around 1,000 vehicles per hour. In the eastbound direction the weekday traffic increased from a low of less than 50 vehicles per hour to a peak of around 900 vehicles between 07:00 and 08:00. There was an inter-peak volume of around 600-700 vehicles per hour, and then an evening peak (17:00-18:00) of close to 900 vehicles per hour. Peak traffic volumes on Saturdays and Sundays were not much lower than those on weekdays. The number of HDVs was lower than on Parramatta Road, peaking at 40 vehicles per hour (late morning on weekdays) or around 10% of the traffic (early hours on weekdays).

5.2 Traffic speed

Some examples of traffic speeds on Parramatta Road and Gipps Street are shown in Figure 23. The Figure shows average values for November and December 2016. On Parramatta Road the speeds in the westbound direction were systematically lower than those in the eastbound direction. This was confirmed by an analysis of separate monthly average speed profiles provided by Roads and Maritime. It may be explained by the westbound carriageway having more vehicles entering and leaving driveways and side streets, which would tend to slow the traffic down, whereas the eastbound carriageway has fewer access/conflict points. The bus depot opposite Concord Oval may also play a role; buses leaving the depot and turning right will interrupt traffic in both directions on Parramatta Road, but buses turning left from the depot will only affect the westbound traffic. However, the size and uniformity of the difference between directions is quite surprising, especially the very low westbound speeds in the afternoon.

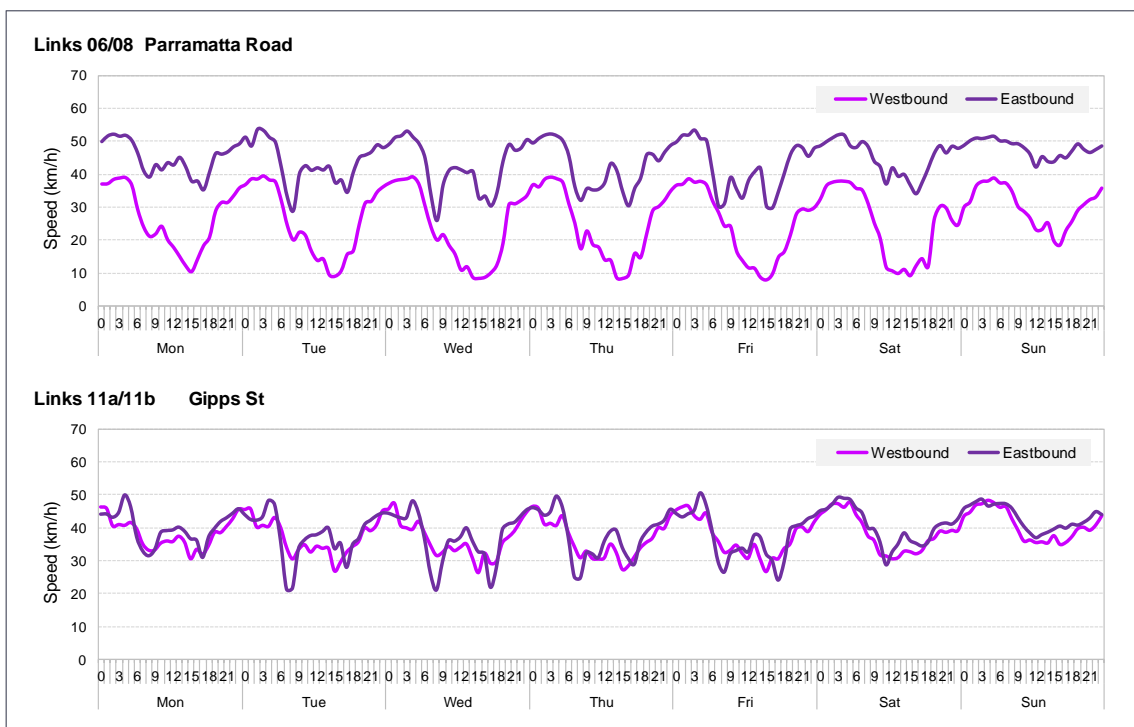


Figure 23: Average weekly traffic speed profiles for Parramatta Road and Gipps Street (Nov/Dec 2016)

5.3 Emissions

Emissions of NO_x, PM₁₀ and PM_{2.5} were calculated on an hourly basis for the dispersion modelling period. Figure 24 and Figure 25 shows examples of average daily profiles of NO_x and PM₁₀ emission rates by road. Unsurprisingly, emissions in the study area are clearly dominated by the traffic on Parramatta Road due to a combination of relatively high volumes, large fractions of HDVs, and low speeds.

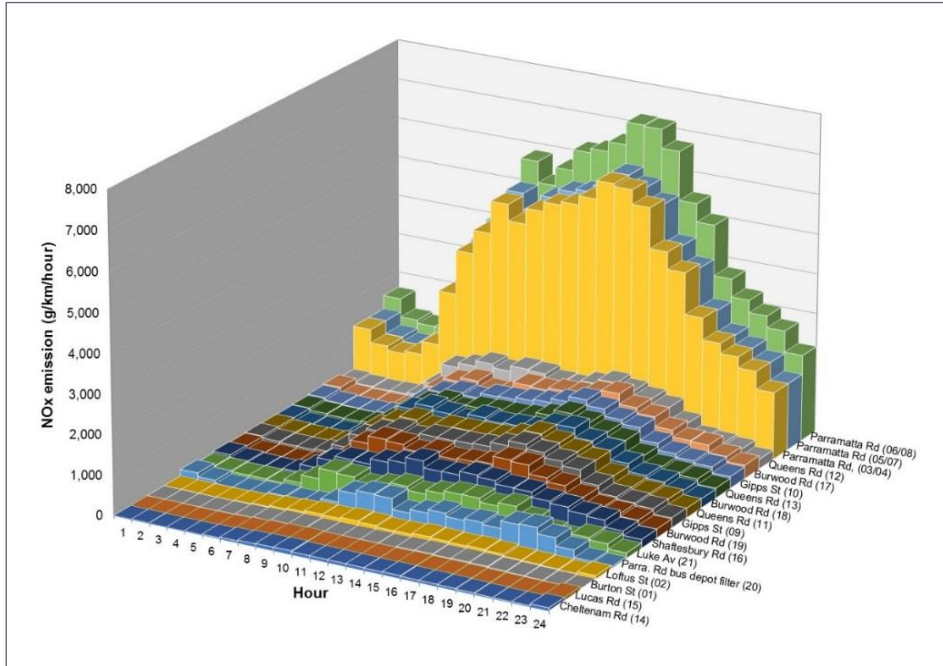


Figure 24: Average daily NO_x emissions profiles by road

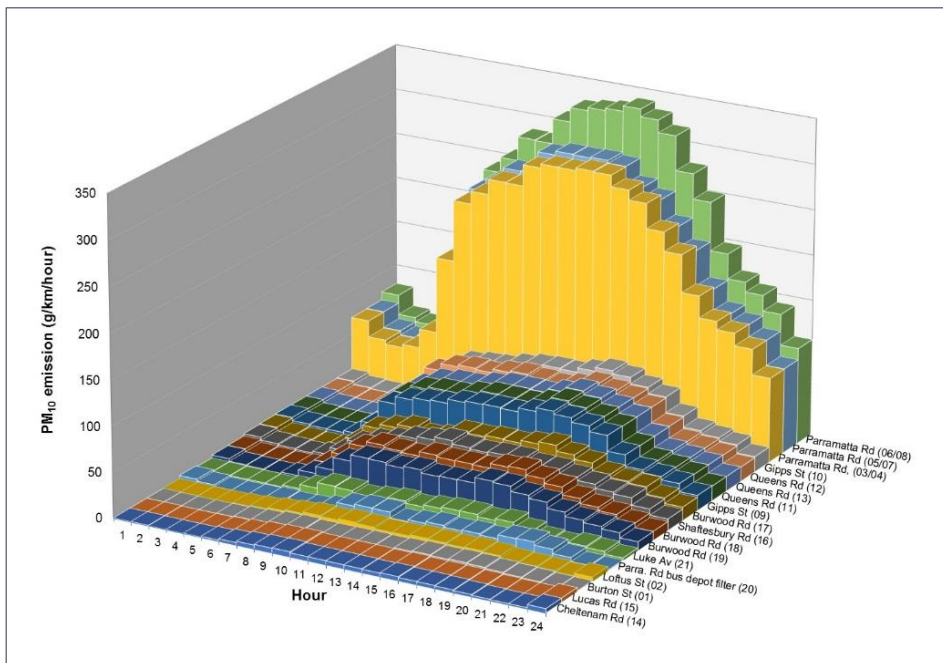


Figure 25: Average daily PM₁₀ emissions profiles by road

The average weekly emission profiles for Parramatta Road (links 06 and 08 combined) during the dispersion model evaluation period are shown in Figure 26. The profiles were very similar on weekdays, but emissions were lower at the weekend. In Figure 22 it was shown that traffic volumes on Parramatta Road were similar on each day of the week. The higher emissions on weekdays are therefore likely to be a consequence of the larger proportion of HDVs and lower speed (particularly in the westbound direction).

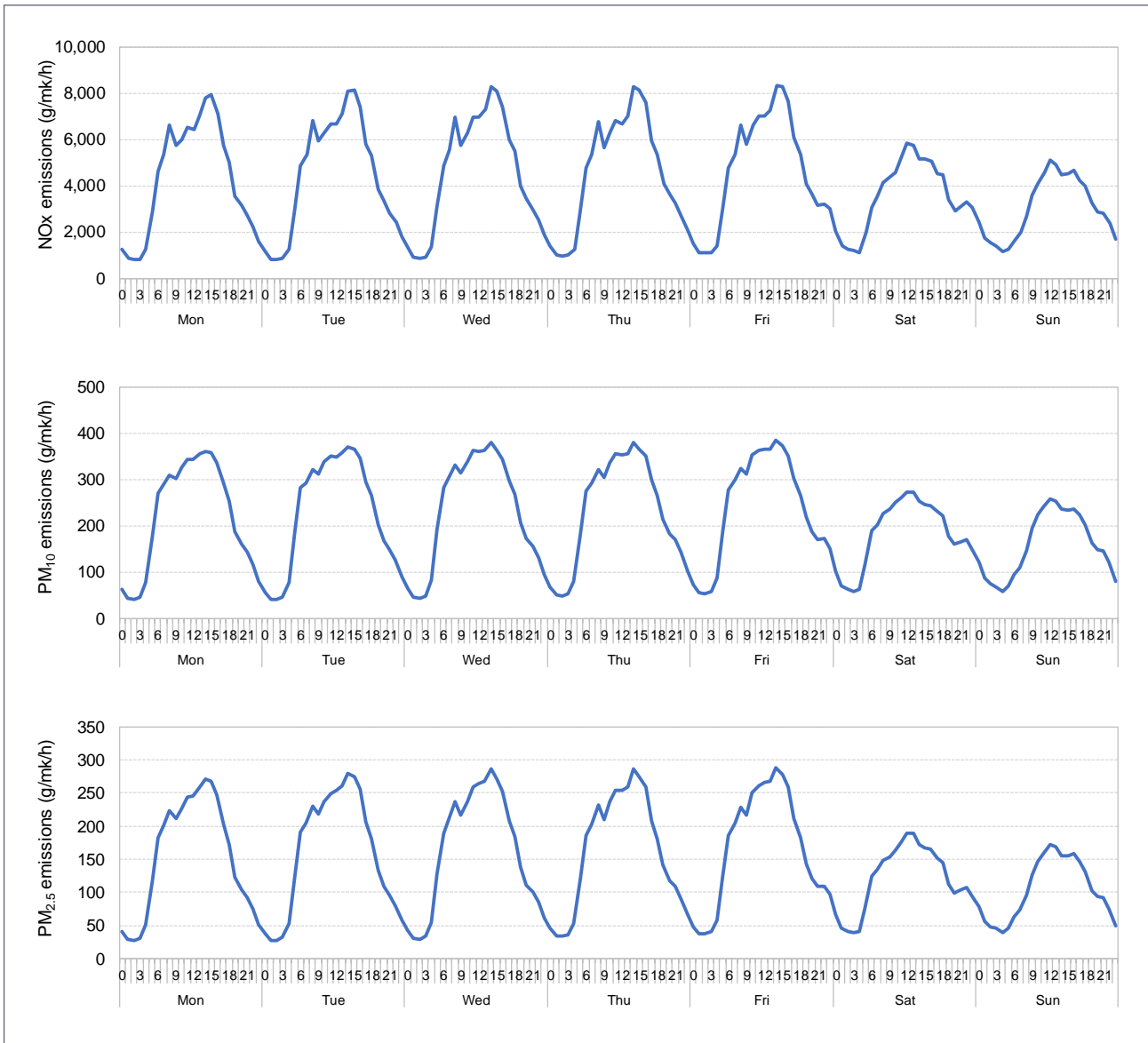


Figure 26: Average weekly emission profiles for Parramatta Road (links 06 and 08 combined)

5.4 Meteorological measurements

The meteorological data collected at all monitoring stations in the meteorological model domain during the model evaluation periods are summarised in this section. For the air quality monitoring stations at Concord Oval and St Lukes Park the data were considered for both the meteorological model evaluation period

(2015) and for the dispersion model evaluation period (November 2016 to February 2017). For the other monitoring stations the data were only considered for 2015.

Descriptive statistics for the parameters measured at the meteorological stations are provided in Appendix D. These statistics relate to data availability, the distribution of values (e.g. maximum, average, percentiles) and, in the case of wind speed, the percentage of calm winds (average wind speed <0.5 m/s).

The availability of data was generally very good. During the meteorological model evaluation period (2015), the availability of most parameters was above 90%. For Concord Oval and St Lukes Park, the availability of meteorological data during the dispersion model evaluation period was close to 100%.

Unsurprisingly, for a given period the data for all other meteorological parameters (temperature, pressure, relative humidity, rainfall and solar radiation) did not show as much between-site variation as the wind data.

An important feature of the data is that average wind speeds and the percentage of calms varied across a surprisingly wide range for a relatively flat urban area such as that covered by the meteorological model domain. For example, in 2015 average wind speeds ranged from 1.3 m/s at St Lukes Park to 3.2 m/s at Canterbury Racecourse, and calms from 7.7% at Canterbury Racecourse to 27.9% at St Lukes Park. Wind speeds were clearly lower at the M4 East and OEH sites than at the BoM sites. The measurements are likely to have been influenced by differences in the instruments used by the organisations, by the age of the instruments, and by local features at each site (e.g. topography, trees, etc.). It is worth noting that the median wind speed also showed a considerable variation across the sites. For example, Canterbury Racecourse and Sydney Olympic Park had median speeds of 2.4-3.0 m/s, whereas Concord Oval and St Lukes Park had median values of 1.0-1.1 m/s. Differences between anemometer types can affect low wind speeds, but would not be expected to have a large effect on the median. It therefore seems likely that other factors, such as the local topography or the presence of trees, are more important. This was an important consideration in terms of how the models were evaluated in the study.

Summaries of the average temporal patterns in wind speed at the Concord Oval (at a height of 2 metres) and St Lukes Park (at a height of 10 metres) stations for the meteorological and dispersion model evaluation periods are provided in Figure 27 and Figure 28 respectively. It should be noted that the data for March to October in the 'month' plot of Figure 28 are inferred by the function and should be ignored. These plots show the following:

- The average wind speed patterns were very similar at the Concord Oval and St Lukes Park monitoring stations.
- Wind speeds are lowest (less than 1 m/s) during the night-time, and start to increase after sunrise. The earlier sunrise in the summer months is reflected in the increase at around 06:00 for the dispersion model evaluation period, compared with the later increase for the full calendar year of 2015.
- Average wind speeds are considerably higher in summer than in winter, and this is again reflected in the higher average wind speeds during the dispersion model evaluation period than the meteorological model evaluation period.

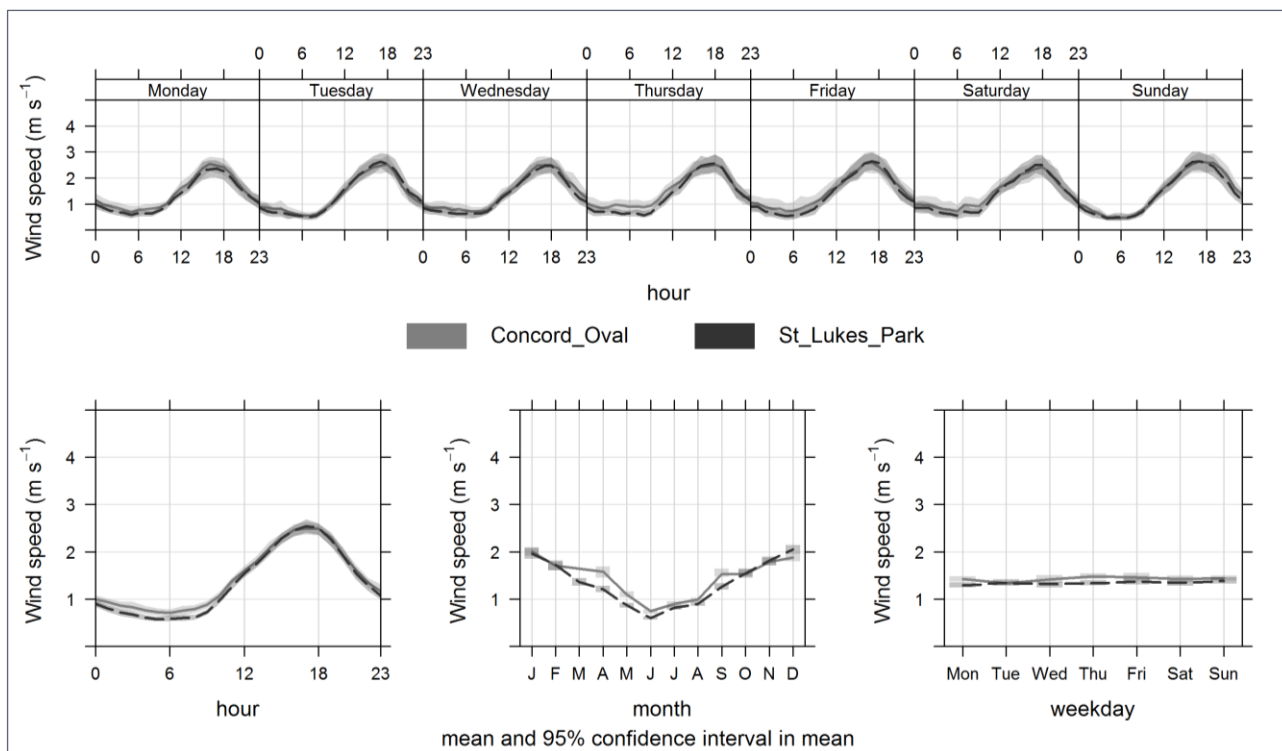


Figure 27: Openair timeVariation plot for wind speed at Concord Oval and St Lukes Park monitoring stations (2015)

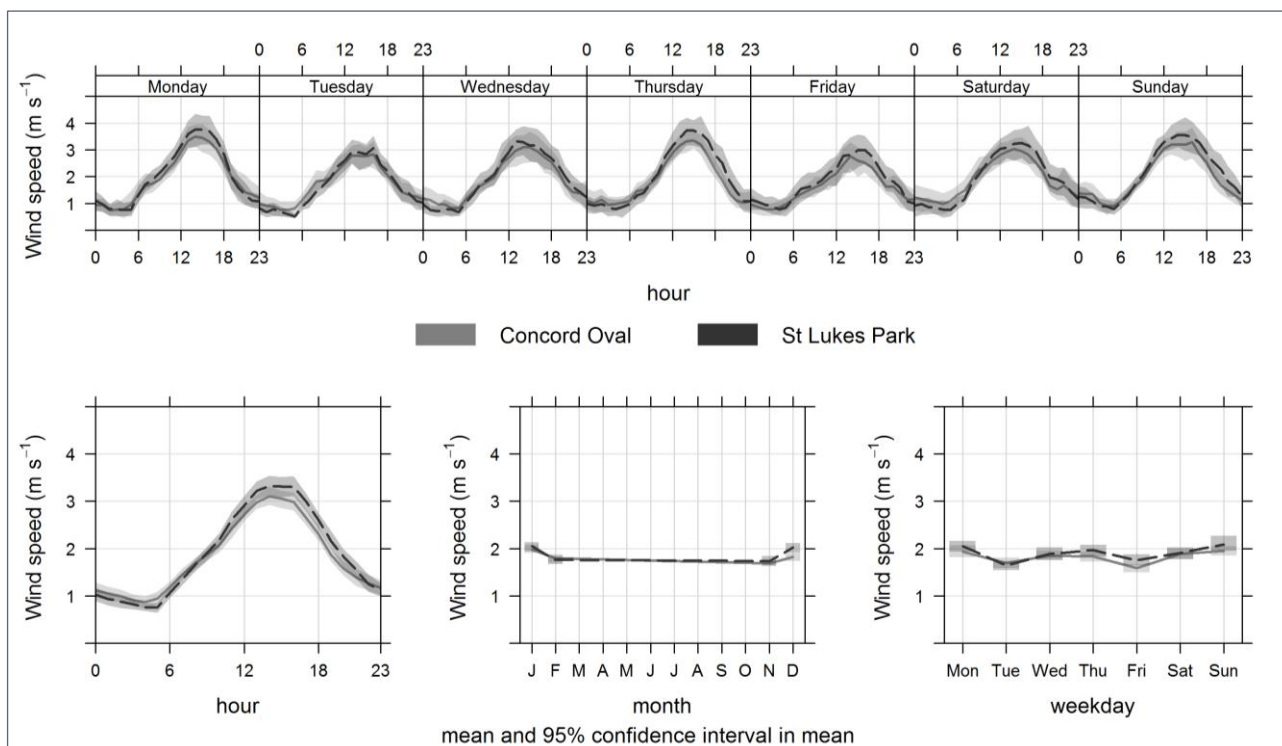


Figure 28: Openair timeVariation plot for wind speed at Concord Oval and St Lukes Park monitoring stations (November 2016 to February 2017)

The average patterns masked the shorter-term differences between the two sites. For example, in Figure 29 the observed hourly wind speed and wind direction values at St Lukes Park are compared with those at Concord Oval. Again, the observations are compared separately for the meteorological and dispersion model evaluation periods. The following points are noted:

- There was a reasonably good overall agreement between the wind speeds at the two sites.
- Two separate groups were apparent at higher wind speeds (and possibly also at lower wind speeds). For some hours, the wind speeds at St Lukes Park showed a good agreement with those at Concord Oval. For other hours, the wind speeds at St Lukes Park were markedly lower than those at Concord Oval. The meteorological data for these two groups were examined further. The two groups of data could be distinguished in terms of wind direction at Concord Oval (Figure 30). Whilst there were exceptions, the hours with a southerly wind direction at Concord Oval (i.e. winds from the direction of Parramatta Road) had higher wind speeds at Concord Oval than at St Lukes Park. It may be the case that these higher wind speeds are due to a road traffic influence. The results may also have been influenced by trees to the south of both measurement stations (these were slightly closer to the monitoring station at St Lukes Park than at Concord Oval).
- Although there is a broad agreement between the wind directions at the two sites, there are clearly some large differences during individual hours, and this could have a significant impact on the evaluation of the model predictions at the monitoring sites. For example, in a given hour the St Lukes Park wind data could indicate that the Concord Oval monitoring station is upwind of Parramatta Road, whereas the Concord Oval wind data could define the monitoring station as being downwind of Parramatta Road.

Additional analyses of the wind speed and wind direction data are provided as part of the model evaluation results in Appendix E. These include annual and seasonal wind roses, and separate consideration of wind speed and wind direction.

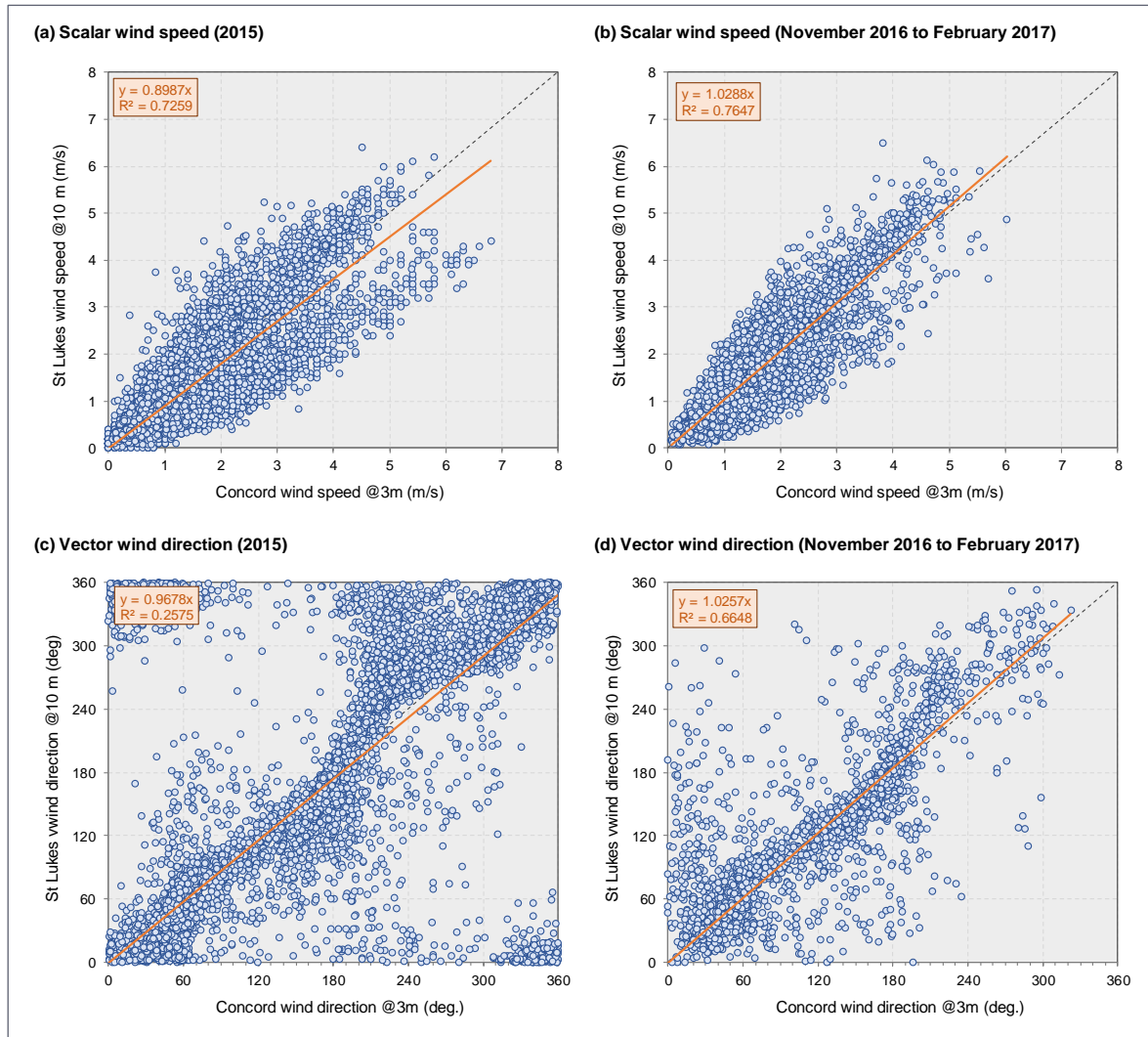


Figure 29: Observed wind speed and wind direction at Concord Oval and St Lukes Park

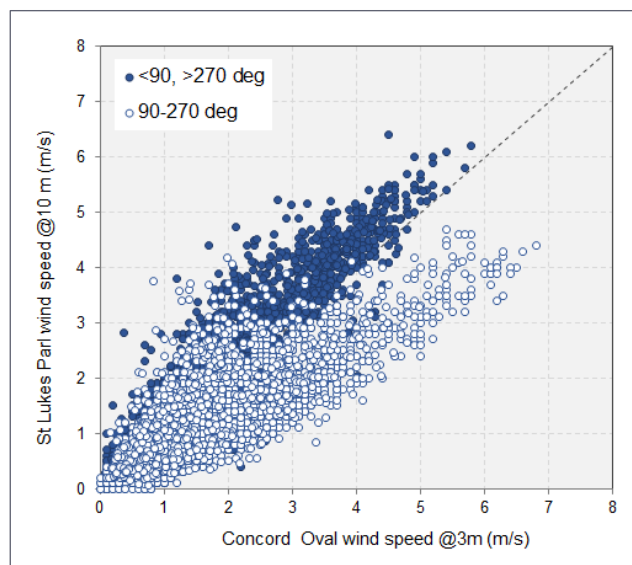


Figure 30: Observed wind speed at Concord Oval and St Lukes Park, by wind direction at Concord Oval (2015)

5.5 Continuous air pollution monitoring

5.5.1 Statistical overview

Statistical summaries of the air quality monitoring data for Concord Oval and St Lukes Park are given in Table 22 and Table 23. The level of data availability was high, and for all parameters it was very close to or greater than 90%.

Although they were not especially relevant to the study, the NSW air quality criteria, and any exceedances of these, are also included in the Tables. There was only one exceedance of a criterion, and this was for the 24-hour value for PM₁₀ (see section 5.5.2).

5.5.2 Temporal analysis

5.5.2.1 All data for Concord Oval and St Lukes Park

The full hourly concentration profiles of NO_x, NO₂, PM₁₀ and PM_{2.5} at Concord Oval and St Lukes Park between November 2016 and February 2017 are shown in Figure 31. These plots have been included mainly to illustrate the variability of the data (typical for air pollution measurements) and the presence of short-term peaks, especially in the case of PM₁₀. In particular, there was a large peak in PM₁₀ at Concord Oval between 14:00 and 18:00 on 14 January 2017.

The temporal patterns in the monitoring data were examined in more detail using the `timeVariation` function, as shown in Figure 32 to Figure 35. The variation of a pollutant by time of day and day of week can reveal useful information concerning the likely sources. For example, road vehicle emissions tend to follow regular patterns both on a daily and weekly basis. The `timeVariation` function produces four plots: day of the week variation, average hour of day variation and a combined hour of day – day of week plot and a monthly plot. Also shown on the plots is the 95% confidence interval in the average. For model evaluation it is important to consider the difference between observations and modelled values over these different time scales (Carslaw, 2015). The average diurnal weekday profiles for NO_x, NO, NO₂ and O₃ (note that the units here are ppb) are also shown in Figure 36, along with the corresponding profiles for traffic volume on Parramatta Road, wind speed and solar radiation.

Table 22: Summary of continuous air pollution measurements: Concord Oval (November 2016 to February 2017)

Statistic	Pollutant										
	CO		NO	NO ₂	NO _x	O ₃		PM ₁₀		PM _{2.5}	
	1-hour mg/m ³	Rolling 8-h mg/m ³	1-hour µg/m ³	1-hour µg/m ³	1-hour µg/m ³	1-hour µg/m ³	Rolling 4-h µg/m ³	1-hour µg/m ³	24-hour µg/m ³	1-hour µg/m ³	24-hour µg/m ³
Availability											
Possible values	2,880	2,873	2,880	2,880	2,880	2,880	2,877	2,880	120	2,880	120
Valid values	2,720	2,845	2,651	2,651	2,651	2,682	2,794	2,714	115	2,702	115
Availability (%)	94%	99%	92%	92%	92%	93%	97%	94%	96%	94%	96%
Concentration statistics											
Average value	0.41	0.40	35.1	21.6	56.7	29.3	28.9	23.9	23.7	9.1	9.0
Maximum value	1.39	1.18	396.6	97.7	471.5	162.2	154.3	619.4	76.7	50.1	17.4
2nd highest value	1.38	1.17	312.2	91.9	392.8	161.4	150.9	322.6	39.6	46.3	15.6
3rd highest value	1.32	1.13	311.6	88.5	381.2	157.0	149.4	233.2	38.8	43.6	15.2
4th highest value	1.26	1.11	298.9	87.6	364.6	152.3	142.3	126.3	37.6	42.6	14.8
5th highest value	1.25	1.07	292.7	85.1	355.2	152.3	135.6	110.2	35.9	42.5	14.3
Minimum value	0.07	0.12	-4.1 ^(a)	-8.8	-8.4	-5.8	-2.8	-6.9	12.4	-9.0	4.1
99th percentile	0.98	0.78	202.0	71.6	256.4	107.6	102.3	56.3	39.5	29.5	15.6
98th percentile	0.87	0.73	159.5	62.2	209.2	90.5	83.0	50.7	38.4	24.2	15.1
95th percentile	0.73	0.64	127.1	52.3	173.6	68.4	65.2	43.1	35.2	20.3	13.9
90th percentile	0.63	0.57	94.2	45.2	138.4	55.2	52.9	37.2	32.6	17.0	13.3
75th percentile	0.50	0.48	48.2	31.9	78.5	38.6	38.1	29.4	27.0	12.7	10.9
50th percentile (median)	0.37	0.39	17.9	18.2	38.0	26.7	26.6	22.0	22.7	8.4	8.5
25th percentile	0.27	0.30	4.9	8.8	15.8	14.1	14.8	15.8	18.2	4.8	6.5
Exceedance statistics											
Standard	30	10	-	246	-	214	171	-	50	-	25
Exceedances (Nov-Feb)	0	0	-	0	-	0	0	-	1	-	0

(a) Negative concentrations can be observed in measurements due to errors in measurement techniques and limitations of calibration procedure.

Table 23: Summary of continuous air pollution measurements: St Lukes Park (November 2016 to February 2017)

Statistic	Pollutant										
	CO		NO	NO ₂	NO _x	O ₃		PM ₁₀		PM _{2.5}	
	1-hour mg/m ³	Rolling 8-h mg/m ³	1-hour µg/m ³	1-hour µg/m ³	1-hour µg/m ³	1-hour µg/m ³	Rolling 4-h µg/m ³	1-hour µg/m ³	24-hour µg/m ³	1-hour µg/m ³	24-hour µg/m ³
Availability											
Possible values	2,880	2,873	2,880	2,880	2,880	2,880	2,877	2,880	120	2,880	120
Valid values	2,654	2,762	2,622	2,622	2,622	2,616	2,722	2,566	110	2,565	110
Availability (%)	92%	96%	91%	91%	91%	91%	95%	89%	92%	89%	92%
Concentration statistics											
Average value	0.27	0.27	7.3	16.3	23.6	41.9	41.4	19.6	19.4	7.6	7.5
Maximum value	1.17	0.88	223.1	89.3	308.3	196.4	164.2	162.6	35.9	39.6	15.1
2nd highest value	1.00	0.87	191.3	88.6	265.7	181.5	157.2	129.7	32.8	38.6	14.8
3rd highest value	0.96	0.83	183.2	85.2	253.4	177.8	156.1	103.2	31.2	35.2	13.6
4th highest value	0.96	0.80	182.4	80.7	232.4	173.0	155.1	72.4	30.7	33.4	13.0
5th highest value	0.96	0.76	162.9	79.7	224.3	172.3	155.0	70.4	30.4	33.3	12.9
Minimum value	0.00	0.02	-5.3	-1.8	-1.4	-0.7	0.2	-1.0	8.5	-9.6	1.4
99th percentile	0.66	0.55	100.5	62.0	148.5	136.1	125.2	50.7	32.7	24.0	14.7
98th percentile	0.55	0.49	66.4	52.3	108.9	114.1	108.7	44.8	31.1	21.6	13.5
95th percentile	0.45	0.42	30.5	43.4	70.2	91.8	86.3	37.2	29.9	17.5	12.3
90th percentile	0.39	0.38	14.9	34.4	48.6	72.9	70.8	32.0	27.7	14.6	11.1
75th percentile	0.32	0.32	6.0	21.9	28.0	52.7	51.9	24.5	23.1	10.8	9.6
50th percentile (median)	0.26	0.26	2.2	12.3	15.3	39.6	38.9	18.2	19.2	7.1	7.4
25th percentile	0.20	0.22	0.8	6.8	8.3	25.3	25.9	12.5	14.6	3.7	5.1
Exceedance statistics											
Standard	30	10	-	246	-	214	171	-	50	-	25
Exceedances (Nov-Feb)	0	0	-	0	-	0	0	-	0	-	0

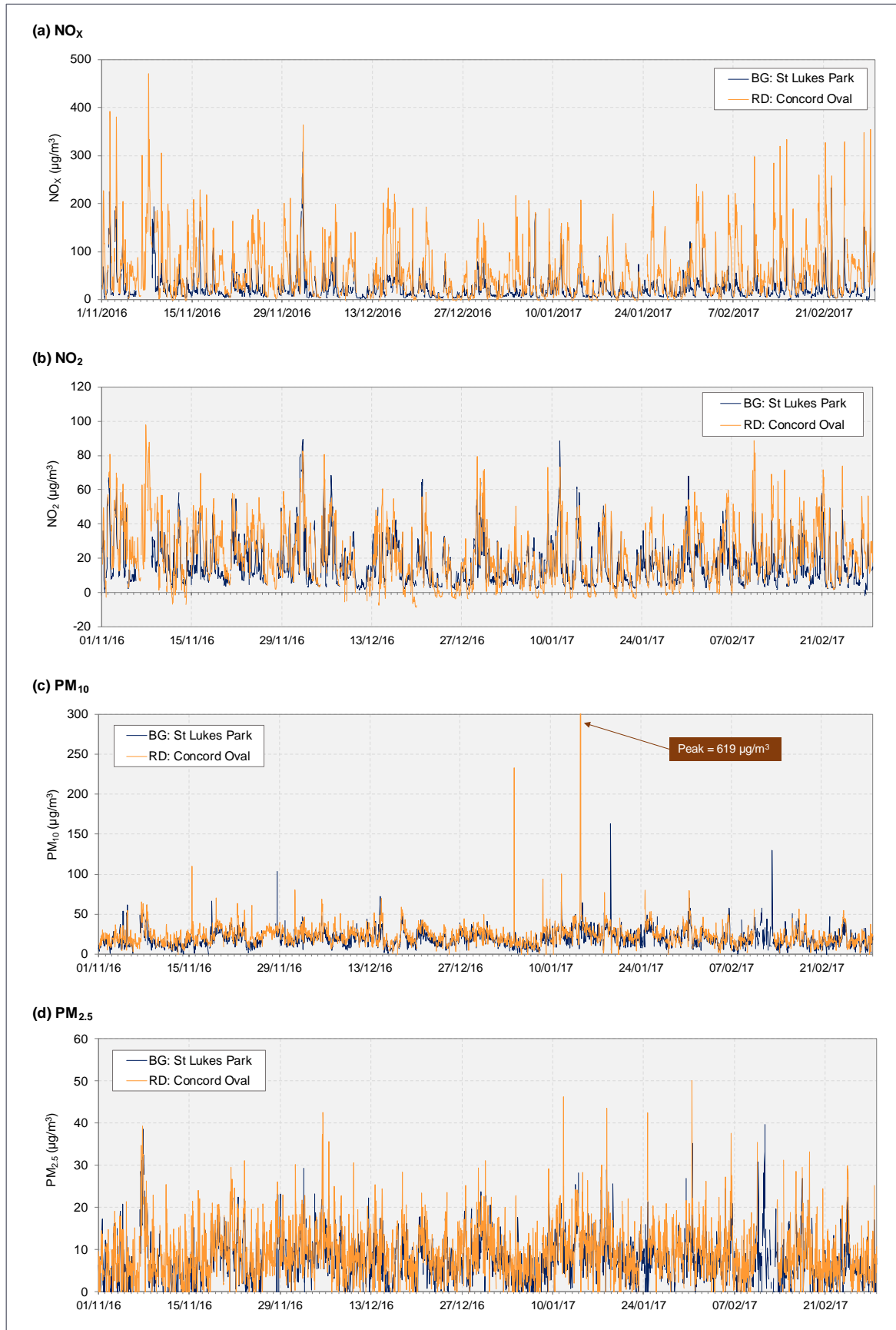


Figure 31: Hourly average pollutant concentrations at Concord Oval and St Lukes Park

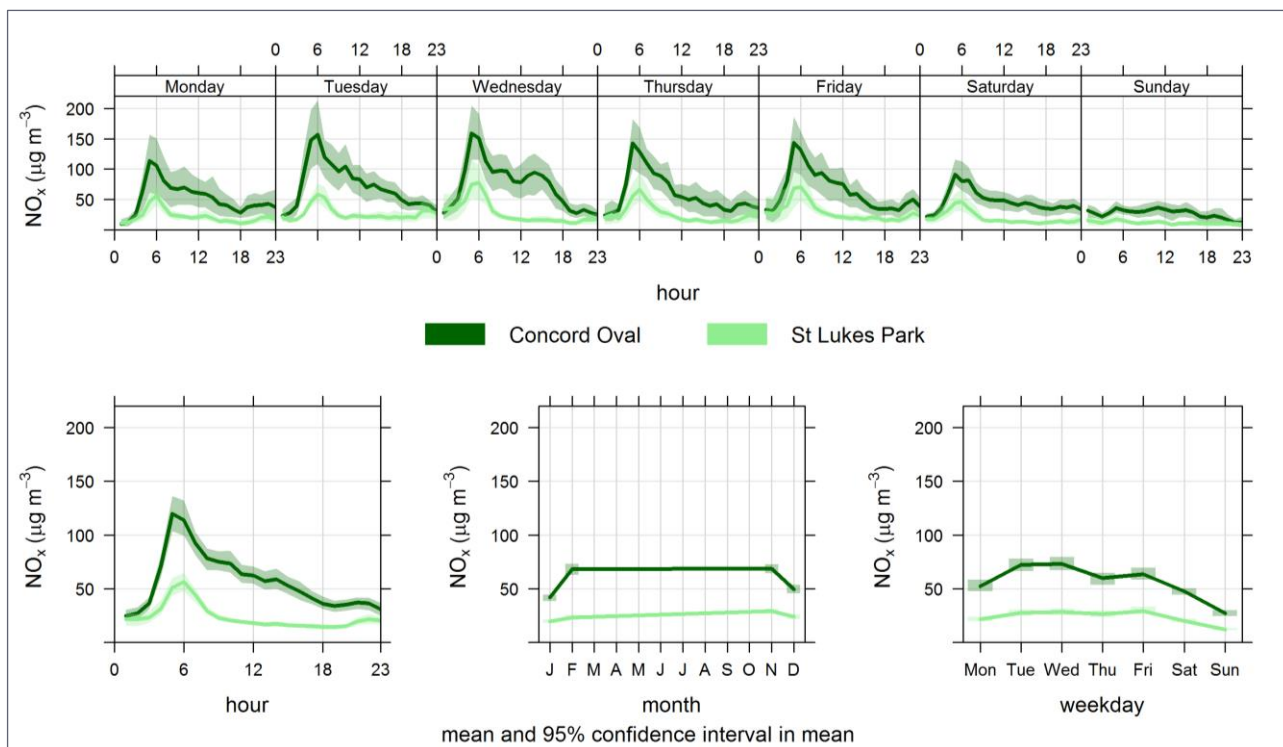


Figure 32: Openair timeVariation plot for NO_x at Concord Oval and St Lukes Park monitoring stations

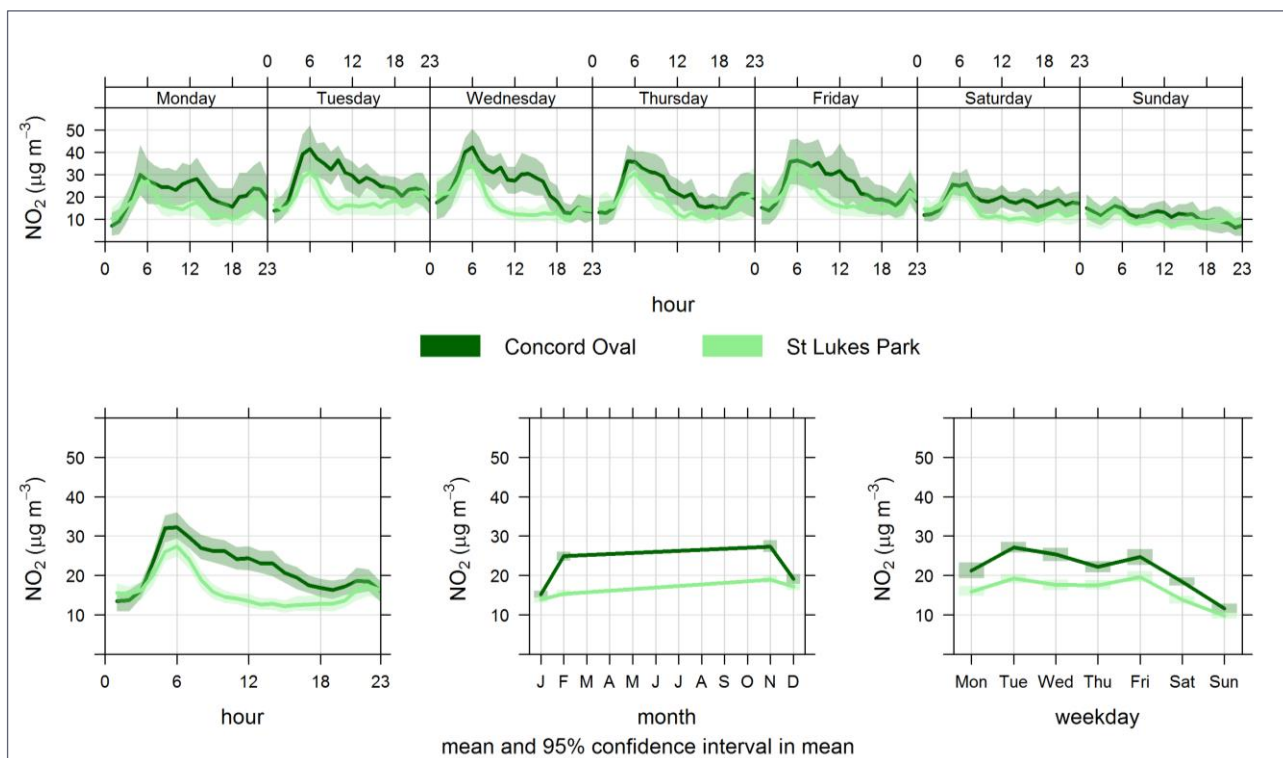


Figure 33: Openair timeVariation plot for NO_2 at Concord Oval and St Lukes Park monitoring stations

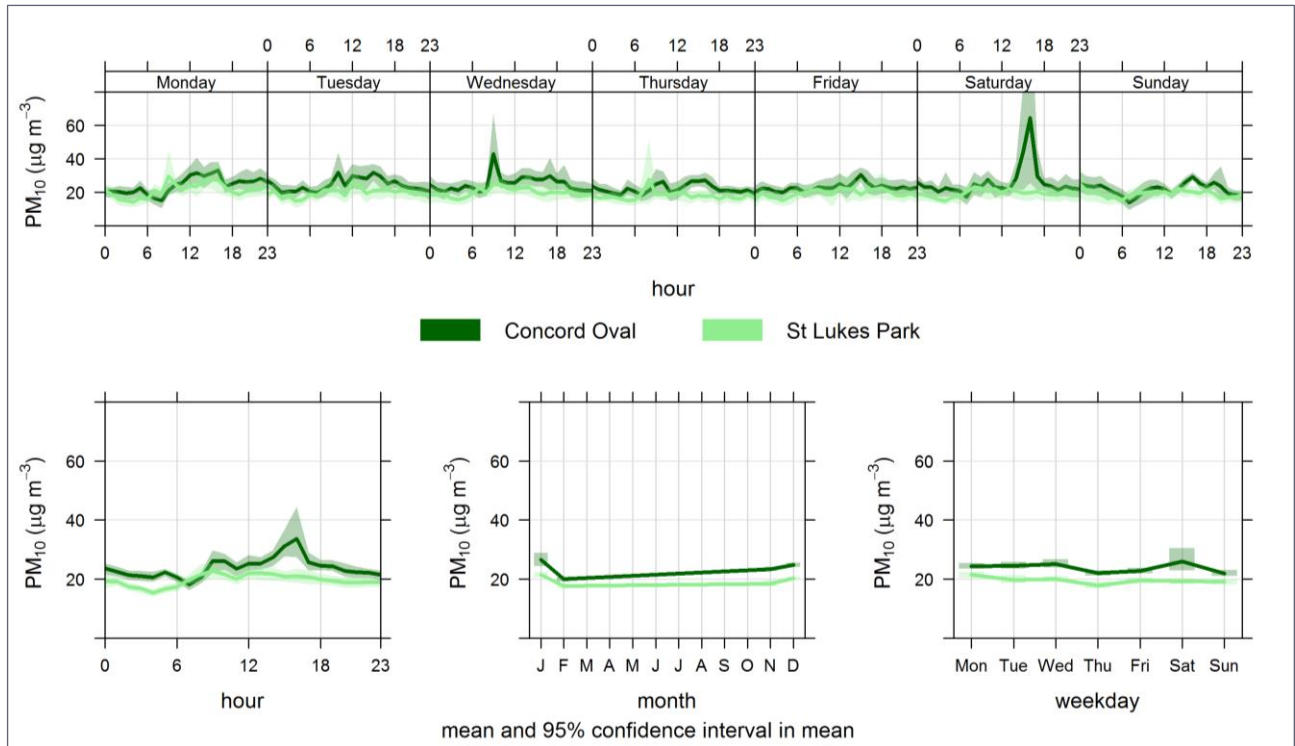


Figure 34: Openair timeVariation plot for PM₁₀ at Concord Oval and St Lukes Park monitoring stations

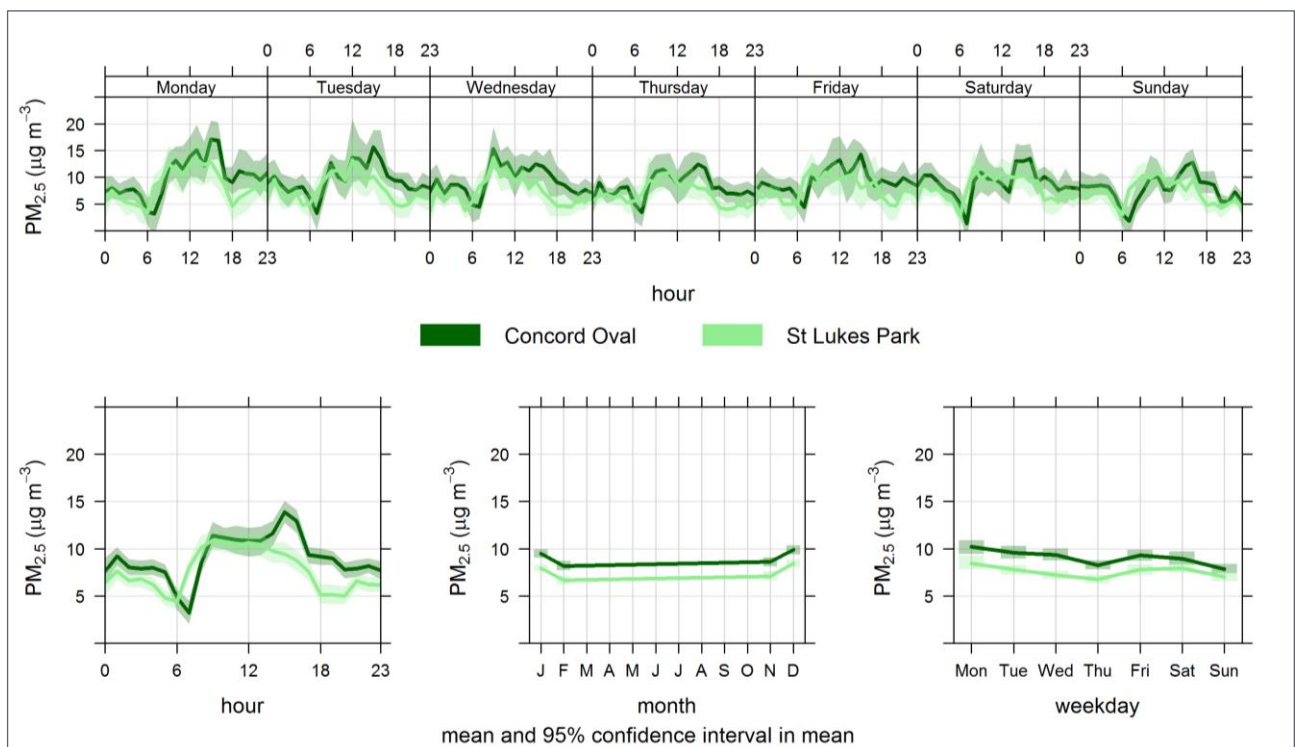


Figure 35: Openair timeVariation plot for PM_{2.5} at Concord Oval and St Lukes Park monitoring stations

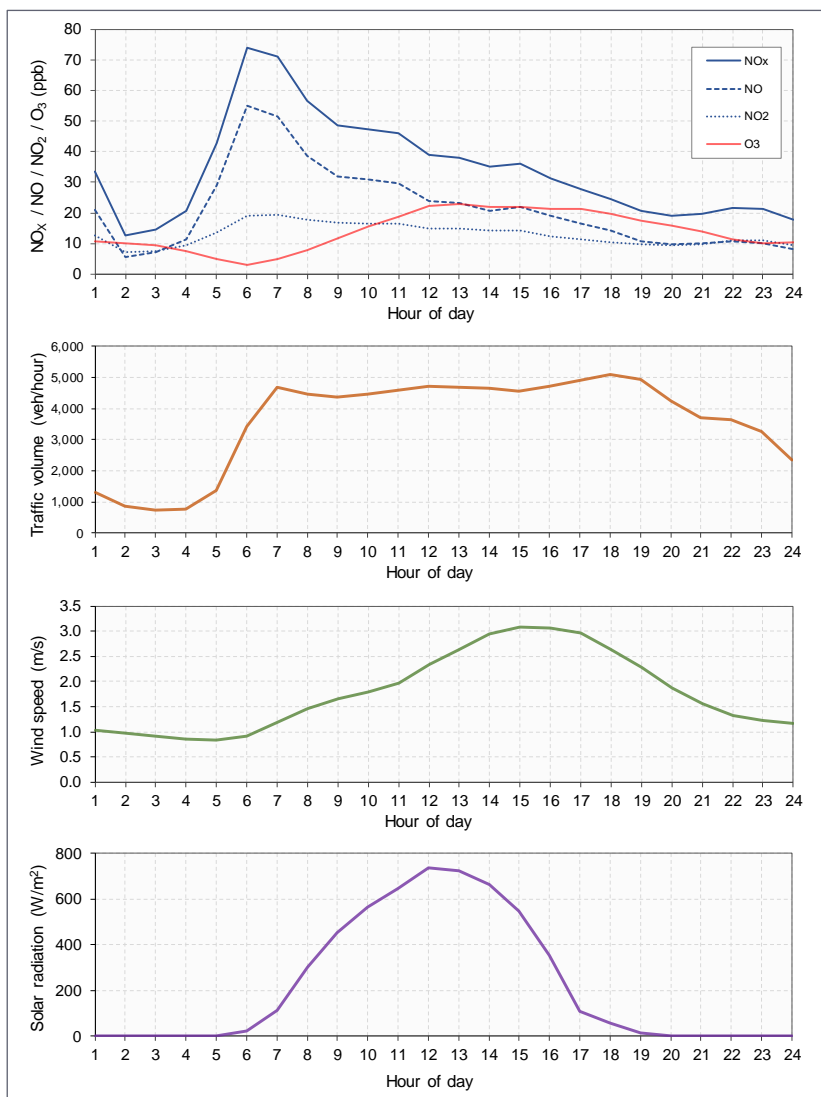


Figure 36: Average weekday profiles for nitrogen oxides, ozone and other parameters at Concord Oval monitoring station

5.5.2.2 Comparison between St Lukes Park and OEH stations

Background sites are located so as to characterise regional air quality, and therefore the data ought to show similar patterns from site to site, albeit with some variation in absolute concentrations. To further investigate the validity of St Lukes Park as a background site, the patterns in the NO_x data were compared with those from several OEH sites

In the recent EIS for the WestConnex M4-M5 Link project, the air quality data from the St Lukes Park monitoring station were compared with the corresponding data from the OEH stations at the Chullora, Earlwood, Randwick and Rozelle sites for the period between August 2014 and February 2017 (Pacific Environment, 2017). The Randwick and Rozelle sites were outside the study area. A summary for NO_x is provided in Figure 39, which presents the time series of concentrations as follows:

- The mean concentration by week. Although none of the air quality criteria relate to a one-week averaging period, this was chosen as a convenient way of representing the whole monitoring period while retaining some of the temporal detail.

- The mean, 75th percentile, 98th percentile and maximum 1-hour concentrations by month. Air quality data are not normally distributed. Most of the measurements tend to be at fairly low values, but there is usually a tail containing higher values (i.e. short-term peaks). The percentile plots are included to show underlying patterns in the data by excluding the highest values.

Although NO_x concentrations at St Lukes Park were generally within the range of concentrations at the OEH sites, the peak values at St Lukes Park tended to be at the upper end of the range.

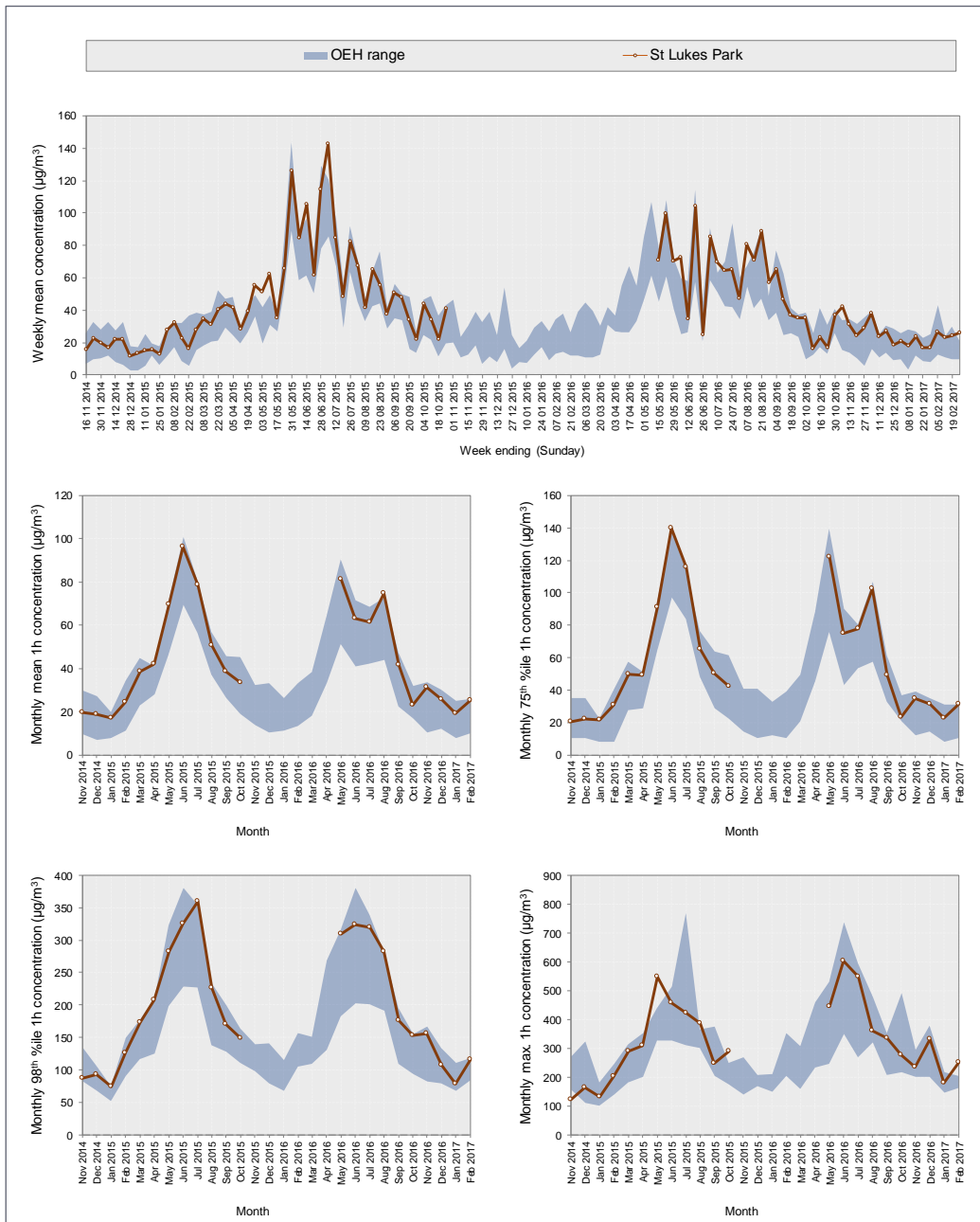


Figure 37: NO_x concentrations at St Lukes Park background air quality monitoring site and OEH background sites (blue shading shows range of values at OEH sites)

Figure 38 shows the Openair `timeVariation` plot for NO_x at St Lukes Park and the four OEH monitoring stations during the period of the dispersion modelling study. The zero concentrations in the early morning at the OEH sites are essentially gaps in the data due to instrument calibration periods. It can be seen that the St Lukes park data are broadly representative of regional air quality in the Sydney area. The morning peak in concentration is present at all sites, illustrating the regional influence of road traffic. It is worth noting that the Randwick site has especially low concentrations on account of its location near to the coast (easterly winds will be associated with very low NO_x).

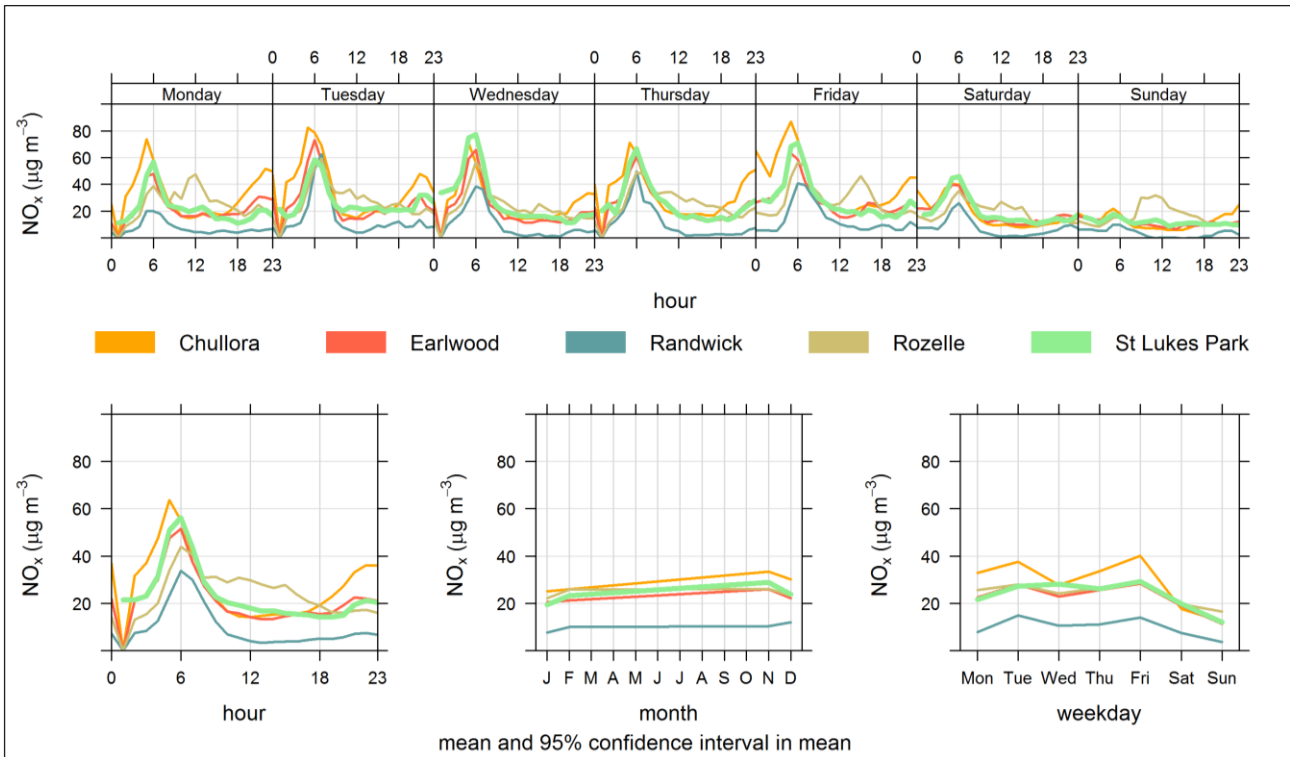


Figure 38: Openair `timeVariation` plot for NO_x at St Lukes Park and OEH monitoring stations (November 2016 to February 2017)

5.5.2.3 Summary

The findings are summarised by pollutant and location as follows:

- NO_x

- Concord Oval

- On weekdays NO_x concentrations tended to increase from a night-time low to quite a sharp peak at 05:00-06:00. Concentrations then decreased almost linearly during the remainder of the daylight period, with a small second peak in the late evening. This can be explained as follows:
 - Between 05:00 and 06:00 a sharp increase in emissions from the traffic (see Figure 26) is combined with low wind speeds at the end of the night-time period (see Figure 28), leading to high concentrations.

- Whilst traffic emissions are maintained between 06:00 and mid-afternoon, the wind speed is generally increasing, resulting in improved dispersion. The net effect is a gradual reduction in concentrations from the earlier peak.
- Traffic levels remain high into the late evening, but with a reduced number of HDVs. Wind speeds are decreasing in the late afternoon. These effects combine to produce the smaller late evening peak in concentrations.
- o Peak concentrations were lower at the weekend (especially on Sunday) than on weekdays. Meteorology does not differ, on average, between weekdays and weekends (see Figure 28), and therefore this would have been a consequence of differences in traffic emissions (see Figure 26).

St Lukes Park

- o The NO_x concentration profiles were similar to those for Concord Oval, but much flatter. For example, the highest concentrations occurred around 05:00-06:00 on weekdays, with lower concentrations on Saturdays and Sundays. This suggests a small general road traffic influence on NO_x concentrations at St Lukes Park, but the data from the OEH sites show that this is a regional effect and not just a feature of the St Lukes Park data.

'Road increment'

- o The difference between the NO_x concentrations at Concord Oval and St Lukes Park (the 'road increment') varied with time of day. On weekdays it ranged from close to zero between 01:00 and 02:00 to around 80 µg/m³ between 05:00 and 06:00.
- **NO₂**
 - o For NO₂ the weekday differences between the concentrations at Concord Oval and St Lukes Park were smaller than those for NO_x and peaked later in the day. The weekday 'road increment' ranged from a slightly negative value (around -3 µg/m³) between 01:00 and 02:00 to around 14 µg/m³ between 10:00 and 11:00.
- **PM₁₀ and PM_{2.5}**
 - o There was no consistent diurnal pattern in PM₁₀ concentration. Notwithstanding the large spike in PM₁₀ at Concord Oval on 14 January, there was little difference between the concentrations at Concord Oval and St Lukes Park, and hence no clear road traffic influence. The weekday road increment ranged from -1 µg/m³ to +9 µg/m³, was it not clearly related to traffic.
 - o PM_{2.5} had a stronger diurnal pattern, but it was not the same as that for NO_x and this suggests a more important contribution from non-road sources. Again, there was little difference between concentrations at the roadside and background sites.

5.5.3 Directional analysis

5.5.3.1 Polar plots

The directional analysis of air pollution at the two monitoring stations was firstly undertaken using the `polarPlot` and `polarAnnulus` functions in `Openair`, and the resulting plots are given in Figure 39 to Figure 46 for Concord Oval, and in Figure 47 to Figure 54 for St Lukes Park.

The polar plot indicates how concentrations vary by wind speed and wind direction, with statistical smoothing techniques giving a continuous surface. The monitoring station is located at the centre of each plot. The axes show the directions from which the wind is coming, and the distance from the origin indicates the wind speed; the further from the centre that concentrations appear, the higher the wind speeds when they were measured. Calm conditions appear close to the centre. The polar plot is a useful diagnostic tool for understanding potential sources of air pollutants at a given site. For many situations an increasing wind speed generally results in lower concentrations due to increased dilution through advection and increased turbulence. Ground-level, non-buoyant sources - such as road traffic – therefore tend to have highest concentrations under low wind speed conditions, but various processes can lead to other concentration-wind speed dependencies. For example, buoyant plumes from tall outlets can be brought down to ground level, resulting in high concentrations under high wind speed conditions. Wind-blown dust (e.g. from exposed areas of soil) also increases with increasing wind speed, and particle suspension can be important close to coastal areas where higher wind speeds generate more sea spray (Carslaw, 2015).

Some typical features of polar plots include the following:

- A maximum concentration, or a 'smeared' peak, at low wind speed, which is indicative of a local, ground-level source such as road traffic. As the wind speed increases concentrations due to a road source will tend to decrease due to the increased dilution of the plume.
- Highly resolved features at high wind speeds, but possibly low concentrations, which indicate more distant point sources.

In addition, relationships between pollutants can provide information on the emission characteristics of different sources.

The polar annulus plot is useful for illustrating how the concentration of a pollutant varies by wind direction and time period. Plotting as an annulus helps to reduce compression of information towards the centre of the plot. The inner part of the annulus represents the earliest time and the outer part of the annulus the latest time. In this analysis, the time dimension is hour of day.

The polar plots for NO_x and NO_2 at Concord Oval clearly illustrate the smeared peak across a range of low wind speeds that is characteristic of a road traffic source, and the dominant influence of southerly winds shows that there is a strong influence of the traffic on Parramatta Road to the south of the monitoring site. The highest PM_{10} and $\text{PM}_{2.5}$ concentrations, on the other hand, occur only for higher wind speeds.

At St Lukes Park there are no strong directional influences from roads on NO_x and NO_2 , indicating the nature of this station as a background site. The time variation plots in the previous Section indicated that the highest concentrations at St Lukes Park occurred around 05:00-06:00, mainly on weekdays, and coincided with the peaks at Concord Oval. However, from the polar annulus plot (Figure 51) it can be seen that the peak concentrations at St Lukes Park were more from a westerly direction than a southerly direction.

There are no highly resolved features at either monitoring site, as could generally be expected for an urban area of this type (i.e. there are no large-scale point sources).

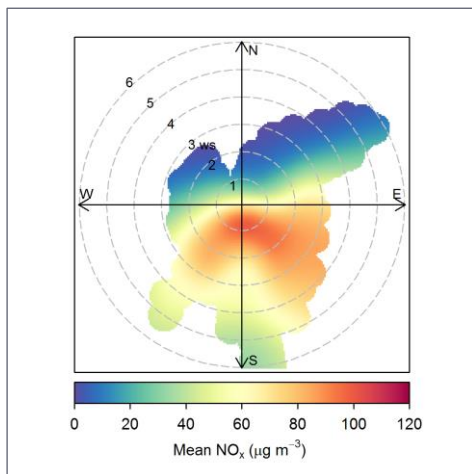


Figure 39: Polar plot for NO_x at Concord Oval

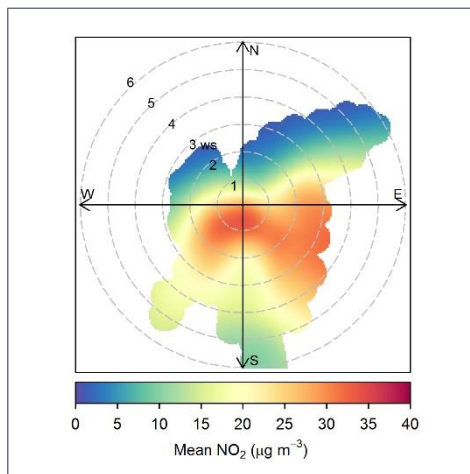


Figure 40: Polar plot for NO₂ at Concord Oval

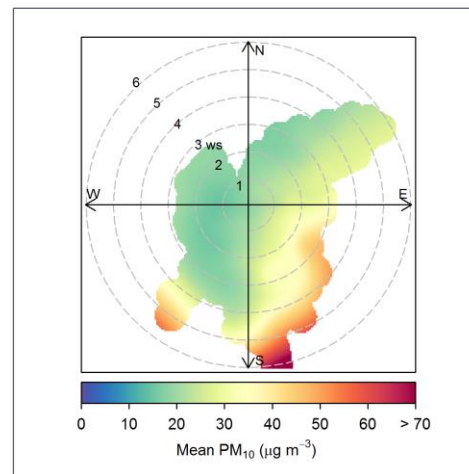


Figure 41: Polar plot for PM₁₀ at Concord Oval

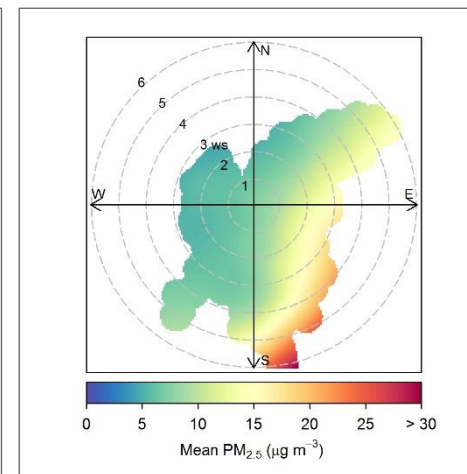


Figure 42: Polar plot for PM_{2.5} at Concord Oval

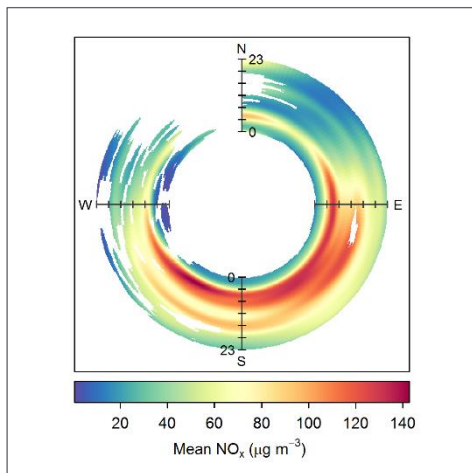


Figure 43: Polar annulus for NO_x at Concord Oval

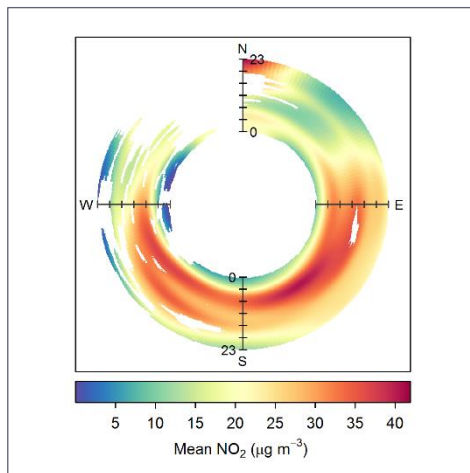


Figure 44: Polar annulus for NO₂ at Concord Oval

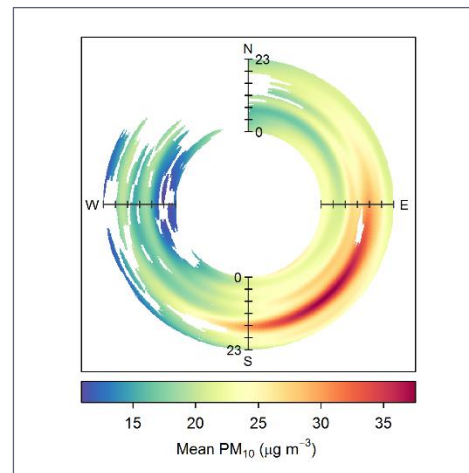


Figure 45: Polar annulus for PM₁₀ at Concord Oval

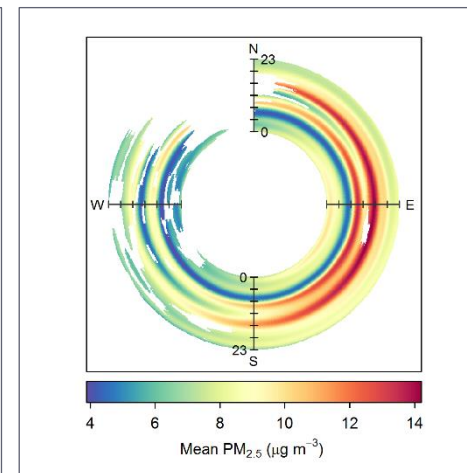


Figure 46: Polar annulus for PM_{2.5} at Concord Oval

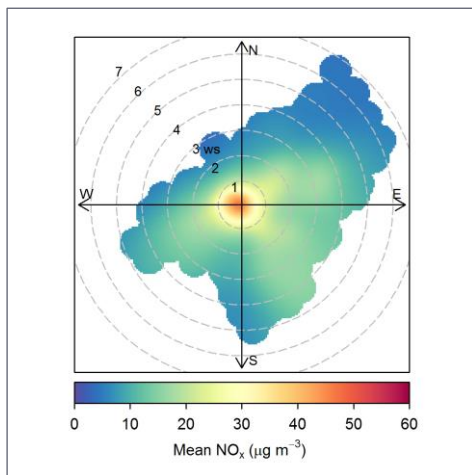


Figure 47: Polar plot for NO_x at St Lukes Park

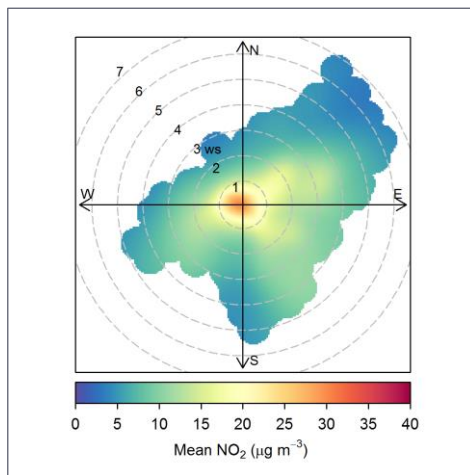


Figure 48: Polar plot for NO₂ at St Lukes Park

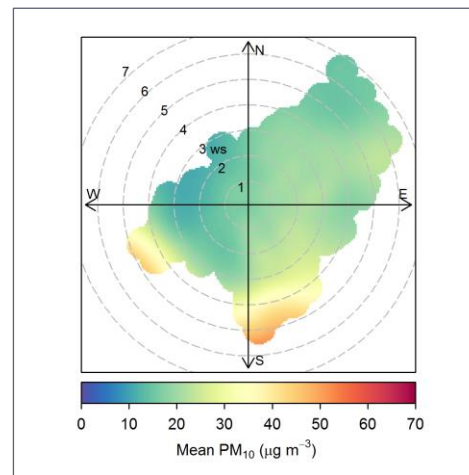


Figure 49: Polar plot for PM₁₀ at St Lukes Park

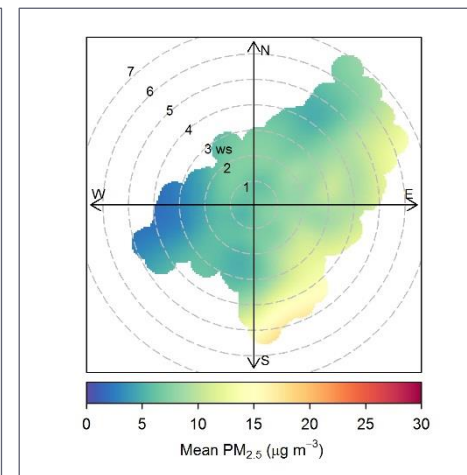


Figure 50: Polar plot for PM_{2.5} at St Lukes Park

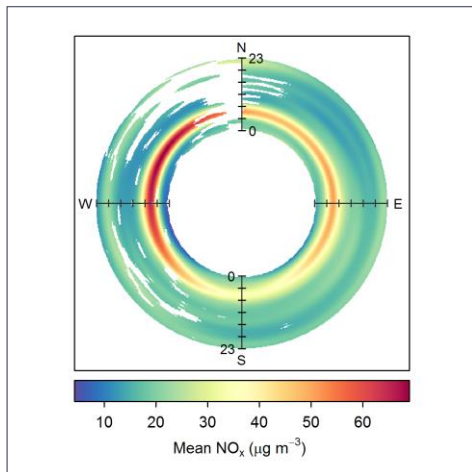


Figure 51: Polar annulus for NO_x at St Lukes Park

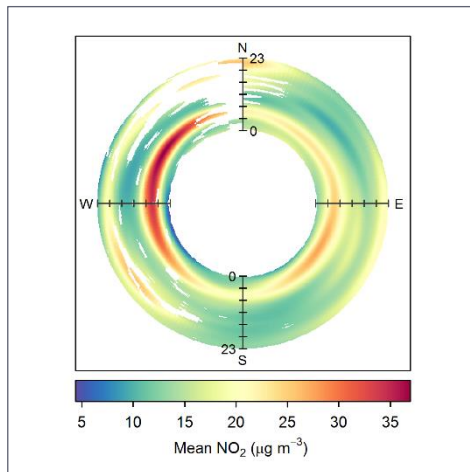


Figure 52: Polar annulus for NO₂ at St Lukes Park

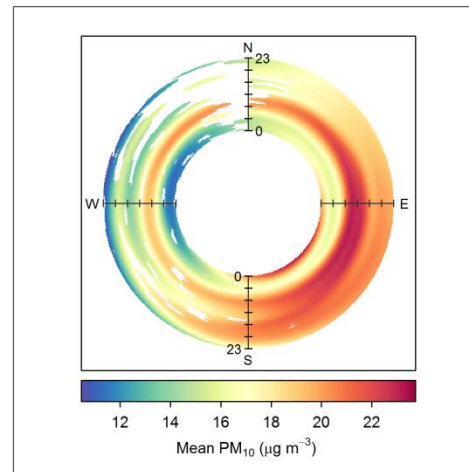


Figure 53: Polar annulus for PM₁₀ at St Lukes Park

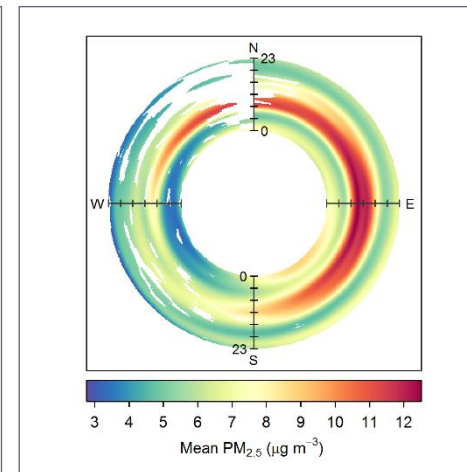


Figure 54: Polar annulus for PM_{2.5} at St Lukes Park

For the NO_x road increment at Concord Oval the corresponding `polarPlot` and `polarAnnulus` plots are given in Figure 55 and Figure 56. Apart from the lower values of the increment than the total (note the lower concentration scale), these plots are similar to those for total NO_x. However, a little more detail appears to be resolved. In particular, the peak concentrations are to the south-east of the monitoring site. This is probably an effect of the junction between Parramatta Road and Shaftesbury Road, as well as the bus depot. It also appears that there is a large increment from this direction at all times of day, which may be related to bus movements at the depot.

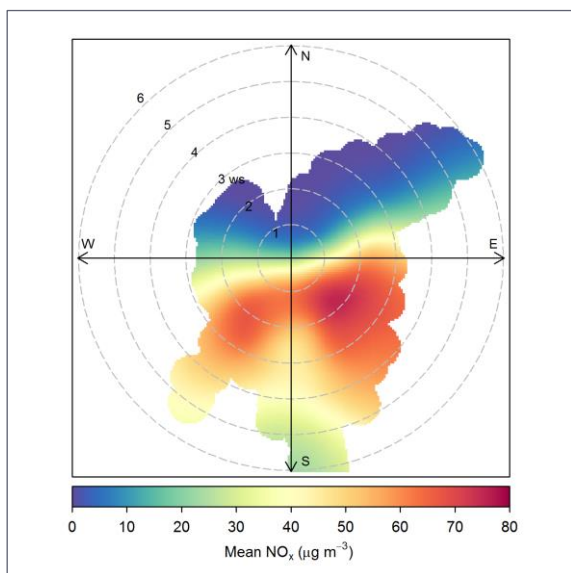


Figure 55: Polar plot - observed NO_x (total) at Concord Oval

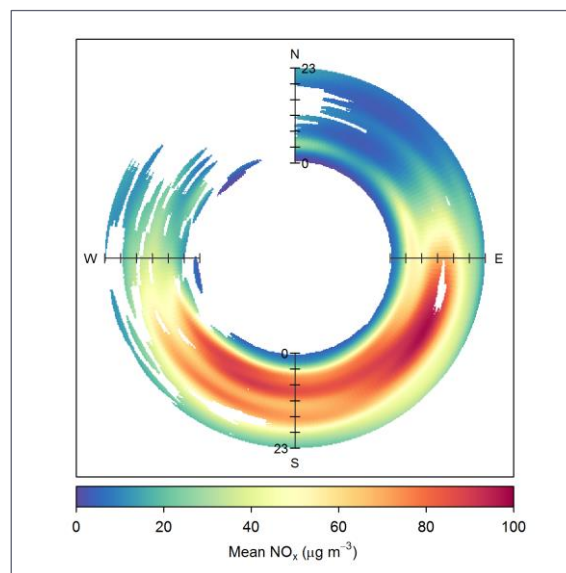


Figure 56: Polar annulus - observed NO_x (road increment) at Concord Oval

5.5.3.2 Wind direction filtering

The pollutant concentrations at Concord Oval and St Lukes Park were filtered by wind direction, with the measurements being sub-divided into 24 15-degree wind direction sectors (Figure 57). Parramatta Road has an approximately east-west alignment near the Concord Oval monitoring station. The monitoring station was considered to be upwind of Parramatta Road when the wind direction was within $\pm 45^\circ$ of a line approximately perpendicular to the road at a wind direction of 15° (i.e. wind directions from 330° and 60°). Similarly, the monitoring station was taken to be downwind of Parramatta Road when the wind direction was between 145° and 235° .

The contemporaneous 'upwind' concentrations at the Concord Oval roadside site were compared with those at the St Lukes Park background site. The latter were also filtered to remove all concentration measurements other than those for wind directions towards Concord Oval. Figure 58 shows that - for NO_x and NO₂ - there was a very strong agreement ($R^2 = 0.83-0.85$), indicating that St Lukes Park was a suitable background site for the study. For PM₁₀ and PM_{2.5} the relationship was much weaker ($R^2 = 0.06-0.23$).

For purposes of comparisons, the contemporaneous 'downwind' concentrations at the Concord Oval roadside site were compared with those at the St Lukes Park background site. In this case the latter were filtered to remove all concentration measurements other than those for wind directions from Concord Oval. The results, shown in Figure 59, illustrate the influence of Parramatta Road traffic on CO, NO_x and NO₂. For PM₁₀ and PM_{2.5} there is a weaker traffic influence.

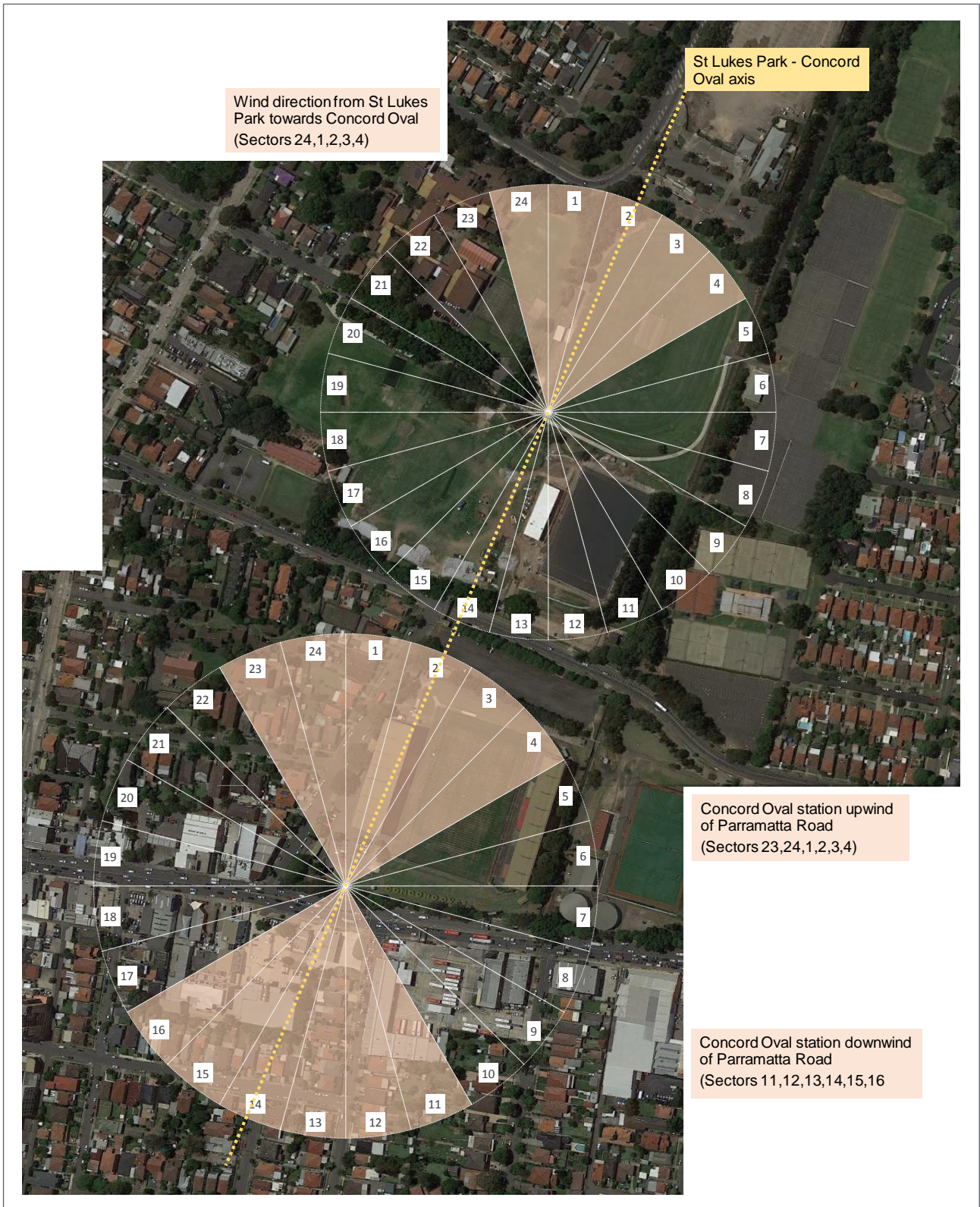


Figure 57: Division of monitoring stations into sectors

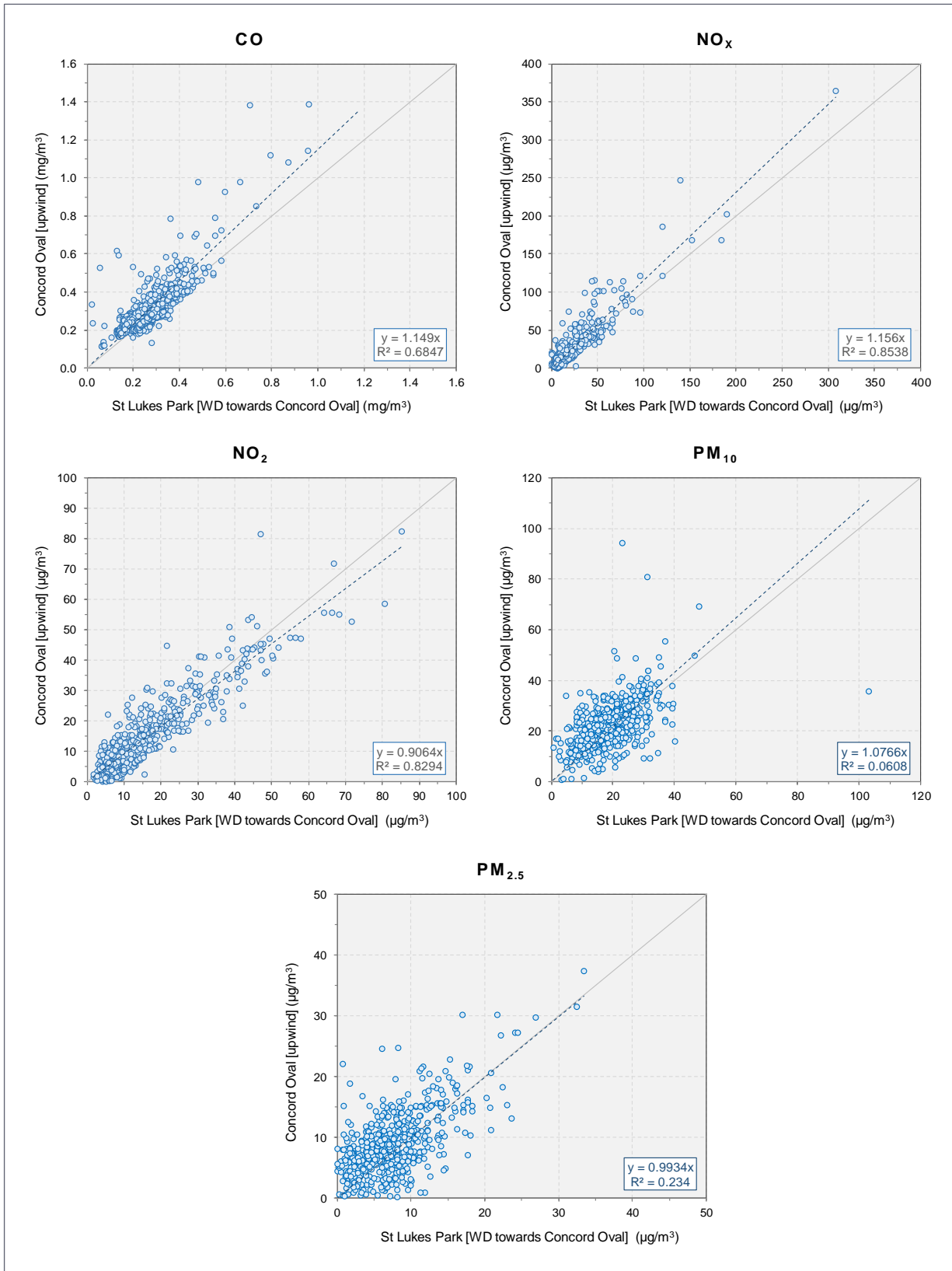


Figure 58: Relationships between pollutant concentrations at Concord Oval and St Lukes Park when both monitoring stations were upwind of Parramatta Road

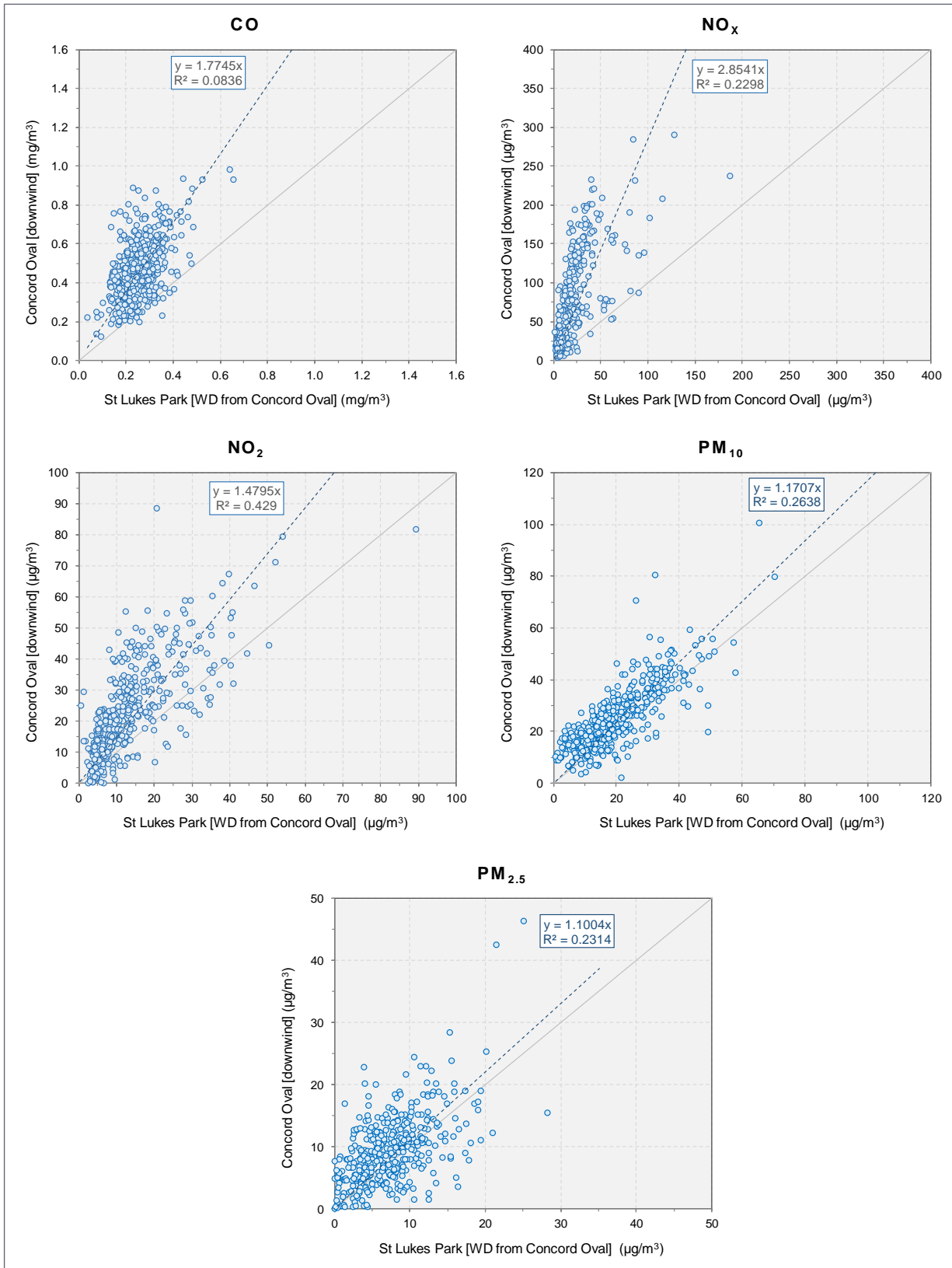


Figure 59: Relationships between pollutant concentrations at Concord Oval and St Lukes Park when both monitoring stations were downwind of Parramatta Road

5.6 Passive air pollution sampling

The passive sampling campaign was completed without any loss of, or damage to, the samplers. The measurements also showed a good level of repeatability, with the standard error on any three measurements being less than $2 \mu\text{g}/\text{m}^3$ at most locations. Almost all the measurements were within the concordance criteria.

The passive sampler results were then calibrated by comparison with reference analysers. In the calibration exercise the Ogawa results for the Concord Oval and St Lukes Park monitoring stations were compared with the average concentrations for the corresponding periods measured by the reference (chemiluminescence) analysers at each station. There were inevitably some gaps in the record from the reference analysers due to, for example, instrument calibration periods. However, the amount of data lost was typically around 5%, and calibrations took place during the night to avoid the loss of data during peak traffic period. One-hour gaps in the data associated with instrument calibration were filled using linear interpolation. Gaps of more than one hour were not filled. It was therefore assumed that the remaining gaps in the data would only have had a small or negligible effect on the period-average concentrations. The results are summarised in Table 24.

One observation was that the average blank concentrations in rounds 2 and 3 were quite high. For NO_x the average results for the blank samples in rounds 1, 2 and 3 were $1.4 \mu\text{g}/\text{m}^3$, $12.5 \mu\text{g}/\text{m}^3$ and $8.2 \mu\text{g}/\text{m}^3$ respectively. The values for rounds 2 and 3 were higher than would be normally expected in field blanks (according to Ogawa, a range of around 0.7 to $2.0 \mu\text{g}/\text{m}^3$ would be typical). Similarly, for NO_2 the average results for the blank samples in rounds 1, 2 and 3 were $0.5 \mu\text{g}/\text{m}^3$, $3.0 \mu\text{g}/\text{m}^3$ and $1.9 \mu\text{g}/\text{m}^3$ respectively, whereas according to Ogawa a typical range would be around 0.4 to $1.0 \mu\text{g}/\text{m}^3$. The triplicate blank samples had a reasonably good level of repeatability, and this suggests that a difference in the sampling procedure may have affected the results. For example, it is possible that the blank sample containers in rounds 2 and 3 were not tightly sealed and exposed inadvertently to the ambient air.

Figure 60 and Figure 61 compare the raw (not blank-adjusted) period-average NO_x and NO_2 concentrations measured by the Ogawa samplers and the reference analysers. For each pollutant a linear regression function has been fitted to the data and forced through zero. The raw NO_x values from the Ogawas showed a stronger agreement with the reference measurements (slope = 0.82, $R^2 = 0.84$) than the blank-adjusted Ogawa values (slope = 0.66, $R^2 = 0.76$ (not shown)), and therefore the calibration of the Ogawa results was applied to the raw values only. The results from the blank samples were not used. This approach was also applied to NO_2 . The raw Ogawa NO_2 data also showed a stronger agreement with the reference measurements (slope = 0.60, $R^2 = 0.69$) than the blank-adjusted values (slope = 0.50, $R^2 = 0.53$ (not shown)), although in both cases the relationship with the reference measurements was weaker than for NO_x .

Calibration factors for NO_x and NO_2 were determined as the inverse of the gradient of each regression function. That is:

$$[\text{NO}_x]_{\text{calibrated}} = 1.225 \times [\text{NO}_x]_{\text{raw}}$$

$$[\text{NO}_2]_{\text{calibrated}} = 1.677 \times [\text{NO}_2]_{\text{raw}}$$

Table 24: Co-location results for passive samplers and reference (chemiluminescence) analysers

Site	Measurement method		NO _x		NO ₂	
			Average	Std. error	Average	Std. error
Round 1 - 13 January to 25 January 2017						
Concord Oval (roadside)	Ogawa (raw)	µg/m ³	38.0	0.8	10.3	0.5
	Reference	µg/m ³	37.7	-	14.2	-
	<i>Difference (Ogawa - reference)</i>	µg/m ³	0.4	-	-3.9	-
	<i>Ratio (Ogawa/reference)</i>	-	1.01	-	0.73	-
St Lukes Park (background)	Ogawa (raw)	µg/m ³	20.2	0.3	5.6	0.2
	Reference	µg/m ³	18.1	-	13.7	-
	<i>Difference (Ogawa - reference)</i>	µg/m ³	2.0	-	-8.1	-
	<i>Ratio (Ogawa/reference)</i>	-	1.11	-	0.41	-
Round 2 - 31 January to 15 February 2017						
Concord Oval (roadside)	Ogawa (raw)	µg/m ³	53.0	0.2	13.5	0.8
	Reference	µg/m ³	66.1	-	24.6	-
	<i>Difference (Ogawa - reference)</i>	µg/m ³	-13.1	-	-11.1	-
	<i>Ratio (Ogawa/reference)</i>	-	0.80	-	0.55	-
St Lukes Park (background)	Ogawa (raw)	µg/m ³	22.5	0.1	6.1	0.1
	Reference	µg/m ³	21.9	-	15.6	-
	<i>Difference (Ogawa - reference)</i>	µg/m ³	0.6	-	-9.6	-
	<i>Ratio (Ogawa/reference)</i>	-	1.03	-	0.39	-
Round 3 - 15 February to 28 February 2017						
Concord Oval (roadside)	Ogawa (raw)	µg/m ³	50.0	0.7	18.6	1.8
	Reference	µg/m ³	67.0	-	24.8	-
	<i>Difference (Ogawa - reference)</i>	µg/m ³	-16.9	-	-6.2	-
	<i>Ratio (Ogawa/reference)</i>	-	0.75	-	0.75	-
St Lukes Park (background)	Ogawa (raw)	µg/m ³	25.5	0.5	9.3	0.2
	Reference	µg/m ³	23.7	-	14.7	-
	<i>Difference (Ogawa - reference)</i>	µg/m ³	1.8	-	-5.4	-
	<i>Ratio (Ogawa/reference)</i>	-	1.08	-	0.63	-

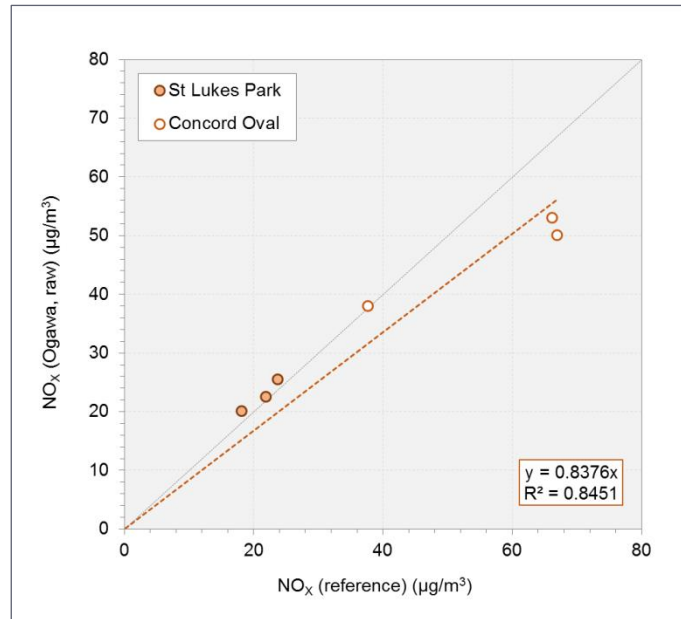


Figure 60: Calibration of Ogawa (NO_x)

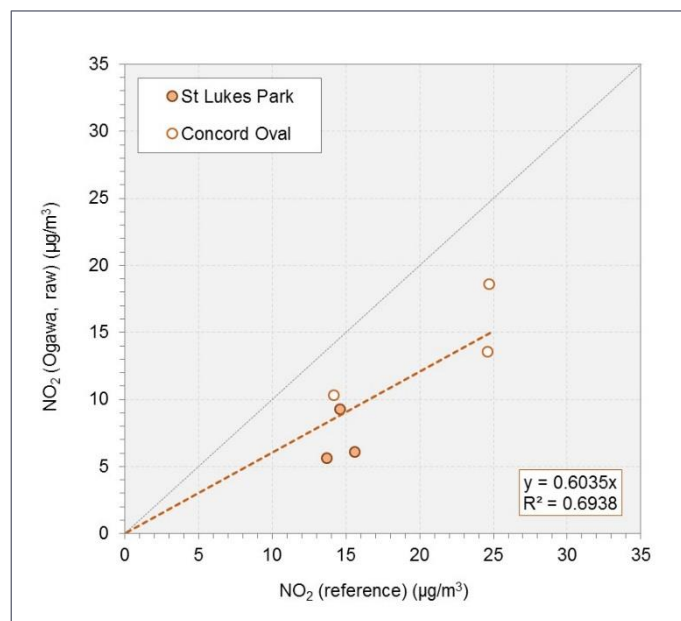


Figure 61: Calibration of Ogawa (NO₂)

The raw Ogawa results for all locations were then multiplied by the calibration factors for use in the model evaluation. Although this approach ignored any potential seasonal bias in the Ogawa data, it was assumed that it would be valid for the four-month (mainly summer) period between November and February.

The raw and calibrated results for NO_x and NO₂ from the Ogawa samplers are summarised in Table 25 and Table 26 respectively. The final calibrated results for the NO_x and NO₂ are also mapped in Figure 62 to Figure 66.

Table 25: Ogawa results for NO_x

Location code	NO _x concentration and standard error (µg/m ³)					
	Round 1		Round 2		Round 3	
	Raw	Calibrated	Raw	Calibrated	Raw	Calibrated
P01	38.0 ± 0.8	46.6	53.0 ± 0.2	65.0	50.0 ± 0.7	61.3
P02	20.2 ± 0.3	24.7	22.5 ± 0.1	27.6	25.5 ± 0.5	31.3
P03	29.8 ± 0.4	36.5	38.9 ± 0.2	47.7	-	-
P04	28.2 ± 0.7	34.6	34.1 ± 1.4	41.8	-	-
P05	52.9 ± 5.0 ^(a)	64.8	73.3 ± 2.1 ^(b)	89.8	-	-
P06	39.9 ± 2.0	48.9	56.6 ± 3.3	69.4	-	-
P07	33.2 ± 0.1	40.7	44.4 ± 0.5	54.4	-	-
P08	29.8 ± 1.8	36.5	35.4 ± 1.7	43.4	-	-
P09	68.3 ± 0.9	83.7	97.0 ± 1.9	118.8	-	-
P10	79.8 ± 2.5 ^(b)	97.8	81.4 ± 3.1 ^(b)	99.8	-	-
P11	31.0 ± 0.8	38.0	36.7 ± 0.9	45.0	-	-
P12	20.0 ± 0.2	24.5	23.5 ± 0.5	28.8	-	-
P13	20.8 ± 0.3	25.5	23.8 ± 0.1	29.2	-	-
P14	47.0 ± 2.4	57.6	44.7 ± 0.3	54.8	-	-
P15	53.9 ± 1.3	66.1	51.3 ± 0.7	62.8	-	-
P16	50.4 ± 0.6	61.7	52.5 ± 0.5	64.4	-	-
P17	26.4 ± 0.2	32.3	30.2 ± 0.4	37.0	-	-
<i>Blank (not used)</i>	1.4 ± 0.5	-	12.5 ± 0.8	-	8.2 ± 1.6	-

(a) One sampler at this location was found on the ground, and therefore the results were not used.

(b) Non-concordant result for one sampler was not used.

Table 26: Ogawa results for NO₂

Location code	NO _x concentration and standard error (µg/m ³)					
	Round 1		Round 2		Round 3	
	Raw	Calibrated	Raw	Calibrated	Raw	Calibrated
P01	10.3 ± 0.5	17.3	13.5 ± 0.8	22.7	18.6 ± 1.8	31.2
P02	5.6 ± 0.2	9.4	6.1 ± 0.1	10.2	9.3 ± 0.2	15.5
P03	10.0 ± 0.7	16.8	12.3 ± 0.4	20.6	-	-
P04	9.9 ± 0.6	16.7	11.6 ± 0.6	19.4	-	-
P05	17.1 ± 0.4 ^(a)	28.6	23.1 ± 1.4	38.7	-	-
P06	13.4 ± 1.3	22.5	17.3 ± 1.7	29.0	-	-
P07	10.5 ± 0.5	17.7	13.0 ± 0.6	21.7	-	-
P08	11.5 ± 0.4	19.3	14.1 ± 0.1	23.7	-	-
P09	22.2 ± 0.7	37.2	30.9 ± 0.5	51.8	-	-
P10	21.3 ± 2.8 ^(b)	35.7	17.9 ± 0.2 ^(b)	29.9	-	-
P11	10.0 ± 0.6	16.8	12.8 ± 0.7	21.5	-	-
P12	6.6 ± 0.2	11.1	7.1 ± 0.3	11.9	-	-
P13	5.7 ± 0.2	9.6	7.3 ± 0.4	12.2	-	-
P14	14.4 ± 0.8	24.2	12.8 ± 0.9	21.5	-	-
P15	15.5 ± 0.4	26.0	13.9 ± 0.3	23.3	-	-
P16	14.9 ± 0.4	25.0	12.9 ± 0.3	21.7	-	-
P17	8.2 ± 0.7	13.8	10.4 ± 0.4	17.4	-	-
<i>Blank (not used)</i>	0.5 ± 0.1	-	3.0 ± 0.8	-	1.9 ± 0.3	-

(a) One sampler at this location was found on the ground, and therefore the results were not used.

(b) Non-concordant result for one sampler was not used.

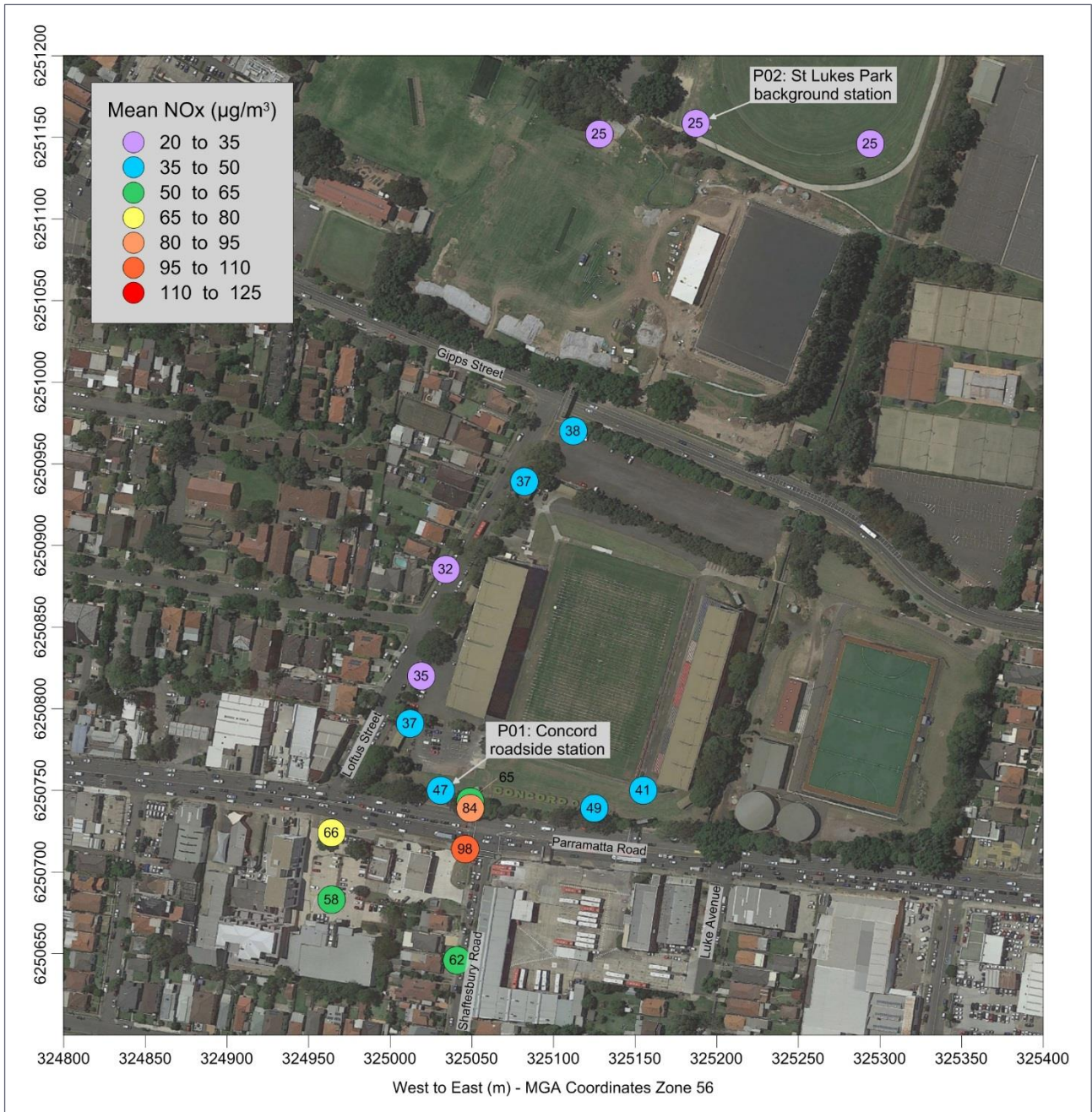


Figure 62: Average NO_x concentrations (calibrated) measured by passive samplers – round 1

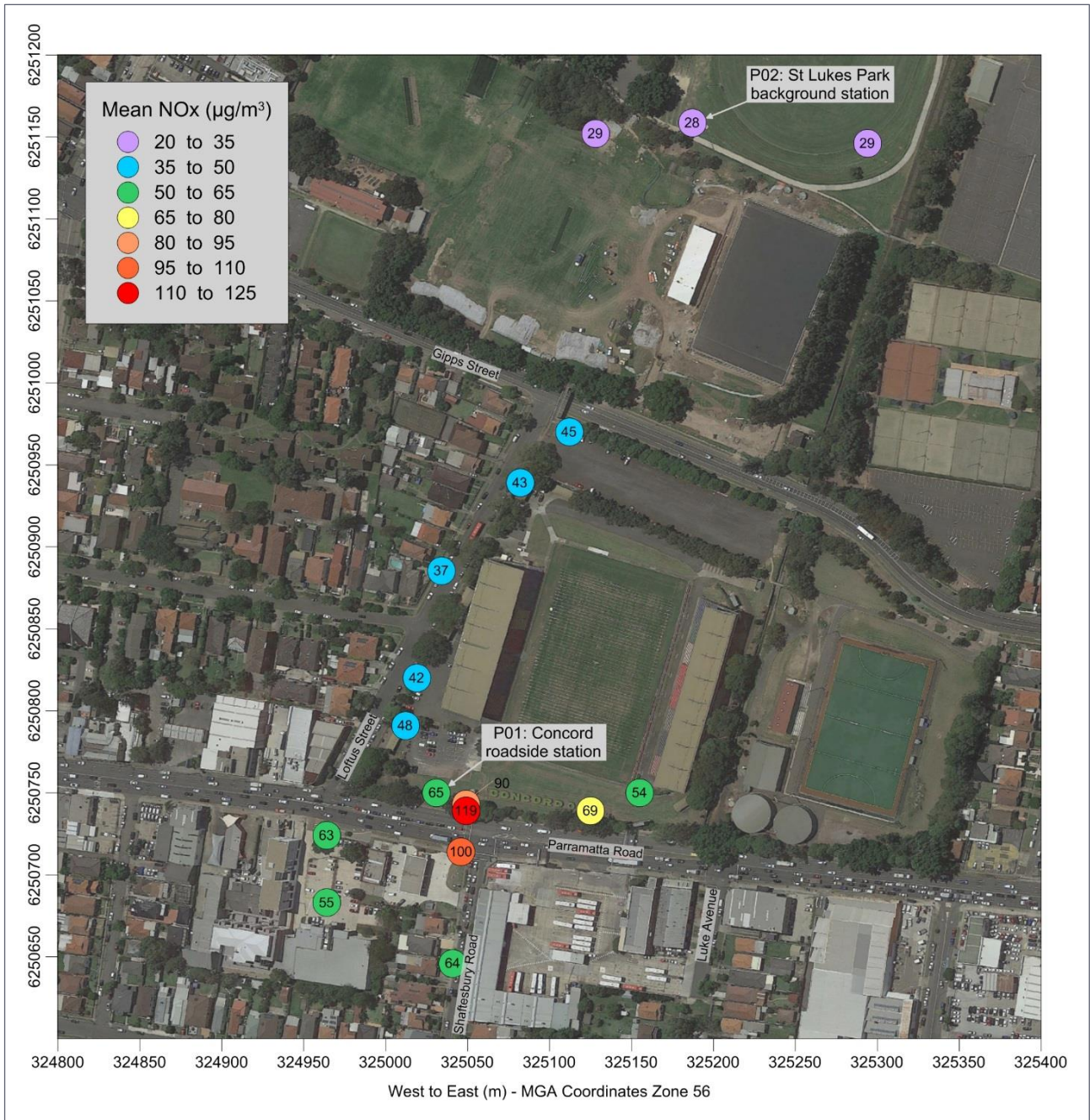


Figure 63: Average NO_x concentrations (calibrated) measured by passive samplers – round 2

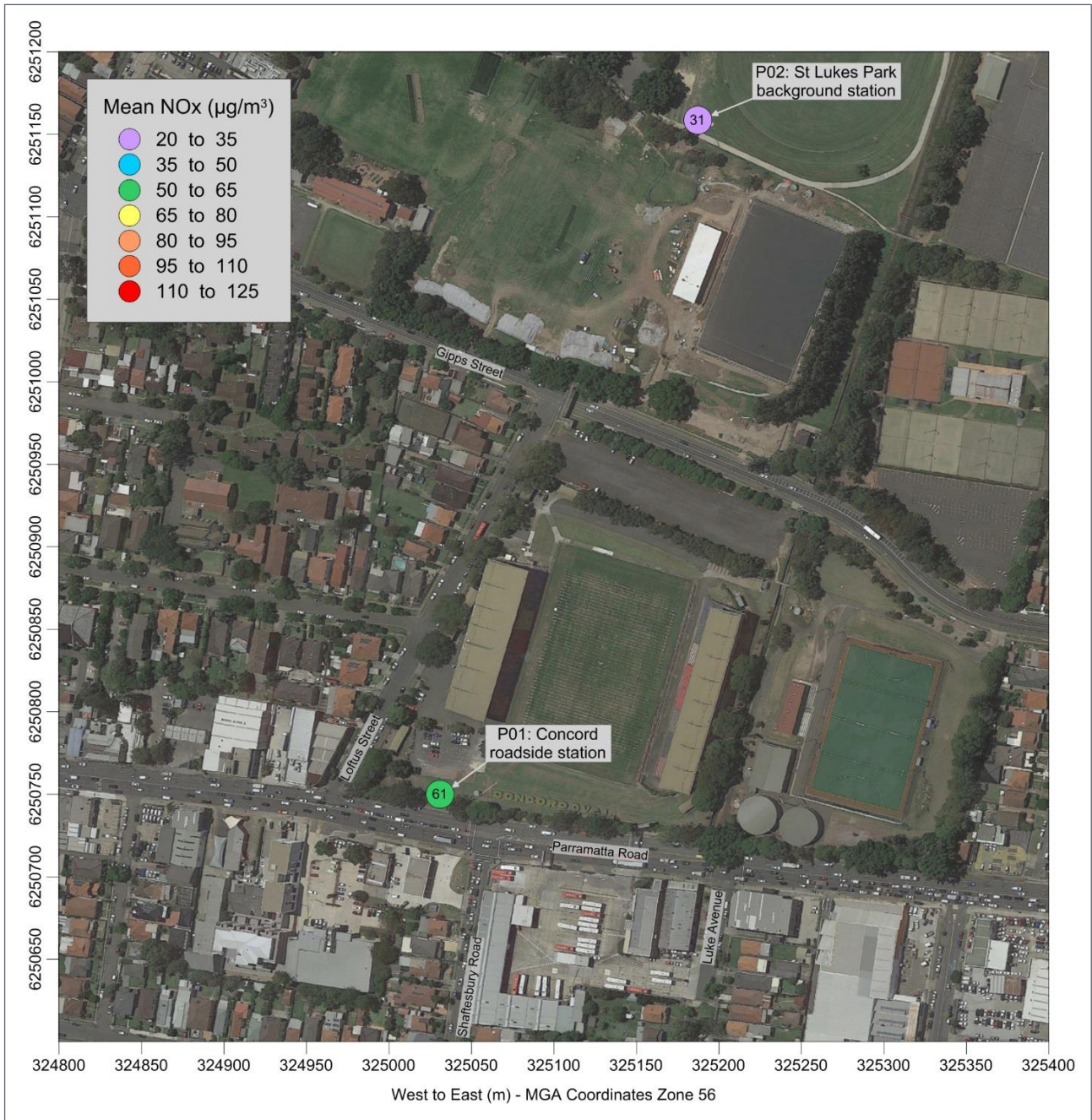


Figure 64: Average NO_x concentrations (calibrated) measured by passive samplers – round 3

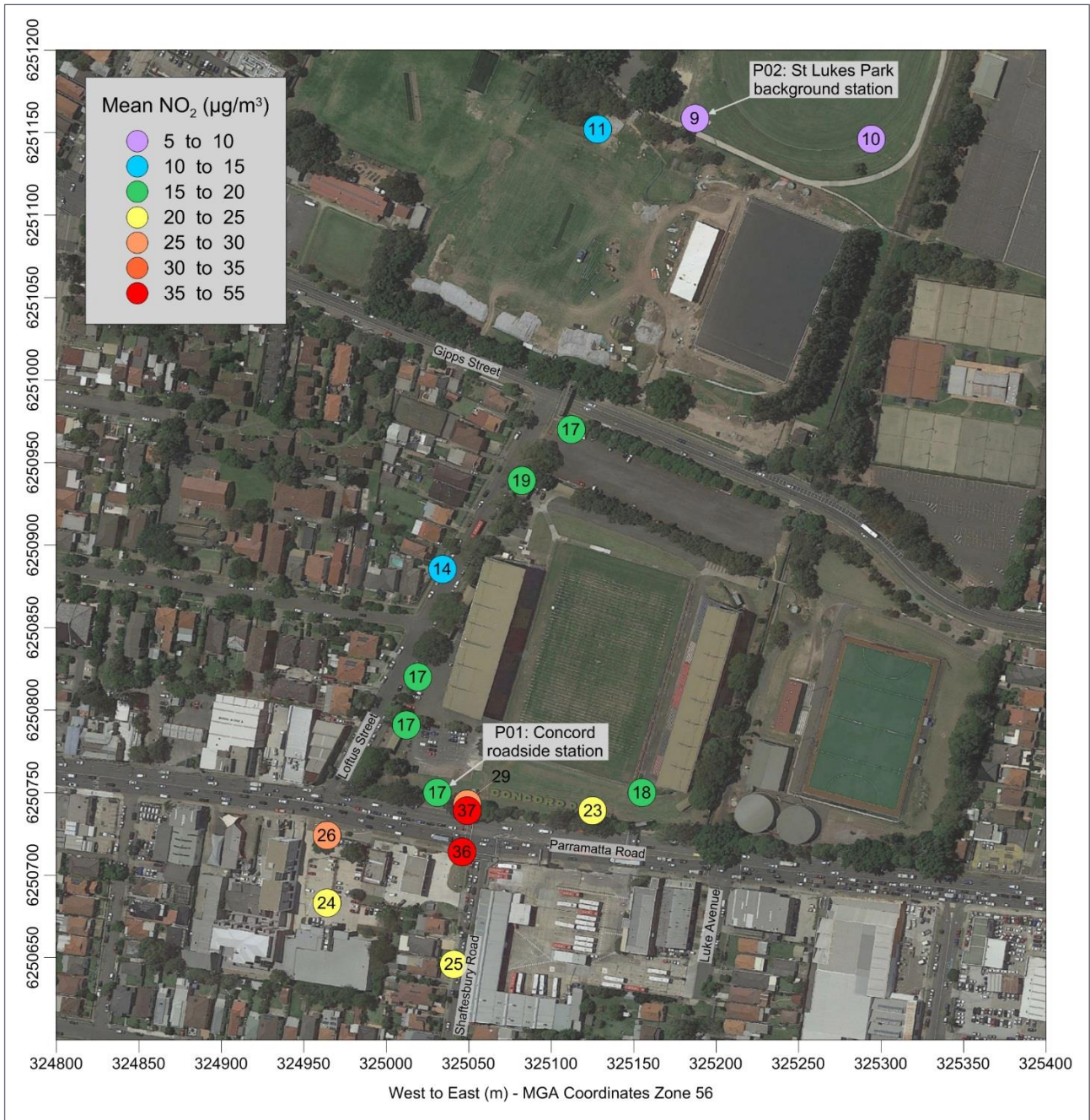


Figure 65: Average NO₂ concentrations (calibrated) measured by passive samplers – round 1

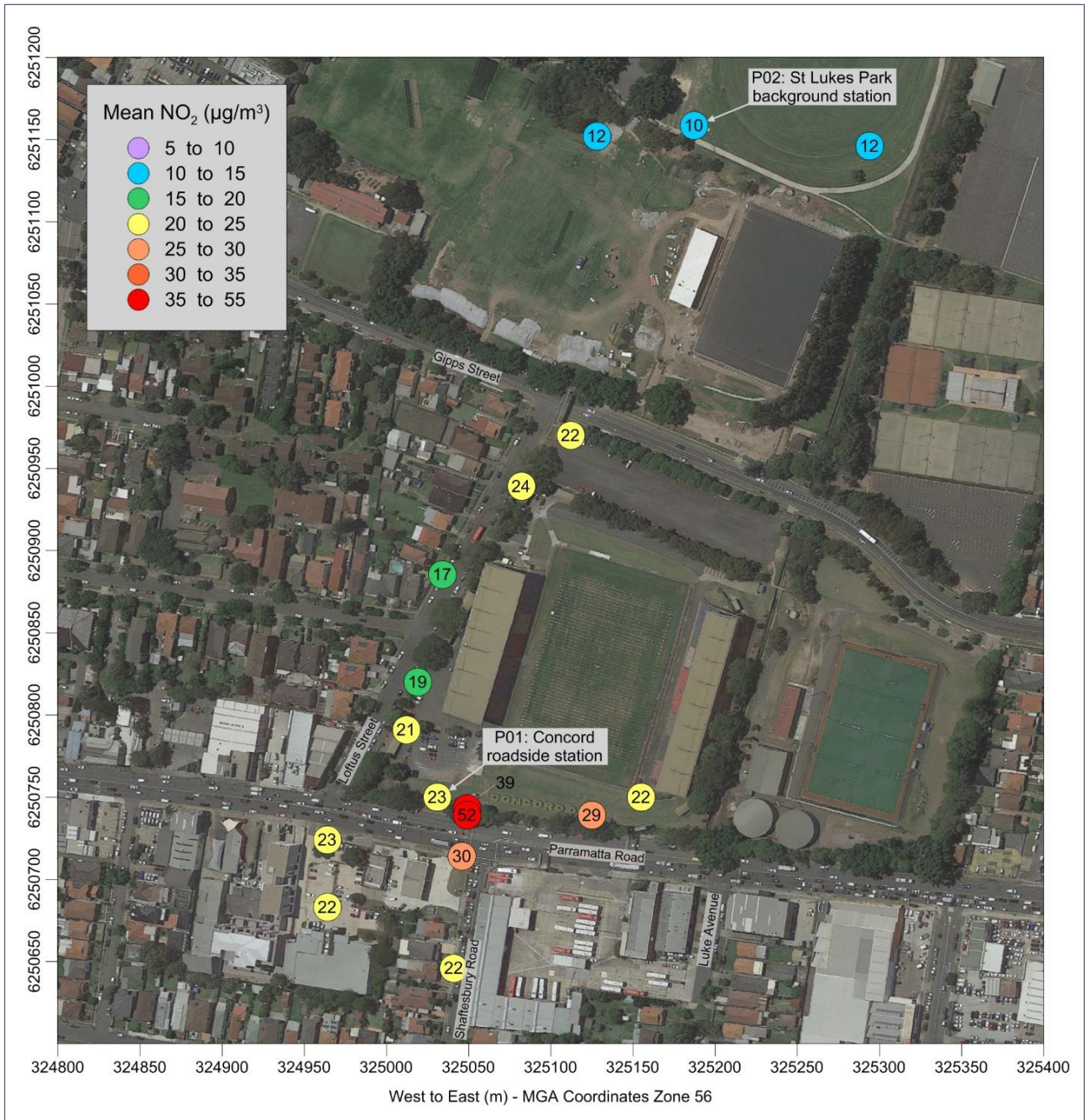


Figure 66: Average NO₂ concentrations (calibrated) measured by passive samplers – round 2

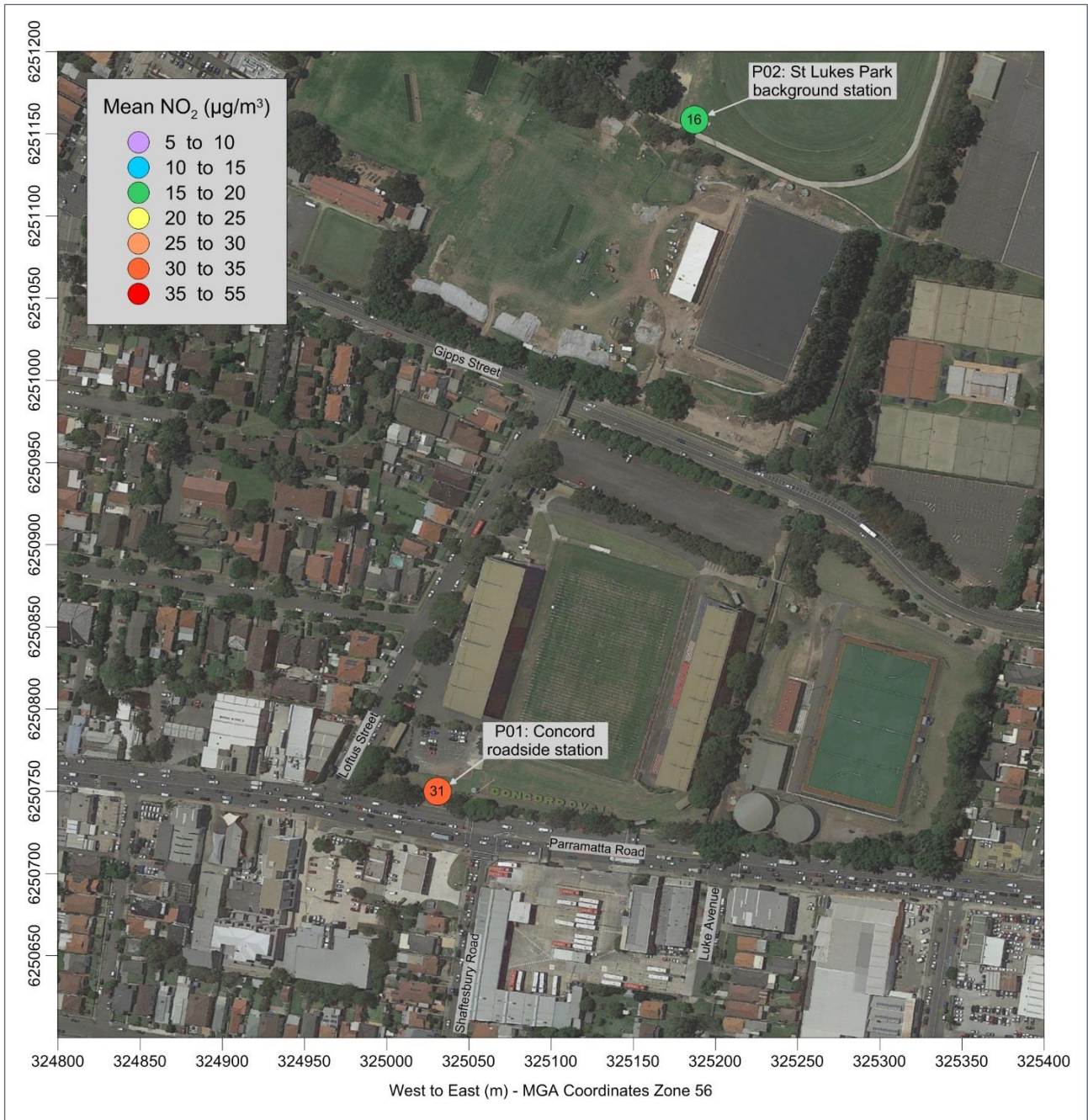


Figure 67: Average NO₂ concentrations (calibrated) measured by passive samplers – round 3

5.7 Background concentrations

Whilst an air pollution dispersion model can provide important information on local concentration gradients, such as in the vicinity of roads, the model predictions are only for the sources that are explicitly included in the model. Where there is a need to compare the model predictions with measurements, estimates of the contributions from other (non-modelled) sources of pollution are also required for all locations in the domain. These other sources are usually defined as 'background'.

The definition of background concentrations can be a major source of uncertainty, especially given that, for some pollutants, the background contribution is substantially higher than the model contribution.

The background concentrations in the dispersion model domain were defined using the data from the St Lukes Park continuous monitoring station, and it was important to establish the following for this station:

- That the measurements were representative of a 'true' background in the dispersion model domain, and were not significantly affected by road traffic.
- That the measurements were representative of background concentrations across the model domain, and in particular at Concord Oval. This point is important because accurate monitoring data were required to support the detailed temporal analysis of dispersion model predictions at Concord Oval.

With respect to NO_x , the information presented in the report indicates that the St Lukes Park station has no strong directional influences on NO_x and NO_2 , indicating the nature of this station as a background site compared with the Concord Oval site and for purposes of this assessment. The temporal and spatial analysis of the continuous monitoring data from St Lukes Park, combined with the passive sampling data, indicated that the NO_x concentrations at St Lukes Park site were only slightly affected by road traffic emissions.

It would not be possible to define the actual background concentrations at all locations in the dispersion model domain from the (necessarily) incomplete monitoring data. For example, as noted earlier, the establishment of a continuous monitoring station on the southern side of Parramatta Road was not possible. This meant that continuous measurements of background concentrations for southerly winds were not available, and hence the background concentrations for these situations had to be inferred.

5.8 Road traffic contribution

The contribution of road traffic to concentrations of NO_x and NO_2 was also investigated temporally (using the continuous measurements) and spatially (using the passive sampling results).

5.8.1 Continuous measurements

The road traffic NO_x increment at the Concord Oval station in each hour was obtained by subtracting the background concentration measured at St Lukes Park from the measurement at Concord Oval, on the assumption that St Lukes Park was representative of background values across the domain. The road increments at Concord Oval were then examined for upwind and downwind situations.

The road increments for NO_x , NO_2 and O_3 are shown in Figure 68, Figure 69 and Figure 70 respectively. In each figure plot (a) shows all available data (i.e. where there was a valid measurement for both Concord Oval and St Lukes Park), and plot (b) shows the data filtered by wind direction (Figure 57). The blue line represents the periods when Concord Oval monitoring station was upwind of Parramatta Road, and the red

line represents the periods when it was downwind of Parramatta Road. Frequency distributions of the increments are also provided.

When unfiltered by wind direction, the NO_x increment ranged from $-24 \mu\text{g}/\text{m}^3$ to $+277 \mu\text{g}/\text{m}^3$, with a mean of $+34 \mu\text{g}/\text{m}^3$. When filtered by wind direction the overall ranges did not change greatly. When the Concord Oval monitoring station was upwind of Parramatta Road the mean increment was $7 \mu\text{g}/\text{m}^3$, whereas when the station was downwind of Parramatta Road the mean increment was $58 \mu\text{g}/\text{m}^3$. For NO_2 the corresponding mean increments for the upwind and downwind situations were $-0.3 \mu\text{g}/\text{m}^3$ and $+10.1 \mu\text{g}/\text{m}^3$ respectively.

Ozone had a negative road increment due to reaction with NO at roadside. The ozone increment for all wind directions ranged from $-72 \mu\text{g}/\text{m}^3$ to $+7 \mu\text{g}/\text{m}^3$, with a mean of $-13 \mu\text{g}/\text{m}^3$. There was no strong influence of wind direction on the ozone increment; when Concord Oval was upwind of Parramatta Road the average ozone increment was $-10.7 \mu\text{g}/\text{m}^3$, and when it was downwind the average increment was $-12.9 \mu\text{g}/\text{m}^3$.

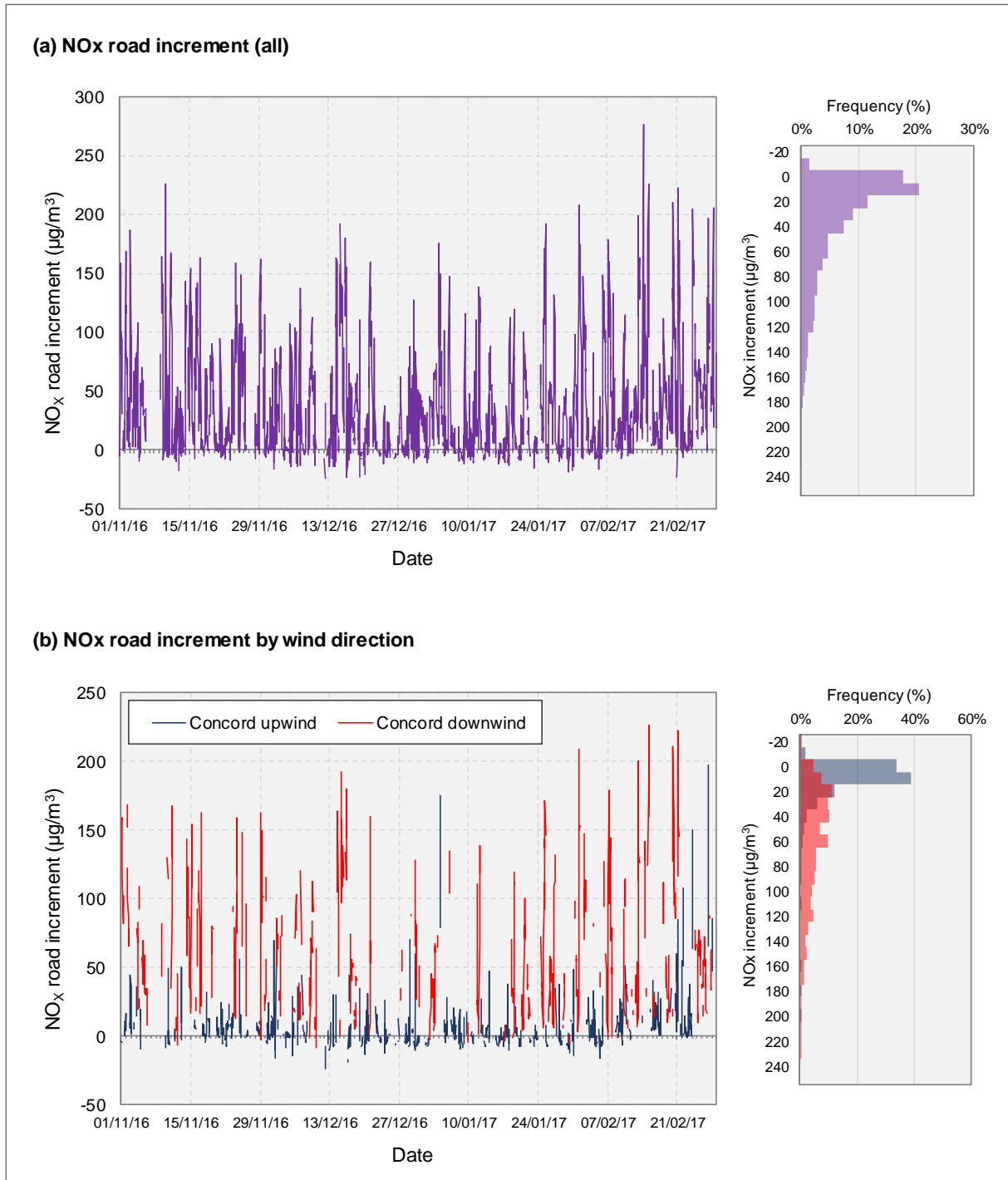


Figure 68: Hourly average NO_x road increments

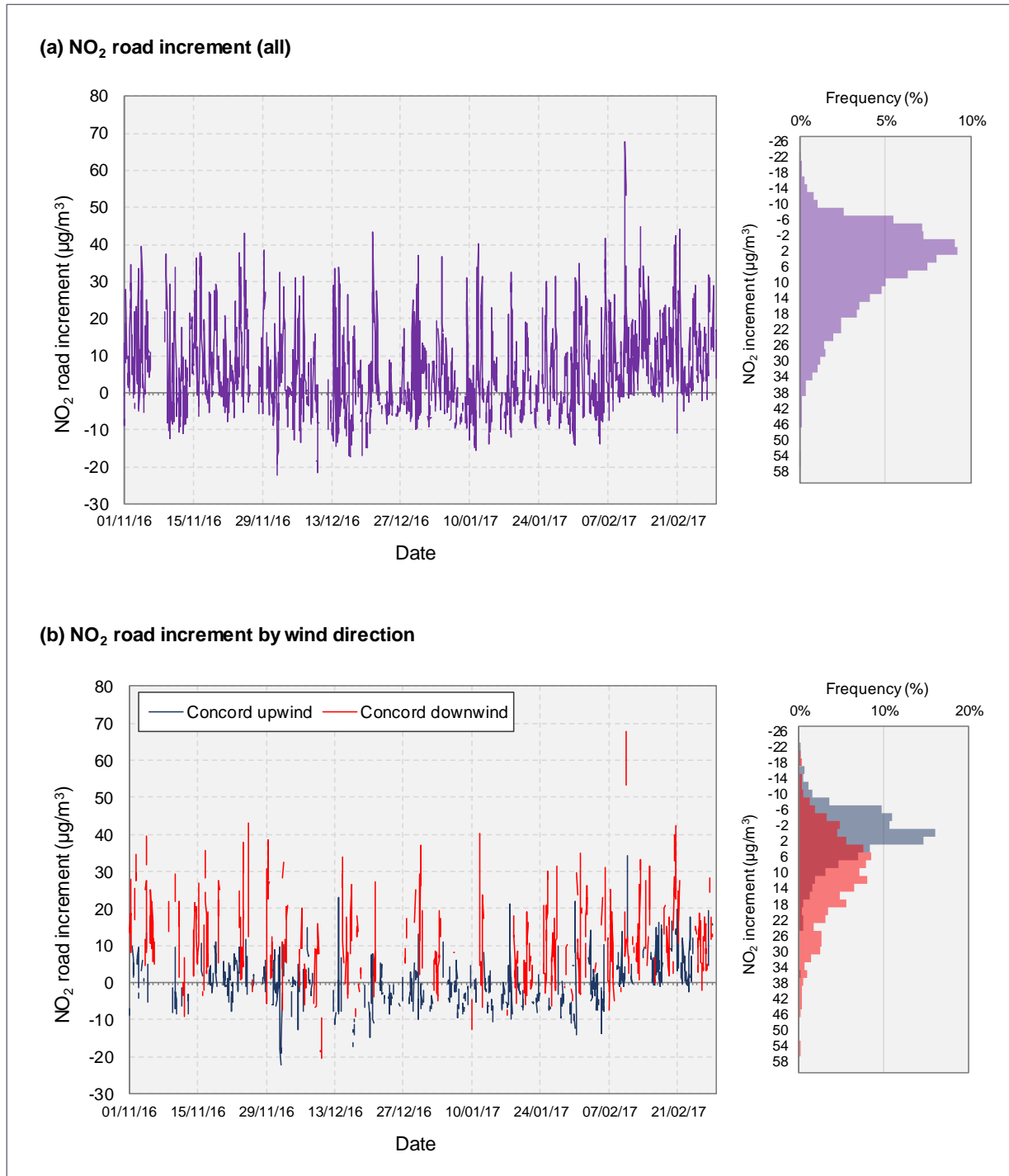


Figure 69: Hourly average NO₂ road increments

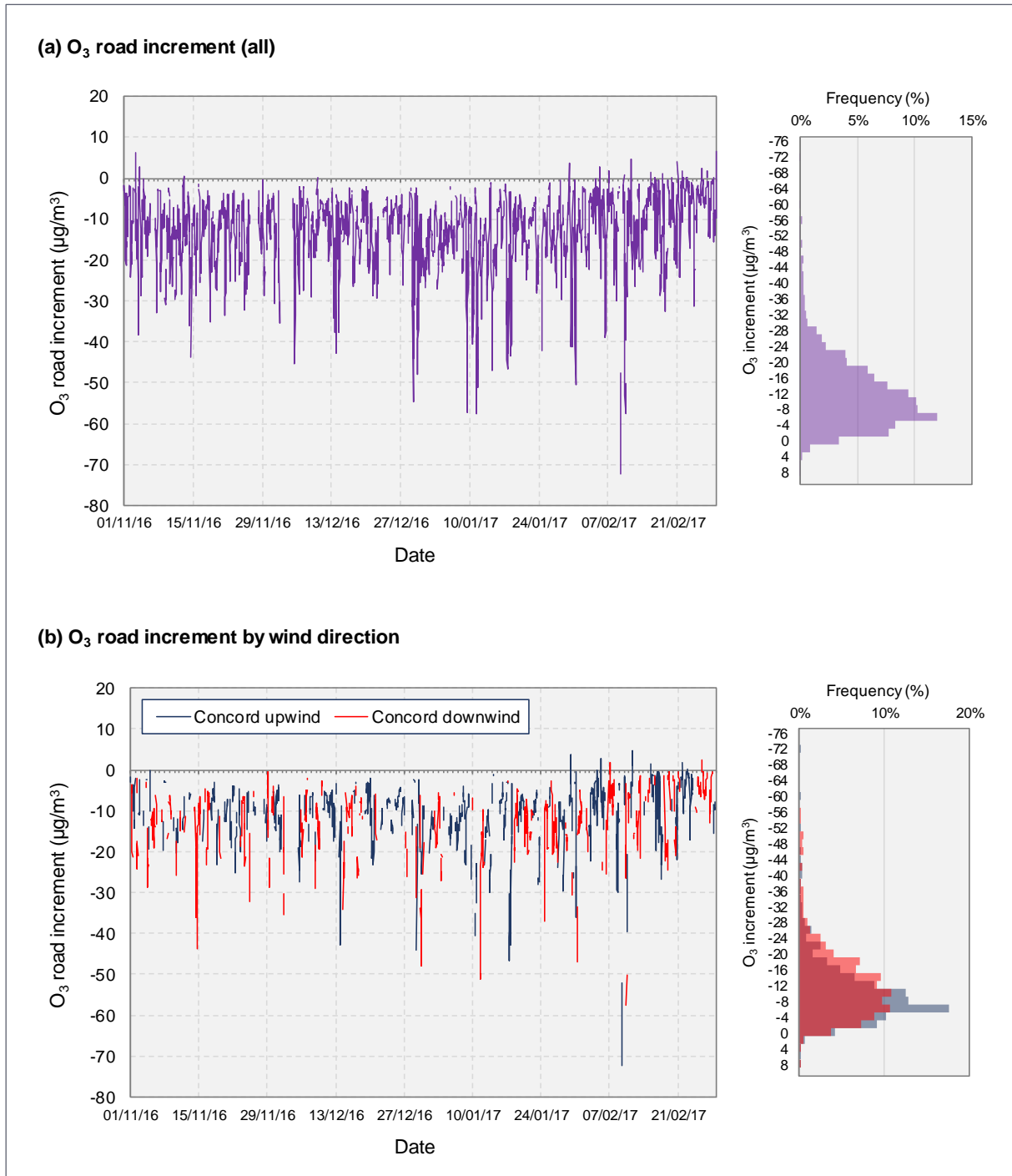


Figure 70: Hourly average O₃ road increments

5.8.2 Passive sampling

The spatial influence of road traffic on pollutant concentrations was considered by examining the Ogawa results as a function of distance from the centre of Parramatta Road during the two rounds of passive sampling. The general areas to the north and south of Parramatta Road were considered separately. The results for NO_x and NO_2 are given in Figure 71 and Figure 72 respectively. To aid the understanding of the results, the hourly wind roses at Concord Oval for the two rounds of passive sampling are also provided in Figure 73 and Figure 74.

The data for the locations to the north of Parramatta Road exhibited a similar pattern in rounds 1 and 2 of the passive sampling, with a sharp decrease in concentration within 30 m from the road. For example, in round 2 the period-average NO_x concentration decreased from around $120 \mu\text{g}/\text{m}^3$ at 15 metres from the road centre (i.e. within a few metres of the kerb) to around $70 \mu\text{g}/\text{m}^3$ at 25 metres. This equated to a reduction in concentration of around 40% over 10 metres. The concentration then decreased to around $30 \mu\text{g}/\text{m}^3$ at a distance of 450 metres from the road centre (i.e. at St Lukes Park), equating to an overall reduction of around 75%. It can be seen that there was an increase in concentration between around 200-250 metres from the centre of Parramatta road. This increase coincided with sites 8 and 11, both to the south of Gipps Street, and was probably due to the contribution of traffic on Gipps Street which is used as an alternative route to Parramatta Road during peak traffic periods. The plots also suggest that concentrations of NO_x and NO_2 are still decreasing at a distance of 450 metres from Parramatta Road. This implies that the background station at St Lukes Park may be slightly overestimating the 'true' background.

The data for locations to the south of Parramatta Road were less extensive than the data for sites to the north. There was a sharp initial decrease in NO_x and NO_2 concentrations within 20 metres, but concentrations did not fall off as sharply as those for locations to the north of Parramatta Road. This may have been due to the additional contribution from the traffic on Shaftesbury Road (around 8,000 vehicles per day). In contrast, the only significant road immediately to the north of Parramatta Road was Loftus Street, and this had a much lower volume of traffic (2,000 vehicles per day).

There were some differences between the results from rounds 1 and 2:

- Immediately to the north of Parramatta Road, markedly higher NO_x and NO_2 concentrations were recorded in round 2 compared with round 1. The results from rounds 1 and 2 converged in the vicinity of St Lukes Park.
- To the south of Parramatta Road the NO_2 concentrations were markedly higher in round 1 than in round 2, whereas NO_x concentrations were quite similar between rounds 1 and 2.

It is likely that meteorology will have had an influence here. For example, in round 1, during the daytime when NO_x emissions were highest, the dominant winds were from a north-easterly direction, and this would have tended to result in higher concentrations to the south of Parramatta Road. Southerly winds were important during the night, but this was when NO_x emissions were relatively low. In round 2 the wind patterns were slightly different to those in round 1, with south-easterly winds being more prominent during the daytime than in round 1. This would have tended to result in higher concentrations at sites to the north of Parramatta Road.

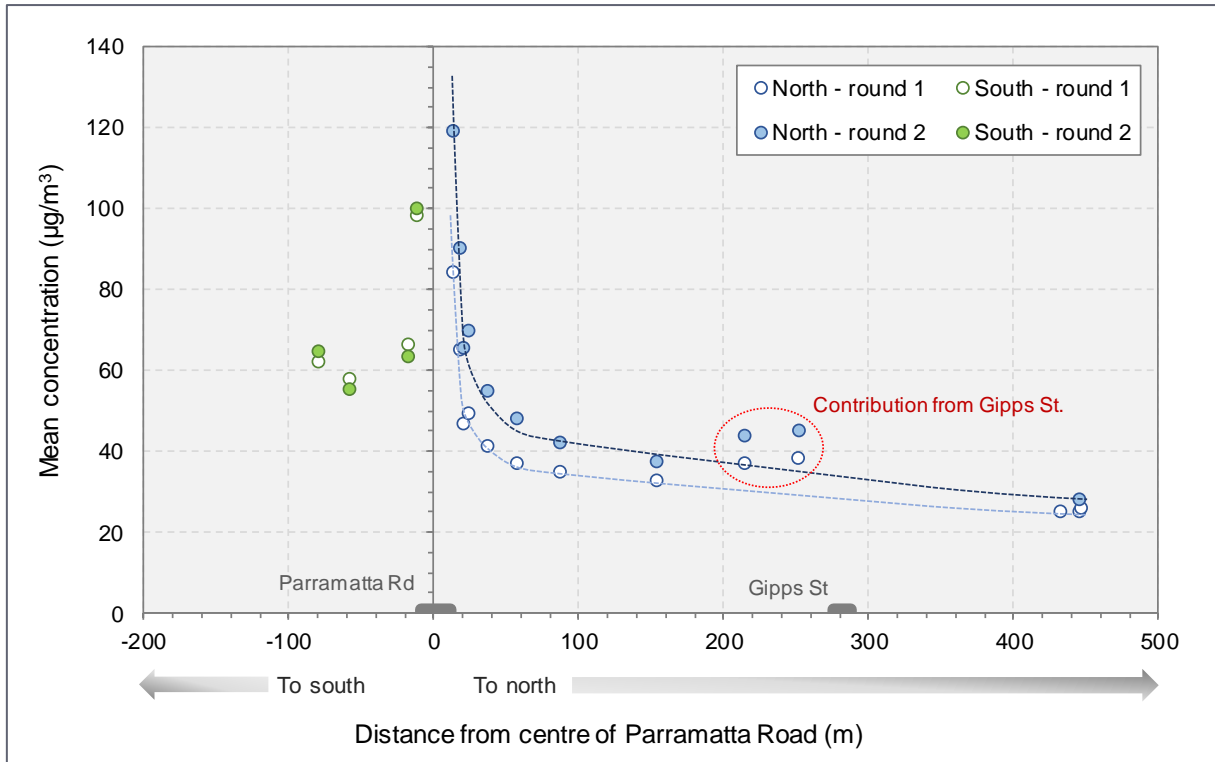


Figure 71: NO_x concentration profiles perpendicular to Parramatta Road

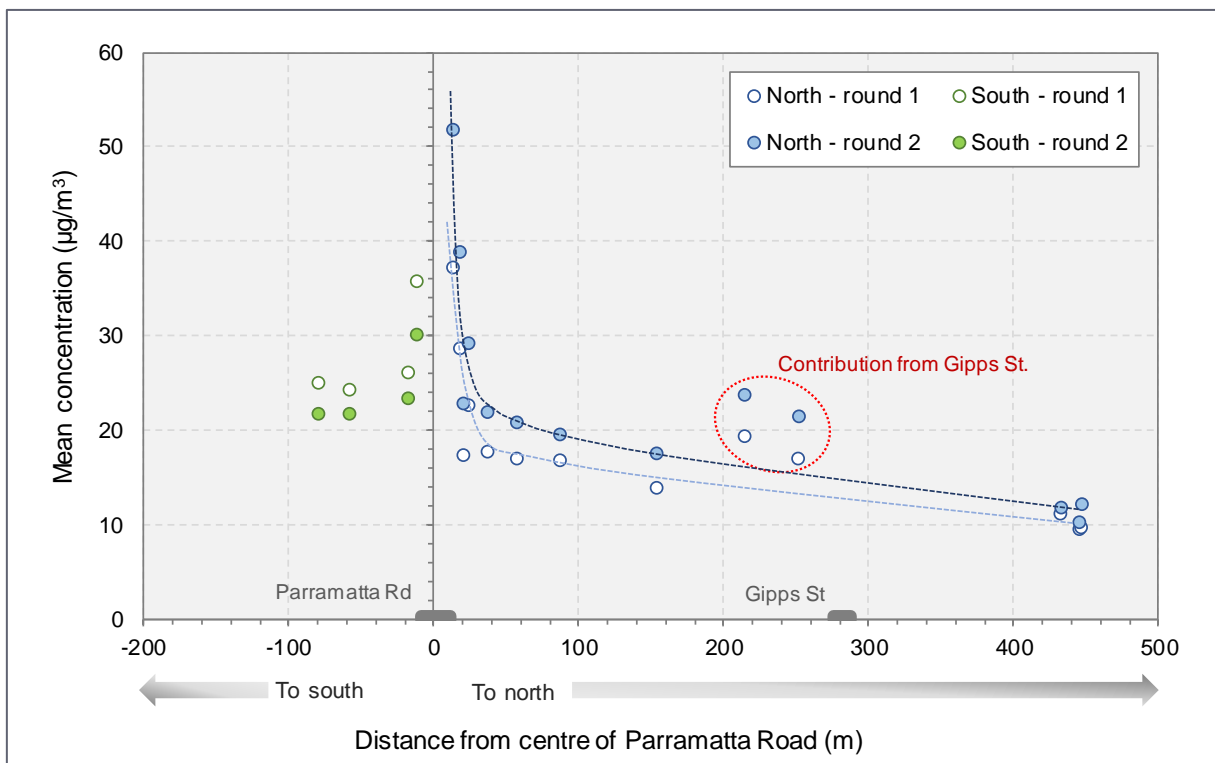


Figure 72: NO₂ concentration profiles perpendicular to Parramatta Road

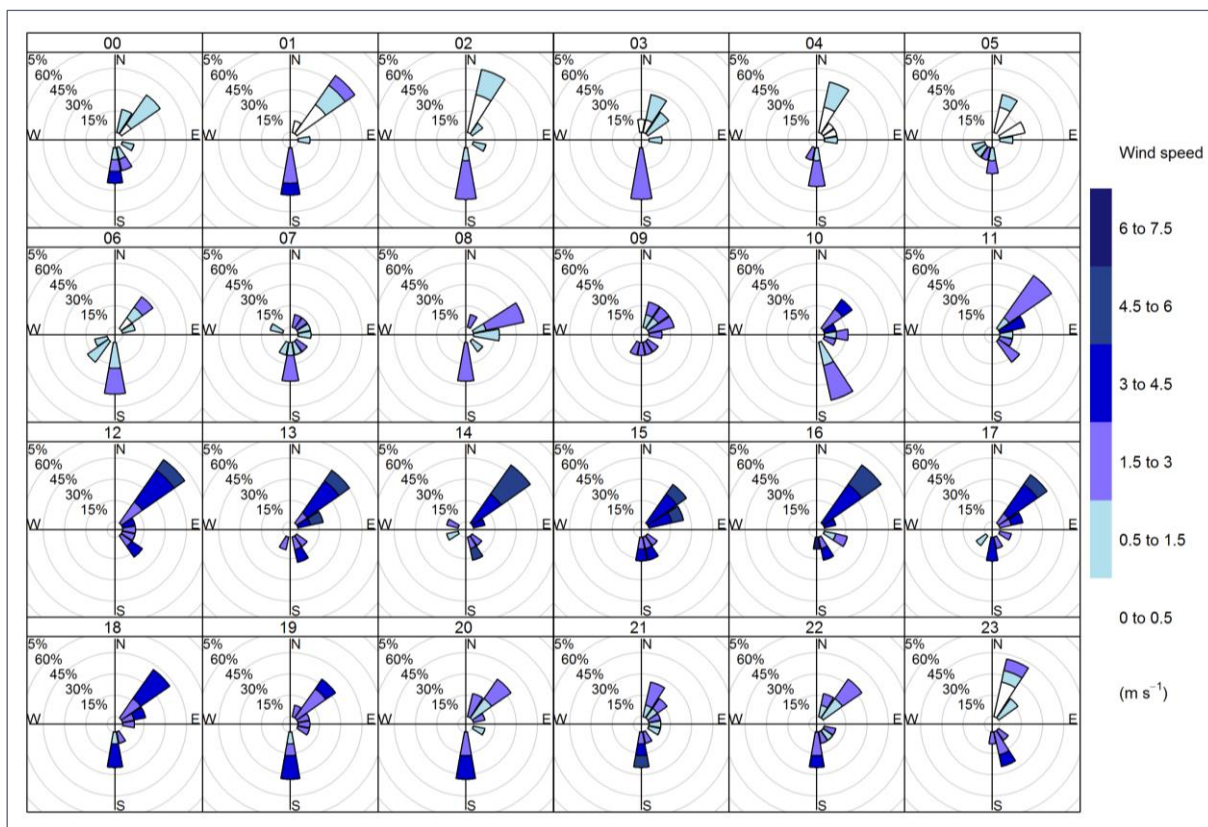


Figure 73: Hourly wind roses at Concord Oval for round 1 of passive sampling

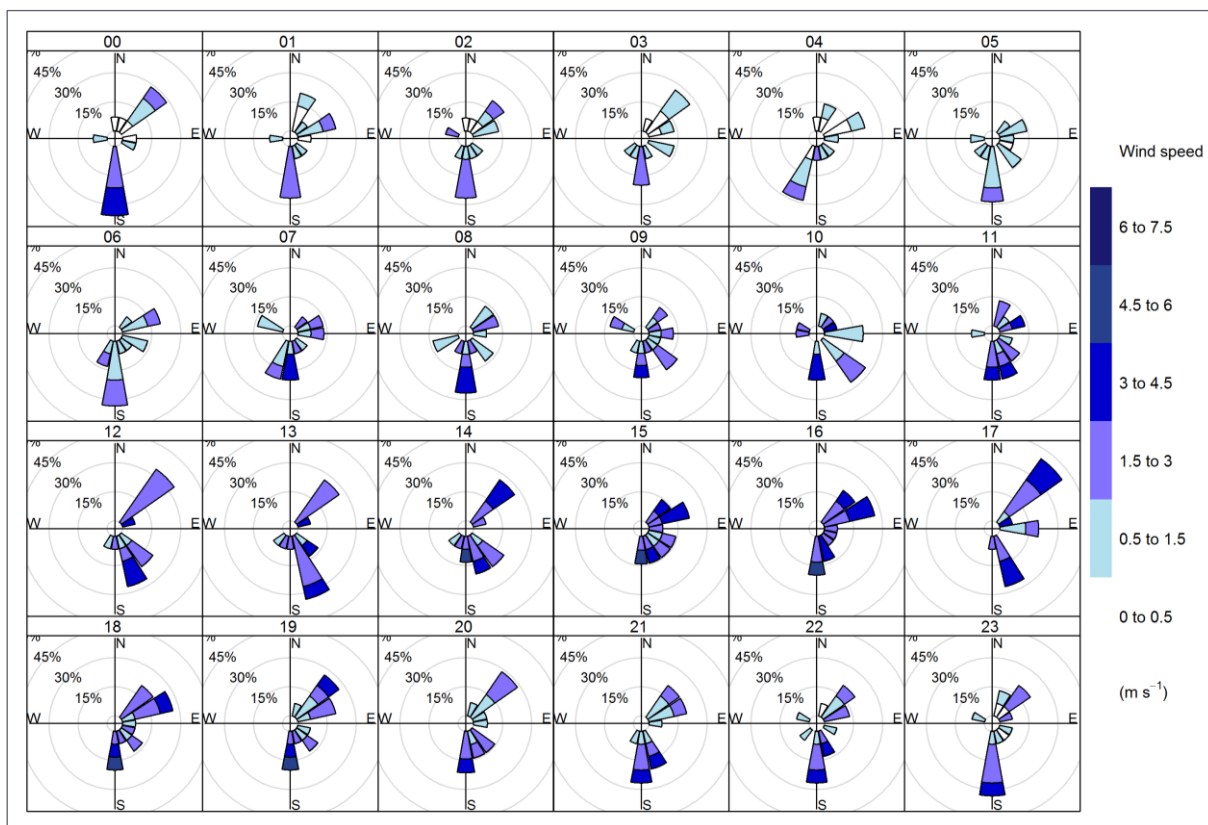


Figure 74: Hourly wind roses at Concord Oval for round 2 of passive sampling

6 Results of modelling

6.1 Emission model sensitivity

The results of the emission model sensitivity testing are summarised in Figure 75. All the analyses presented here relate to the calendar year 2016, but the model sensitivity would vary by year. Whilst this would not matter on short timescales (e.g. a few years), it may become more important on timescales of environmental assessments, which often involve projections for 15 years into the future.

Plots (a) and (b) show the effects of road type on NO_x emissions, firstly using an appropriate default traffic mix for each road type from the NSW EPA inventory, and then using a single traffic mix (in this case, for arterial roads). Plot (a) therefore shows the combined effects of different emission factors and traffic mix assumptions, whereas plot (b) shows the differences between the emission factors alone. It can be seen in plot (a) that there are some significant differences between the different road types, but the more closely grouped results in plot (b) indicates that these are mainly due to the traffic mix assumptions. In terms of this study, most of the roads were classified as either residential or arterial (see Table 8), and it is considered unlikely that errors in the allocation of road type would have had a large effect on the outcomes.

Plot (c), which again relates to arterial roads, shows that NO_x emissions are rather sensitive to the road gradient, and small errors in the definition of road gradient can significantly affect the results. For example, at a speed of 40 km/h the emission factors for a level road (0% gradient) is 0.63 g/vehicle-km, whereas for a 2% downhill gradient it is 0.37 g/vehicle-km (42% lower than a level road) and for a 2% uphill gradient it is 1.05 g/vehicle-km (66% higher than a level road). Of most relevance to this study are the gradients on Parramatta road, which were generally negligible (see Table 8). However, the section between Burwood Road and Shaftesbury Road, which ran alongside the Concord Oval station, did have a significant gradient ($\pm 3.3\%$). Although an effort was made to characterise the gradient accurately, uncertainty in the values used (as well as in the emission factors) could have significantly affected the overall model accuracy.

Plot (a) shows that the relationships between speed and emissions are non-linear. Any error in the definition of speed therefore leads to an error in emissions that depends on the actual speed. Plot (d) shows the effects on NO_x emissions (in percentage terms, although the absolute effects are similar) of a 10% underestimation and a 10% overestimation in speed, as a function of the 'correct' speed. Because the relationship between speed and emissions is quite flat between around 30 km/h and 60 km/h, the effect of an error in speed on emissions within this range is relatively small (a 10% error in speed results in an error in emissions of less than 5%). The effects on emissions are larger at around 20 km/h and above 60 km/h.

Small errors in traffic composition can also lead to significant errors in emissions. This is especially important for HDVs. On a per vehicle basis the NO_x emissions from HGVs are considerably higher than those from LDVs. For example, in 2016 the base emission factor for an articulated truck is around 30 times higher than that for a petrol car, and around 10 times higher than that for a diesel car. Plot (e) shows that, for the middle of the speed range, it will be more important to accurately define the proportion of HDVs in the traffic than the speed.

The effects of including cold-start emissions are shown for the default fleet on arterial roads in plot (f). The cold start emission is a fixed value that is added to the hot emission at all speeds. In the case of arterial roads the value in plot (f) is 0.2 g/vehicle-km.

These examples are, of course, rather simplistic, and where the road network being modelled is complex there will be a range of errors on different roads and for different parameters. These errors would not be

consistent. However, this analysis has shown that, in addition to the accurate quantification of traffic volume, it is important to accurately quantify the road gradient and the proportion of heavy duty vehicles. Errors in traffic speed will be important unless the prevailing speed is between around 20 and 60 km/h.

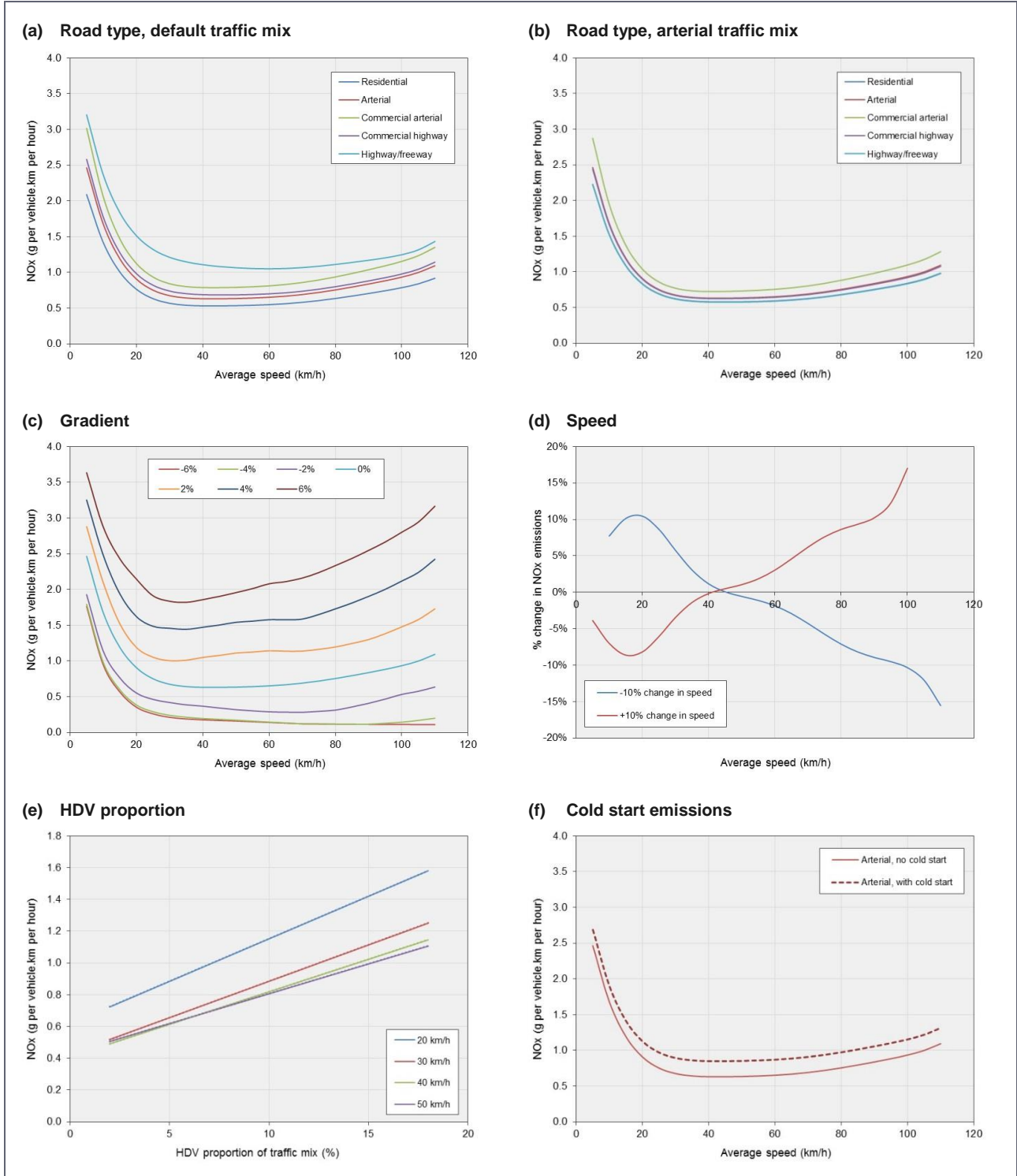


Figure 75: Sensitivity of NO_x emissions to model inputs

6.2 Meteorological model evaluation

6.2.1 Overview

One of the objectives of the study was to provide an evaluation of the GRAMM performance for a specific set of local conditions. This was done by:

- Completing GRAMM simulations using local meteorological measurements.
- Investigating the response of GRAMM to model inputs and settings using statistical and visual presentation methods.
- Assessing the response of GRAMM by comparing it against another meteorological model (in this case, CALMET).

The tests that were conducted were described in Section 4.5.1. The results for the different test series are summarised in the following Sections.

6.2.2 Wind speed analysis

The full results of the wind speed analysis are presented in Appendix E, and a summary is provided in Table 27. More detailed discussions of the results for test series A and B are provided in the following sections.

Table 27: Summary of wind speed tests

Test	Results at St Lukes Park	Results for other stations
Series A – Single measurement station (St Lukes Park)		
CT-01	CALMET extract almost identical to observations.	CALMET did not perform as well at St Lukes.
GM-01 GM-02 GM-03	A grid spacing of 50 metres gave the strongest relationship with observations ($R^2 = 0.79$). The results for the 100 and 200 metre spacing tests were similar, and showed a higher degree of overestimation of lower wind speeds compared with the 50 metre spacing test.	GRAMM did not perform as well at the other stations, generally overestimating lower wind speeds.
GM-04	GRAMM with Re-Order showed an improvement in model performance (R^2 of 0.79 without Re-Order compared with 0.88 with Re-Order). The Re-Order test showed an improvement in the prediction of the higher wind speeds.	GRAMM did not perform as well at the other stations, generally overestimating lower wind speeds. However, the Re-Order test gave better results than without Re-Order for all stations.
Series B – Multiple measurement stations (CALMET) or synthetic meteorology (GRAMM)		
CT-02	Markedly worse than in test CT-01.	CALMET extract almost identical to observations.
GM-05	GRAMM did not perform as well as previous tests but slightly better than CALMET (R^2 of 0.47 for GRAMM compared with 0.43 for CALMET).	GRAMM gave a fair to good performance at other stations, and markedly better than at St Lukes Park.
GM-06	GRAMM gave a fair to good performance at St Lukes Park and was markedly improved compared with GM-05 ($R^2 = 0.74$).	GRAMM did not perform as well at other stations, generally overestimating lower wind speeds.
GM-07	Match-to-Observations showed much improved GRAMM results, especially when compared with GM-01, GM-02 and GM-03 ($R^2 = 0.96$).	GRAMM did not perform as well at the other stations generally overestimating lower wind speeds. This was also seen in the equivalent CALMET test (CT-01_GM-01, GM-02 and GM-03 showed better model performance.

6.2.2.1 Series A (single station reference meteorology - St Lukes Park)

In Series A the reference meteorology was taken from St Lukes Park only. The descriptive statistics for the wind speed tests are given in Table 28, and the model performance metrics are summarised in Table 29. The metrics are explained in Appendix B.

Table 28: Wind speed statistics for Series A tests (2015)

Statistic	1-hour average wind speed (m/s)					
	Observed	CT-01	GM-01	GM-02	GM-03	GM-04
St Lukes Park						
N	8,720	8,760	8,693	8,693	8,693	8,693
Average value	1.3	1.3	1.1	1.0	1.0	1.2
Maximum value	6.4	6.4	3.5	3.3	3.2	3.5
98th percentile	4.5	4.5	2.6	2.5	2.4	3.1
50th percentile (median)	1.0	1.0	1.0	0.9	1.0	0.9
% calms	27.9%	27.5%	32.9%	33.3%	35.2%	33.3%
Sydney Olympic Park						
N	7,762	8,760	8,693	8,693	8,693	8,693
Average value	2.6	1.9	1.2	1.1	1.0	1.2
Maximum value	8.6	6.4	3.4	3.2	3.2	3.4
98th percentile	6.4	4.4	2.5	2.4	2.3	3.0
50th percentile (median)	2.4	1.8	1.2	1.0	0.9	1.0
% calms	11.1%	2.3%	13.0%	28.7%	26.4%	23.7%
Canterbury Racecourse						
N	7,807	8,760	8,693	8,693	8,693	8,693
Average value	3.2	1.6	1.1	1.0	1.0	1.2
Maximum value	10.1	4.9	3.4	3.5	3.4	3.4
98th percentile	7.5	3.7	2.6	2.5	2.4	3.1
50th percentile (median)	3.0	1.5	1.0	0.8	0.8	0.8
% calms	7.7%	4.4%	32.0%	34.1%	38.1%	32.5%
Rozelle						
N	8,443	8,760	8,693	8,693	8,693	8,693
Average value	1.7	2.2	1.2	1.0	1.0	1.2
Maximum value	16.3	7.1	3.1	3.4	3.5	3.1
98th percentile	5.4	4.9	2.5	2.5	2.5	2.8
50th percentile (median)	1.2	2.1	1.1	1.0	1.0	1.0
% calms	20.3%	2.6%	6.5%	27.7%	27.6%	18.4%
Chullora						
N	8,648	8,760	8,693	8,693	8,693	8,693
Average value	1.7	1.9	1.1	1.0	1.0	1.1
Maximum value	8.2	5.8	3.4	3.2	3.3	3.4
98th percentile	4.9	4.0	2.4	2.3	2.4	3.2
50th percentile (median)	1.5	1.7	1.1	1.0	1.0	0.9
% calms	9.4%	1.8%	26.4%	34.0%	33.2%	31.5%

Table 29: Summary of model performance for wind speed by statistical metric (Series A)

Extract location	Test ^(a)	Statistical metric ^(b)									
		FAC2 (Ideal = 1)	MB (Ideal = 0)	MGE (Ideal = 0)	NMB (Ideal = 0)	NMGE (Ideal = 0)	RMSE (Ideal = 0)	r (Ideal = 1)	R ² (Ideal = 1)	COE (Ideal = 1)	IOA (Ideal = 1)
St Lukes Park	CALMET (CT-01)	1.00	-0.001	0.001	-0.001	0.001	0.01	1.00	1.00	1.00	1.00
	GRAMM (GM-01)	0.92	-0.27	0.46	-0.20	0.34	0.70	0.89	0.79	0.50	0.75
	GRAMM (GM-02)	0.85	-0.37	0.53	-0.27	0.40	0.80	0.84	0.71	0.42	0.71
	GRAMM (GM-03)	0.81	-0.36	0.55	-0.27	0.41	0.82	0.83	0.69	0.41	0.70
	GRAMM (GM-04)	0.97	-0.16	0.29	-0.12	0.22	0.49	0.94	0.88	0.69	0.84
Sydney Olympic Park	CALMET (CT-01)	0.67	-0.53	1.14	-0.21	0.45	1.46	0.58	0.33	0.16	0.58
	GRAMM (GM-01)	0.46	-1.27	1.45	-0.50	0.57	1.87	0.61	0.37	-0.07	0.46
	GRAMM (GM-02)	0.42	-1.40	1.53	-0.54	0.60	1.98	0.58	0.33	-0.13	0.43
	GRAMM (GM-03)	0.37	-1.46	1.58	-0.57	0.62	2.04	0.56	0.31	-0.17	0.42
	GRAMM (GM-04)	0.47	-1.23	1.39	-0.48	0.54	1.80	0.62	0.39	-0.03	0.49
Canterbury Racecourse	CALMET (CT-01)	0.51	-1.49	1.69	-0.46	0.53	2.11	0.72	0.52	-0.04	0.48
	GRAMM (GM-01)	0.25	-2.06	2.10	-0.64	0.66	2.57	0.73	0.54	-0.29	0.35
	GRAMM (GM-02)	0.19	-2.16	2.20	-0.67	0.69	2.68	0.70	0.50	-0.35	0.32
	GRAMM (GM-03)	0.18	-2.18	2.23	-0.68	0.69	2.72	0.66	0.44	-0.37	0.31
	GRAMM (GM-04)	0.30	-1.93	1.97	-0.60	0.61	2.42	0.74	0.55	-0.21	0.39
Rozelle	CALMET (CT-01)	0.59	0.52	1.13	0.31	0.68	1.50	0.38	0.14	-0.01	0.50
	GRAMM (GM-01)	0.62	-0.48	0.88	-0.29	0.53	1.25	0.59	0.35	0.22	0.61
	GRAMM (GM-02)	0.53	-0.64	0.91	-0.38	0.55	1.31	0.60	0.36	0.19	0.60
	GRAMM (GM-03)	0.53	-0.64	0.91	-0.38	0.55	1.31	0.60	0.35	0.19	0.60
	GRAMM (GM-04)	0.62	-0.49	0.82	-0.30	0.49	1.17	0.67	0.45	0.27	0.64
Chullora	CALMET (CT-01)	0.75	0.14	0.75	0.08	0.44	0.99	0.58	0.34	0.18	0.59
	GRAMM (GM-01)	0.64	-0.59	0.80	-0.34	0.47	1.16	0.54	0.29	0.12	0.56
	GRAMM (GM-02)	0.54	-0.73	0.85	-0.42	0.50	1.22	0.57	0.33	0.06	0.53
	GRAMM (GM-03)	0.58	-0.69	0.84	-0.40	0.49	1.22	0.54	0.29	0.08	0.54
	GRAMM (GM-04)	0.59	-0.58	0.83	-0.34	0.48	1.15	0.56	0.32	0.09	0.54

(a) Dark green shading indicates best model/set-up performance overall for each site. Light green shading indicates where no single model/set-up gave the best performance for all metrics.

(b) Table B-2 in Appendix B provides definitions for the statistical metrics shown in this table.

Tests **C3-01** and **GM-01** compared the performance of CALMET and GRAMM, with the following outcomes at the evaluation stations:

- St Lukes Park (reference station)
 - CALMET exhibited 'perfect' performance, as expected for this location.
 - Whilst the level of agreement with observations was lower for GRAMM than for CALMET at St Lukes Park (reflecting the meteorological situation modelling approach in GRAMM), the relationship was still very strong ($R^2 = 0.79$).
 - GRAMM typically underestimated the wind speed when the observed wind speed was greater than around 2 m/s.
 - GRAMM did not fully simulate the diurnal variation in wind speed. The model performed well between 18:00 and 06:00, but less so at around 15:00 (when the average underestimation was around 1 m/s). GRAMM performed well in winter (especially April to August), and adequately in summer.
- Sydney Olympic Park
 - CALMET overestimated the wind speed at the lowest end of the wind speed distribution and underestimated the wind speed for higher quantiles.
 - CALMET showed a good prediction of the average wind speed at night-time, but during the daytime the wind speed was underestimated by almost 2 m/s. The underestimation was also greater during the summer than during the winter.
 - The GRAMM predictions were systematically lower than those from CALMET (by around 0.8 m/s on average), and did not simulate the temporal agreement with the observations as well.
- Canterbury Racecourse
 - CALMET underestimated the wind speed. The underestimation ranged from, on average, around 1 m/s during the night-time to around 2.5 m/s during the mid-afternoon. Again, the underestimation was also greater during the summer than during the winter.
 - CALMET overestimated wind speeds where the value for a quantile in the observations was less than around 1 m/s, and underestimated the wind speed for higher quantiles.
 - Again, the GRAMM predictions were systematically lower than those from CALMET, and did not simulate the temporal agreement with the observations as well.
- Rozelle
 - For CALMET the relationship between the predicted and observed values was weak ($R^2 = 0.14$).
 - In contrast to all other stations, at Rozelle CALMET overestimated wind speeds by up to 1 m/s at night-time and gave a more accurate prediction during the afternoon.

- The CALMET underestimation was greater during the winter than during the summer.
- GRAMM showed a better agreement with the observations than CALMET at night-time and during winter, and CALMET gave better agreement with observations during the afternoon and during summer.
- On average, GRAMM underestimated wind speeds by around 0.5 m/s.
- Chullora
 - The average diurnal variation in wind speed was reproduced well by CALMET. However, the hourly paired observations and predictions were again not highly correlated.
 - GRAMM again underestimated wind speeds (by around 0.6 m/s on average), and at this station GRAMM had a weaker relationship with observations than CALMET.

The general observations from tests C3-01 and GM-01 were as follows:

- For the stations other than St Lukes Park, the performance of both models was not as good as at St Lukes Park. For some situations GRAMM performed better than CALMET, and for other situations the CALMET performance was better. Both CALMET and GRAMM predicted wind speeds that had less variation than the observations.
- Neither CALMET nor GRAMM predicted the between-station variation in wind speed. In fact, GRAMM predicted little site-to-site variation. Overall, the results showed that it is a challenge for both CALMET and GRAMM to predict wind speeds accurately across a domain in a situation such as the one investigated, where wind speeds vary quite considerably from location to location. This is, however, confounded by the use of different instrumentation (e.g. cup-and-vane and sonic anemometers) by BoM and OEH. It is likely that this difference in instrumentation played a role in the comparisons.

Tests **GM-01**, **GM-02** and **GM-03** examined the effects of the GRAMM grid spacing. These tests involved running GRAMM with reference meteorology taken from the St Lukes Park station only, and with grid spacing of 50 metres, 100 metres and 200 metres respectively. Notwithstanding the general under-prediction by GRAMM identified earlier, the use of a 50 metre grid generally resulted in better predictions than the 100 metre and 200 metre grids. However, the results for the different grid spacings were generally quite similar. This implies that for a simulation of this kind (flat terrain, no buildings, single station reference meteorology), the results will not be very dependent on the GRAMM grid resolution. In other words, the effect of grid resolution is likely to be small relative to the differences between the predictions and the observations.

Tests **GM-01** and **GM-04** examined the GRAMM Re-Order function. A comparison between these two tests illustrated the effects of running GRAMM without the Re-Order function (test GM-01) and with the Re-Order function (test GM-04). The main effects of the Re-Order function were as follows:

- It slightly improved the prediction of the higher wind speeds. Conversely, the prediction of low wind speeds was made slightly worse.
- It gave a slight improvement in the correlation between the predictions and the observations.
- It resulted in a variability in the predictions that was slightly closer to that in the observations.

6.2.2.2 Series B (multiple station or synthetic reference meteorology)

In Series B the reference meteorology was taken from either multiple stations (CALMET) or from a synthetic meteorological file with Match-to-Observations (GRAMM). Descriptive statistics for the wind speed tests are given in Table 30, and the model performance metrics are summarised in Table 31.

Tests **CT-02** and **GM-05** compared CALMET and GRAMM. In contrast to tests CT-01 and GM-01, where the only reference meteorology was St Lukes Park, these tests illustrated the behaviour of CALMET when several meteorology stations were used as input, except the station for which CALMET predictions were obtained (in this case, St Lukes Park). This provided a more independent test of model performance at St Lukes Park than tests CT-01 and GM-01.

General observations:

- At St Lukes Park, the performance of CALMET deteriorated significantly ($R^2 = 0.43$) compared with test CT-01. With reference meteorology not including this station, the performance of CALMET was similar to that of GRAMM. The following points can also be noted:
- Wind speeds were systematically overestimated by both CALMET and GRAMM, and low wind speeds were overestimated more than high wind speeds. To some extent this would have been a consequence of the measured wind speeds at St Lukes Park, which were the lowest of all the stations.
- On average, the performance of GRAMM was better than that of CALMET at low wind speeds. CALMET gave slightly better predictions at high wind speeds.
- Both models gave a variability in predictions that was quite close to that in the measurements (CALMET was slightly better than GRAMM).
- On an hourly basis the performance of both models could be said to be typical for this temporal resolution ($R^2 = 0.43$ to 0.47).
- At the other stations the performance of GRAMM in Series B was markedly better than in series A. As the other stations were included in CALMET the expected 'perfect' performance was observed.

In tests **CT-02** and **GM-06** the Match-to-Observations function in GRAMM was applied to all stations.

- For St Lukes Park the performance of GRAMM was much improved relative to tests GM-01, GM-04 and GM-05. The ability of GRAMM to simulate the wind speeds at St Lukes Park was still somewhat constrained by the algorithms in the Match-to-Observations function. This is because the function provides an optimised fit across all reference stations included, and therefore for some meteorological situations the fit will have been better at other stations than at St Lukes.
- For the other stations the results for test GM-06 were actually worse than in test GM-05, with the exception of Rozelle. It therefore appears that simply adding more reference stations to GRAMM does not automatically improve its performance.

In tests **CT-01** and **GM-07** GRAMM was run with Match-to-Observations for St Lukes Park only, and the predictions were compared with those from CALMET test CT-01 from series A. Given that GRAMM was not constrained by the need to match the observations at the other stations, this test gave by far the best performance of all GRAMM tests for St Lukes Park ($R^2 = 0.96$). At the other stations neither GRAMM nor CALMET gave systematically the better performance.

Table 30: Wind speed statistics for Series B tests (2015)

Statistic	1-hour average wind speed (m/s)				
	Observed	CT-02	GM-05	GM-06	GM-07
St Lukes Park					
N	8,720	8,760	7,761	8,718	8,719
Average value	1.3	2.1	2.0	1.5	1.3
Maximum value	6.4	6.5	5.4	5.4	5.5
98th percentile	4.5	4.8	4.7	4.6	4.4
50th percentile (median)	1.0	1.9	1.8	1.3	0.9
% calms	27.9%	3.0%	17.8%	25.4%	24.5%
Sydney Olympic Park					
N	7,762	8,760	7,761	8,717	8,720
Average value	2.6	2.4	2.1	1.6	1.4
Maximum value	8.6	8.6	5.6	5.5	5.7
98th percentile	6.4	6.3	5.0	4.5	4.4
50th percentile (median)	2.4	2.2	1.9	1.5	1.1
% calms	11.1%	10.4%	10.8%	19.7%	26.1%
Canterbury Racecourse					
N	7,807	8,760	7,761	8,717	8,720
Average value	3.2	3.0	2.0	1.5	1.3
Maximum value	10.1	10.1	5.4	5.3	5.8
98th percentile	7.5	7.4	5.1	4.5	4.4
50th percentile (median)	3.0	2.7	1.7	1.2	1.0
% calms	7.7%	7.5%	17.8%	25.4%	25.0%
Rozelle					
N	8,443	8,760	7,761	8,718	8,693
Average value	1.7	1.7	2.0	1.5	1.4
Maximum value	16.3	16.3	5.8	5.0	5.5
98th percentile	5.4	5.3	4.5	3.9	4.4
50th percentile (median)	1.2	1.3	1.8	1.5	1.2
% calms	20.3%	19.9%	16.1%	23.5%	23.8%
Chullora					
N	8,648	8,760	7,761	8,718	8,666
Average value	1.7	1.7	1.8	1.4	1.3
Maximum value	8.2	8.2	4.9	4.9	5.3
98th percentile	4.9	4.9	4.0	3.9	4.2
50th percentile (median)	1.5	1.5	1.7	1.4	1.2
% calms	9.4%	9.4%	14.1%	21.9%	25.7%

Table 31: Summary of model performance for wind speed by statistical metric (Series B)

Extract location	Reference meteorology	Test ^(a)	Statistical metric									
			FAC2	MB	MGE	NMB	NMGE	RMSE	r	R ²	COE	IOA
			(Ideal = 1)	(Ideal = 0)	(Ideal = 1)	(Ideal = 1)	(Ideal = 1)	(Ideal = 1)				
St Lukes Park	All stations except St Lukes Park	CALMET (CT-02)	0.55	0.76	1.00	0.52	0.68	1.21	0.66	0.43	-0.07	0.47
		GRAMM (GM-05)	0.63	0.50	0.87	0.34	0.60	1.15	0.68	0.47	0.06	0.53
	All stations	CALMET (CT-02)	1.00	0.00	0.00	0.00	0.00	0.01	1.00	1.00	1.00	1.00
		GRAMM (GM-06)	0.78	0.14	0.44	0.10	0.33	0.62	0.86	0.74	0.52	0.76
		St Lukes Park only	CALMET (CT-01)	1.00	-0.001	0.00	-0.001	0.001	0.01	1.00	1.00	1.00
		GRAMM (GM-07)	0.99	-0.01	0.16	-0.01	0.12	0.25	0.98	0.96	0.82	0.91
Sydney Olympic Park	All stations except St Lukes Park	CALMET (CT-02)	1.00	0.00	0.00	0.00	0.00	0.00	1.00	1.00	1.00	1.00
		GRAMM (GM-05)	0.78	-0.47	0.73	-0.18	0.29	1.03	0.84	0.70	0.46	0.73
	All stations	CALMET (CT-02)	1.00	0.00	0.00	0.00	0.00	0.00	1.00	1.00	1.00	1.00
		GRAMM (GM-06)	0.59	-0.86	1.17	-0.34	0.46	1.52	0.66	0.43	0.14	0.57
		St Lukes Park only	CALMET (CT-01)	0.67	-0.53	1.14	-0.21	0.45	1.46	0.58	0.33	0.16
		GRAMM (GM-07)	0.49	-1.06	1.32	-0.41	0.51	1.71	0.59	0.35	0.03	0.51
Canterbury Racecourse	All stations except St Lukes Park	CALMET (CT-02)	1.00	0.00	0.00	0.00	0.00	0.00	1.00	1.00	1.00	1.00
		GRAMM (GM-05)	0.65	-1.28	1.39	-0.38	0.41	1.75	0.79	0.62	0.62	0.12
	All stations	CALMET (CT-02)	1.00	-0.002	0.002	-0.001	0.001	0.00	1.00	1.00	1.00	1.00
		GRAMM (GM-06)	0.46	-1.61	1.69	-0.50	0.53	2.09	0.76	0.57	-0.04	0.48
		St Lukes Park only	CALMET (CT-01)	0.51	-1.49	1.69	-0.46	0.53	2.11	0.72	0.52	-0.04
		GRAMM (GM-07)	0.35	-1.75	1.81	-0.55	0.56	2.21	0.76	0.57	-0.11	0.44
Rozelle	All stations except St Lukes Park	CALMET (CT-02)	1.00	0.00	0.00	0.00	0.00	0.00	1.00	1.00	1.00	1.00
		GRAMM (GM-05)	0.75	0.16	0.72	0.09	0.40	0.98	0.74	0.55	0.55	0.37
	All stations	CALMET (CT-02)	1.00	0.00	0.00	0.00	0.00	0.00	1.00	1.00	1.00	1.00
		GRAMM (GM-06)	0.73	-0.17	0.62	-0.10	0.37	0.89	0.79	0.62	0.45	0.72
		St Lukes Park only	CALMET (CT-01)	0.59	0.52	1.13	0.31	0.68	1.50	0.38	0.14	-0.01
		GRAMM (GM-07)	0.61	-0.28	0.76	-0.17	0.46	1.05	0.70	0.49	0.32	0.66
Chullora	All stations except St Lukes Park	CALMET (CT-02)	1.00	0.00	0.00	0.00	0.00	0.00	1.00	1.00	1.00	1.00
		GRAMM (GM-05)	0.78	-0.09	0.64	-0.05	0.35	0.88	0.70	0.49	0.49	0.29
	All stations	CALMET (CT-02)	1.00	0.00	0.00	0.00	0.00	0.0	1.00	1.00	1.00	1.00
		GRAMM (GM-06)	0.74	-0.29	0.71	-0.17	0.41	0.99	0.63	0.39	0.22	0.61
		St Lukes Park only	CALMET (CT-01)	0.74	0.14	0.75	0.08	0.44	0.99	0.58	0.34	0.18
		GRAMM (GM-07)	0.62	-0.38	0.84	-0.22	0.49	1.11	0.58	0.33	0.08	0.54

(a) Dark green shading indicates best model/set-up performance overall for each site. Light green shading indicates where no single model/set-up gave the best performance for all metrics.

6.2.3 Wind direction analysis

The results of the wind direction tests are summarised for St Lukes Park and the other stations separately in Table 32.

Table 32: Summary of wind direction tests

Test	Results at St Lukes Park	Results for other stations
Series A – Single measurement station (St Lukes Park)		
CT-01	CALMET extract almost identical to observations	CALMET did not perform as well at St Lukes
GM-01 GM-02 GM-03	Grid spacings of 50 and 200 metres gave a good wind direction distribution. A grid spacing of 100 metres decreased the GRAMM performance, with underestimation of the frequency of northerly winds.	GRAMM did not perform as well at the other stations generally overestimating the frequency of northerly winds.
GM-04	GRAMM with Re-Order showed an improvement in model performance.	
Series B – Multiple measurement stations (CALMET) or synthetic meteorology (GRAMM)		
CT-02	Markedly worse than in test CT-01	CALMET extract almost identical to observations
GM-05 GM-06	GRAMM did not perform as well as previous tests.	GRAMM gave a fair to good performance at other stations.
GM-07	Match-to-Observations showed much improved GRAMM results especially when compared to GM-01, GM-02 and GM-03.	GRAMM did not perform as well at the other stations.

6.2.4 Wind roses

In Appendix E3 annual and seasonal wind roses are shown for all tests. These have not been analysed in detail, and are provided for reference.

6.3 Dispersion model evaluation

6.3.1 Temporal analysis of NO_x

6.3.1.1 Overview

In the temporal analysis of model performance the NO_x concentrations predicted by CAL3QHCR and GRAL were compared with observations from the St Lukes Park and Concord Oval monitoring stations, and for the period between November 2016 and February 2017. The analysis was based on one-hour average data.

As noted in the methodology, the dispersion model predictions for NO_x were combined with a background contribution from St Lukes Park to give total concentrations, and two alternative approaches were used:

- ‘Unadjusted background’ approach. For each hour, the model contribution at each location was added to the corresponding concentration from the St Lukes Park background site.

- 'Adjusted background' approach. For each hour, the model contribution at the St Lukes Park background site was subtracted from the observation at the same site to give an 'adjusted' background. The adjusted background was then added to the model prediction at each location.

The detailed findings of the dispersion model evaluation are provided in Appendix F. A summary of model performance for NO_x by statistical metric, and using the unadjusted background approach, is given in Table 33. An equivalent summary for the 'adjusted background' approach (Concord Oval only) is provided in Table 34. For each performance metric the test with the best performance is shown in green font, and the GRAMM set-up with the best performance is shown in blue.

Whilst the adjusted background approach naturally gave a perfect fit at St Lukes Park, it did not significantly improve the predictions at Concord Oval and has not been presented elsewhere in the report. The lack of improvement with the adjusted approach was probably due to the generally small modelled contribution at St Lukes Park relative to the observations. For example, Figure 19 presents a *timeVariation* plot for NO_x at St Lukes Park for the dispersion model evaluation period. The plot shows the observed concentrations and smaller model increments for GRAL (test GL-01) and CAL3QHCR (test C3-01).

Because the model predictions were added to the background observations from St Lukes Park, the predicted total concentration was always larger than or equal to the observed concentration. However, this was not considered to be a significant drawback.

For NO_x at the Concord Oval site the model predictions (without background) were also compared directly with the 'road increment', which was calculated by subtracting the St Lukes Park observation from the Concord Oval observation in each hour. Table 35 summarises the results for the road increment at Concord Oval. The relationships between the predictions and observations were weaker than for the total concentration. Figure 77 and Figure 78 show the Taylor diagrams for all tests at Concord Oval and St Lukes Park respectively. Overall, it can be seen that, for this particular site and conditions, CAL3QHCR gave the best overall temporal performance, with test GL-03 (GRAMM excluded) giving the best performance for GRAL.

Table 33: Summary of model performance for NO_x by statistical metric (unadjusted background)

Extract location	Test	FAC2	MB	MGE	NMB	NMGE	RMSE	r	R ²	COE	IOA
		(Ideal = 1)	(Ideal = 0)	(Ideal = 1)	(Ideal = 1)	(Ideal = 1)	(Ideal = 1)				
Concord Oval	CAL3QHCR (C3-01)	0.73	-2.20	23.42	-0.04	0.42	35.95	0.77	0.59	0.45	0.72
	GRAL (GL-01)	0.61	13.88	34.56	0.25	0.62	56.75	0.66	0.43	0.18	0.59
	GRAL (GL-02)	0.58	27.92	40.14	0.50	0.72	62.62	0.66	0.44	0.05	0.53
	GRAL (GL-03)	0.54	37.69	49.51	0.68	0.89	80.51	0.62	0.38	-0.17	0.41
	GRAL (GL-04)	0.61	24.92	36.69	0.45	0.66	56.42	0.69	0.47	0.13	0.57
	GRAL (GL-05)	0.54	35.37	49.89	0.63	0.89	86.68	0.56	0.31	-0.18	0.41
	GRAL (GL-06)	0.55	37.21	47.94	0.67	0.86	76.83	0.63	0.40	-0.13	0.43
	GRAL (GL-07)	0.52	45.28	57.34	0.81	1.03	98.21	0.58	0.34	-0.36	0.32
	GRAL (GL-08)	0.54	37.93	50.10	0.68	0.90	81.43	0.61	0.37	-0.19	0.41
St Lukes Park	CAL3QHCR (C3-01)	0.95	3.57	3.57	0.15	0.15	6.19	0.98	0.97	0.79	0.89
	GRAL (GL-01)	0.92	4.37	4.37	0.19	0.19	8.72	0.97	0.94	0.74	0.87
	GRAL (GL-02)	0.86	6.46	6.46	0.27	0.27	11.84	0.95	0.90	0.62	0.81
	GRAL (GL-03)	0.88	5.56	5.56	0.24	0.24	12.81	0.93	0.86	0.67	0.84
	GRAL (GL-04)	0.84	6.82	6.82	0.29	0.29	12.13	0.95	0.90	0.60	0.80
	GRAL (GL-05)	0.87	6.24	6.24	0.26	0.26	16.44	0.88	0.78	0.63	0.82
	GRAL (GL-06)	0.86	6.11	6.11	0.26	0.26	12.65	0.93	0.87	0.64	0.82
	GRAL (GL-07)	0.87	5.82	5.82	0.25	0.25	14.41	0.91	0.83	0.66	0.83
	GRAL (GL-08)	0.87	5.33	5.33	0.23	0.23	11.91	0.94	0.88	0.68	0.84

Table 34: Summary of model performance for NO_x by statistical metric (adjusted background)

Extract location	Test	FAC2	MB	MGE	NMB	NMGE	RMSE	r	R ²	COE	IOA
		(Ideal = 1)	(Ideal = 0)	(Ideal = 1)	(Ideal = 1)	(Ideal = 1)	(Ideal = 1)				
Concord Oval	CAL3QHCR (C3-01)	0.73	-5.81	23.12	-0.10	0.41	35.85	0.78	0.60	0.45	0.73
	GRAL (GL-01)	0.63	9.42	32.21	0.17	0.58	52.46	0.66	0.44	0.24	0.62
	GRAL (GL-02)	0.61	21.37	36.14	0.38	0.65	56.96	0.66	0.44	0.14	0.57
	GRAL (GL-03)	0.55	32.06	46.52	0.57	0.83	75.97	0.61	0.37	-0.10	0.45
	GRAL (GL-04)	0.64	18.00	33.54	0.32	0.60	52.14	0.67	0.45	0.21	0.60
	GRAL (GL-05)	0.54	29.05	47.68	0.52	0.85	83.58	0.54	0.29	-0.13	0.44
	GRAL (GL-06)	0.58	31.01	43.95	0.56	0.79	71.44	0.63	0.39	-0.04	0.48
	GRAL (GL-07)	0.53	39.42	53.11	0.71	0.95	92.27	0.57	0.33	-0.26	0.37
	GRAL (GL-08)	0.55	32.53	46.59	0.58	0.83	76.39	0.61	0.37	-0.10	0.45

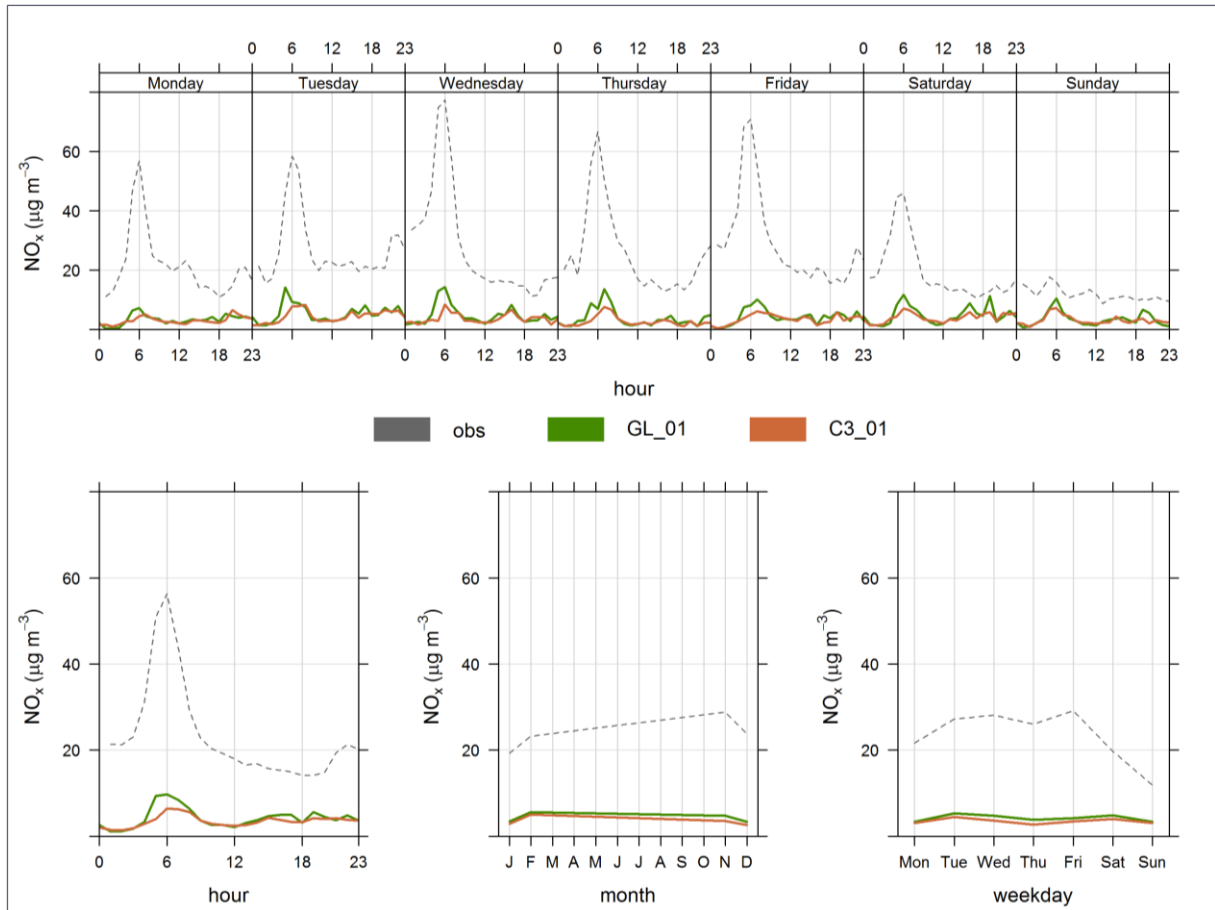


Figure 76: Openair `timeVariation` plot for NO_x at St Lukes Park monitoring station (**November 2016 to February 2017**). The plot shows the observed concentrations and model increments for GRAL (test GL-01) and CAL3QHCR (test C3-01).

Table 35: Summary of model performance for NO_x by statistical metric (road increment)

Extract location	Test	FAC2	MB	MGE	NMB	NMGE	RMSE	r	R ²	COE	IOA
		(Ideal = 1)	(Ideal = 0)	(Ideal = 1)	(Ideal = 1)	(Ideal = 1)	(Ideal = 1)				
Concord Oval, road increment	CAL3QHCR (C3-01)	0.39	-2.20	23.42	-0.07	0.73	35.95	0.57	0.33	0.30	0.65
	GRAL (GL-01)	0.29	13.88	34.56	0.43	1.07	56.75	0.47	0.22	-0.03	0.49
	GRAL (GL-02)	0.33	27.92	40.14	0.87	1.25	62.62	0.48	0.23	-0.19	0.40
	GRAL (GL-03)	0.26	37.69	49.51	1.17	1.54	80.51	0.47	0.22	-0.47	0.26
	GRAL (GL-04)	0.37	24.92	36.69	0.77	1.14	56.42	0.50	0.25	-0.09	0.45
	GRAL (GL-05)	0.23	35.37	49.89	1.10	1.55	86.68	0.40	0.16	-0.48	0.26
	GRAL (GL-06)	0.29	37.21	47.94	1.15	1.49	76.83	0.48	0.23	-0.43	0.29
	GRAL (GL-07)	0.24	45.28	57.34	1.40	1.78	98.21	0.43	0.19	-0.70	0.15
	GRAL (GL-08)	0.25	37.93	50.10	1.18	1.55	81.43	0.45	0.20	-0.49	0.26

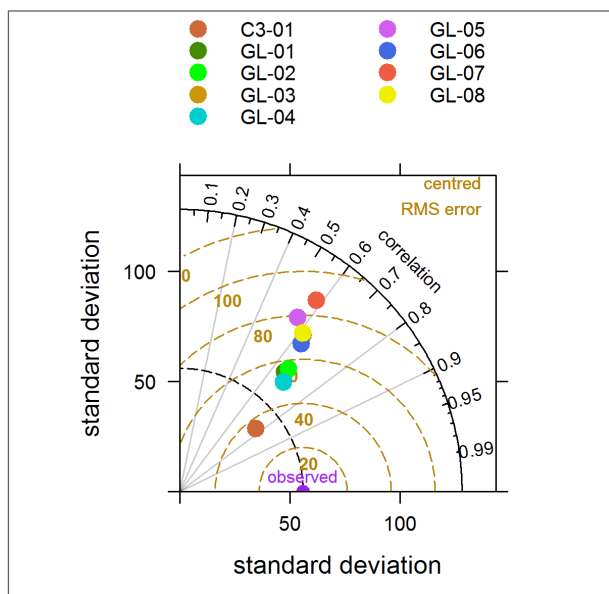


Figure 77: Taylor diagram for all models – Concord Oval

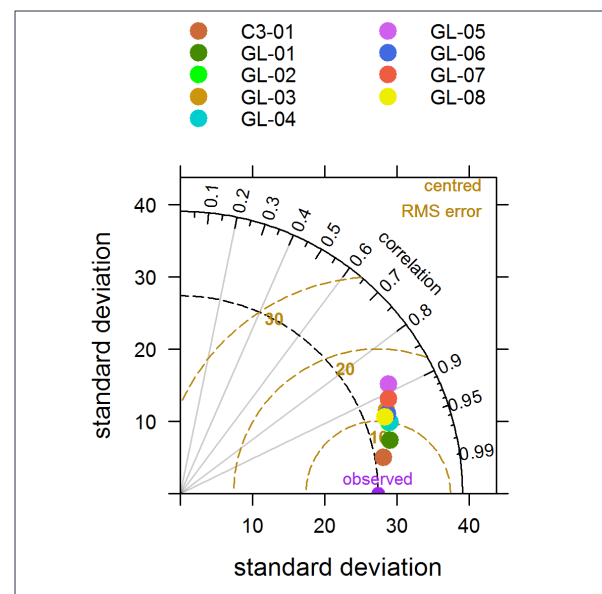


Figure 78: Taylor diagram for all models – St Lukes Park

The results for the different test series are summarised in the following Sections.

6.3.1.2 Series C: CAL3QHCR and GRAL

In these tests the Concord Oval meteorology was used directly in CAL3QHCR (test C3-01) and GRAL (test GL-01). GRAMM was not used in GRAL.

It is helpful to firstly consider the results for the St Lukes Park background site. Because the model predictions were added to the observations from St Lukes Park, the predicted total concentration was always larger than or equal to the observed concentration. However, as the modelled contribution was generally small at this location, the relationship between the predictions and the observations was naturally very good. The over-prediction was slightly higher on average using GRAL than using CAL3QHCR. For a small proportion of hours GRAL significantly over-estimated the concentration at St Lukes Park.

For the Concord Oval site at this high temporal resolution, the R^2 value for CAL3QHCR (0.59) was higher than that for GRAL (0.43). However, CAL3QHCR resulted in a general under-prediction of NO_x (by around 35% for an observed concentration of $400 \mu\text{g}/\text{m}^3$), whereas GRAL was more accurate overall.

The simulation of the average temporal patterns in the NO_x concentrations at Concord Oval was much better, with a reasonably accurate representation of diurnal patterns. GRAL tended to overestimate concentrations during the morning peak traffic period, whereas CAL3QHCR tended to underestimate these. Because of the use of an average weekday emissions profile in the modelling, both models overestimated NO_x concentrations on Saturdays and Sundays. Although the removal of the results for weekends improved the predictions, the improvement was not very large overall (at Concord Oval the R^2 for CAL3QHCR increased from 0.59 to 0.61, and for GRAL it increased from 0.43 to 0.48).

GRAL tended to overestimate the variation in the observations, and CAL3QHCR tended to underestimate it.

On balance, and from an air quality assessment point of view, the slight over-estimations of concentrations in GRAL would be preferable to the slight underestimation in CAL3QHCR.

6.3.1.3 Series D: GRAL meteorological input (tests GL-01 and GL-02)

The tests in Series D examined the effects of the meteorological input in GRAL. In test GL-02 GRAMM (Concord Oval Match-to-Observations) was used rather than the direct observations from Concord Oval in test GL-01. Other model settings were not changed.

There were only quite small differences between the GRAL predictions in the two tests. On average, the predictions in test GL-02 were higher than those in test GL-01, especially in the afternoon and evening. During the morning peak period the predictions in both tests were very similar. Most of statistical metrics indicated a slight deterioration in overall model performance when GRAMM was used.

6.3.1.4 Series E: GRAL grid spacing (tests GL-02, GL-03 and GL-04)

The Series E tests examined the influence of the grid spacing in GRAL (2, 10 and 20 metres). The number of particles in GRAL was fixed at 400 per second. At Concord Oval, the predictions for the three grid spacings were quite similar. The highest concentrations were obtained using the finest resolution, and the lowest concentrations with the coarsest resolution. Overall the test using the coarsest resolution actually resulted in the closest agreement with the predictions.

6.3.1.5 Series F: GRAL particle number

The number of particles per second used in GRAL was investigated in tests GL-03, GL-05 and GL-06. The number of particles used in GRAL (200, 400 or 800) had little effect on the model predictions. The only noticeable difference between the test results was that test GL-03 (400 particles per second) gave markedly higher morning peak concentrations on Mondays and Wednesdays than tests GL-05 or GL-06. The reason for this specific behaviour is unclear.

6.3.1.6 Series G: GRAL buildings

The effects of including buildings in GRAL were examined in tests GL-03, GL-7 and GL08. This involved the separate testing of prognostic (GL-07) and diagnostic (GL-08) approaches. The results were compared with those from test GL-03 (no buildings).

The inclusion of buildings in the modelling had little effect on the results at Concord Oval. The results for test GL-08 were almost identical to those for test GL-03, whereas test GL-07 appeared to slightly compound the existing over-estimation in test GL-03. These findings are not especially surprising, given that there were no large buildings in the vicinity of the Concord Oval monitoring station.

6.3.2 Directional analysis of NO_x

The NO_x predictions from CAL3QHCR (test C3-01) and GRAL (test GL-01) at Concord Oval were analysed directionally, again using the `polarPlot` and `polarAnnulus` functions in Openair in a similar way to the observational analysis (see Section 5.5.3.1). The observed wind speed and wind direction data were used. The resulting plots, which exclude the background contribution, are shown in Figure 81 to Figure 86. The observations (total and road increment) are also shown again for comparison. It should be noted that the predictions for the GRAL model increment are considerably higher than those for the CAL3 model increment, and therefore different scales are used in the plots to enable the spatial features within each dataset to be resolved.

The polar plots for the model predictions again illustrate the strong influence of the traffic on Parramatta Road to the south of the monitoring site. The peak NO_x increments during the middle of the day from the south-east are not picked up in the modelling. It is possible that this may be related to specific bus operations at the depot, including engine idling (which is not represented in the models).

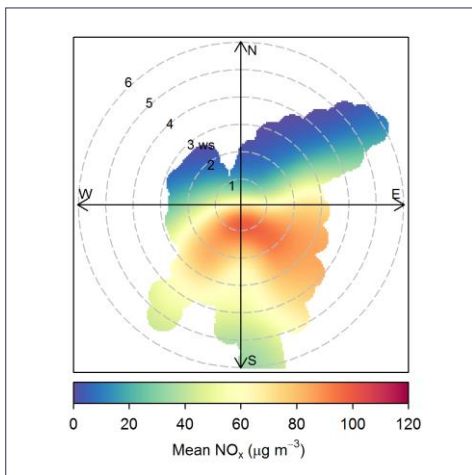


Figure 79: Polar plot - observed NO_x (total) at Concord Oval

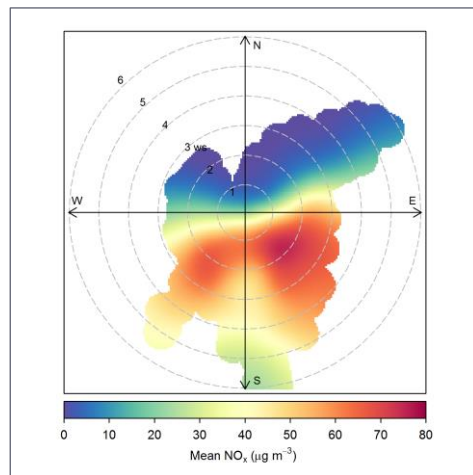


Figure 80: Polar plot - observed NO_x (road increment) at Concord Oval

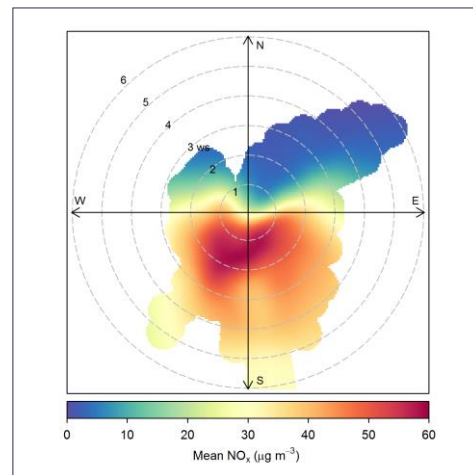


Figure 81: Polar plot for modelled NO_x (C3-01) with measured met at Concord Oval

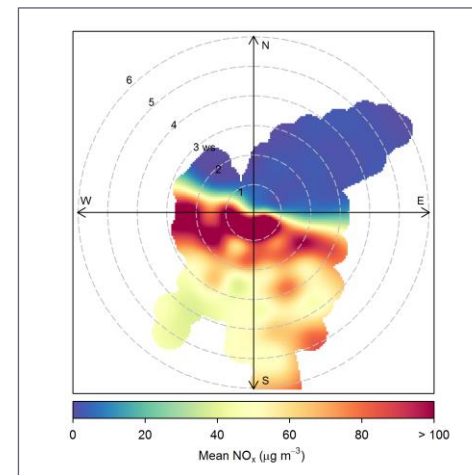


Figure 82: Polar plot for modelled NO_x (GL-01) with measured met at Concord Oval

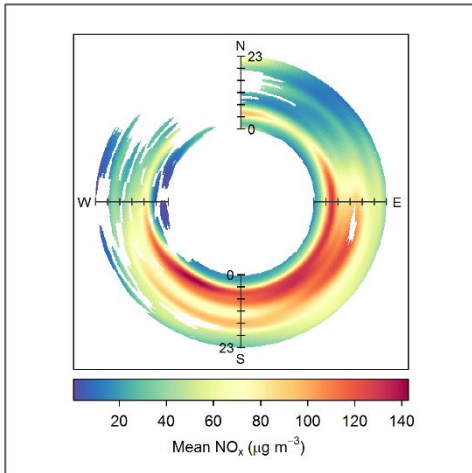


Figure 83: Polar annulus - observed NO_x (total) at Concord Oval

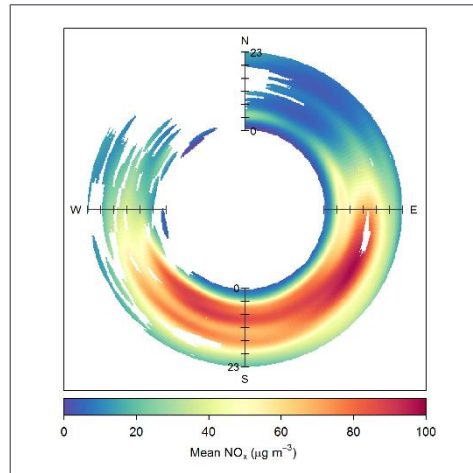


Figure 84: Polar annulus - observed NO_x (road increment) at Concord Oval

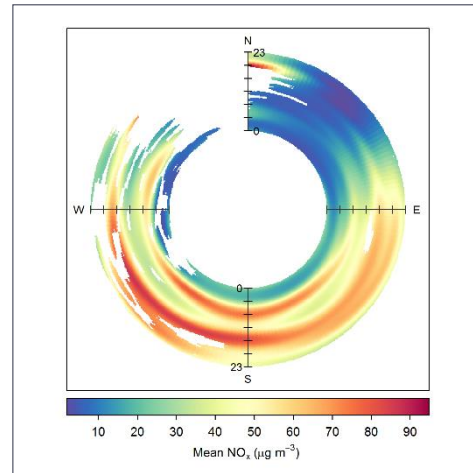


Figure 85: Polar annulus - modelled NO_x (C3-01) with measured met at Concord Oval

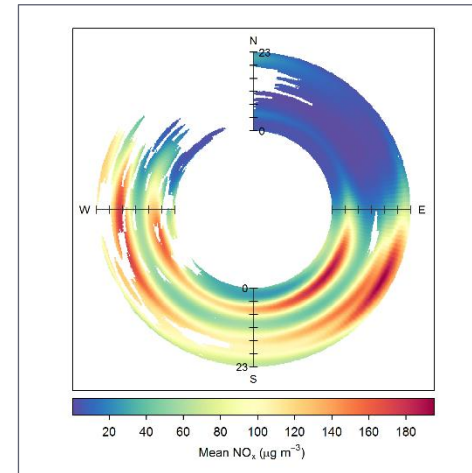


Figure 86: Polar annulus - modelled NO_x (GL-01) with measured met at Concord Oval

6.3.3 Spatial analysis of NO_x

The following sections describe the spatial relationships between the model predictions and observations for NO_x. Contour plots for mean and maximum 1-hour NO_x are given in Appendix F.

6.3.3.1 Regression

For NO_x the performance of CAL3QHCR and GRAL was examined using the period-average concentrations at the passive monitoring locations, as shown in Figure 87. A linear regression function has been fitted to the predicted and observed data for each test (the observed data do not change). In each plot the data from all three periods of passive sampling have been combined, and the regression function has been forced through the origin. It can quickly be seen that, in all cases, the relationship between the predicted and observed values was very strong, with R² values of between 0.79 and 0.90, depending on the test.

The first plot of the Figure shows the comparison between CAL3QHCR and GRAL. To enable a cross-reference to the temporal analysis, the six results for the location of the Concord Oval monitoring station are indicated with red circles. The plot shows that CAL3QHCR (test C3-01) underestimated period-average NO_x concentrations by around 30% on average. For a comparable GRAL set-up (test GL-01), GRAL overestimated NO_x concentrations by around 7% on average. In the case of GRAL this would tend to represent a good outcome for an air quality assessment, where a small amount of conservatism is usually desirable. It is worth noting that, based on this limited dataset, the performance of GRAL at the Concord Oval station was in agreement with its overall performance at other locations, whereas for CAL3QHCR the performance at Concord Oval was slightly better than its overall performance. In other words, the underestimation with CAL3QHCR at Concord Oval was slightly lower than the general trend with this model would suggest.

The use of GRAMM in conjunction with GRAL (test GL-02) had little impact on the results; the agreement with the observations was marginally better than in test GL-01.

The effects of changing the GRAL grid spacing from 10 metres in test GL-01 to 2 metres in test GL-03, and to 20 metres in test GL-04, were also small on average. However, the use of a 2 metre spacing reduced the R² value to 0.81, and a closer inspection of the data revealed that this was influenced by an over-prediction at Concord Oval. With this site removed the R² value was 0.89 and the gradient 1.01. Increasing the GRAL grid spacing to 20 metres had little effect on R², but it increased the average over-prediction to 13%.

In test GL-03 the number of particles in GRAL was set at 400 per second. Decreasing this to 200 particles per second (test GL-05), or increasing it to 800 particles per second (test GL-06), had little effect on the results. Both the 200 and 800 particles per second test had a slightly improved R² value compared with the 400 particles per second run, and it is likely that this linked to the randomness inherent in a Lagrangian model such as GRAL. Normally, increasing the number of particles should result in a more accurate result, all else being equal.

In tests GL-07 and GL-08, the effects of including buildings in the GRAL set-up were investigated. In test GL-07 a prognostic approach was used, whereas in test GL-08 a diagnostic approach was used. All other model settings were the same as in test GL-03. The inclusion of buildings did not markedly improve the performance of the model relative to test GL-03. Using the prognostic model the R² value increased slightly, but the general over-prediction increased from an average of 6% to an average of 18%. Using the diagnostic model the over-prediction decreased to 2% but the R² decreased to 0.79. In test GL-07 the over-prediction was again influenced by the results for Concord Oval, as well as the roadside receptor P10.

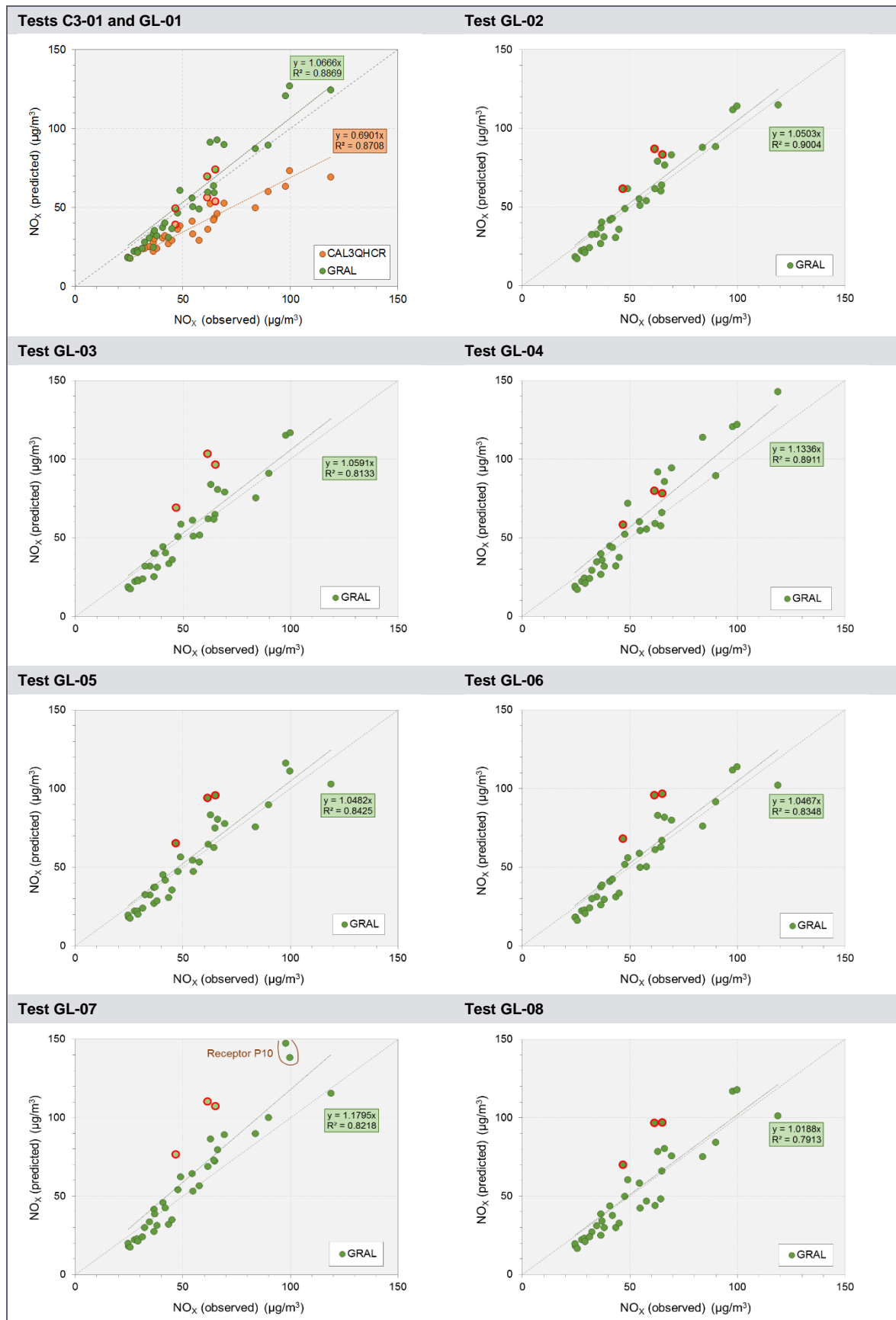


Figure 87: Model evaluation at passive sampling locations (NO_x, periods 1, 2 and 3 combined)

6.3.3.2 Concentration profiles perpendicular to Parramatta Road

The spatial influence of road traffic on measured pollutant concentrations was considered by examining the Ogawa results as a function of distance in Section 5.8.2. These results were examined for the two rounds of passive sampling monitoring completed.

Figure 88 and Figure 89 present the passive sampling NO_x results with GRAL (test GL-01) and CAL3QHRC model results overlaid for rounds 1 and 2 respectively.

The GRAL and CAL3QHRC modelled results for the locations to the north of Parramatta Road exhibited a similar pattern in rounds 1 and 2 of the passive sampling with GRAL showing higher results than CAL3QHRC in both cases. There was more variation to the south of Parramatta Road between the two models and when compared to the passive sampling results.

Generally, GRAL showed an overestimation of high NO_x concentrations closer to Parramatta Road, and an underestimation of low concentrations at locations further away. The near-road overestimation may be due, in part, to a general overestimation of NO_x in the EPA emission factors, as observed in the LCT study. However, as noted earlier, the conditions along Parramatta Road quite different to those in the LCT.

CAL3QHRC showed much lower results than both the measurements and GRAL predictions, closer to Parramatta Road as well as at locations further away.

These results encapsulate the overall effects of the model chain, such as the emission factors, the configuration of the roads in the model, the meteorology, and the dispersion algorithms. If any of these important elements are wrong, then it would be exposed in this comparison. In this respect, the results (particularly for GRAL) are very encouraging.

The effects of the GRAL settings on the prediction of concentrations with distance from Parramatta Road are shown in Figure 90. Consideration is given here to the more detailed set of data to the north of Parramatta Road.

The use of GRAMM in conjunction with GRAL (test GL-02) tended to increase the overprediction within 200 metres of Parramatta Road compared with test GL-01, but there was an improved agreement with the observations beyond 200 metres.

As noted earlier, the effects of changing the GRAL grid spacing from 10 metres in test GL-01 to 2 metres in test GL-03, and to 20 metres in test GL-04, were relatively small overall. The differences between tests were more substantial within around 40 metres of Parramatta Road, but were not systematic.

Increasing the number of particles had little effect on the results.

As before, the inclusion of buildings did not markedly improve the performance of the model.

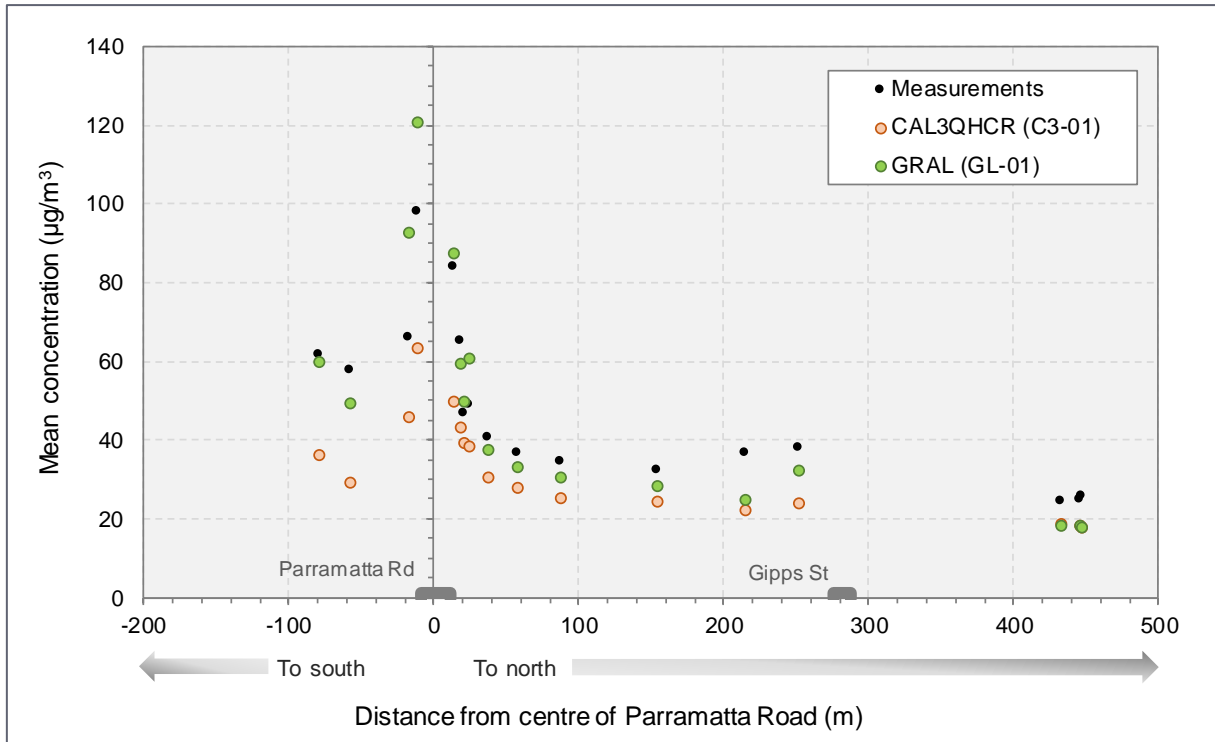


Figure 88: Passive sampling observations and predictions from GRAL (GL-01) and CAL3QHCR (C3-01) perpendicular to Parramatta Road – NO_x , round 1

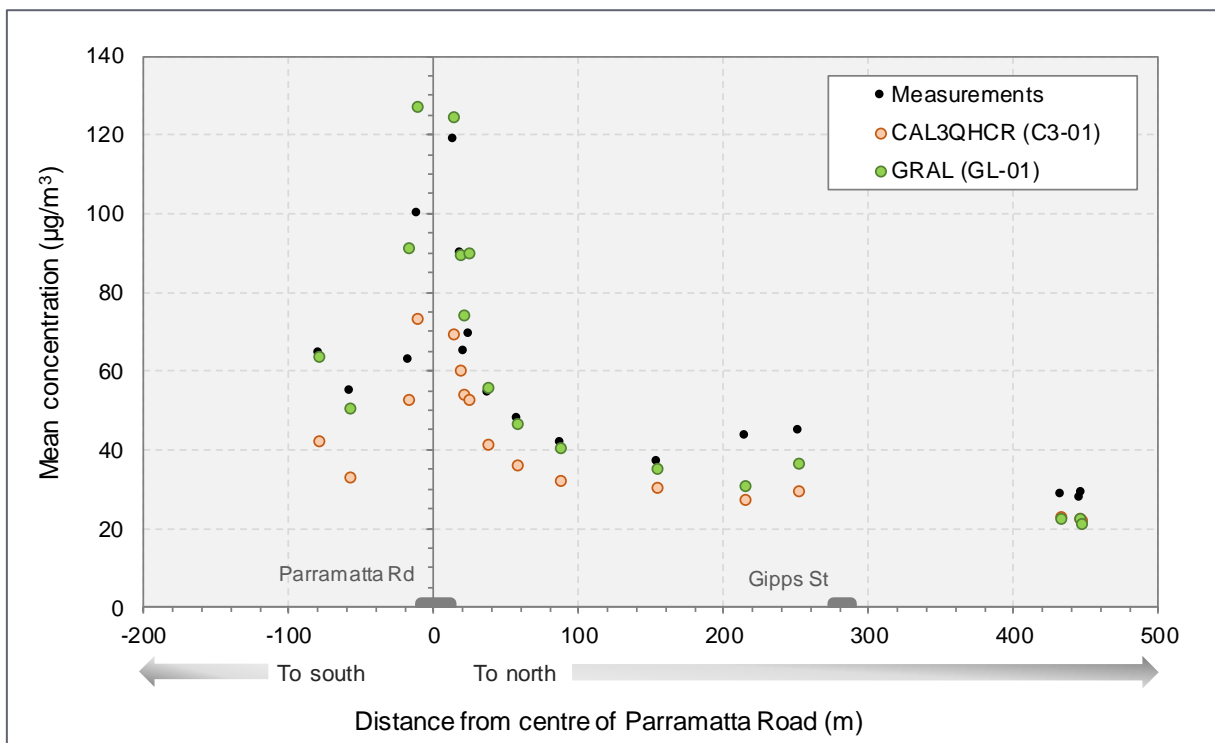


Figure 89: Passive sampling observations and predictions from GRAL (GL-01) and CAL3QHCR (C3-01) perpendicular to Parramatta Road – NO_x , round 2

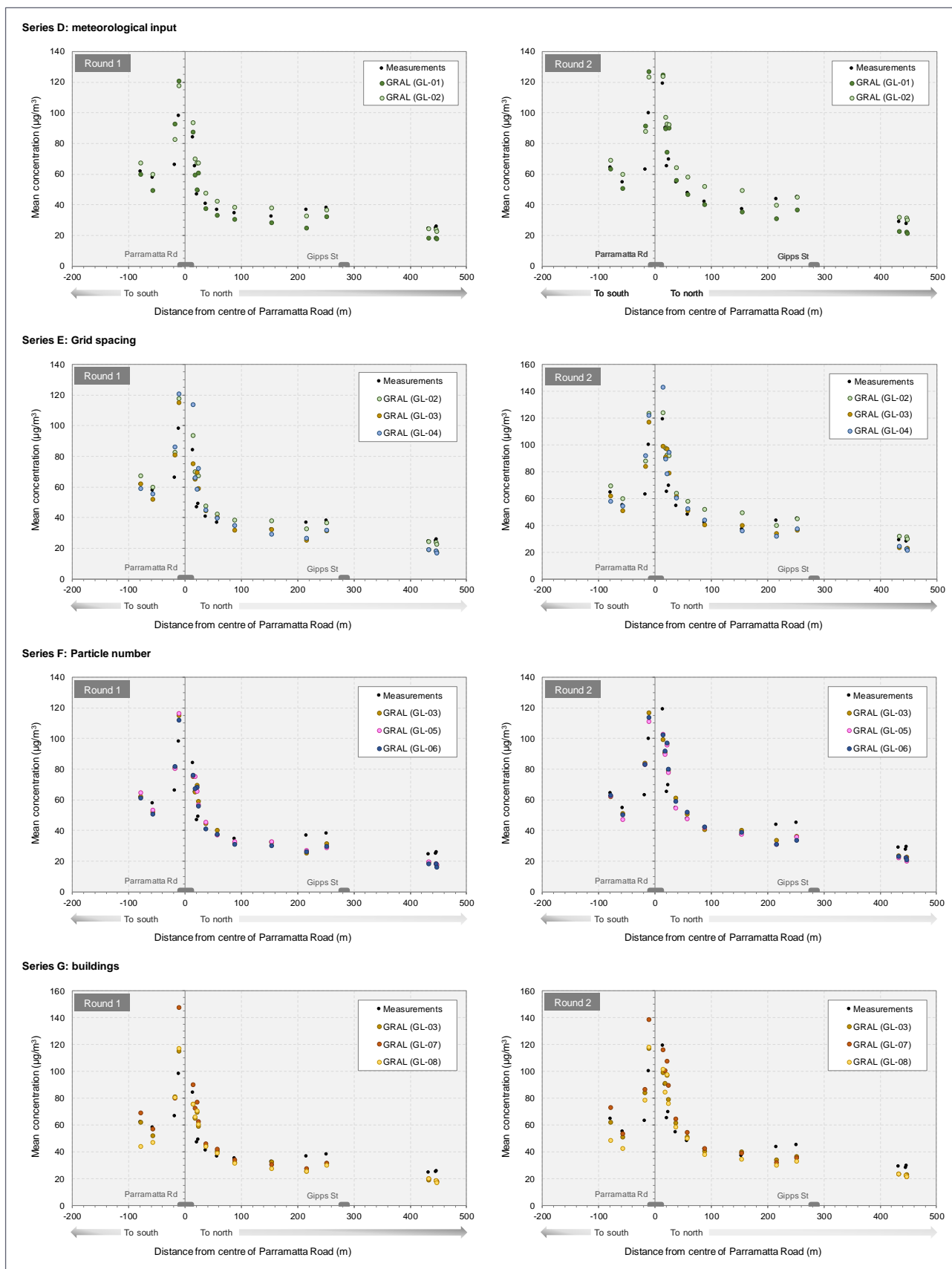


Figure 90: Passive sampling observations and model predictions for NO_x perpendicular to Parramatta Road – effects of GRAL settings

6.4 Treatment of NO₂ concentrations

Several methods for estimating NO₂ concentrations have been included in this study, as NO₂ is important in terms of health, and has air quality criteria. However, NO₂ is strongly influenced by atmospheric chemistry, and GRAL does not include a chemical reaction scheme. The evaluation of NO₂ does not, therefore, represent an evaluation of GRAL itself.

NO₂ was estimated using five different methods, none of which could be considered ideal given the short averaging times involved in the study. The results for the different calculation methods are shown in Figure 91. Given the uncertainty in the calculation of NO₂, only the NO_x results for tests GL-01 and C3-01 were used. The results should therefore be considered relative to the first plot in Figure 87.

The OLM was firstly used in conjunction with the NO₂ and O₃ measurements from Concord Oval and then in conjunction with the NO₂ and O₃ measurements from St Lukes Park. This did not have a large effect on the outcome, with both methods resulting in a general overprediction of NO₂.

The two WestConnex empirical conversion methods gave quite different results. For GRAL the annual mean method actually gave quite good predictions of NO₂ up to around 30 µg/m³, but under-predicted higher concentrations. For CAL3QHCR the annual mean method generally under-predicted concentrations for observations higher than around 20 µg/m³, but then the model already under-predicted NO_x. Unsurprisingly, the WestConnex 1-hour conversion method overestimated NO₂ concentrations for both models.

The use of the study-specific 1-hour conversion method reduced the overestimation substantially, and it would be worth exploring this further in future work.

Overall, the combination of GRAL and the WestConnex annual mean conversion method gave the best match with the observations, but the under-prediction of higher NO₂ concentrations would not be desirable in an air quality impact assessment.

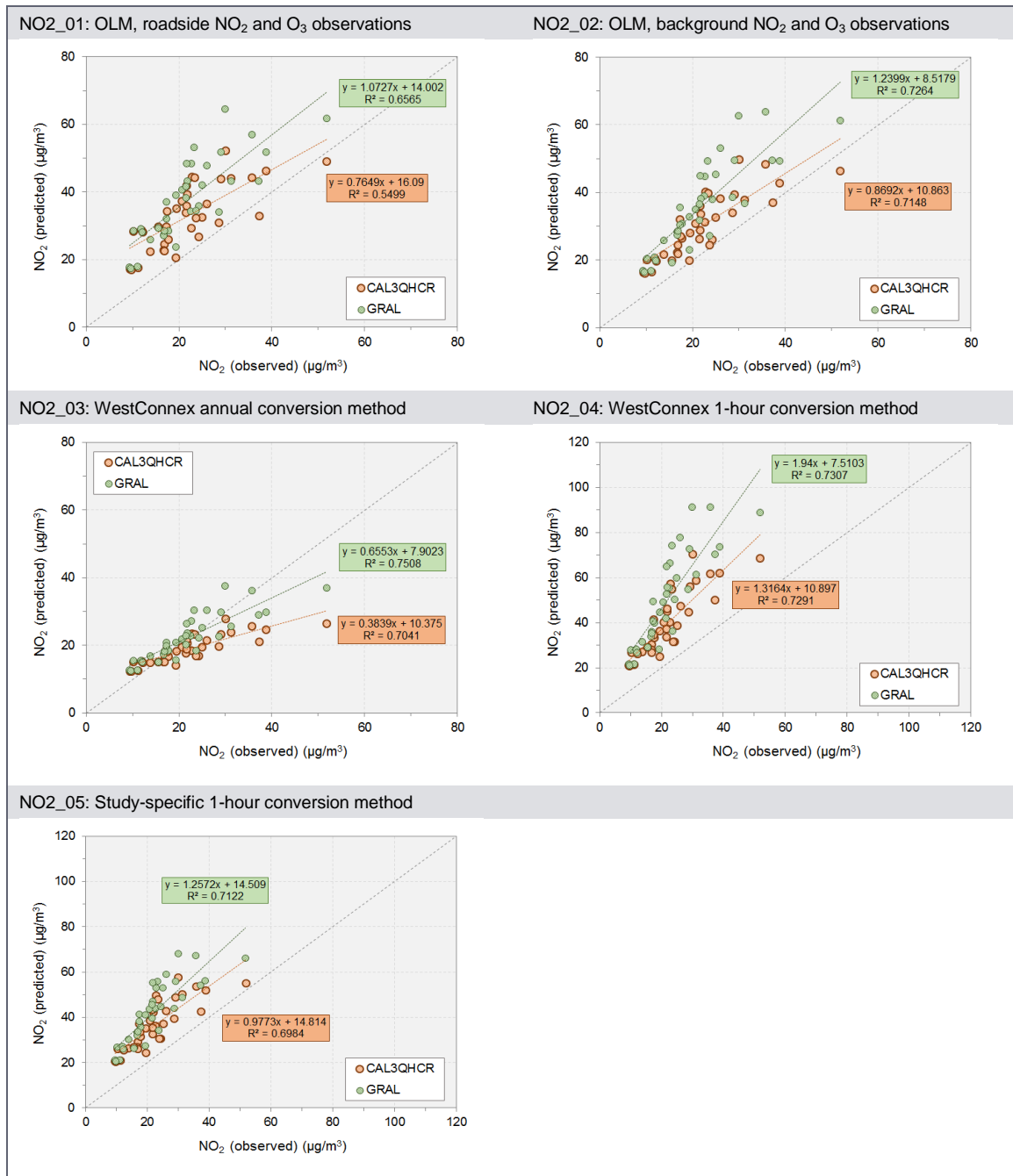


Figure 91: Model evaluation at passive sampling locations (NO₂, periods 1, 2 and 3 combined)

7 Summary and conclusions

7.1 Summary

7.1.1 Emission model sensitivity testing

The sensitivity of the emission model to input parameters, and the implications for modelling uncertainty in the study, was examined for NO_x. Whilst there were some significant differences between emissions for the different road types, these were mainly due to the traffic composition assumptions. Indeed, small errors in traffic composition can also lead to significant errors in emissions. This is especially important for HDVs. Emissions were also not very sensitive to speed between around 30 km/h and 60 km/h.

NO_x emissions are rather sensitive to the road gradient, and small errors in the definition of road gradient can significantly affect the results. Although an effort was made to characterise the gradient accurately, uncertainty in the values used (as well as in the emission factors) could have significantly affected the overall model accuracy.

7.1.2 Meteorological modelling

7.1.2.1 Series A (single station reference meteorology)

At the reference meteorology station - St Lukes Park - the CALMET extract was almost identical to the observed meteorology in terms of both wind speed and wind direction. This is a known characteristic of the model in relation to reference meteorology. GRAMM (without Match-to-Observations) did not match CALMET performance at St Lukes Park, reflecting the met situation modelling approach in GRAMM. The performance of both models was not as good at the other stations.

The effect of the GRAMM grid spacing on wind speed was small. The use of the Re-Order function slightly improved the prediction of higher wind speeds and gave a better overall agreement with observations. Conversely, the prediction of low wind speeds was made slightly worse. Unsurprisingly, this improvement was most pronounced at the St Lukes Park station. Whilst there was also an improvement in the GRAMM predictions at the other stations, this was less clear-cut.

7.1.2.2 Series B (multiple station or synthetic reference meteorology)

With reference meteorology taken from *all stations except St Lukes Park*, the performance of CALMET and GRAMM at St Lukes Park was similar. When the observations from St Lukes Park were not included in CALMET, its performance at this station deteriorated significantly and was similar to that of GRAMM. On average, GRAMM gave better results than CALMET at low wind speeds, whereas CALMET performed slightly better at high wind speeds. At the other stations the performance of GRAMM was markedly better than in series A.

With the reference meteorology taken from *all stations*, the performance of GRAMM at St Lukes Park improved relative to Series A and the test with all stations except St Lukes Park. However, GRAMM was still constrained by the match-to-observations for other sites.

Using the reference meteorology from *St Lukes Park only* (with Match-to-Observations for this site), gave the best performance of all GRAMM tests for St Lukes Park. At the other stations the performance of GRAMM in series B was markedly better than in series A.

7.1.3 Dispersion modelling

7.1.3.1 Temporal performance

At a high temporal resolution (1 hour), the performance of neither CAL3QHCR nor GRAL was especially good, but the level of performance was quite consistent with previous studies. Both models were better at simulating *average* diurnal NO_x profiles.

For Concord Oval the overall performance of CAL3QHCR and GRAL was similar; GRAL tended to overestimate NO_x concentrations whereas CAL3QHCR tended to underestimate them. The performance of GRAL at Concord Oval was better when the Concord Oval meteorological data were used directly, rather than when GRAMM was used.

Changing the settings of GRAL (grid resolution, particles or buildings) had little effect on the predictions at Concord Oval. The small effects of buildings in the modelling was not especially surprising, given that there were no large buildings in the vicinity of the Concord Oval monitoring station.

7.1.3.2 Spatial performance

The performance of both CAL3QHCR and GRAL at simulating the average NO_x concentrations at the passive sampling sites, and hence the fall-off in concentration with distance from the road, was good. However, GRAL slightly overestimated concentrations, whereas CAL3QHCR significantly underestimated concentrations.

The GRAL settings had only a small effect on on the fortnightly-average NO_x predictions at the passive sampling locations. These effects were smaller than the differences between the GRAL and CAL3QHCR predictions.

From an air quality assessment point of view, the slight over-estimations of concentrations in GRAL would be preferable.

7.2 Conclusions

The main conclusions of the study are provided below. When considering these, it should be borne in mind that the purpose of the study was not to provide a validation of the GRAMM-GRAL model itself, but rather to evaluate its performance for the set-up of this particular study.

Emission modelling

1. It is considered unlikely that errors in the allocation of road type would have had a large effect on the outcomes of the study.
2. Uncertainty in road gradient is probably a significant contributor to overall uncertainty in the modelling in the vicinity of the Concord Oval monitoring station, but the gradient was characterised as accurately as possible.
3. It is important to accurately define the proportion of HDVs in the traffic than the speed, except when speeds are particularly low (below 30 km/h).

Meteorological modelling

4. Overall, the results showed that, whilst *average* predictions can be quite good at some locations (especially reference sites), it is a challenge for both CALMET and GRAMM to predict wind speeds accurately across a domain in a situation such as the one investigated, where wind speeds varied quite considerably from location to location. This is, however, confounded by the use of different instrumentation (e.g. cup-and-vane and sonic anemometers) by BoM and OEH, as well as site characteristics such as local topography and the presence of trees.
5. The prediction of *hourly* wind speeds is very challenging for models, especially for stations not included as reference meteorology.
6. The Match-to-Observations function in GRAMM provides an improved prediction of wind speeds compared with a set-up in which it is not used, and also compared with GRAMM using the Re-Order function. This is particularly clear when matching to only one station, but is also likely to be true when multiple stations in a model domain show a similar meteorological pattern.

Dispersion modelling

7. With respect to temporal variation, the combination of GRAMM and GRAL captured the diurnal, seasonal and weekday variations in NO_x well, even though there was a lot of scatter in the hourly comparisons.
8. Overall, CAL3QHCR and GRAL gave a similar overall temporal performance at Concord Oval.
9. GRAL generally gave a better spatial performance than CAL3QHCR. From an air quality assessment point of view, the slight over-estimation of concentrations in GRAL would be preferable to the slight underestimation in CAL3QHCR. Following convention, in this study the minimum wind speed in CAL3QHCR was set to 1 m/s to avoid zero concentration predictions for periods with wind speeds below 1 m/s. It is important to consider the implications of this when comparing CAL3QHCR results (or other Gaussian model results) with GRAL results.
10. For the type of situation investigated ((i.e. flat terrain, no large buildings, varying in meteorological data across stations etc.), the direct use of measured meteorological data in GRAL can result in model performance that is at least as good as when GRAMM is used. For example, test GL-03 (direct input of Concord Oval meteorology) gave the best overall performance with GRAL.
11. The results of GRAL were not very sensitive to settings for grid resolution and number of particles.
12. The inclusion of buildings and therefore wake effects, may be more important where there are many buildings within the study area and close to model sources. This should be considered prior to including buildings in a model given the implications on grid resolution (fine resolution required) and therefore computation times.

Overall conclusions

13. The observational data illustrate how complex and variable air quality is in an urban location with a complex road network, and how demanding the modelling task is. Poor agreement of modelled results with observations (for any model) may be caused by several factors, including

- a. Limitations of the model itself.
- b. Significant processes or factors influencing observations that have not been modelled (due to lack of input data, or processes that are highly localised).

This study was not designed to distinguish between these possibilities.

14. The results show that the combination of GRAMM and GRAL can produce good average predictions which reflect the spatial distribution of concentrations near roads with reasonable accuracy. The model chain gives results that are at least as good as those produced by other models that are currently in use in Australia. As with all air pollution models, the prediction of short-term (1-hour) concentrations remains a challenge. This is not surprising given the complexity of the processes involved. The GRAMM-GRAL model system is therefore suitable for any type of study involving the modelling of road networks. One caveat here is that it may be an unnecessary complication to use GRAMM where appropriate meteorological data are already available.
15. One of the challenges for the study was the treatment of short-term average NO₂ concentrations, especially given the focus on the health impacts of this pollutant rather than total NO_x. This is a challenging problem because of the processes involved, including adequate representation of background concentrations, quantification of primary NO₂ (which is uncertain, and the short-term chemical formation of NO₂ through its reaction with ozone. The latter point was particularly important for this study; the time scales for atmospheric mixing and chemical reactions are very similar, which makes this task difficult. Ideally, what is required is a closely-coupled treatment of mixing and chemistry. As shown in the study, the OLM and empirical approaches for estimating short-term NO₂ concentrations do not work especially well.

8 Recommendations

Various recommendations for the application of GRAMM and GRAL have resulted from this study. When considering these, the following should be borne in mind:

- The purpose of the study was not to provide a complete validation of the GRAMM-GRAL system itself, but rather to evaluate its performance for the set-up of the study.
- Any recommendations made for the use of the model system in an Australian regulatory assessment context should be viewed with an understanding that they are based on the set-up for the study.

In particular, it should be noted that the recommendations apply to *road traffic sources in a small study area with relatively simple terrain and few large buildings*. However, it can reasonably be assumed that the findings are transferable from Sydney to similar urban areas of Australia.

The recommendations for GRAMM-GRAL application are as follows:

1. For the type of study area investigated, the direct use of measured meteorological data in GRAL can result in model performance that is at least as good as when GRAMM is used. Nevertheless, it would generally be advisable to run GRAMM to confirm this, and to run GRAMM for more complex situations and larger domains.
2. Where GRAMM is used, then it will be important to use the Match-to-Observation function for an appropriate (nearby, representative) meteorological station.
3. In order to reduce the uncertainty in emission calculations, it is important to use an accurate temporal profile of traffic volume and traffic composition. It will also be important to accurately characterise traffic speed, especially when this is outside the range of around 30-60 km/h. These factors have been known for a long time, and are not exclusive to GRAL.
4. The results of GRAL will probably not be sensitive to settings such as grid resolution and number of particles, although these should clearly be within the recommended ranges.
5. The likely advantages of including buildings in a model run should be considered prior to modelling, given the implications on grid resolution (fine resolution required) and therefore computation times.
6. In general, the prediction of short-term NO₂ concentrations needs to be improved to properly account for local chemical processes. Empirical methods should be further investigated. It would be useful to know, for example, how NO₂ predictions vary according to conditions.

The data obtained in the study could be useful in future studies, and there are further opportunities for data mining. The information presented in the report will be available to anyone interested in understanding or modelling near-road air quality.

For more detailed recommendations on model settings the GRAMM and GRAL documentation should be consulted.

9 References

- AECOM (2014). NorthConnex - Environmental Impact Statement - Submissions and Preferred Infrastructure Report. ISBN 978-1-925093-99-5.
- ASTM (2015). Standard Guide for Statistical Evaluation of Atmospheric Dispersion Model Performance. ASTM D6589-05, ASTM International, West Conshohocken, PA.
- Barclay J and Scire J (2011). Generic Guidance and Optimum Model Settings for the CALPUFF Modeling System for Inclusion into the 'Approved Methods for the Modeling and Assessment of Air Pollutants in NSW, Australia' Prepared for NSW Office of Environment and Heritage, March 2011.
- Boulter P and Bennett S (2015). A review and analysis of primary nitrogen dioxide emissions from road vehicles in Sydney. Report AQU-NW-003-20187. Report prepared for NSW Roads and Maritime Services, April 2014. Pacific Environment, North Sydney.
- Boulter P, Manansala F and Barnett J (2015). WestConnex M4 East – Environmental Impact Statement. Appendix H, Volume 2B, Air Quality Assessment Report. WestConnex Delivery Authority, September 2015.
- Bull M (2011). DMRB air quality model verification – good practice guide. Report 210664.26. Ove Arup and Partners, London.
- Carslaw D (2011). Defra urban model evaluation analysis – Phase 1. Department for the Environment, Food and Rural Affairs, London.
- Carslaw D C (2015). The openair manual: -open-source tools for analysing air pollution data. Manual for version 1.1-4, King's College London.
- Chang J C and Hanna S R (2005). Technical Descriptions and Users' Guide for the BOOT statistical Model Evaluation Software package, available at http://www.harmo.org/kit/Download/BOOT_UG.pdf
- Cole H S and Summerhays J E (1979). A review of techniques available for estimating short-term NO₂ concentrations. Journal of Air Pollution Control Association. 29(8), pp. 812-817.
- Corsmeier I, Imhof F, Kohler M, Kuhlwein J, Kurtenbach R, Petrea M, Rosenbohm E, Vogel B and Vogt U (2005). Comparison of measured and model-calculated real-world traffic emissions. Atmospheric Environment, Vol. 39, pp. 5760-5775.
- D'Abreton P (2009). Air quality modelling best practice guidance for the Australian alumina industry. Report 3143. PAEHolmes, Brisbane.
- Defra (2016). Local Air Quality Management Technical Guidance (TG16). April 2016. Department for the Environment, Food and Rural Affairs, London.
- Denby B et al. (2010). Guidance on the use of models for the European Air Quality Directive - A working document of the Forum for Air Quality Modelling in Europe (FAIRMODE). ETC/ACC report Version 6.2. European Topic Centre on Air and Climate Change.

Derwent D, Fraser A, Abbott J, Jenkin M, Willis P and Murrells T (2010). Evaluating the Performance of Air Quality Models. Issue 3/June 2010. Department for the Environment, Food and Rural Affairs, London.

EEA (2016). EMEP/EEA Air Pollutant Emission Inventory Guidebook 2016. Report No 21/2016. European Environment Agency EEA, Copenhagen.

<http://www.eea.europa.eu/publications/emep-eea-guidebook-2016>

Evans, J. D. (1996). Straightforward statistics for the behavioral sciences. Pacific Grove, CA. Brooks/Cole Publishing.

Hanna S R (1989). Confidence Limits for Air Quality Models, as Estimated by Bootstrap and Jackknife Resampling Methods. *Atmospheric Environment*, Vol. 23, pp. 1385-1395.

Hu J, Ying Q, Chen J, Mahmud A, Zhao Z, Chen S-H and Kleeman M J (2010). Particulate air quality model predictions using prognostic vs. diagnostic meteorology in central California. *Atmospheric Environment*, Vol. 44, pp. 215-226.

Hurley P (2000). Verification of TAPM meteorological predictions in the Melbourne region for a winter and summer month, *Australian Meteorological Magazine*, Vol. 49(2), pp. 97-107.

Hurley P J, Physick W L and Luhar A K (2002). The Air Pollution Model (TAPM) Version 2. Part 2: Summary of some Verification Studies. CSIRO Atmospheric Research technical paper no.57.

Hurley, P. (2008) TAPM V4. Part 1: Technical Description, CSIRO Marine and Atmospheric Research Paper.

John C, Friedrich R, Staehelin J, Schläpfer K and Stahel W A (1999). Comparison of emission factors for road traffic from a tunnel study (Gubrist tunnel, Switzerland) and from emission modeling. *Atmospheric Environment*, Vol. 33, pp. 3367-3376.

Levitin J, Härkörknen J, Kukkonen J and Nikmo J (2005). Evaluation of the CALINE4 and CAR-FMI models against measurements near a major road. *Atmospheric Environment*, 39, pp. 4439–4452.

Longley I, Kingham S, Dirks K, Somervell E, Pattinson W and Elangasinghe A (2013). Detailed observations and validated modelling of the impact of traffic on the air quality of roadside communities. NZ Transport Agency research report 516. NZ Transport Agency, Wellington, New Zealand.

Manansala F, Boulter P and Barnett J (2015). WestConnex New M5 – Environmental Impact Statement. Appendix H, Volume 2B, Air Quality Assessment Report. WestConnex Delivery Authority, November 2015.

NSW EPA (2012a). Air Emissions Inventory for the Greater Metropolitan Region in New South Wales - 2008 Calendar Year. Technical Report No. 1 - Consolidated Natural and Human-Made Emissions: Results. NSW Environment Protection Authority, Sydney South.

NSW EPA (2012b). Air Emissions Inventory for the Greater Metropolitan Region in New South Wales - 2008 Calendar Year. Technical Report No. 7 - On-Road Mobile Emissions: Results. NSW Environment Protection Authority, Sydney South.

<http://www.environment.nsw.gov.au/resources/air/120256AEITR7OnRoadMobile.pdf>

<http://www.environment.nsw.gov.au/resources/air/120256AEITR7OnRoadMobileAppendix.pdf>

NSW EPA (2016). Approved Methods for the Modelling and Assessment of Air Pollutants in NSW. NSW Environment Protection Authority, Sydney.

<http://www.epa.nsw.gov.au/resources/epa/approved-methods-for-modelling-and-assessment-of-air-pollutants-in-NSW-160666.pdf>

NSW OEH (2014). NSW Air Quality Monitoring Network: Quality Assurance Procedures. NSW Office of Environment and Heritage, Sydney.

<https://www.environment.nsw.gov.au/resources/aqms/140754AQMNqa.pdf>

NZMfE (2004). Good Practice Guide for Atmospheric Dispersion Modelling. New Zealand Ministry for the Environment, Wellington.

O'Kelly D (2016). NSW Fleet Forecast for Tunnel Ventilation Design: 2016 to 2040. NSW Roads and Maritime Services, September 2016.

Öttl D (2016a). Documentation of the prognostic mesoscale model GRAMM (Graz Mesoscale Model) Vs. 16.1. Report LU-05-16. Government of Styria, Graz, Austria.

Öttl D (2016b). Documentation of the Lagrangian Particle Model GRAL (Graz Lagrangian Model) Vs. 16.8. Report LU-09-16. Government of Styria, Graz, Austria.

Öttl D (2016c). Recommendations when using the GRAL/GRAMM modelling system. Government of Styria, Graz, Austria.

Öttl D and Kuntner M (2010). H13-223 - The Austrian Guideline for Short Scale dispersion modelling. HARMO13 - 1-4 June 2010, Paris, France - 13th Conference on Harmonisation within Atmospheric Dispersion Modelling for Regulatory Purposes.

Öttl D and Kuntner M (2016). GRAL Manual - GRAL Graphical User Interface 16.8. Government of Styria, Graz, Austria.

Öttl D, Sturm P J, Bacher M, Pretterhofer G and Almbauer R A (2002): A simple model for the dispersion of pollutants from a road tunnel portal. *Atmospheric Environment*, Vol. 36, pp. 2943-2953.

Pacific Environment (2017). WestConnex M4-M5 Link – Environmental Impact Statement. Technical Working Paper: Air Quality. Appendix I. NSW Roads and Maritime Services, August 2017.

Pastramas N, Samaras C, Mellios G and Ntziachristos L (2014). Update of the Air Emissions Inventory Guidebook – Road Transport 2014 Update. Report. No: 14.RE.011.V1. Emisia, Thessaloniki, Greece.

PIARC (2012). Road tunnels: vehicle emissions and air demand for ventilation. World Road Association, Paris. Report 2012R05, December 2012.

PRC (2001). National Environment Protection Measure (NEPM). Technical Paper No. 5 - Data Collection and Handling. Peer Review Committee.

<http://www.nepc.gov.au/resource/ephc-archive-ambient-air-quality-nepm>

Stevenson K, Yardley R, Stacey B and Maggs R (2009). QA/QC Procedures for the UK Automatic Urban and Rural Air Quality Monitoring Network (AURN). Report AEAT/ENV/R/2837, September 2009. AEA group, Harwell, United Kingdom.

http://uk-air.defra.gov.uk/assets/documents/reports/cat13/0910081142_AURN_QA_QC_Manual_Sep_09_FINAL.pdf

Stocker J, Heist D, Hood C, Isakov V, Carruthers D, Perry S, Snyder M, Venkatram A and Arunachala S (2013). Road source model intercomparison study using new and existing datasets. 15th International Conference on Harmonisation, Madrid, Spain.

Tesche T W, McNally D E and Tremback C (2002). Operational Evaluation of the MM5 Meteorological Model Over the Continental United States: Protocol for Annual and Episodic Evaluation. Prepared for USEPA by Alpine Geophysics, LLC, Ft. Wright, KY, and ATMET, Inc., Boulder, CO.

Thunis P, Pederzoli A and Pernigotti D (2012). Performance criteria to evaluate air quality modeling applications. Atmospheric Environment 59 (2012), pp. 476-482.

Tikvart J A (1996). Application of O₃ limiting Method; Model Clearinghouse Memorandum #107; US Environmental Protection Agency: Research Triangle Park, NC, August 15.

Uhrner U, Lackner B C, Reifeltshammer R, Steiner M, Forkel R and Sturm P J (2014). Inter-Regional Air Quality Assessment: Bridging the Gap between Regional and Kerbside PM Pollution - Results of the PMinter Project. Report of the Institute for Internal Combustion Engines and Thermodynamics, Graz University of Technology, Vol. 98. ISBN: 978-3-85125-364-1.

USEPA (2007). Guidance on the Use of Models and Other Analyses for Demonstrating Attainment of Air Quality Goals for Ozone, PM_{2.5}, and Regional Haze. Publication No. EPA-454/B-07-002, April 2007. United States Environmental Protection Agency, North Carolina.

USEPA (2009). Guidance on the Development, Evaluation, and Application of Environmental Models. EPA/100/K-09/003. U.S. Environmental Protection Agency, Washington, DC 20460.

Willmot C J (1982). Some Comments on the Evaluation of Model Performance. Bulletin of the American Meteorological Society, Vol 63, 1982, pp. 1309-1313.